AUTONOMOUS UNIVERSITY OF MADRID
FACULTY OF SCIENCES
DEPARTMENT OF MOLECULAR BIOLOGY

Pathogenesis and Targeted Therapy of T-cell Lymphoma

by

Magdalena Barbara Woźniak

****

A thesis submitted to
the Autonomous University of Madrid
for the degree of
Doctor of Philosophy

Madrid 2010

This thesis, submitted for the degree of Doctor in Philosophy at the Autonomous University of Madrid, has been performed in the laboratory of Lymphoma Group at Spanish National Cancer Research Centre (CNIO). The presented work was done under the guidance of Dr Miguel Ángel Piris (CNIO) and Dr Pablo Luis Ortiz-Romero (Hospital 12 de Octubre). This work was supported by the grant from Ministerio de Sanidad y Consumo (FISP05/1710) and RETICS.

El trabajo descrito en esta memoria para optar al grado de doctor en la Universidad Autónoma de Madrid, ha sido realizado en el Laboratorio de Linfomas del Centro Nacional de Investigaciones Oncológicas (CNIO), bajo la dirección de los doctores Miguel A. Piris (CNIO) y Pablo Luis Ortiz-Romero (Hospital 12 de Octubre). La realización de este trabajo ha sido posible gracias a la financiación proporcionada por unas becas de Ministerio de Sanidad y Consumo (FISP05/1710) y por el RETICS.

The joy of discovery is certainly the liveliest that the mind of man can ever feel.

Claude Bernard (1813-78) French physiologist.

Dedicated to my family

ACKNOWLEDGEMENTS

Almost four years have passed since my arrival to Spain and the start of my PhD Project in the Lymphoma Group. Now, when I am almost finished, the time has come to acknowledge the people that in one way or other have contributed to both my scientific as well as personal development during my stay in Madrid.

In the first place, I would like to thank Miguel Angel Piris and Pablo Ortiz-Romero for their excellent supervision and for giving me the opportunity to perform my PhD thesis at Spanish National Cancer Research Centre in collaboration with Hospital 12 de Octubre. Thank you both for your help, support and a good word when needed.

However, it is with sadness that in this paragraph of my thesis I must also acknowledge the passing of a friend and colleague Raquel Villuendas, and I would like to thank her for introducing me to the Lymphoma Group and for keeping an eye on the progress of my project in the first year of my thesis.

It is fair to say that most of the lab members have made a contribution to this work. Many thanks to Paloma and Elena for the help with hybridizations and to Mari Cruz, Helena, Pier, Mar and Ruben for their excellent technical support. Thanks to May for being friendly and supportive along all those years and to Maria and Santiago for the input of their knowledge of pathology in my work.

Thanks to all the members of the 307A for being not only great lab buddies but also for your friendship throughout the years. To Dani aka “God” (according to some individuals who will remain anonymous) and Bea “Maribel”, my “hermanos de tesis”, for the four years we spend together, for sharing the moments of both happiness and sorrows, for hours of conversations (also scientific), for your unconditional help, for your patience to my endless questions, for assisting in my “mudanzas” and for being wonderful friends also outside the lab. To my “evil twin” – Lina (“Choffis”) – for being my kindred spirit in the last years, for all the jokes we have made, for being a great flat- and lab-mate, for Magda’s room at your place, for your friendship, for….. well I think you probably know better what I was going to write as “great minds think alike”. To Lorena for all the dinners, parties and journeys we have experienced together and for being one “bananero” more. To Helen for making me laugh, Pilar for giving us hugs whenever needed and to all lab members that I did not mention due to space limitation for being friendly and supportive. To Laura for always finding a solution to my problems, for driving me home and for all the breakfasts we had together. There is nothing better for a good start of the day.

To Josue (“Wey”), Ricardo (“Ramiro”), Fabian (“Caipira”), Lina (“Choffis”), Matt, Olivia (“Newton”) and Julio (“Listo”) for being the best flatmates ever, for all the dinners, parties, for sharing your everyday life with me, for making me smile and for giving me your company every evening. “Bombon” – Josue, there are not enough words to express how wonderful flatmate and friend you were - “ya estoy!”. I wish you all the best in the future.
Special thanks must go also to Ricardo for teaching me how to see the positive side of everything, your happiness is contagious and together we lived so many unforgettable moments across so many different places. Thank you for always cheering me up and for letting us know “how big we are”! To Fabian for the trips to Portugal, to Matt for friendship and support and to Olivia for having enough energy to share with all of us.

Many thanks to Gonzalo Gomez for his patience and help in solving all my bioinformatics queries. To Lorenzo and Denise for all the good moments and to the Polish community at CNIO (Aneta, Agnieszka, Magda, Jarek…) for bringing a little bit of “polishness” while being so far away from home.

Finally, to my parents for their unconditional love, for supporting me in various ways since my educational journey began more than 20 years ago, and for providing me with everything I needed. Thanks to you I became who I am, and for all of it I would like to dedicate this thesis to you.

Last but not least, to Patrick, for his friendship, for being with me, for putting up with all my journeys, parties and huge phone bills and of course thanks for all the English corrections. Thank you for your love and the precious, but too infrequent moments we shared together these last couple of years as well as the commitment to our future together… Ik hou van jou.

Once Michael Vance said:

“Life is not measured by the breaths you take, but by its breathtaking moments”.

For those moments and for making me smile I would like to say to all of you:

Thank you

Magdalena

INDEX

Table of Contents

PUBLICATIONS

ARTICLES

The following articles have been published in scientific journals:

Wozniak MB, Tracey L, **Ortiz-Romero PL**, Montes S, Alvarez M, Fraga J, Fernández Herrera J, Vidal S, Rodriguez-Peralto JL, **Piris MA**, Villuendas R.
Psoralen plus ultraviolet A +/- interferon-alpha treatment resistance in mycosis fungoides: the role of tumour microenvironment, nuclear transcription factor-kappaB and T-cell receptor pathways.
Br J Dermatol. 2009 Jan; **160**(1):92-102. Epub 2008 Oct 16.

Wozniak MB, Villuendas R, Bischoff JR, Blanco-Aparicio C, Martínez-Leal JF, de La Cueva P, Rodriguez ME, Herreros B, Martin-Perez D, Longo MI, Herrera M, **Piris MA**, **Ortiz-Romero PL**.
Vorinostat interferes with the signaling transduction pathway of T cell receptor and synergizes with PI3K inhibitors in cutaneous T-cell lymphoma.
Haematologica 2010; **95**(4). Epub 2010 Feb 4.

Wozniak MB, Rodriguez Pinilla SM, Villuendas R, Herrera M, **Ortiz PL**, **Piris MA**
Cutaneous T-cell lymphoma, new insights.
Hematology Meeting Reports 2009; **3**(1):85–86

Wozniak MB, **Piris MA**.
Cutaneous T-cell lymphoma: two faces of the same coin.
J Invest Dermatol. 2010 Feb; **130**(2):348-51.

BOOK CHAPTERS

Wozniak MB.
Chapter III: "Molecular abnormalities and prognostic factors in mycosis fungoides."
Book Title: New Research on Cutaneous Lymphomas.
Editor: Angel Fernandez-Flores
Nova Publishers Inc. 2007
ISBN: 1600214037

SUMMARY / RESUMEN

SUMMARY

Lymphomas are neoplasms derived from B or T lymphocytes. Peripheral T-cell lymphomas (PTCL) are a group of malignancies that vary in their biology, genetics, clinical presentation, response to therapy, and outcome. While B-cell lymphomas are relatively well studied, only limited research has been performed to elucidate the pathobiology and identify novel pharmacological approaches in PTCL. With the purpose of delineating the mechanisms responsible for PTCL tumorigenesis, a variety of approaches including microRNA, mRNA and protein expression analysis was used. The microRNA analysis revealed a series of aberrantly expressed microRNAs including downregulation of let-7 family, miR-10, miR-15, miR-16, miR-101, miR-29, miR-215, miR-150, miR-139, miR-126 and miR-195 regulating stemness, stress response, apoptosis, proliferation, angiogenesis, and cell cycle pathways. Furthermore, a group of PTCL with a null-phenotype (lacking normal T-cell subpopulations' markers) has been identified, expressing an oncogenic microRNA signature. This group showed an increased proliferation with enrichment of Ras and Rho associated pathways.

At present, no curative treatment is available for cutaneous T-cell lymphoma (CTCL) patients and many commonly used therapeutic strategies achieve remission in only a subset of cases. Although PUVA and IFNα are commonly used therapies in CTCL, a large proportion of patients show resistance to treatment, and the factors responsible for this resistance are unknown. In order to identify factors responsible for resistance to PUVA and IFNα treatment in mycosis fungoides (MF) patients, the gene expression profiling of pre-treatment samples from 29 MF patients enrolled in a randomized clinical trial was analyzed using cDNA microarrays. Genes involved in NF-κB, T-cell receptor, cytokine signaling and proliferation were differentially expressed between responders and non-responders. Moreover, many of the markers identified to be associated with PUVA and IFNα resistance, were expressed not only by tumoral cells but also by the tumor microenvironment, highlighting the important role of the stroma in conferring therapy resistance in MF.

Vorinostat (SAHA), a pan-histone deacetylase inhibitor, is the FDA approved treatment for refractory CTCL. However, despite emerging information on vorinostat effect on many cancer types, there is still little knowledge on mechanism and the kinetics of gene expression, essential for its effective use in combination therapy. Time course experiments in CTCL derived cell lines, showed that vorinostat decreased T-cell receptor (TCR) signaling through inhibition of kinase phosphorylation (ZAP70, AKT). Additionally, combined concomitant administration of vorinostat and PI3K inhibitors (LY249002 and new ETP-45658) resulted in synergism and could be potentially efficacious for the treatment of CTCL. Besides, vorinostat and PIM inhibitors showed an additive effect while the use of vorinostat and HSP90 inhibitor (17-AAG) produced antagonistic reaction.

In summary, our findings bring new ideas on the molecular heterogeneity of PTCLs and suggest combination therapies using HDACi and PI3K inhibitors for the treatment of CTCLs.

RESUMEN

Los Linfomas son neoplasias derivadas de linfocitos B o T. Los Linfomas periféricos de célula T (LPCT) son un grupo de enfermedades que varían en su biología, genética, presentación clínica, respuesta a terapia y resultado. Mientras que los linfomas de célula B están relativamente bien estudiados, sólo se ha realizado una investigación limitada para elucidar la patobiología de LPCT e identificar nuevas estrategias farmacológicas. Se han usado gran variedad de aproximaciones para delinear los mecanismos responsables de la generación de los LPCT incluyendo análisis de la expresión de microARN, ARNm y proteínas. El análisis de microARN reveló una serie de microARNs que se expresaban de manera aberrante, incluyendo la disminución en los niveles de expresión de la familia de let-7, miR-10, miR-15 miR-16, miR-101, miR-29, miR-215, miR-150, miR-139, miR-126 y miR-195 que regulan las rutas implicadas en las propiedades de células troncales, respuesta a estrés, apoptosis, proliferación, angiogénesis y ciclo celular. Además, se ha identificado un grupo de LPCT con un fenotipo nulo (carecen de los marcadores de las subpoblaciones normales de células T), que expresan una firma de microARNs oncogénicos. Este grupo mostró una mayor proliferación y un enriquecimiento en la expresión de genes de las rutas asociadas a Ras y Rho.

Aún no hay disponible ningún tratamiento curativo para los pacientes con linfomas cutáneos de célula T (LCCT) y muchas de las terapias comunes consiguen la remisión sólo en un grupo de casos. Aunque rutinariamente se usan PUVA e IFNα, una gran proporción de los pacientes son resistentes al tratamiento y los factores responsables de esta resistencia son desconocidos. Con el objetivo de identificar los factores responsables de esta resistencia en pacientes con micosis fungoides (MF), se analizó la expresión génica de muestras antes del tratamiento de 29 pacientes con MF inscritos en un ensayo clínico aleatorizado usando micromatrices de ADNc. Los genes implicados en la vía de NF-κB, receptor de célula T, señalización por citoquinas y proliferación se expresan de manera diferencial entre pacientes sensibles y resistentes al tratamiento. Además, muchos de los marcadores identificados como asociados a la resistencia a PUVA e IFNα se expresaban en las células tumorales y también en el microambiente, subrayando la importancia del estroma en otorgar resistencia a la terapia en MF.

Vorinostat (SAHA), un inhibidor de desacetilasas de histonas (HDACi), es el tratamiento aprobado por la FDA contra el LCCT resistente al tratamiento. Sin embargo, a pesar de la emergente información sobre vorinostat en diferentes tipos de cáncer, aún poco se sabe sobre su mecanismo de acción y la cinética de expresión génica, esenciales para su uso eficaz en combinación con otras terapias. Los experimentos realizados a diferentes tiempos en líneas derivadas de LCCT mostraron que el vorinostat disminuye la señalización del receptor de célula T mediante la inhibición de la fosforilación de quinasas (ZAP70, AKT). Adicionalmente, la administración combinada de vorinostat e inhibidores de PI3K (LY249002 y ETP-45658) resultó en un comportamiento sinérgico y podría ser potencialmente eficaz para el tratamiento de LCCT. El vorinostat y los inhibidores de PIM mostraron un efecto aditivo mientras que el uso de vorinostat y un inhibidor de HSP90 (17-AAG) indujo una reacción antagonista.

En resumen, nuestros descubrimientos aportan nuevas ideas sobre la heterogeneidad molecular de los LCCT y sugieren la aplicación de terapias combinadas usando HDACi e inhibidores de PI3K para el tratamiento de LCCT.

ABBREVIATIONS

17-AAG	17-allylamino-geldanamycin
AITL	Angioimmunoblastic T-cell Lymphoma
ALCL	Anaplastic Large Cell Lymphoma
aRNA	Amplified RNA
ATCC	American Type Culture Collection
BCNU	Topical Carmustine
BSA	Bovine Serum Albumin
CDK	Cyclin-Dependent Kinases
CI	Combination Index
CLA	Cutaneous Lymphocyte Antigen
cMap	Connectivity Map
CNIO	Spanish National Cancer Centre
CR	Complete Remission
CTCL	Cutaneous T-Cell Lymphoma
Cy3	Cyanine 3-conjugated dUTP
Cy5	Cyanine 5-conjugated dUTP
DMSO	Dimethyl Sulphoxide
DNA	Deoxyribonucleic acid
dNTP	2'-Deoxyribonucleoside-5'-triphosphate
DSS	Disease-Specific Survival
DTT	Dithiothreitol
EBV	Epstein Barr virus
ECP	Extra-corporeal Photopheresis
EORTC	European Organisation for Research and Treatment of Cancer
FAM	6-carboxyfluorescein
FBS	Fetal Bovine Serum
FDA	U.S. Food and Drug Administration
FDC	Follicular Dendritic Cell
FDR	False Discovery Rate
FE	Feature Extraction
GEP	Gene expression profiling
GSEA	Gene Set Enrichment Analysis
H/E	Haematoxylin and Eosin
HDAC	Histone Deacetylase
HDACi	Histone Deacetylase Inhibitor
HIF-1α	Hypoxia-inducible Factor 1a
HL	Hodgkin Lymphoma
HSP	Heat Shock Protein
HTLV-1	Human T-lymphotropic virus type 1
IC50	Inhibitory Concentration 50%
ID	Inflammatory Dermatoses
IFNα	Interferon Alpha
IPI	International Prognostic Index
IRF	Interferon Regulatory Factor
iTreg	Induced Regulatory T cells

IκB	Inhibitor of Kappa B
JAK	Janus Kinase
LDH	Lactate dehydrogenase
LN	Lymph Node
MF	Mycosis Fungoides
mRNA	Messenger RNA
NF-κB	Nuclear Factor Kappa B
NHL	Non-Hodgkin Lymphoma
NK	Natural Killer Cell
NR	Non-Responders
PBMC	Peripheral Blood Mononuclear Cells
PBS	Phosphate Buffered Saline
PCR	Polymerase Chain Reaction
PD1	Programmed death-1
PI	Propidium Iodide
PI3K	Phosphatidylinositol-3-kinase
PTCL	Peripheral T-cell Lymphoma
PTCLU	Peripheral T-cell Lymphoma, Unspecified (PTCLU)
PUVA	Psoralen in combination with Ultraviolet A radiation
R	Responders
Rb	Retinoblastoma
RNA	Ribonucleic acid
rpm	Revolutions per Minute
RT	Reverse Transcription
SAHA	Suberoylanilide Hydroxamic Acid
SAM	Significance Analysis of Microarrays
SDS	Sodium Dodecyl Sulfate
SKY	Spectral Karyotyping
SOCS	Suppressor of Cytokine Signaling
SS	Sézary Syndrome
STAT	Signal Transducer and Activator of Transcription
STEM	Short Time Series Expression Miner
T_{CYT}	Cytotoxic T cell
T_{FH}	Follicular helper T cells
Th1	T helper 1 cell
Th17	T helper 17 cell
Th2	T helper 2 cell
TMA	Tissue Microarrays
TNF	Tumor Necrosis Factor
TRAF	Tumor Necrosis Factor Receptor Associated Factor
TSEB	Total Skin Electron Beam
UVA	Ultraviolet A Radiation
VEGF	Vascular Endothelial Growth Factor
WB	Western Blot
WHO	World Health Organization
ZAP70	Zeta-chain-associated Protein Kinase 70

INTRODUCTION

1 Lymphoma

Lymphoma is a type of cancer that involves the white blood cells of the immune system, called lymphocytes. Just as cancer represents many different diseases, lymphoma represents many different cancers of lymphocytes. There are many entities of lymphomas, and in turn, lymphomas are a part of the broad group of diseases called hematological neoplasms. The first description of lymphoma has been published in 1832 by Thomas Hodgkin, specifically the form bearing his name, Hodgkin lymphoma (Hellman, 1999). There are two main types of lymphoma that include Hodgkin lymphoma (HL) and non-Hodgkin lymphoma (NHL). Lymphoma is a malignant transformation of B or T lymphocytes and the most common blood cancer. It arises from abnormal growth of lymphocytes in many parts of the body, including the lymph nodes, spleen, bone marrow, blood or other organs. Although both cell types – B and T lymphocytes can develop into lymphomas, B-cell lymphomas are more common and better studied.

1.1 T cell lymphoma

The T cell non-Hodgkin´s lymphomas (T-NHL) are a group of malignancies that vary in their biology, genetics, clinical presentation, response to therapy, and outcome (Table 1). Of all cancers involving the same class of blood cells, 8% of cases are mature T cell lymphomas. Among those cases, 2% are precursor T lymphoblastic and 2% are cutaneous T cell lymphomas (Turgeon, 2005).

Table 1. WHO Classification of T-Cell Lymphomas (Cheson, 2007)

Type	Examples
Precursor	T-LBL/T-ALL
Peripheral	T-PLL
	Large granular lymphocytic leukemia
	MF/Sézary
	Peripheral T-cell lymphoma, unspecified type
	Angioimmunoblastic lymphoma
	Angiocentric lymphoma
	Intestinal T-cell lymphoma
	Subcutaneous panniculitis-like lymphoma
	Gamma-delta T-cell lymphoma
	Adult T-cell leukemia/lymphoma
	Anaplastic large cell lymphoma

Abbreviations: MF, mycosis fungoides; T-ALL, T-cell acute lymphoblastic leukemia; T-LBL, T-cell lymphoblastic leukemia; T-PLL, T-cell prolymphocytic leukemia; WHO, World Health Organization

T-cell lymphoma (TCL) accounts for about 15% of all cases of NHL in the United States, although some forms of TCL are more common in Asia and other parts of the world. There are many different types of TCL and some are extremely rare, occurring in only a few patients per year throughout the world.

1.1.1 Peripheral T-cell lymphoma

Malignancies derived from mature (post-thymic) T cells and NK cells, collectively referred to as peripheral T-cell lymphomas (PTCLs), encompass a variety of uncommon and rare diseases, altogether accounting for about 15% of all NHL on a worldwide basis. T-cell and NK-cell lymphomas demonstrate significant variations in incidence in different geographical regions and racial populations, showing higher prevalence in Asia and Central/South America than in Western countries (Rudiger et al., 2002). Human T-lymphotropic virus-1 (HTLV-1) and Epstein-Barr virus (EBV) have been observed to be associated with increased risk of PTCLs (Vose, 2008). PTCLs show great morphological diversity, and a spectrum of histological appearances can be seen within individual disease entities. These neoplasms often present an advanced stage at diagnosis, and most commonly have an aggressive clinical course requiring prompt treatment. These disorders are among the most aggressive of all lymphoid neoplasms, with only four exceptions, the mycosis fungoides (MF), the primary cutaneous anaplastic large cell lymphoma (ALCL), primary cutaneous CD4-positive small/medium-sized pleomorphic T-cell lymphoma (CSMTCL) and the large granular lymphocytic (LGL) leukemia, which have usually a more indolent course. The rarity of these tumors requires additional studies to better understand their biology and search for new therapies which may hopefully improve the dismal outcome of most patients.

Immunophenotypic markers have been less useful in the classification of T-cell lymphomas than B-cell lymphomas, as one marker is frequently shared by multiple disease entities. Additionally, the molecular pathogenesis for most T-cell lymphomas is yet undiscovered. However, the World Health Organisation (WHO) classification of PTCLs takes into account a combination of morphologic, immunophenotypic, genetic and clinical features in attempt to correlate disease entities with the normal cellular counterpart (Swerdlow, 2008). The list of entities according to the updated WHO classification is presented in Table 2.

Table 2. WHO 2008 classification of mature T/NK-cell neoplasms (Swerdlow, 2008).

Leukemic or disseminated
T-cell prolymphocytic leukemia
T-cell large granular lymphocytic leukemia
Chronic lymphoproliferative disorders of NK cells*
Aggressive NK-cell leukemia
Adult T-cell lymphoma/leukemia (HTLV1-positive)
Systemic EBV-positive T-cell lymphoproliferative disorders of childhood
Extranodal
Extranodal NK/T-cell lymphoma, nasal type
Enteropathy-associated T-cell lymphoma
Hepatosplenic T-cell lymphoma
Extranodal – cutaneous
Mycosis fungoides
Sézary syndrome
Primary cutaneous CD30+ lymphoproliferative disorders
Primary cutaneous anaplastic large cell lymphoma
Lymphomatoid papulosis
Subcutaneous panniculitis-like T-cell lymphoma
Primary cutaneous $\gamma\delta$ T-cell lymphoma*
Primary cutaneous aggressive epidermotropic CD8+ cytotoxic T-cell lymphoma*
Primary cutaneous small/medium CD4+ T-cell lymphoma*
Nodal
Angioimmunoblastic T-cell lymphoma
Anaplastic large cell lymphoma, ALK-positive
Anaplastic large cell lymphoma, ALK-negative*
Peripheral T-cell lymphoma, not otherwise specified

* designates provisional entities

The most common subtypes of mature T-cell lymphomas are peripheral T-cell lymphoma, unspecified (PTCLU), angioimmunoblastic T-cell lymphoma (AITL), anaplastic large cell lymphoma (ALCL) and cutaneous T-cell lymphoma (CTCL).

1.1.1.1 Peripheral T-cell lymphoma, unspecified (PTCLU)

Peripheral T-cell lymphoma, unspecified (PTCLU) represents the largest PTCL subtype constituting 40-50% (Savage et al., 2004). Pathologically, there is typically a diffuse atypical infiltrate of intermediate and large lymphoid cells that are CD4+, CD2+ and CD3+ but they often lack mature T-cell antigens, such as CD7. Approximately a third may be CD30+ or EBV+. Usually, PTCLU occurs in the fifth to sixth decade of life, and there is no evidence of sex

predilection. PTCLU more often presents in stage III-IV, with nodal, skin, liver, spleen, bone-marrow or peripheral blood involvement (Evens and Gartenhaus, 2004; Gisselbrecht et al., 1998; NHL-Group, 1997). PTCL can express CD30 irrespectively of anaplastic morphology as well as cytotoxic markers, including TIA1, granzyme B, perforin, CD56 and CD57 (Rudiger et al., 2002). Activation markers are often expressed, including HLA-DR, CD25 or CD71 and antigen expression may change over time (Rodriguez-Abreu et al., 2008). Most cases of PTCLU are CD4+ CD8-, prompting speculation that within the CD4+, T-helper (Th) phenotype some of the biological heterogeneity may be explained by variable expression of Th1 and/or Th2 surface chemokine receptors (Ishida et al., 2004).

Despite being classified in as a nodal PTCL in the WHO, the majority of patients have extranodal site involvement including the gastrointestinal tract, liver, bone marrow and skin (Savage, 2007). On clinical grounds, PTCLU are among the most aggressive non-Hodgkin lymphomas. The 5 year survival of patients with PTCLU is approximately 30% using standard chemotherapy (Gisselbrecht et al., 1998).

1.1.1.2 Angioimmunoblastic T-cell lymphoma (AITL)

Angioimmunoblastic T-cell lymphoma (AITL), initially described in 1970s, is an aggressive peripheral T-cell lymphoma that comprises 5-20% of peripheral T-cell lymphomas and 1-2% of all non-Hodgkin lymphomas (Dogan A, 2008; Rudiger et al., 2002). Approximately, 75% of patients are clinical stages III–IV at diagnosis and despite aggressive therapies their median survival is less than 3 years (Lachenal et al., 2007). The disease preferentially affects elderly males (male-to-female ratio 3:1, median age around 60 years). Patients present with symptoms, such as generalized lymphadenopathy (up to 90%), hepatosplenomegaly (50–79%), cutaneous rash (50%), hypergammaglobulinemia (50%), B-symptoms (70%), pleural effusion (37%) and autoimmune phenomena (20%) (Iannitto et al., 2008; Lachenal et al., 2007). Histologically, the majority of cases show regressed follicles, a polymorphous infiltrate of medium-sized lymphocytes with mild cytological atypia, Epstein-Barr virus (EBV)-positive large B blasts and characteristically expanded follicular dendritic cell meshworks encircling high endothelial venules (Dogan A, 2008). AITL usually has the phenotype of a mixture of CD4+ and CD8+ T-cells, with a CD4:CD8 ratio greater than unity. The neoplastic T cells in AITL express CD10 and sometimes BCL6, suggesting origin of germinal center (known as follicular helper T (T_{FH}) cells) (Dunleavy and Wilson, 2007; Kim et al., 2004; Pautier et al., 1999). T_{FH} derivation is also supported by demonstration of CXCL13 expression, a chemokine produced in high quantities by normal T_{FH} cells following costimulation via the CD28 and T cell receptors (Dupuis

et al., 2006a; Kim et al., 2004). Additional markers of normal T_{FH} cells, including CXCR5, CD154, programmed death-1 (PD-1), a member of the CD28 costimulatory membrane receptor family, and SLAM-associated protein (SAP), a cytoplasmic adaptor protein were demonstrated (Krenacs et al., 2006; Roncador et al., 2007). Moreover, polyclonal plasma cells and CD21+ follicular dendritic cells were also seen (Jaffe, 2001). Clonality studies demonstrated a monoclonal rearrangement of the β-chain of the T-cell receptor (TCR) in the majority of cases.

1.1.1.3 Anaplastic large cell lymphoma (ALCL)

Anaplastic large cell lymphoma (ALCL) was first recognized by Stein *et al* in 1985, who reported the consistent expression of the Ki-1 antigen (later designated as CD30) in tumors with frequent cohesive proliferation of large pleomorphic cells of T- or null-cell lineage (Stein et al., 1985). CD30 is a transmembrane receptor and a member of tumor necorosis factor superfamily that is normally expressed by activated T cells (Al-Shamkhani, 2004). ALCL occurs as two distinct clinical entities, as a widespread systemic disease, or as a localized cutaneous disease. When ALCL presents in the cutaneous form it is called primary cutaneous anaplastic large cell lymphoma. Systemic ALCL comprises 2% to 8% of non-Hodgkin lymphomas in adults and 10% to 15% of these lymphomas in children (Kadin et al., 1986). ALCL is heterogenous and includes two subtypes: neoplasms that aberrantly express ALK (anaplastic lymphoma kinase) and others that are ALK negative. ALK, also known as CD246, is a tyrosine kinase that belongs to the insulin receptor superfamily (Pulford et al., 2004). The ALK+ ALCLs represent approximately 50% to 80% of all ALCLs and usually affects children and young adults and has striking male predominance. The ALK- ALCLs is more commonly found in older patients over age 60. It is recognized that patients with ALK+ have a favorable prognosis compared with other types of T-cell lymphoma, including ALK- ALCL (Benharroch et al., 1998; Gascoyne et al., 1999). The majority of ALK+ ALCL cases present as advanced stage (III or IV) systemic disease with generalized lymphadenopathy and extranodal involvement (Gascoyne et al., 1999). The immunophenotype of ALK- ALCL shares many features with ALK+ ALCL (Falini et al., 1999; Saffer et al., 2002). In T-cell ALK- ALCLs, an abberant T-cell immunophenotype is common, and these neoplasms are commonly negative for pan-T-cell antigens (e.g. CD3 and T-cell receptors) (Bonzheim et al., 2004). These tumors usually have a high proliferation rate and express activation markers, similar to ALK+ ALCL. However, in contrast to ALK+ ALCL, many ALK- ALCL express BCL-2 (Rassidakis et al., 2001) and can be positive for CD15 and Epstein-Barr virus (Herling et al., 2004).

1.1.1.4 Cutaneous T-cell lymphoma (CTCL)

One of the most common forms of T-cell lymphoma is cutaneous T-cell lymphoma (CTCL) which actually describes many different disorders with various signs and symptoms, outcomes, and treatment considerations. Mycosis fungoides (MF) is the most common type of CTCL and is an indolent T-cell lymphoma attributed to the clonal expansion of skin-homing, epidermotropic CD4+ helper T-cells (Willemze et al., 1997). The term "mycosis fungoides" originally referred to the mushroom-like nodules in the tumor stage of disease. MF accounts for approximately 1% of all NHL and 65% of all lymphomas originating in the skin, with a median age of presentation of 57 years and a male/female ratio of 2:1 (Edelson, 1980; Kim et al., 2003). The incidence is estimated at 0.36-0.90 cases per 100,000 per year and is rising (Bradford et al., 2009; Chuang et al., 1990; Weinstock and Gardstein, 1999). However, onset may occur at any age, from infancy upwards. MF present with patch type skin lesions (Figure 1A), plaque type lesions (Figure 1B) and tumor type lesions (Figure 1C). The Sézary syndrome (SS), a more aggressive form of cutaneous T-cell lymphoma, also defined as the leukemic variant of MF, is characterized by erythroderma and measurable presence of malignant pleomorphic T-lymphocytes with convoluted nucleus in the peripheral blood as well as skin involvement.

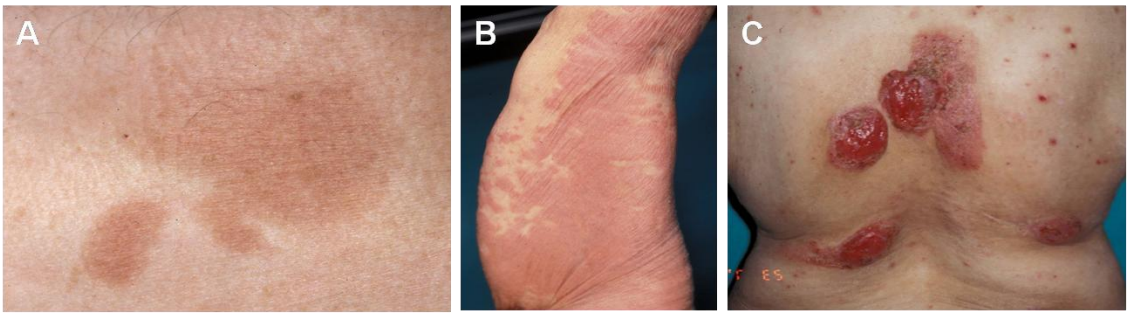

Figure 1. Clinical manifestation of MF

A) Patch stage lesions are oval or ring-shaped (annular) pink dry patches on covered skin; **B)** MF plaques are infiltrated lesions due to epidermal hyperplasia or significant neoplastic lymphoid infiltrate;
C) Tumor-stage CTCL may arise from patches, from plaques or de novo. Lesions are typically erythematoviolaceous, exophytic, mushroom-shaped tumors.

Since symptoms of early MF bear many resemblances to common inflammatory dermatoses, it is often misdiagnosed as chronic contact dermatitis, atopic dermatitis, or psoriasis. The malignant T cell of MF expresses surface markers characteristic of a skin-homing memory T cell, such as CD2, CD3, CD4, CD5, CD45RO and cutaneous lymphocyte antigen (CLA). The MF/SS malignant cells frequently lack CD7, CD26, CD49 and CD60 expression (Kim et al., 2005). In the early stages of MF a clonally expanded population of T cells can be detected by analysis of T-

cell-receptor-γ rearrangement (Wood et al., 1994). With the progression of the disease the number of the normal $CD8^+$ lymphocyte population in skin lesions and in the peripheral blood decreases (Heald et al., 1994; Hoppe et al., 1995; Lu et al., 2002). Cytotoxic ($CD8^+$) T lymphocytes mount an antitumor response in cutaneous T-cell lymphoma and may induce apoptosis by the expression of Fas ligand (FasL) and the engagement of cell-surface Fas (CD95) on the malignant cells. This is consistent with the decrease in Fas expression within the CD8+ T-cell population in the later stages of MF (van Doorn et al., 2002). Depending on the stage of the disease, different cytokine profiles have been identified. In the early patch stage of MF the Th1 cytokines dominate whereas in the late stages of the disease as well as in SS a bias towards a Th2 profile has been identified (Saed et al., 1994). The malignant T cells of MF/SS express such cytokines as IL-4, IL-5 and IL-10, which are representative for Th2 cytokines and fail to display IL-12 and IFN-γ - characteristic of Th1 (Vowels et al., 1994). Both, neoplastic MF cells and reactive T cells have been found to express abundant amounts of CCR4, CXCR3, CXCR4 and CCR7 in the early patch and plaque stages of MF. Involvement of the chemokine receptors – CCR4 and CXCR3 – in skin homing of T cells in early MF and its loss is associated with the progression of the disease (Lu et al., 2001).

Staging of patients with MF and SS is based on the tumor-node-metastasis system (Bunn and Lamberg, 1979), though a new WHO – EORTC classification has recently been developed on the base of the EORTC classification for cutaneous lymphomas (Willemze et al., 1997) and the WHO classification for nodal lymphomas (Jaffe ES). The new consensus WHO – EORTC classification reconciles these two systems, and takes into account different clinical behaviors of primary cutaneous lymphomas as well as their distinct histological, phenotypical and molecular features as compared to nodal counterparts. This staging expands the traditional staging system to include a B rating on the basis of molecular evidence of leukemic involvement (Sausville et al., 1988; Vonderheid et al., 2002). Staging of CTCL patients is summarized in Table 3. The most frequent forms of CTCL, MF proceeds slowly (5-20 years) but leads mostly to death, which is often caused in the late phase of CTCL by rapidly growing, ulcerating tumors and immune disorders. In addition to generalized erythroderma, patients with SS have leukemic T cells in the blood and life expectancy is generally shorter (3 years) than it is for patients with MF.

Table 3. TNMB staging system for CTCL - ISCL/EORTC revision (Olsen et al., 2007).

	Clinical signs
T: Tumor stage (skin)	
T1	Patches/plaques < 10% body surface area
T2	Patches/plaques ≥ 10% body surface area
T3	Tumors (rounded or dome-shaped lesions ≥ 1cm in diameter)
T4	Erythroderma (≥ 80% of body surface area affected)
N: Nodal stage	
N0	No clinically abnormal peripheral lymph nodes, pathological findings not CTCL
N1	Clinically abnormal (palpable) peripheral lymph nodes, pathological findings not CTCL
N2	No clinically abnormal peripheral lymph nodes, pathological findings positive for CTCL
N3	Clinically abnormal (palpable) peripheral lymph nodes, pathological findings positive for CTCL
M: Visceral organs	
M0	No visceral organ involvement
M1	Visceral involvement with pathological confirmation
B: Peripheral blood	
B0	Atypical circulating cells not present (≤ 5%)
B1	Atypical circulating cells present (5% or more)
B2	High blood tumor burden: ≥ 1000/μl Sézary cells with positive clone; CD4/CD8 ratio ≥ 10, aberrant expression of normal T-cell markers, molecular evidence of clonality, or chromosomal abnormality in a T-cell clone

Stage	**T**	**N**	**M**	**B**
IA	1	0	0	0-1
IB	2	0	0	0-1
II	1-2	1-2	0	0-1
IIB	3	0-2	0	0-1
III	4	0-2	0	0-1
IIIA	4	0-2	0	0
IIIB	4	0-2	0	1
IVA_1	1-4	0-2	0	2
IVA_2	1-4	3	0	0-2
IVB	1-4	0-3	1	0-2

1.1.2 Biological and Molecular Prognostic Factors in T-cell lymphoma

Apart from the pathologic characterization according to different cytokine and chemokine expression by PTCLs, several other biological and prognostic factors have been identified in these types of lymphomas. Interestingly, a proliferation signature has recently been reported to correlate with an aggressive clinical course (Cuadros et al., 2007) and EBV has been proposed as a negative prognostic factor in PTCL (Cheng et al., 1993; Dupuis et al., 2006b; Kluin et al., 2001). The relationship between the overexpression of p53 and Ki-67 has also been

suggested as representative of high proliferation and subsequently worse prognosis. Consistently, elevated Ki-67 expression, EBV status and CD15 staining were related to worse outcome in PTCLU patients (Went et al., 2006). Recently, CD26 and a positive regulatory domain 1 (PRDM1) have emerged as unfavorable prognostic factors in PTCL (Carbone et al., 1994; Carbone et al., 1995). PRDM1 is upregulated in PTCLU, ALCL and in T/NK lymphomas and is characteristically lost in AITL. High CYP3A4 expression was found to be significantly associated with lower complete remission rate (Rodriguez-Antona et al., 2007). In contrast, PTCL patients with tumors expressing a CD57 or CD4+/CD8- profile showed a tendency towards a more favorable outcome (Bekkenk et al., 2003; Kojima et al., 2004).

In addition, the factors reported to herald a poor prognosis in MF include: age $\geq$ 60, elevated LDH (Diamandidou et al., 1999), elevated soluble interleukin-2 receptor levels (Wasik et al., 1996), a low percentage of CD8+ tumor infiltrating lymphocytes (Hoppe et al., 1995), extent of skin involvement in patients with T3 disease (Quiros et al., 1996), T-cell clonality within the cutaneous infiltrate (Guitart et al., 2003), an identical T-cell clone in the skin and peripheral blood (Berth-Jones, 2005), and T-cell clonality in dermatopathic lymph nodes (Bakels et al., 1993). Moreover, increased expression of cell death regulating genes, such as MCL-1 and inactivation of cell death promoting BAD and BAX proteins have been observed in the course of MF/SS progression.

Several predictors related to therapy outcome have been identified. These include predictors of chemotherapy efficacy, such as the expression of TOPO2-alpha and other detoxifying agents including GST-pi, which are related to resistance to anthracycline and alkylating agents therapy in PTCL (Rodriguez et al., 2008). Interestingly, p53+ patients overexpressing p-glycoprotein, were found to be resistant to most major drugs effective in the aggressive lymphomas, such as anthracyclins, etoposide or vincristine (Dalton et al., 1989; Pescarmona et al., 2001). In the case of ALK+ ALCL, the presence of less antiapoptotic active mechanisms (BCL-2, BCL-xL) than in other subtypes may explain the better prognosis with standard chemotherapy (Rassidakis et al., 2003).

1.1.3 Gene Expression Profiling of T-cell lymphoma

The molecular pathogenesis of most PTCLs is poorly understood. One of the disadvantages of genomic profiling studies is related to the lack of suitable cell lines in most of the aggressive PTCL. Thus most studies have been performed on cutaneous T-cell lymphoma (CTCL). Although there is a great overlapping between entities some authors have found differences between

some PTCL, such as AITL and ALCL (de Leval et al., 2007; Thompson et al., 2005). PTCL have been the subject of a limited number of GEP studies. In particular, our group (Tracey et al., 2003), Lamant (Lamant et al., 2007) and Leval (de Leval et al., 2007) focused on MF, ALK-positive and –negative ALCLs, and AITL, respectively.

Peripheral T-cell lymphoma, unspecified (PTCLU): There are several studies aiming at identification of different molecular subgroups within PTCLU based on gene expression profile. They define discrete subgroups based on differences in expression levels of genes related to NF-κB (Martinez-Delgado et al., 2005) and IFN/JAK/STAT pathways (Ballester et al., 2006). The latter study allowed the division of PTCLU into three groups named U1, U2, U3 based on gene expression signature and prognosis. Additionally, enrichment of CD8+ T cell signature and a repertoire of cytotoxic molecules (perforin, granulysin, granzymes and cathepsins) have been lately suggested in PTCLU (Iqbal et al., 2009).

Angioimmunoblastic T-cell lymphoma (AITL): Recent gene-expression profiling studies suggested that T_{FH} (follicular helper T cells) may be the cell of origin of AITL (de Leval et al., 2007; Piccaluga et al., 2007). T_{FH} cells are CXCR5+/CCR7- T cells, located in germinal centres, which provide help to B cells in cellular immune responses, through the acquisition of other molecules, such as ICOS (immune costimulatory molecule), CD40L and IL-21 (King et al., 2008). Among the genes upregulated in T_{FH} cells are CXCL13, BCL6 and programmed death-1 (PD1) (Kim et al., 2004). PD1 and CXCL13 are particularly useful markers in the diagnosis of AITL, helping to differentiate this condition from lymphoid hyperplasias and PTCLU (Dorfman et al., 2006; Dupuis et al., 2006a). In addition, gene expression profiling revealed a strong microenvironment imprint with overexpression of B cell and follicular dendritic cell-related genes, chemokines, and genes related to extracellular matrix and vascular biology (de Leval et al., 2007). Different cytokine and chemokine expression analysis demonstrated a T_{H1} phenotype of AITL characterized by expression of T_{H1} related markers, CXCR3, TNF receptor, OX40 and CXCL13 (Ohshima et al., 2004; Tsuchiya et al., 2004). Recently, AITL classifier has been described, which included B-cell, a follicular dendritic cell (FDC) and cytokine signatures confirming previously published data (Iqbal et al., 2009).

Anaplastic large cell lymphoma (ALCL): Recently, differences in molecular signature of ALCL with or without ALK expression have been established. Overexpression of four genes CCR7, CNTFR, IL22 and IL21 were related to ALCL ALK- while BCL6, PTPN12, CEBPB and SERPINA1 genes were upregulated in ALCL ALK+ (Thompson et al., 2005). With regards to the expression

of cytokines and chemokines, ALCL have been associated to a T_{H2} phenotype. Neoplastic cells of these lymphomas usually show expression of CCR4 and CCR3, but are negative for the T_{H1}-associated chemokine receptor CXCR3 (Ohshima et al., 2004; Tsuchiya et al., 2004). Expression of other genes, such as IL13R, FOS and JUNB also suggests association of ALCL with T_{H2} differentiation. The newly reported ALCL classifier by Iqbal and colleagues (Iqbal et al., 2009) includes ALK, TNFRSF8 (CD30), MUC1, T_H17-cell associated molecules (IL17A, IL17F, RORγ) and immunoregulatory cytokines/receptors modulating STAT3 (IL26, IL31RA) and JAK3 activation (IL9).

Cutaneous T-cell lymphoma (CTCL): Several studies have indicated the importance of NF-κB activation in CTCL (both in cell lines as well as patient samples) demonstrating the involvement of p50 and RELA/p65 (Izban et al., 2000). Besides, our group showed that a deregulation of TNF and PI3K-PTEN-AKT signaling pathways impairs apoptosis of malignant cells in MF (Tracey et al., 2003). In addition, it has been suggested that BCL2 and BAX play a role in pathogenesis of MF (Dummer et al., 1995; Nielsen et al., 1999). Other members of BCL2 gene family, such as apoptosis-inhibiting members: BCL-xL and MCL1 and apoptosis-promoting: BAD and BAX are expressed in CTCL cell lines as well as cutaneous lesions. The increase of MCL1 expression was observed in the later-stage skin lesions and associated with the disease progression and could be implicated in resistance of CTCL cells to some anti-cancer drugs (Zhang et al., 2003). The study of the role of oncogenes in the pathogenesis of MF revealed an increased protein expression of K-RAS in tumor cells in the late stages of MF (Tosca et al., 1991).

1.1.4 MicroRNAs in T-cell lymphoma

Mature microRNAs (miRNAs) are 19-24 nucleotide non-coding single-stranded RNA molecules which regulate the expression of target genes through perfect (in plants) or imperfect (in animals) binding to the 3'-UTR (un-translated region) and possibly 5'-UTR (Lytle et al., 2007) of mRNA. miRNAs are processed by Drosha and Dicer (Wiemer, 2007) and cause translation repression or mRNA degradation of their target genes. There are currently over 600 human miRNA sequences annotated in the miRBase database (http://microrna.sanger.ac.uk/sequences/), although it is believed that the true figure is closer to one thousand (Bentwich et al., 2005; Berezikov et al., 2005). Despite the relatively small number of miRNAs, because a single miRNA can target several hundred genes, and conversely a single target gene can cooperatively bind to multiple miRNAs (Lewis et al., 2003), it is currently believed that between 10% and 30% of all human genes are a target for miRNA regulation (John et al., 2004; Lewis et al., 2005). miRNAs are expressed in a tissue-/cell-specific

manner, some expressed ubiquitously whilst others appear to be restricted to single cell types (Landgraf et al., 2007).

There is now compelling evidence that dysfunctional expression of miRNAs is a common feature of malignancy (Calin and Croce, 2006). Aberrant expression of specific miRNAs has now been associated with all cancer types including solid and haematopoietic tumors. Germline and somatic mutations in miRNAs or polymorphisms in the mRNAs targeted by miRNAs may also contribute to cancer predisposition and progression (Calin and Croce, 2007). Moreover, it has been suggested that miRNA expression profiling can distinguish cancers according to diagnosis and developmental stage of the tumor to a greater degree of accuracy than traditional gene expression analysis (Lu et al., 2005). miRNAs are proposed to play a direct role in oncogenesis as they can function as both oncogenes (e.g., miR-155 and members of miR-17-92 cluster) and tumor suppressor molecules (e.g., miR-15a and miR-16). There are currently understood to be at least three mechanisms whereby miRNAs are de-regulated in cancer; (i) chromosomal lesions at regions encoding miRNAs, (ii) defects in the miRNA biosynthetic pathway machinery and (iii) epigenetic regulation (Lawrie, 2008).

Little research has been carried out to study the direct role of miRNAs in T cell lymphomas. Recently the T lymphoma causing murine leukemia virus (MLV) was used in a screen to identify common proviral integration sites and found a high density of integrations upstream of the miR-106a cistron (Lum et al., 2007). The same group has shown that the miR-17-92 cluster was also a common integration site (Wang et al., 2006). Additionally, miRNAs have been found to be encoded in the avian T-cell lymphoma causing virus, Marek's disease virus (MDV). EBV-associated microRNAs were recently profiled in a peripheral T cell lymphoma case, which were consistent with a type II latency infection (Jun et al., 2008). So far no miRNA profiling has been performed for T-cell lymphoma.

1.1.5 Clinical Management of T-cell lymphoma

There is no consensus as to the appropriate standard therapy for PTCL. The optimal therapy for most PTCL is an area of controversy for multiple reasons including the rarity of the diseases, the difficulty to make a rapidly and definite histopathologic diagnosis, their variable clinical course with a number of more unusual presentation and different clinical "syndrome" which they can present, and especially for the lack of randomized clinical trials that focus specifically on T-cell lymphoma. Indeed, the problem of T-cell lymphoma has been defined "the next, and largely unexplored, frontier in lymphoma management" (Armitage et al., 2004)

and undoubtedly is one of the most challenging problems for clinicians. In case of CTCL there is no cure, so palliation and symptom control comprise current treatment objectives. Although partial and complete remission can be achieved, subsequent relapses are common and curative therapy remains elusive (Duvic et al., 2001; Kim et al., 2005; Olsen et al., 2001; Prince et al., 2003; Querfeld et al., 2005). Prognosis of PTCL is generally poor when treated with conventional chemotherapy regimens used in B-cell aggressive lymphomas. Clearly, better therapeutic regimens are needed to improve the long-term outcome of these patients. The present treatment modalities include:

Skin-directed therapies: Skin-directed therapies are the appropriate first-line treatment for early stages (I-IIA) CTCL patients who have limited patch/plaque disease and include:

- Topical corticosteroids
- Topical mechlorethamine (nitrogen mustard)
- Topical carmustine (BCNU)
- Topical retinoids/rexinoids
- Psoralen plus UVA irradiation (PUVA)
- Total skin electron beam therapy (TSEB) and
- Superficial X-irradiation

Psoralen and ultraviolet A photochemotherapy (PUVA) is one of the treatments analyzed in the presented work hence its use will be briefly explained. PUVA combines the oral or topical administration of psoralen (to sensitize skin) with exposure to UVA light. Psoralens are tricyclic aromatic compounds which have phototherapeutic activities. The mechanism of action is not precisely known, however generation of reactive oxygen species, inhibition of DNA synthesis and mitochondrial dysfunction caused by opening of the permeability transition pore have been proposed as possible mechanism of apoptosis generation (Caffieri et al., 2007; Parrish et al., 1974; Potapenko, 1991; Yoo et al., 1996).

At present, PUVA is used for the treatment of several hyperproliferative skin diseases, such as MF (Stern, 2007). The clinical benefit of PUVA is well established and response rates of 79–88% in stage IA and 52–59% in stage IB patients have been reported. However, relapse is frequent after treatment suspension, resulting in frequent re-treatment leading to high total cumulative UVA dose and increased risk of skin cancers.

Systemic therapy: Patients with refractory early-stage MF or more severe disease stages (IIB-IV) are likely to receive systemic therapies, either alone or in combination with skin-directed therapies (Trautinger et al., 2006). These agents comprise the main treatment categories:

- Chemotherapy
- Extra-corporeal photopheresis (ECP)
- Biological response modifiers
- Immunotherapy

CHOP-type (cyclophosphamide, doxorubicin, vincristine and prednisone) chemotherapy is considered as the standard therapy for PTCLs, however, with the notable exception of ALK+ ALCL, outcomes utilizing anthracycline-based regiments has been uniformly disappointing (Fisher et al., 1993). In CTCL CHOP regimen demonstrated only moderate anti-tumor activity (Bagot, 2008).

ECP in the treatment of CTCL isolates the malignant cells in the blood, irradiates them and then reintroduces into patients for potential immunization against disease. Response rates of 63% were reported in CTCL, however, the high cost and availability limit its use.

Biological response modifiers such as interferon alpha (IFNα), retinoids, rexinoids, and denileukin diftitox, alemtuzumab, have shown considerable activity in the treatment of advanced CTCL. IFNs are cytokines that exhibit pleiotropic cellular effects, including immunomodulatory, anti-proliferative and pro-apoptotic effects (Stark et al., 1998). IFNα has a stimulatory effect upon natural killer cells and macrophages, inducing them to produce IFNγ and IL1 in addition to stimulating their cellular cytotoxicity and inducing cellular proliferation of T-lymphocyte effector cells (Jonasch and Haluska, 2001). Direct cytostatic effects, induction of apoptosis and inhibition of cell growth are observed in tumor cells in response to IFNα, with targeting of specific components of the cell cycle control apparatus such as c-MYC, Rb, CyclinD3, CDC25A and BCL2 (Kumar and Atlas, 1992; Melamed et al., 1993; Resnitzky et al., 1992; Tiefenbrun et al., 1996) as well as other cell cycle regulators such as p15, p21, p27 (Sangfelt et al., 1999) and IFN Regulatory Factor (IRF) transcription factors (Xie et al., 2003). IFNα monotherapy has been reported to produce clinical response in over 50% of patients (Olsen, 2003), while others have reported overall response rates of 45–74% and complete response rates in 10–27% of patients (Stadler, 2003). When IFNα is used in combination with PUVA, both response and response duration are improved (Chiarion-Sileni et al., 2002; Rupoli et al., 2005), with recent studies reporting overall response and complete response rates of

98% and 84%, respectively. A randomised study of IFNα and/or PUVA in early-stage MF suggests that the response rates are similar, but the cumulative dose is lower and the duration of response is prolonged for the combined regimen (Stadler, 2003).

Homozygous and hemizygous deletions of the IFNα gene (Colamonici et al., 1992), alterations in some of the IFNα response genes, such as well known members of the JAK/STAT signalling pathway (STAT1, STAT2, STAT3, SOCS1 or IFNR) (Abramovich et al., 1994; Gamero et al., 2004; Landolfo et al., 2000; McKendry et al., 1991; Roman-Gomez et al., 2004; Sakamoto et al., 1998; Sun et al., 1998; Yang et al., 1998), changes in membrane microdomain gene expression (Tracey et al., 2002) and infection by Epstein Barr Virus (Nanbo et al., 2002) have all been implicated in IFNα resistance. However, these studies are largely confined to in vitro studies and have therefore not been able to explain the frequent clinical phenomenon of IFNα resistance.

Denileukin diftitox (Ontak) is a fusion molecule of IL-2 to diphtheria toxin and has been shown to have efficacy in patients with CTCL. Limited reports have also demonstrated tumor responses to denileukin diftitox in relapsed PTCLs. IL-2 receptor (IL-2R) is a marker of T-cell differentiation and the CD25 subunit of this receptor is expressed in a subset of patients with PTCLU and CD30+ ALCL. Denileukin diftitox targets cells expressing the IL-2R, interrupts protein synthesis and precipitates cell death (Smith and Wilson, 2003). The US Food and Drug Administration have granted approval for its use in refractory CTCL tumors expressing the IL-2R (Olsen et al., 2001).

There are several novel agents – including interferons (Armitage and Coiffier, 2000), denileukin diftitox (Di Venuti et al., 2003), campath-1H (Enblad et al., 2004), cyclosporine (Cooper et al., 1993), pentostatine (Mercieca et al., 1994) and cladribine (Saven et al., 1992), which have shown some benefit in relapsing patients and will need to be carefully studied in order to be optimally incorporated in front line treatments. At present, some ongoing European trials are investigating the role of Campath-1H (and anti-CD52 monoclonal antibody) in combination (contemporary or sequentially) with chemotherapy using low dose of the monoclonal antibody. Moreover, several histone deacetylase inhibitors are in clinical development and suberoylanilide hydroxamine acid (vorinostat) has been approved in US for treatment of aggressive and refractory CTCL (Vorinostat will be discussed in section 1.3.1).

Although infrequent, these types of lymphomas are behind the other lymphomas in both molecular biology knowledge and treatment results. Only recently international efforts are

putting into motion both biological studies and targeted new treatments for this type of lymphomas.

1.2 Epigenetics and Cancer

Epigenetics is the study of heritable changes in gene expression that are not due to any alteration in the DNA sequence (Feinberg, 2008; Fraga et al., 2005a). Epigenetic modification can be viewed as "on" and "off" switches for gene expression, where shutting down tumor-suppressor genes or activating oncogenes can lead to dysregulated cellular proliferation and apoptosis (Mack, 2006).

Histones are a family of proteins that interact with DNA, resulting in DNA being coiled around a histone octameric core within the nucleosome. Histone deacetylase (HDAC) enzymes catalyse the deacetylation of lysine residues in the histone N-terminal tails and are also found in large multiprotein complexes with transcriptional corepressors. The addition of an acetyl group to histones (acetylation) loosens this binding and allows expression of tumor suppressor genes. Conversely, deacetylation can result in tumor formation. HDACs are enzymes that regulate chromatin structure and function through the removal of acetyl groups from lysine residues of core histones, facilitating a closed chromatin state and transcriptional repression. The opposing activities of HDAC and histone acetyltransferases regulate histone acetylation and chromatin architecture (Bolden et al., 2006). Human HDACs are classified into four classes based on their similarity to yeast factors, with 18 different HDACs identified to date (Table 4) (Bhalla, 2005; Gregoretti et al., 2004). Class I HDACs are primarily detected in the nucleus, while Class II and IV HDACs shuttle between the cytoplasm and nucleus (Bolden et al., 2006; Dokmanovic et al., 2007).

The organization of chromatin into either a relatively open or condensed form impacts on key molecular processes such as transcription, DNA repair, recombination and replication, with clear evidence that gene expression controlled by epigenetic changes can play an important role in cancer onset and progression (Baylin and Ohm, 2006; Lund and van Lohuizen, 2004). Increased acetylation of histones H3 and H4 is associated with open and active chromatin and increased transcription, while deacetylation of these histone residues is associated with condensed chromatin and transcriptional repression (Rice and Allis, 2001). Alteration in the balance of activity between HDACs, in association with aberrant gene transcription, has been observed in cancer cells in both hematological and solid malignancies (Cress and Seto, 2000;

Jones and Saha, 2002; Redner et al., 1999; Timmermann et al., 2001). Moreover, the finding that global hypoacetylation of histone H4 is a common hallmark of human cancer adds to the rationale that HDACs are important potential therapeutic targets in anticancer therapy (Fraga et al., 2005b). There is a growing evidence that epigenetic changes play a crucial role in cancer and it has been widely recognized in recent years that HDAC are promising targets for therapeutic interventions intended to reverse aberrant epigenetic states associated with cancer (Lund and van Lohuizen, 2004; Rasheed et al., 2007).

Table 4. Known classes of histone deacetylases

Class	Enzyme
I	HDAC 1, HDAC 2, HDAC 3, HDAC 8
IIa	HDAC 4, HDAC 5, HDAC 7, HDAC 9
IIb	HDAC 6, HDAC 10
III	SIRT 1,2,3,4,5,6,7
IV	HDAC 11

HDAC: Histone deacetylase; SIRT: Sirtuin

1.3 Biological pathways as targets for new therapies in PTCL

1.3.1 Histone Deacetylase Inhibitors

Histone deacetylase inhibitors (HDACi) are a new class of chemotherapeutic drugs shown in preclinical studies to have potent anticancer activities (Bolden et al., 2006; Rasheed et al., 2007). Although it is not yet clear exactly how HDACi achieve therapeutic anticancer responses, these agents induce rapid histone hyperacetylation, chromatin remodeling and can activate or repress genes regulating apoptosis, proliferation, differentiation, angiogenesis, and immune responses (Figure 2) (Bolden et al., 2006). However, the exact pathways that lead to the anticancer effects observed in various tumor types remain to be fully elucidated. Despite encouraging in vitro activity, early compounds derived from natural products, such as depudecin, trapoxin, and trichostatin, have limited in vivo antineoplastic activity, partly because of poor retention, instability, and toxicity. The therapeutic action of HDACi in CTCL patients may relate to induction of histone hyperacetylation, altered gene expression, and subsequent apoptosis of malignant T cells (Zhang et al., 2005), although other effects such as loss of cell proliferation and decreased angiogenesis may also play a role (Duvic et al., 2007).

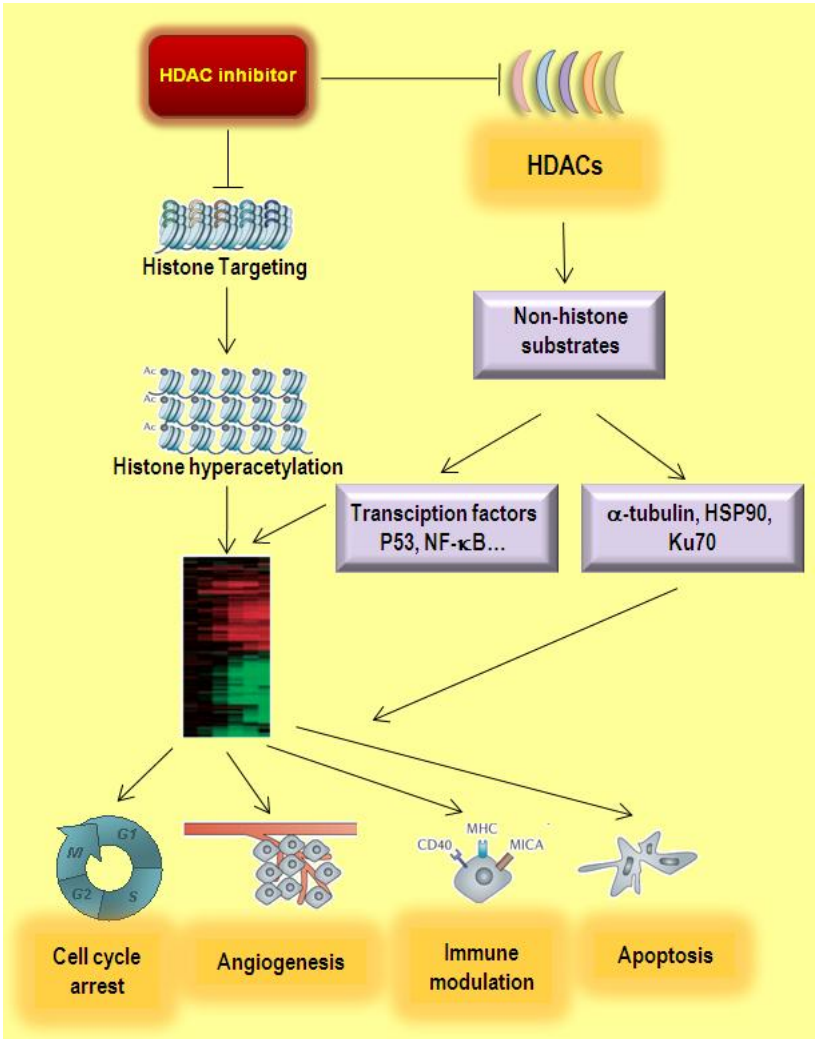

Figure 2. Effects of histone deacetylase inhibition

Vorinostat (suberoylanilide hydroxamine acid, SAHA) is the first HDACi in its class to be approved by the FDA for cancer therapy (Mann et al., 2007). Vorinostat is a pan-HDACi, which inhibits the enzymatic activity of histone deacetylases (HDACs) resulting in the accumulation of acetylated histones and nonhistone proteins. Vorinostat causes caspase-dependent apoptotic cell death, caspase-independent autophagic cell death and cell cycle arrest of a wide variety of transformed cells (Marks et al., 2001; Marks and Dokmanovic, 2005; Marks and Jiang, 2005; Shao et al., 2004). Modulated expression of 2-10% of genes in malignant cells has been described (Butler et al., 2002; Gray et al., 2004; Marks et al., 2004; Mitsiades et al., 2004; Richon et al., 2000). CDKN1A (p21, WAF1/CIP1) is a commonly induced gene following vorinostat treatment and could be related to the arrest in G1 phase of the cell cycle (Richon et al., 2000), while cyclin D1, ERBB2 and thymidylate synthase belong to genes repressed following vorinostat treatment (Gui et al., 2004). Other targets of vorinostat include transcription factors (MyoD, E2F-1, Smad 7, TF11E and GATA1), tumor suppressors (p53, Rb),

as well as factors involved in cell motility (α-tubulin), apoptosis (Bcl-2 family), angiogenesis (HIF-1α) and reactive oxygen species (thioredoxin) (Bolden et al., 2006; Drummond et al., 2005; Johnstone and Licht, 2003; Marks and Dokmanovic, 2005; Marks and Jiang, 2005; Rosato et al., 2003; Shao et al., 2004; Ungerstedt et al., 2005). In addition, HDACi cause hyperacetylation of nonhistone protein, such as chaperone protein Hsp90, Raf, AKT, ErbB2, and Bcr-Abl, thus achieving antitumor effects (Kim et al., 2006b). Such a multiplicity of targets could partly explain the efficacy of vorinostat as an anticancer agent. However, the exact mechanism, the kinetics of gene expression and players involved in resistance to this drug are still unknown.

Clinical trials in patients with refractory CTCL demonstrate an objective overall response of 30% (Duvic et al., 2007) following vorinostat treatment. Presently, vorinostat is in clinical trials both as monotherapy and in combination with various anticancer drugs. Vorinostat has been reported to have synergistic or additive effects when used with several anticancer agents, including anthracyclines, fludarabine, flavopiridol, imatinib, bortezomib, isotretinoin, antiangiogenic agents and TNFS10 (Johnstone and Licht, 2003; Marks et al., 2004). At present, there are 137 clinical trials registered for this drug (www.cancer.gov). In 41 trials vorinostat is used as a monotherapy, while in as many as 96 clinical trials, vorinostat is used in combination with other therapies. The conversion from mono- to combination- therapy clinical trials is heralding future applications of specific HDACi. However, in order to achieve the desired effect following administration of combinatorial drug therapies, the exact mode of action as well as the time at which expression of particular genes is altered needs to be identified.

1.3.2 Heat Shock Protein Inhibitors

Heat shock proteins (HSPs) were originally defined according to their increased expression in response to a cellular insult, such as elevated temperature, heavy metals and oxidative stress (Hartl and Hayer-Hartl, 2002; Young et al., 2004). Most, but not all HSPs are molecular chaperones that are organized into families according to their molecular size or function, including Hsp100, Hsp90, Hsp70, Hsp60, Hsp40 and small HSPs. Chaperones are required for essential housekeeping functions, such as de novo protein folding during nascent polypeptide-chain synthesis, translocation of proteins across membranes, quality control in the endoplasmic reticulum, and normal protein turnover as well as regulation of post-translational protein homeostasis (Figure 3) (Wegele et al., 2004; Whitesell and Lindquist, 2005).

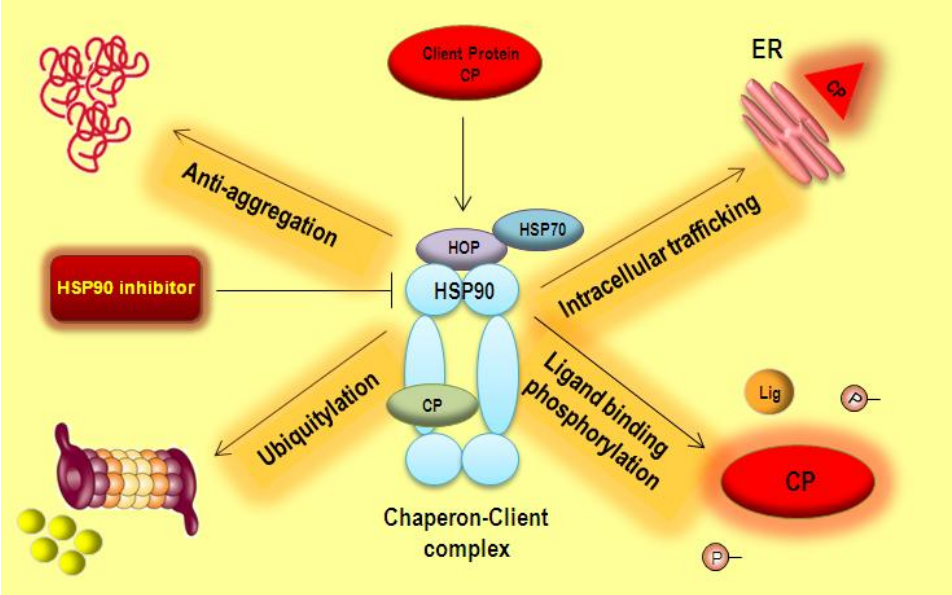

Figure 3. Participation of molecular chaperones in regulating many aspects of post-translational protein homeostasis

Hsp90 is an abundant molecular chaperone which constitutes 1-2% of total cellular protein. Hsp90 and other family members control intracellular trafficking and folding of diverse cellular proteins, particularly those involved in signal transduction, cell cycle regulation, and survival decisions (Garrido et al., 2001; Richter and Buchner, 2001). However, increased Hsp90 activity may also allow survival of genetically unstable cancer cells allowing escape from the apopototic death and overexpression of Hsp90 has been reported in many cancers (Ferrarini et al., 1992; Lebeau et al., 1991). Hsp90 client proteins include mutated and/or overexpressed signaling proteins implicated in cancer, such as mutated p53 (Blagosklonny et al., 1996), Bcr-Abl (An et al., 2000; Shiotsu et al., 2000), Raf-1 (Schulte et al., 1996), AKT (Hostein et al., 2001; Sato et al., 2000), ErbB2(Miller et al., 1994), hypoxia-inducible factor 1α (HIF-1α) (Minet et al., 1999), cyclin-dependent kinases Cdk4 and Cdk6 (Stepanova et al., 1996) and steroid receptors including estrogen and androgen receptors (Bagatell et al., 2001). Additionally, it has been reported that Hsp90 and its co-chaperones modulate tumor cell apoptosis through effects on AKT (Basso et al., 2002), tumor-necrosis factor (TNF)-receptors (Vanden Berghe et al., 2003) and nuclear factor-κB (NF-κB) function (Chen et al., 2002a).

Hsp90 inhibition has several advantages in cancer therapy. First, Hsp90 inhibition minimizes toxicities in normal tissues while it maximizes target-specific damage in tumor tissues. This is due to increased Hsp90 expression in tumors and preferential accumulation of Hsp90 inhibitors in malignant tissues (Kitano, 2003). Second, multiple signaling pathways can be

targeted simultaneously with Hsp90 inhibition because many of the signaling proteins are HSP90 client proteins. Third, as Hsp90 inhibition targets multiple pathways, the likelihood that tumor cells will escape a single-target therapy lessens. This is especially relevant in solid tumors because by the time of diagnosis, most solid tumors harbor multiple genetic abnormalities that could have conferred the ability to overcome a single-target therapy. 17-allylamino-geldanamycin (17-AAG), a geldanamycin analog, is the first of its class to enter clinical trials. 17-AAG inhibits Hsp90-dependent conformational folding and promotes degradation of oncoproteins, such as ErbB2, mutant p53, c-Raf, and Bcr-Abl, and has shown antitumor activities in preclinical experiments (Ramanathan et al., 2005). 17-AAG is currently being tested in various solid and hematological malignancies, either as a single agent or in combination therapies. However, clinical trials with 17-AAG failed to show anti-tumor efficacy so far, despite extensive testing. It is felt that second-generation and third-generation inhibitors may be needed to adequately determine whether Hsp90 is a valid target for cancer therapy.

Disruption of HSP-client protein complex can also be achieved by the nonhistone effects of HDAC inhibitors. Several reports demonstrate the enhanced acetylation of Hsp90 by HDACi and suggest involvement of HDAC6 in modulation of Hsp90 acetylation. These reports document the connection between HDACi-mediated Hsp90 acetylation and the depletion of numerous Hsp90 client proteins (Atadja et al., 2004; Yu et al., 2002).

1.3.3 PI3K inhibitors

The phosphatidylinositol-3-kinase (PI3K) signaling pathway is crucial to many aspects of cell growth and survival. It is targeted by genomic aberrations including mutation, amplification and rearrangement more frequently than any other pathway in human cancer (with the possible exception of the p53 and retinoblastoma (Rb) pathways). There are three classes of PI3K, each with its own substrate specificity and distinct lipid products (Engelman et al., 2006; Katso et al., 2001). The Class IA of PI3K is the most widely implicated class in cancer and consists of three known isoforms of p110 (p110α/p110β/p110δ) with the first two isoforms being widely expressed and the third of which is restricted to lymphocytes (Fruman, 2004). The most frequent genetic aberrations in breast cancer are somatic missense mutations in the gene encoding p110α (*PIK3CA*). Amplification or mutation of the *PIK3CA* gene also commonly occur in bowel cancer, ovarian cancer, head and neck and cervical squamous cancers, gastric and lung cancers, anaplastic oligodendrogliomas, anaplastic astrocytomas, glioblastoma

multiforme and medulloblastomas which emphasizes the importance of the pathway (Broderick et al., 2004; Campbell et al., 2004; Ma et al., 2000; Mizoguchi et al., 2004; Shayesteh et al., 1999; Woenckhaus et al., 2002). PI3K activation initiates a single transduction cascade that promotes cancer cell growth, survival and metabolism. AKT, a serine-threonine kinase that is directly activated in response to PI3K, is a major effector of PI3K in cancer. There are three different AKT isoforms in mammalian cancers, and emerging data suggest that they have overlapping and distinct roles in cancers. AKT in response to PI3K activation phosphorylates and regulates the activity of a number of targets including kinases, transcription factors and other regulatory molecules. These targets include GSK3, BAD, human caspase 9, NF-κB transcription factors, mTOR, eNOS (Figure 4), Raf protein kinase, BRCA1 and $p21^{Cip1/WAF1}$ (Altiok et al., 1999; Datta et al., 1999; Montagnani et al., 2001; Zhou et al., 2001; Zimmermann and Moelling, 1999). AKT, directly or indirectly, phosphorylates and inhibits glycogen synthase kinase-3 (GSK3), phosphodiesterase-3B, protein phosphatase 2A and possibly PI3K signaling also controls angiogenesis, growth, proliferation, senescence and other processes through mechanisms including vascular endothelial growth factor (VEGF) transcriptional activation and induced hypoxia inducible factor-1α (HIF1α) expression (Hennessy et al., 2005; Kim and Kaelin, 2004; Skinner et al., 2004). AKT signaling leads to increased cellular growth and survival (Engelman, 2009). One of the major effectors downstream of AKT is mTOR complex 1 (mTORC1), which integrates many inputs, such as growth factor signaling, the energy state of the cell (AMP levels) and nutrient and O_2 availability.

Several small molecule inhibitors of PI3K-AKT signaling pathway are in clinical development. Two chemical inhibitors have been used to probe the function of PI3K: wortmannin, a fungal metabolite that irreversibly inhibits p110 by reacting covalently with the catalytic site, and the flavenoid derivative LY294002, a reversible inhibitor which, like wortmannin, inhibits all class I PI3Ks. However, both inhibitors have off-target activity. Many inhibitors with greater selectivity are under development, including GDC-0941, PX-866, SF-1126, XL-147, XL-765, CAL-101 and RAD-001. However, as the PI3K pathway is important for many normal cellular functions and, in particular, signaling by insulin, the main limiting factor for implementing drugs that inhibit the pathway will probably be the identification of targets and drugs with a sufficient therapeutic index to warrant clinical implementation.

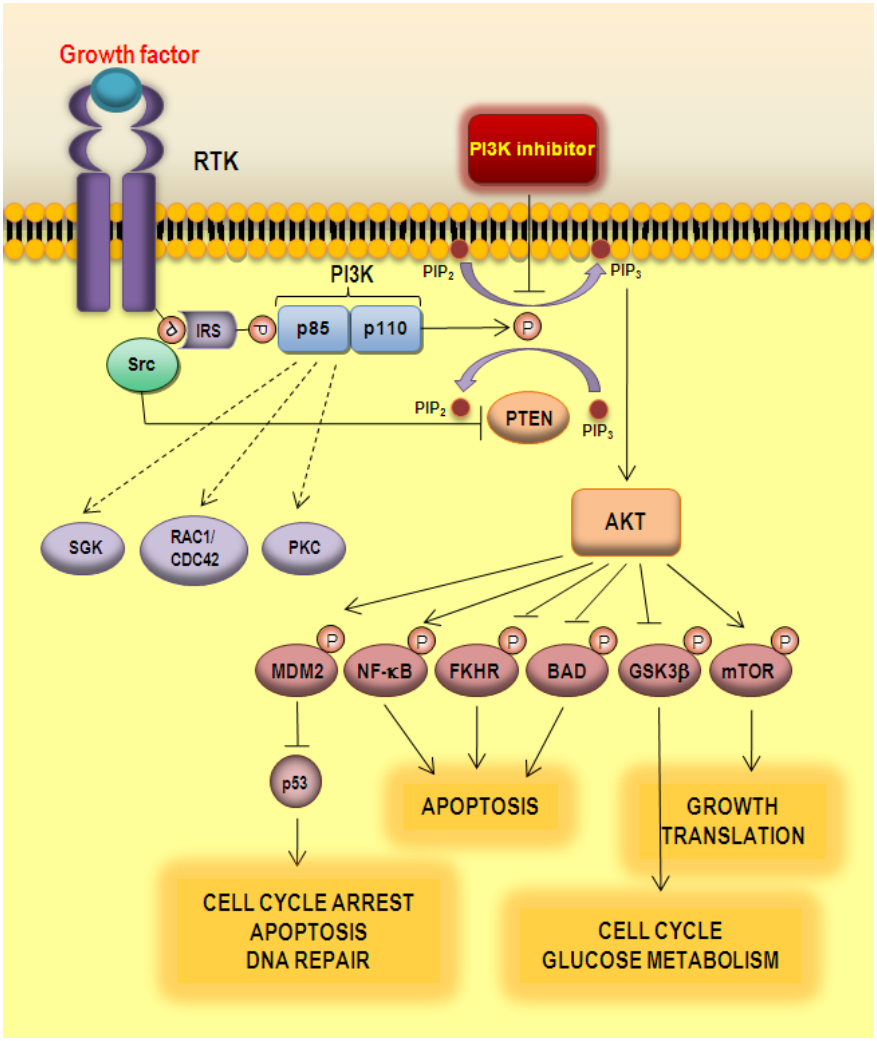

Figure 4. Signaling through the phosphatidylinositol-3-kinase (PI3K)/AKT pathway.

1.3.4 PIM Inhibitors

The Pim family of proto-oncogenes encodes serine/threonine specific kinases involved in cytokine-mediated signaling pathways in hematopoietic cells. The Pim gene family consists of three members, Pim-1, Pim-2 and Pim-3 (Bachmann and Moroy, 2005), which are substantially homologous, but differ in tissue distribution (Eichmann et al., 2000). Pim-1 and Pim-2 are expressed in most hematopoietic cells whereas the highest Pim-3 expression has been reported in brain, kidney, and mammary tissue (Mikkers et al., 2004). The Pim protein kinases were first cloned as proviral insertions in murine T-cell lymphomas induced by the c-Myc oncogene (Cuypers et al., 1984; Hoover et al., 1991). Unlike other serine/threonine kinases, the Pim kinases are not regulated by membrane recruitment or phosphorylation but primarily by transcription. Activated cytokine receptors recruit JAKs to induce STAT-dependent transcription of the Pim genes. The role of Pim signaling for cell survival in nontransformed cells has only recently been identified (Fox et al., 2005). Pim-1 contributes to the regulation of

cell apoptosis and antiapoptotic activity (Pircher et al., 2000; Shirogane et al., 1999; Wang et al., 2001) through its association with and phosphorylation of Bcl-xL/Bcl-2–associated death promoter (Bad), which is a proapoptotic member of the Bcl-2 family and capable of forming heterodimers with Bcl-2 or Bcl-xL (Datta et al., 2002). Several recently reported substrates of Pim are significant of its involvement in cell proliferation at both G1/S and G2/M transition, such as $p21^{Cip1/WAF1}$ (Wang et al., 2002; Zhang et al., 2007), CDC25A (Mochizuki et al., 1999), PTPU2 (Wang et al., 2001), NuMA (Bhattacharya et al., 2002), C-TAK1 (Bachmann et al., 2004), and CDC25C (Bachmann et al., 2006). Other Pim targets have been described, these include the mentioned proapoptotic protein Bad (Fox et al., 2003; Yan et al., 2003), members of the suppressor of cytokine signaling (SOCS) family (Chen et al., 2002b; Peltola et al., 2004), the translational repressor eIF-4E binding protein 1 (4E-BP1), GSK3β (Fox et al., 2003) and the transcription factor Myb (Winn et al., 2003). Additionally, Pim-1 and Pim-2 have been reported to be essential components of an endogenous pathway that regulates T cell growth and survival (Figure 5) (Fox et al., 2005).

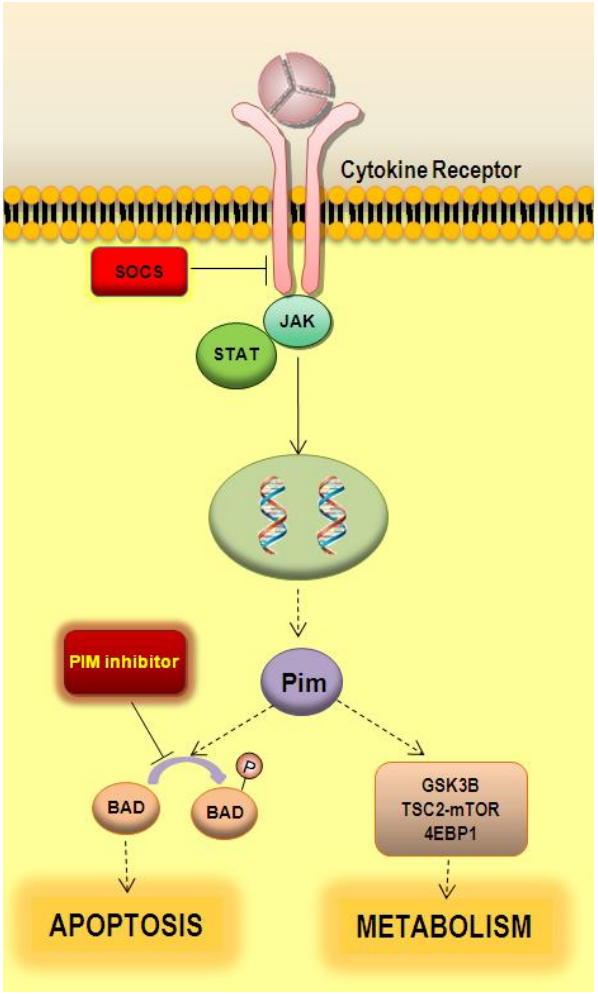

Figure 5. Schematic representation of PIM signaling pathway.

In human, Pim-1 overexpression is reported in diffuse B-cell lymphoma, chronic lymphocytic leukemia, acute myelogenous leukemia, head and neck cancer, and prostate cancer (Amaravadi and Thompson, 2005; Cibull et al., 2006) and increase in Pim levels has been correlated with progression to a more aggressive disease (Dhanasekaran et al., 2001). Similarly, Pim-2 is found to be overexpressed in multiple myeloma, leukemia, lymphoma, and prostate cancer and its expression correlates with clinical outcome (Amson et al., 1989; Claudio et al., 2002; Dhanasekaran et al., 2001; Neill and Kelsell, 2001; Yoshida et al., 1999). Consistently, enhanced levels of nuclear Pim-2 in the tumor cells have been associated with a higher risk of prostate-specific antigen recurrence and with perineural invasion of the prostate gland (Dai et al., 2005).

Besides cancer, Pim kinase activity has been shown to be of importance in the pathogenesis of vascular smooth muscle proliferation in vessel injury models (Katakami et al., 2004). However, in spite of the interest in Pim-mediated signaling, there are few known inhibitors of these enzymes. The only reported inhibitor of Pim function is LY294002, which was originally identified as a specific PI3K inhibitor (Jacobs et al., 2005). Development of specific inhibitors of Pim is underway and several groups have reported structurally novel Pim kinase inhibitors, such as imidazo[1,2-*b*]pyridazines (inhibit Pim and block the growth of leukemia cells) (Bullock et al., 2005; Pogacic et al., 2007), substituted pyridines (Cheney et al., 2007) and specific flavinoids (Holder et al., 2007a; Holder et al., 2007b). Evidence already exists to suggest that inhibitors of survival kinases can contribute to cancer therapy.

OBJECTIVES

Peripheral T-cell lymphoma (PTCL) is a relatively uncommon disease, accounting for 10-15% of Non-Hodgkin Lymphomas. The most common subtypes of peripheral T-cell lymphomas in Europe are peripheral T-cell lymphoma, unspecified (PTCLU), angioimmunoblastic T-cell lymphoma (AITL), anaplastic large cell lymphoma (ALCL) and cutaneous T-cell lymphoma (CTCL). Our group has significantly contributed to understanding of the pathogenesis and resistance to treatment in the field of cutaneous T-cell lymphoma (Tracey et al., 2003; Tracey et al., 2002). However, there is still a need to investigate new treatments as new therapies appear. The diagnosis of systemic PTCL is frequently challenging, and up to 50% of the cases are categorized as PTCL, unspecified (PTCLU) and the molecular alterations underlying the pathogenesis of PTCL are largely unknown. Hence, the objectives of the present thesis were the following:

1. Exploring the ontogeny and molecular heterogeneity of PTCL through a microRNA and gene expression profiling analysis of a series of AITLs and PTCLU samples

2. Finding the molecular signature associated with response and resistance to PUVA +/- IFNα treatment in twenty-nine CTCL patients enrolled in phase IV randomized open clinical trial comparing PUVA vs. PUVA + IFNα

3. Identification of genes and pathways that are differentially regulated by two histone deacetylase inhibitors (HDACi): vorinostat (SAHA) and panobinostat (LBH589) in five CTCL cell lines

4. Providing rationale for novel drug combination partners and identification of a core set of HDACi-regulated genes

MATERIALS & METHODS

2. Materials and Methods

2.1 Case selection

The tissue samples used in the present work were obtained from the Tumor Bank Network coordinated by the Molecular Pathology Program at Spanish National Cancer Research Centre. The complete procedures for obtaining and processing the samples by Tumor Bank Network can be found on http://www.cnio.es/ing/programas/progTumor11.asp. Immediately after biopsy the samples were processed according to two different protocols:

1. Paraffin-embedded tissue: samples were fixed in 10% buffered formalin for a minimum of 16 hours and a maximum of 48 hours after which time; they were embedded in paraffin following conventional techniques.
2. Frozen tissue: samples were frozen and duly identified in plastic cryomoulds (Cryomold standard, Tissue-Tek 4557, Bayer S.A) embedded in a cryosolidifiable medium (OCT-Compound, Tissue-Tek 4583, Bayer S.A) through immersion in a highly cryogenic medium allowing rapid freeze such as isopentane.

The diagnostics of all samples was centrally revised according to World Health Organization Criteria (WHO) using paraffin embedded sections with the help of immunohistochemistry techniques.

For PTCL study of **T-cell lymphoma pathogenesis**, twenty peripheral T-cell lymphoma (PTCL) and seven reactive lymph node (LN) samples were selected from the medical records of hospitals included in the Spanish Tumor Bank Network. The PTCL cases comprised a total of 20 cases, 9 of which represented diagnostic samples of patients with PTCLU and 11 patients with AITL. Clinical characteristics of all the patients included in PTCL study is presented in Table 5.

Table 5. Clinical characteristics of the peripheral T-cell lymphoma patients included in PTCL study

ID	Patient number	Sex	Age	Diagnosis	Stage	PS
TCL1	01040202	F	77	AITL	IVA	1
TCL2	01040203	F	42	PTCL	IVA	1
TCL3	01030422	F	73	AITL	--	1
TCL4	01030195	M	49	PTCL	IA	1
TCL5	20030222	--	--	PTCL	--	--
TCL6	00000326	M	42	AITL	IVB	1-2
TCL7	05011364	M		AITL	--	--
TCL8	02010182	M	63	PTCL	IV	2
TCL9	02010235	M	39	PTCL	IIA	1
TCL10	05030174	--	--	AITL	--	--
TCL11	01030194	M	78	PTCL	IIA	1
TCL12	00030729	M	69	PTCL	--	--
TCL13	00000110	M	--	AITL	--	--
TCL14	00000183	M	27	AITL	--	--
TCL15	00000311	F	70	AITL	IIIA	0
TCL16	00010062	F	81	AITL	IVA	1
TCL17	00011340	M	65	PTCL	IVB	3
TCL18	00020012	M	66	AITL	IIIB	1
TCL19	00030177	F	--	PTCL	--	--
TCL20	01030191	M	71	AITL	IIIA	1

Abbreviations: PS, Performance Status; AITL, Angioimmunoblastic T-cell lymphoma; PTCL, Peripheral T-cell lymphoma; --, no data available

For **PUVA +/- IFNα study**, twenty nine pre-treatment mycosis fungoides (MF) samples and 18 inflammatory dermatitis (ID) samples were included. MF patients were enrolled in a randomised clinical trial, MF99 (ClinicalTrials.gov, registration number NCT00630903) to test the efficacy of PUVA vs. PUVA + IFNα and were all stage IA, IB or IIB patients. Previous treatments included PUVA, topical corticosteroids, PUVA+IFNα, BCNU, TSEB, Methotrexate and 8-MOP and are listed in Table 6 for each patient. Thirteen patients were previously untreated. Patients received no treatment for at least 1 month prior to beginning of the study protocol. All paraffin embedded and frozen samples represented biopsies taken in the 2 weeks preceding treatment commencement on MF99.

Table 6. Characteristics of the 29 MF patient group included in a randomized clinical trial to test the efficacy of PUVA vs PUVA + IFNα

ID	Patient number	Sex	Age	Stage	Previous treatment	Arm treatment	Response	TT-REM [weeks]	TT-REL [weeks]
MF 01	00-0292	H	40	3	Topical corticosteroids	PUVA + IFNα	R	26	35
MF 02	00-0295	M	78	2	PUVA (84, 85, 87, 90), Topical corticosteroids, BCNU (83)	PUVA	R	12	171
MF 03	00-0296	M	45	1	PUVA, (91, 97), Topical corticosteroids	PUVA + IFNα	R	24	128
MF 04	00-0406	M	52	2	PUVA (1992)	PUVA	R	8	>177
MF 05	01-0002	M	59	3	None	PUVA	R	16	109
MF 06	01-0024	M	54	1	Ropheron (VI-98); PUVA+IFNa (VII-96)	PUVA	R	8	188
MF 07	01-0025	M	66	1	None	PUVA	R	25	49
MF 08	01-0157	H	52	3	Sun + 8-MOP	PUVA + IFNα	R	20	74
MF 09	01-0867	M	41	1	PUVA	PUVA	R	8	165
MF 10	01-0204	H	65	3	None	PUVA	R	8	96
MF 11	01-0205	M	69	3	None	PUVA + IFNα	R	14	44
MF 12	01-0209	H	62	2	Topical corticosteroids	PUVA	NR	30	20
MF 13	01-1960	M	29	3	None	PUVA + IFNα	R	12	35
MF 14	01-0158	M	29	2	PUVA, TSEB , topical BCNU, topical corticosteroids, MTX	PUVA + IFNα	NR	30	24
MF 15	01-1640	H	68	1	None	PUVA	R	18	59
MF 16	01-1676	M	61	3	PUVA (VI-97, VI-98), PUVA+IFNa (IX-XII 98,II-VIII 99)	PUVA	R	24	45
MF 17	02-2087	M	59	3	None	PUVA + IFNα	R	12	78
MF 18	02-0628	M	24	3	PUVA + IFNa, PUVA	PUVA + IFNα	R	16	44
MF 19	02-1679	H	52	2	PUVA (98, 00)	PUVA + IFNα	NR	30	17
MF 20	02-1770	M	44	2	Topical corticosteroids	PUVA	R	16	53
MF 21	03-0472	H	74	1	None	PUVA + IFNα	R	10	154
MF 22	03-0454	M	18	1	PUVA	PUVA	NR	30	24
MF 23	02-2075	M	24	1	PUVA	PUVA	R	16	27
MF 24	03-0462	H	59	1	None	PUVA + IFNα	NR	30	24
MF 25	03-0463	H	21	1	Topical corticosteroids	PUVA	R	13	>175
MF 26	03-0464	H	62	1	None	PUVA + IFNα	R	6	39
MF 27	03-0455	H	45	1	None	PUVA	NR	30	24
MF 28	0702-0554	M	37	1	None	PUVA	R	8	80
MF 29	0702-0579	H	25	1	None	PUVA	NR	30	8

Abbreviations: PUVA, psoralen plus ultraviolet A irradiation; BCNU, Topical carmustine; TSEB, Total skin electron beam irradiation therapy; MTX, methotrexate; 8-MOP, 8-Methoxsalen; R, responders; NR, non-responders; TT-REM, time to remission; TT-REL, time to relapse

Both study arms consisted of a 24 week treatment period. In the PUVA monotherapy arm, the patients were treated with PUVA at the dose dependent on the skin phototype for 24 weeks. In the PUVA + IFNα arm, IFNα alone was given for the first two weeks of treatment in a dose of 3-6-9MU for 3 days in the first week and the combination PUVA + IFNα (IFNα dose – 9MU/3 days per week) was used during the remaining 23 weeks. Treatments continued until complete remission, disease progression, significant toxicity, or withdrawal of consent. Responders (R) are defined as patients who achieve complete remission (CR) within 24 weeks of the commencement of the treatment while non-responders (NR) are patients that do not achieve CR within 24 weeks or show disease progression. Twenty nine MF samples were used for expression profiling (7 NR and 22 R) while immunohistochemistry analysis was performed on paraffin embedded sections from all patients enrolled in the study (35).

The ID samples used represented cases of interface and spongiotic dermatitis including rosacea, lupus erythematosus, dermatitis herpetiformis, seborrheic dermatitis, lichenoid dermatitis, psoriasis and spongiotic dermatitis. All control cases were previously untreated at biopsy.

Informed consent was obtained from all patients under the supervision of the local Ethics Committees and followed the Declaration of Helsinki protocols. All samples were centrally reviewed by a panel of pathologists and diagnosed using generally accepted criteria (Kallinich et al., 2003), with the aid of Haematoxylin/Eosin, CD3, CD4, and CD8 staining, and TCRγ gene rearrangement analysis by PCR.

For **HDACi (vorinostat) study** peripheral blood lymphocytes (PBL) before and after treatment with vorinostat were obtained from CTCL patients (SS) with high percentage of circulating malignant cells. The study was conducted after informed consent has been obtained and in accordance with regulation of the Hospital 12 de Octubre (Madrid, Spain). PBL from patients was isolated on Lymphoprep™ (Axis-Shield, Oslo, Norway).

2.2 Cell culture

2.2.1 Tumor cell lines

Human MJ, HuT78 and HH CTCL cell lines, derived from peripheral blood of patients with MF, SS and non-MF/SS aggressive CTCL, respectively (Gootenberg et al., 1981; Popovic et al., 1983; Starkebaum et al., 1991), were obtained from American Type Culture Collection (Rockville, MD). The cell line MyLa (Kaltoft et al., 1992) (MF origin) was obtained from European

Collection of Cell Cultures (Wiltshire, UK); and SeAx (Kaltoft et al., 1988) (SS) was a kind gift of Dr Reinhard Dummer, University Hospital of Zurich, Switzerland. Characteristics and origin of all the cell lines used are presented in Table 7. Cells were periodically tested for Mycoplasma infection and found to be negative.

Table 7. Characteristics of the cell lines used.

Cell line	Species	Source	Culture medium	Growth	Origin
HH	Human	Non-MF/SS aggressive CTCL	RPMI + 10% FBS	Suspension	ATCC
HuT78	Human	Sézary syndrome	RPMI + 20% FBS	Suspension	ATCC
MJ	Human	Mycosis fungoides	RPMI + 20% FBS	Suspension	ATCC
MYLA	Human	Mycosis fungoides	RPMI + 20% FBS	Suspension	ECCC
SeAx	Human	Sézary syndrome	RPMI + 10% FBS	Suspension	Zurich

Additionally, spectral karyotyping (SKY) method performed by Cytogenetics Unit at CNIO was used to identify and confirm chromosome aberration in cancer cells. SKY is a molecular cytogenetic technique used to simultaneously visualize all the pairs of chromosomes in an organism in different colors. Briefly, fluorescently-labeled probes for each chromosome are made by labeling chromosome-specific DNA with different fluorophores. Due to a limited number of spectrally-distinct fluorophores, a combinatorial labeling method is used to generate many different colors. Spectral differences generated by combinatorial labeling are captured and analyzed using an interferometer attached to a fluorescence microscope. Image processing software assigns a pseudo color to each spectrally different combination allowing the visualization of the individually colored chromosomes (Schrock et al., 1996). The SKY results for all cell lines used in the present study are shown in Table 8.

Table 8. Spectral Karyotyping

Cell line	Spectral Karyotype (SKY)
HH	 Karyotype: 45,XY, der(3)t(2;3)(?;p24), t(3;12)(q12;q23), der(4)t(1;4)(?;q32), der(5)t(5;9;10)(p15;q?;?), t(6;14)(q25;q12), +8, -9, del(10)(q21), -15, der(18)t(3;18)(?;q22)
HuT78	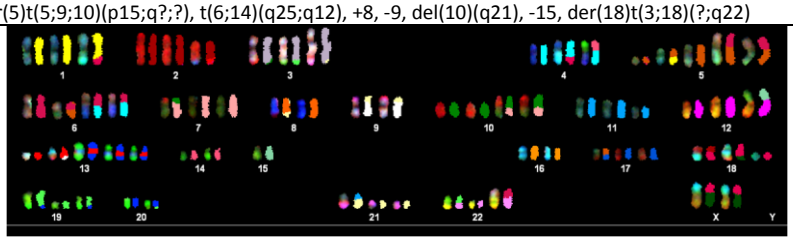 Karyotype: der(X)t(X;18)(p11.2;q11.2)x2, der(1)t(1;18)(q21;q12), der(2)t(2;13)(q21;?), der(3)t(3;10)(q2?;?), der(3)t(3;19)(q2?;?), der(3)t(3;?;21)(q;?;?), der(4)t(4;18)(q12;q12), der(4)t(4;14)(p11.2;p11.2), del(5)(q11.2qter), t(5;6)(p11.2;q11.2)x2, der(6)t(4;6)(q13;q121)x2, der(7)t(7;10)(p13;?), der(8)t(8;21)(q24;?), der(9)t(9;21)(p21;?), del(10)(q22qter), der(10)t(7;10)(q?;q22)x2, del(11)(q13qter), del(12)(p12pter), der(12)t(12;15)(p13;p11.2), del(13)(q14qter), der(13)t(2;13)(?;q14), der(13)i(13)t(13;20)(q14;q11.2), del(14)(q21q32), der(17)t(5;17)(p?;p11.2), del(18)(q11.2qter), der(18)t(2;18)(?;p11.2), der(18)t(X;18)(?;q21), der(19)t(19;20)(q13;?)hsr(19)(q13.1?), der(19)t(19;20)(q13.1;?), del(20)(q11.2qter), der(21)t(11;21)(q12;p11.2), der(22)t(6;22)(q/:p11.2), der(22)t(19;22)(?;p11.2)
MJ	 Karyotype: 47,XY, der(15)t(5;15)(q21;q25-26), der(17)t(2;17)(q?;q25)  Karyotype: 46,XY, t(9;15)(p24;q21), del(15), der(17)t(2;17)(q?;q25)
MYLA	 Karyotype: 47,XY, del(1)(q31), t(1;15)(p36;q23), t(2;14)(q33;q12), t(4;5)(q21;q31), del(6)(q21), del(9)(p21), der(10)t(10;13)(p15;q?), -13, t(16;22)(p10;p10), +r(17), der(21)t(13;21)(?;q22), +Y
SeAx	 Karyotype: 47,XY, del(1)(q31), t(1;15)(p36;q23), t(2;14)(q33;q12), t(4;5)(q21;q31), del(6)(q21), del(9)(p21), der(10)t(10;13)(p15;q?), -13, der(13)t(13;14)(q34;q12), del(14), t(16;22)(p10;p10), +r(17), der(21)t(13;21)(?;q22), +Y

2.2.2 Culture and conservation of cell lines

Cells were grown in RPMI 1640 medium (Sigma Chemical, St Louis, MO) supplemented with 10-20% heat-inactivated fetal bovine serum – FBS (10% FBS from Euroclone, Ltd, UK and 10% FBS from Lonza, Qalkersville, MD), 2mM L-glutamine (Life Technologies, Inc., Grand Island, NY), 100mg/ml penicillin/streptomycin (Life Technologies, Inc.), and 2.5μg/ml fungizone (amphotericin B) (Life Technologies, Inc) and grown in a humidified atmosphere at 37^{O}C with 5% CO_2. All the cell lines were cultured in suspension in cell culture flasks (Corning, NY) and passaged every 3-4 days. All cell manipulation was performed in the *Telstar* Biological Safety Cabinets (*Bio IIA*) with the laminar air flow systems.

For long term storage the cells were cryopreserved. The basic principle of successful cryopreservation is a slow freeze and quick thaw. The cells were stored in their habitual medium supplemented with 10% of cryoprotectant such as dimethyl sulphoxide (DMSO) to help protect the cells from rupture by the formation of ice crystals. Although the precise requirement may vary with different cell lines, as a general guide cells should be cooled at a rate of –1^{O}C to –3^{O}C per minute and thawed quickly by incubation in a 37^{O}C water bath for 3-5 minutes.

2.2.3 Compounds

Vorinostat (SAHA) was provided by Merck (Boston, Massachusetts). LY294002 was purchased from Calbiochem (La Jolla, CA), 17-AAG was obtained from Sigma (St Louis, MO) and Panobinostat (LBH589) from Novartis Pharmaceuticals (Basel, Switzerland). ETP-45628 (3-(1-methyl-4-morpholin-4-yl-pyrazolo[5,4-d]pyrimidin-6-yl)phenol) and ETP-39010 (4-[6-[(4-fluorophenyl)methylamino]imidazo[2,3-f]pyridazin-3-yl]phenol) were developed by Experimental Therapeutics Program at CNIO (Madrid, Spain). All the drugs were dissolved in DMSO to stock concentration of 50mM or 10mM and stored at –20^{O}C. Serial dilutions were freshly made in RPMI 1640.

2.2.4 Cell transfection – Microporation

To transfect HuT78, MYLA and SeAx cells with a plasmid DNA containing ZAP70 target gene microporation technology was used. pcDNA3-ZAP70 vector was a kind gift of professor Dimitar Efremov, ICGEB, Italy. The MicroPorator (MP-100 MicroPorator) and its accompanying devices and materials are manufactured by Digital Bio (Seoul, Korea) (http://www.microporator.com).

First, careful calibrations for microporation of each cell line, leading to improved transfection yields and cell survival rates were performed.

Tumor cell preparation for microporation: one day prior to microporation the cells were cultured in a fresh growth medium without antibiotics in order to reach 60 to 80% confluency.

On the day of microporation: The microporations were done in 10μl or 100μl gold-tips, which were inserted into the microporation tube. The size of the tip, whether 10μl ($3.0x10^5$ cells) or 100μl ($2.0x10^6$ cells), depended on the amount of cells undergoing microporation, were used according to the manufacturer's instructions.

First, to prepare the apparatus, 3ml of Buffer E were added into the microporation tube. Then the pulse conditions of the pipette station were set up, as follows:

for HuT78 cells: pulse voltage, 1150; pulse width, 20; pulse number, 2.

for MYLA cells: pulse voltage, 1300; pulse width, 20; pulse number, 2.

for SeAx cells: pulse voltage, 1300; pulse width, 20; pulse number, 2.

The appropriate amount of cells resusupended in Buffer R was mixed with plasmid DNA and the cell-DNA mixture was aspirated using the MicroPorator pipette carrying the gold-tip. Afterwards, the MicroPorator pipette was inserted into the Pipette Station and the Start button was pressed on the LCD panel. After the pulse, the cell sample was immediately transferred into the culture flask containing medium and supplements (including antibiotics).

2.3 Cell – based assays

2.3.1 Cell proliferation/Viability

Cell proliferation/viability was measured by the CellTiter-Glo® Luminescent Cell Viability Assay (Promega, Madison, WI). The CellTiter-Glo® Luminescent Cell Viability Assay is a homogeneous method of determining the number of viable cells in culture based on quantitation of the ATP present, which signals the presence of metabolically active cells. The assay relies on the properties of a proprietary thermostable luciferase (Ultra-Glo™ Recombinant Luciferase), which generates a stable "glow-type" luminescent signal and improves performance across a wide range of assay conditions. Briefly, aliquots of $1x10^4$ cells per well were distributed in 96-well flat bottom tissue culture plates (BD Falcon; New Jersey) in 100μL of medium and incubated at 37^OC in the presence or absence of the drug for 72h (unless stated otherwise). Following incubation for the indicated time period, 100μl of a single CellTiter-Glo reagent (prepared before adding from the CellTiter-Glo buffer and substrate) was added directly to cells cultured in serum-supplemented medium. This addition resulted in cell lysis and

generation of a luminescent signal proportional to the amount of ATP present. The plates were then mixed for 2min on an orbital shaker and incubated for 10min at room temperature to stabilize. Following, the luminescent signal was recorded using Wallac 1420 multilabel counter (PerkinElmer Life and Analytical Sciences, Turku, Finland). Wells containing medium alone were used as a control for background luminescence.

2.3.2 Apoptosis measurement

Evaluation of the early apoptotic populations (Annexin V^+/PI^-) and late apoptotic or secondary necrotic population (Annexin V^+/PI^+) was performed by Annexin V-APC/PI surface staining. Briefly, cells were collected, washed twice with cold PBS, and centrifuged at 1200rpm for 5min. Cells were resuspended in 1X binding buffer (Sigma-Aldrich, St Louis, MO) at a concentration of $1x10^6$ cells/ml, 100μl of the solution were transferred to a 5μl culture tube, and 5μl of annexin V-APC (BD Biosciences, Pharmingen, San Jose, CA), and 5μl of PI (Sigma-Aldrich) were added. Cells were incubated for 15min at room temperature in the dark. Finally, 400μL of 1X binding buffer was added to each tube and samples were analyzed with FACSCalibur flow cytometer (Becton Dickinson, Franklin Lakes, NJ). For each sample, 20,000 gated events were acquired and the data were analysed using CellQuest Pro software (Becton Dickinson).

2.3.3 Cell cycle analysis

HH, Hut79, MJ, Myla and SeAx cells ($1x10^6$ cells) were incubated with DMSO or vorinostat (SAHA) at indicated concentrations for 24 and 48h. Cells were collected, washed with cold phosphate buffered saline (PBS) and fixed in ice cold 70% ethanol. This suspension was stored at -20^OC for at least 30min. Next, the cells were washed with 5ml of PBS, centrifuged at 2000rpm during 5min and resuspended in 500μl of PBS. The cell suspension was treated with DNase-free Rnase (Quiagen, Inc., Valencia, CA), and stained with 50μg/mL propidium iodide (PI). Distribution of the cell-cycle phase by different DNA content was determined with a FACSCalibur flow cytometer (Becton Dickinson). For each sample, 10,000-gated events were acquired. Analyses of cell-cycle distribution (including apoptosis: sub-G0) were performed using CellQuest Pro software (Becton Dickinson).

2.3.4 Determination of drug synergy

Cells were seeded in 96-well plates and treated with serial dilutions of each drug individually or with both drugs simultaneously at a fixed ratio of doses 0.25, 0.5, 1, 2, 4 times the individual

IC_{50} (ED_{50}) values (Table 9). After 72h of exposure, the luminescence was measured using CellTiter-Glo Assay.

Table 9. Scheme of drug combinations.

		DRUG 1					
DRUG 2		0	0.25 x $(ED_{50})_1$	0.5 x $(ED_{50})_1$	1 x $(ED_{50})_1$	2 x $(ED_{50})_1$	4 x $(ED_{50})_1$
	0	Control $(f_a)_0$	$(f_a)_1$	$(f_a)_1$	$(f_a)_1$	$(f_a)_1$	$(f_a)_1$
	0.25 x $(ED_{50})_2$	$(f_a)_2$	$(f_a)_{1,2}$				
	0.5 x $(ED_{50})_2$	$(f_a)_2$		$(f_a)_{1,2}$			
	1 x $(ED_{50})_2$	$(f_a)_2$			$(f_a)_{1,2}$		
	2 x $(ED_{50})_2$	$(f_a)_2$				$(f_a)_{1,2}$	
	4 x $(ED_{50})_2$	$(f_a)_2$					$(f_a)_{1,2}$

f_a – the fraction affected by the dose

To determine synergism the isobologram analyses based on the Chou and Talalay method implemented in Calcusyn software (Biosoft, Ferguson, MO) were applied.

Combination Index (CI) values were calculated using CalcuSyn program. The dose-effect relationships analyzed using the median-effect equation was first obtained for each single drug by its serial dilution. A CI value for each combination treatment was then calculated based on the following formula:

$$CI = \frac{(D)_1}{(Dx)1} + \frac{(D)_2}{(Dx)2}$$

where Dx_1 and Dx_2 are the doses of drug 1 and drug 2 alone required to produce x% effect, and D_1 and D_2 are the doses of drug 1 and drug 2 in combination required to produce the same effect (Chou and Talalay, 1984). CI was used to express synergism (CI < 1), additive effect (CI = 1), or antagonism (CI > 1). Detailed definition of synergism and antagonism with respect to CI values can be found in Table 10.

Table 10. Description of combination index (CI) values.

Range of CI	Symbol	Description
< 0.1	+++++	Very strong synergism
0.1 – 0.3	++++	Strong synergism
0.3 – 0.7	+++	Synergism
0.7 – 0.85	++	Moderate synergism
0.85 – 0.90	+	Slight synergism
0.90 – 1.10	±	Nearly additive
1.10 – 1.20	-	Slight antagonism
1.20 – 1.45	--	Moderate antagonism
1.45 – 3.3	---	Antagonism
3.3 – 10	----	Strong antagonism
> 10	-----	Very strong antagonism

2.4 mRNA – based techniques

2.4.1 RNA isolation

2.4.1.1 microRNA extraction

Total RNA isolation for microRNA hybridization was performed using Trizol protocol (Invitrogen, Carlsbad, CA, USA) as follows: Sections of the frozen tissue were made using a microtome at -20^{O}C and 1ml of Trizol (monophasic solutions of phenol and guanidine isothiocyanate) was added to the tube containing the sectioned tissue and kept in dry ice until homogenisation. The tissue was homogenised using a polytron or syringe, and 1µl of linear acrylamide (Life technologies Inc.) was added. During sample homogenization or lysis, TRIZOL Reagent maintains the integrity of the RNA, while disrupting cells and dissolving cell components. The sample containing the linear acrylamide was incubated at room temperature for 5-10 minutes. 200µl of chloroform was added and the tubes were mixed for 15 seconds. The tubes were incubated at room temperature for 10min and centrifuged at 12,000g for 15min at 4^{O}C. Addition of chloroform followed by centrifugation separates the solution into an aqueous phase and an organic phase. RNA remains exclusively in the aqueous phase. The aqueous phase was removed to a fresh tube and the RNA was precipitated using isopropyl alcohol. The pellet was washed twice using ice-cold 70% ethanol, dried and re-suspended in RNase-free water. RNA quality was checked using a total RNA (small fraction chip) with the Agilent 2100 Bioanalyzer (Agilent Technologies Inc., Santa Clara, CA, USA). In addition, total RNA integrity was evaluated by 1% agarose electrophoresis, following the standard procedure.

2.4.1.2 total RNA extraction from frozen tissue

Total RNA extraction from whole frozen tissue was carried out using the Trizol reagent (Invitrogen) as described in section 2.4.1.1. The resulting RNA was further purified using the RNeasy kit (Qiagen Inc., Valencia, CA) and digested with RNase-free DNase I following the manufacturer's instructions and procedures described in the following section.

The integrity of RNA was verified by electrophoresis and/or automatically using the 2100 Bioanalyzer (Agilent Technologies) and the quantity was measured by NanoDrop ND-100 (NanoDrop, Wilmington, DE) or by the 2100 Bioanalyzer (Agilent Technologies).

2.4.1.3 total RNA extraction from cell lines

Total cellular RNA was extracted from cells using QIAshredder spin column (homogenization) and purified with RNeasy Mini-Kit (Qiagen Inc., Valencia, CA) following the manufacturer's RNA Clean-up protocol with the optional on-column digestion with RNase free DNase I. Briefly, cells were lysed and homogenized in the presence of highly denaturing buffer RLT containing guanidine isothiocyanate and 2-mercaptoethanol (10µl of 2-mercaptoethanol for 350µl of RLT buffer). Ethanol was then added to the lysate, creating conditions that promote selective binding of RNA to RNeasy silica-gel membrane. Following, the sample was applied to the RNeasy mini column. Total RNA binds to the membrane, contaminants are efficiently washed away, and a high quality RNA is eluted in RNase-free water. All centrifugation steps were performed at 20-25^{O}C in a standard microcentrifuge. RNA quality and integrity were verified using the RNA 6000 Nano Chips, Agilent 2100 Bioanalyzer (Agilent Technologies, Palo Alto, CA).

2.4.2 Reverse transcription and RT-PCR

First-strand cDNA was synthesized from 500ng of total RNA using the High-Capacity cDNA Archive Kit (Applied Biosystems, Foster City, CA) according to manufacturer's protocol. Reverse transcription reactions were performed in the total volume of 20µl containing 500ng DNase treated total RNA, 1x reaction buffer, dNTP mixture, random primers, Rnase inhibitor and 50U MultiScribe reverse transcriptase. Reaction mixtures were incubated at 25^{O}C for 10min followed by incubation at 37^{O}C for 2h and 5sec at 85^{O}C.

2.4.3 Quantitative Real-Time PCR

Expression of mRNA for eight differentially expressed genes associated with TCR pathway was measured with the use of TaqMan Gene Expression Assays on demand (Applied Biosystems, Foster City, CA). The following assays has been used: FYN (Hs00941608_g1), IFNGR1 (Hs00988302_m1), STAT3 (Hs00374286_g1), ZAP70 (Hs00896347_m1), CD3G (Hs00962185_g1), LAT (Hs01065378_g1), IL4R (Hs00965052_m1) and CD3E (Hs99999153_m1). Quantitative reverse transcriptase PCR (RT-PCR) reactions were performed in triplicate with the ABI Prism 7900 Sequence Detector System (Applied Biosystems). The PCR cycling conditions were standard: 95^{O}C for 10min for one cycle, 95^{O}C for 15sec, and 60^{O}C for 1min for 40 cycles. The relative changes in gene expression were calculated by the $\Delta\Delta$Ct method using the Sequence Detection System (SDS) 2.1 software (Applied Biosystems). The $\Delta\Delta$Ct method gives the amount of target normalized to an endogenous reference and relative to a calibrator. The expression of each of the genes in all specimens was related to its expression in a reference RNA pool (Stratagene) used as a calibrator. The level of each transcript was quantified by the cycle at which the PCR amplification was in log phase where there was significant fluorescent signal (Ct) with HGUSB as the endogenous control. All standards and samples were run in the total volume of 15µl in triplicate.

2.4.4 Gene expression microarrays

Gene expression microarrays are powerful techniques, which allow the analysis of the expression of thousands of genes simultaneously. The past decade has witnessed a revolution in the field of expression profiling in cancer. Microarray technology has changed both the view of cancer and how research in molecular oncology can be conducted (Raetz and Moos, 2004).
The schematic diagram of gene expression microarray labeling, hybridization and analysis is presented in Figure 6.

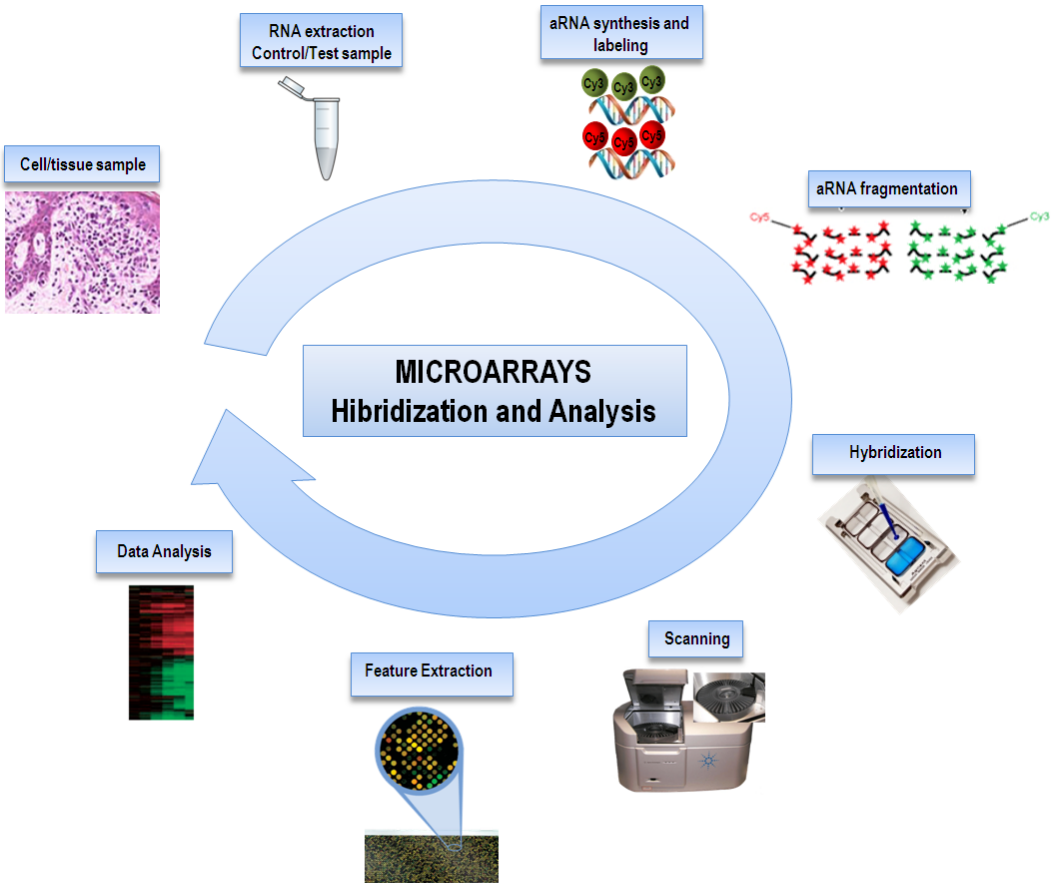

Figure 6. Gene expression microarray labeling, hybridization and analysis.

2.4.4.1 Oncochip v. 1.1c

In PUVA +/- IFNα study, the CNIO OncoChip was used. The OncoChip is a cDNA microarray developed at the Genomics Unit of Spanish National Cancer Centre (CNIO) that has been especially designed for the study of cancer and contains 6386 genes including a core of 2489 cancer-relevant genes in addition to genes involved in drug-response, tissue-specific genes and control genes. The 6386 genes are represented by a total of 7237 clones represented by 13057 spots on the array.

2.4.4.1.1 RNA amplification

T-7 based mRNA amplifications were carried out as described previously (Eberwine, 1996; Van Gelder et al., 1990). Briefly, 0.5-5µg of total RNA was converted to double stranded cDNA. For first strand cDNA synthesis, an oligo-dT primer containing a T7 RNA polymerase promoter (Ambion, Austin, TX) was used. The first strand cDNA synthesis reaction was performed using Superscript II Reverse Transcriptase, DTT (Dithiothreitol) and 10mM dNTPs (2'-Deoxyribonucleoside-5'-triphosphates) (all supplied by Life Technologies, Inc.) and RNase

inhibitor (RNAsin) (Promega, Madison, WI), and was incubated for 2 hours at 42^{O}C. Second strand cDNA synthesis was performed using DNA polymerase, *Escherischia coli* DNA ligase, RNaseH and dNTPs (Life Technologies, Inc.) at 16^{O}C for 2h. The double stranded cDNA was purified using phenol-chloroform-isoamyl alcohol (25:24:1) pH 8.0 (Ambion) and precipitated using ethanol, 7.5M ammonium acetate (Sigma Chemical Company) and linear acrylamide (Ambion). T7 *in vitro* transcription was carried out using the Megascript T7 *in vitro* transcription kit (Ambion), following the manufacturer's instructions. T7 *in vitro* transcription was allowed to continue for between 2 and 14 hours at 37^{O}C, depending on the quantity of total RNA used.

2.4.4.1.2 Preparation of fluorescent cDNA from aRNA

Fluorescent first strand cDNA was made with 2.5 or 5µg of amplified RNA (aRNA) in the presence of Cy3 or Cy5 (Amersham, Uppsala, Sweden), random hexamer primers (Promega), DTT (Life Technologies Inc), RNase inhibitor (RNAsin) (Promega), unlabelled dNTPs (Fermentas Life sciences, Lithuania) and Superscript II Reverse Transcriptase (Life Technologies Inc). 10µg of Cot1 human DNA (Life Technologies Inc.) was added to the labeled probe. The microarray slides were denaturalized by placing in boiling water for 3min. Slides were incubated in a buffer filtered using a 45µm filter and containing 4X SSC (Saline Sodium Citrate buffer), 1X BSA (Bovine serum albumin)(Sigma Chemical Co.), 2µg/ml denatured salmon sperm DNA (DNAs) (Sigma Chemical Co.) and 0.1% SDS (Sodium Dodecyl Sulphate) for 45min at 65^{O}C, followed by washing with sterile water. The probe was added to a solution containing 50% formamide, 20X SSC (Saline Sodium Citrate buffer) and 10% SDS (Sodium Dodecyl Sulphate) and incubated at 100^{O}C for 3min followed by 20min at 42^{O}C before applying to the microarray slide.

2.4.4.1.3 Hybridization

The slides were prepared for hybridization first by submerging in hot water for 3min, followed by incubation in prehybridization buffer (SSC 4X, SDS 0.1%, 0.001% BSA) at 65^{O}C for 45-60min and washed in water at room temperature. The hybridization mixture was then applied on the printed side of the array and carefully the cover slide was placed on the top (Hybri-slips 22 x 60mm; Sigma). Slides were inserted in the hybridization chamber (Corning) and the hybridization was carried out at 42^{O}C overnight (15-20h). After that time, the slides were washed three times (3X) with 600ml of SSC 2X, 0.5% SDS and another 3X with 600ml of SSC 0.5X, 0.5% SDS. All the washing steps were carried out at 42^{O}C for 15min, with shaking. Slides

were scanned for Cy3 and Cy5 fluorescence using Scanarray 5000 XL (GSI Lumonics, Kanata, Ontario, Canada).

2.4.4.1.4 Data analysis

Using GenePix Pro 4.0 software (Axon instruments Inc., Union City, CA), the fluorescence intensity ratios (Cy3/Cy5 o Cy5/Cy3) were quantified for each point. Fluorescence intensity measurements were subjected to automatic background subtraction and the Cy5/Cy3 ratio values were normalized to the median ratio value of all spots in the array. For patient samples, the sum of the median background for each channel was calculated and spots with total intensity values below the calculated sum of median backgrounds were discarded. Additionally, all spots with total intensity values lower than 250 were discarded. Furthermore, bad spots or areas of the array with obvious defects were manually flagged and discarded from analysis. All ratio values were log-transformed (base 2). Inconsistent duplicates were discarded and all consistent duplicate spots and genes were averaged (Herrero et al., 2003). The genes with less than 70-80% of valid data were excluded from the analysis. The preprocessing was performed using bioinformatics tools developed at the Bioinformatics Unit at CNIO (Gene Expression Pattern Analysis Suite (GEPAS), available at http://gepas.bioinfo.cnio.es).

2.4.4.2 Agilent Spike-In v. 44K and v. 4X 44K

2.4.4.2.1 cDNA synthesis from total RNA

2µg of total RNA was mixed with 2µl of a 5,000-fold dilution of Agilent's Two-Color Spike-in RNA control and amplified using Agilent Low RNA Input Fluorescent Amplification Kit (Agilent Technologies, Inc., Santa Clara, CA). The mixture in a final volume of 6.5µl (total concentration at least 5ng/µl) was mixed with 5µl of T7 promoter primer. The primer and the template were denatured by incubating the reaction at 65^{O}C for 10min and placing on ice for 5min. Following, 8.5µl of cDNA Master Mix was added and the samples were incubated first at 40^{O}C in a circulating water bath for 2h and then at 65^{O}C in a heating block for 15min to inactivate MMLV-RT. Following that time, the samples were incubated on ice for 5min.

cDNA Master Mix composition: 4µl of 5X First strand buffer, 0.1M DTT 2µl, 10mM dNTP mix 1µl, 1µl of MMLV-RT and 0.5µl of RNaseOUT.

2.4.4.2.2 Fluorescent cRNA synthesis: in vitro trasnscription and incorporation of fluorochromes

To each sample tube, either 2.4µl of 10mM cyanine 3-CTP (sample) or 2.4µl of 10mM cyanine 5-CTP (Stratagene Universal Human Reference RNA) was added and mixed. Following, to each sample, 57.6µl of Transcription Master Mix was added an incubated in a circulated water bath at 40^{O}C for 2h. Following amplification and labeling, each sample was assessed on the Nanodrop ND-1000 to measure yield and specific activity.

Transcription Master Mix composition: 15.3µl of Nuclease-free water, 20µl of 4X Transcription buffer, 0.1M DTT 6µl, 8µl of NTP mix, 50% PEG 6.4µl, 0.5µl of RNase OUT, 0.6µl of Inorganic pyrophosphatase and 0.8µl T7 RNA Polymerase.

2.4.4.2.3 Hybridization

cRNA target was prepared as follows: 0.75µg cyanine 3-labeled, linearly amplified sample cRNA was mixed with 0.75µg cyanine 5-labeled, linearly amplified reference pool cRNA, 50µl of 10X control targets and Nuclease-free water to final volume of 240µl. The hybridization solution was prepared by adding 240µl of 2X target solution to 10µl of 25X fragmentation buffer. The mixture was incubated at 60^{O}C in the heating block for 30min. Following, 250µl of 2X hybridization buffer (from In situ Hybridization kit) to the final volume of 500µl, mixed, spinned and 490µl of the hybridization solution was applied to 60-mer Agilent 44K (or 4X 44K) Human Whole Genome oligonucleotide microarrays and assembled in microarray hybridization chamber (G2534A). Once fully assembled, the chambers were loaded into the hybridization rotator rack and set to rotate at 4rpm. The hybridization was performed in a rotating oven at 60^{O}C for 17h.

All the washing steps were performed at room temperature. First the sandwiched slides were submerged in Wash Solution 1 to remove oligo microarray slide. The slides were washed for 1min in the Wash Solution 1 with the magnetic stir. The slides were then transferred to the staining dish containing Wash Solution 2 and washed for 1min. Following, the slides were transferred to the staining dish containing the Wash Solution 3 and washed for 30sec. All steps were performed in the dark. The dried slides were scanned with a G2565BA Microarray Scanner System (Agilent Technologies, Palo Alto, CA).

Wash solution 1 composition: 6X SSPE, 0.005% N-Lauroylsarcosine, deionized nuclease free water.

Wash solution 2 composition: 0.06X SSPE, 0.005% N-Lauroylsarcosine, deionized nuclease free water.

The buffers 1 and 2 are passed through a 0.2μm sterile filtration unit before use.

Wash solution 3 composition: The Agilent Stabilization and Drying Solution contain an ozone scavenging compound dissolved in acetonitrile.

2.4.4.2.4 Data analysis

The data were processed and normalized with the use of Feature Extraction (v.9.0) software. In HDACi (vorinostat) study each time point was additionally normalized to time 0 and genes with more than 30% of missing values were discarded. The preprocessing was performed using bioinformatics tools developed at the Bioinformatics Unit at CNIO (Gene Expression Pattern Analysis Suite (GEPAS), available at http://gepas.bioinfo.cnio.es).

2.4.5 MicroRNA expression microarrays

2.4.5.1 Agilent v. 1.0

2.4.5.1.1 Labeling

100ng of total RNA were hybridized onto an Agilent 8x15K Human microRNA Microarray Kit for the detection of 470 human and 64 viral microRNAs, following the manufacturer's instructions (Agilent Technologies). Briefly, this procedure consisted of a RNA dephosphorylation step where the mixture of 100μg RNA, 10X CIP Buffer and CIP (16U/μl) was incubated at 37^{O}C for 30min. Following, a denaturation step was performed through addition of DMSO to samples carried out at 100^{O}C for 5min. Samples were then treated with T4 ligase (15U/μl) and labeled with Cy3 at 16^{O}C for 2h. The reaction was performed in a total volume of 20μl. Subsequently, RNA was purified with Bio-spin 6 columns (BioRad, Hercules, CA) and dried in a speed vacuum (45^{O}C, 45min).

Ligation master mix compostition: 10X T4 ligase Buffer 2μl, 0.1% BSA 2μl, pCp-Cy3 3μl and T4 ligase diluted (15U/μl)* 1μl.

2.4.5.1.2 Hybridization

Labeled RNA was resuspended in the appropriate volume of hybridization mix (H_2O 18μl, blocking agent 4.5μl and hybridization buffer 22.5μl) to a final volume of 45μl and incubated at 100^{O}C for 5min, quickly cooled and pipetted into the 8X gasket, closed with the Agilent 8x15K Human miRNA platform, and locked with the appropriate support. Hybridization was carried out at 55^{O}C for 20h at 20rpm. After that time the slides were washed first with WB1 buffer and then with WB2 buffer. Both washing steps were performed at 37^{O}C for 7min each,

with shaking. Finally, the array was submerged in acetonitrile for 1min and dried. The arrays were scanned for Cy3 fluorescence with a G2565BA Microarray Scanner System (Agilent Technologies, Palo Alto, CA).

2.4.5.1.3 Data analysis

The data were extracted using Feature Extraction (v.9.0) software. Following, the average values of the replicate spots of each miRNA were background subtracted, normalized, and subjected to further analysis. microRNA was normalized using Loess within array normalization and quantile between-array normalization. microRNAs were retained when present in at least 30% of samples, (meaning the miRNAs were measured as present in at least the smallest group in the dataset) and when at least 30% of the miRNA had fold change of more than 1.5 from the gene median. Following the data was analyzed using the bioinformatics tools described in section 2.4.6.

2.4.6 Bioinformatics tools

2.4.6.1 Significance Analysis of Microarrays (SAM)

Significance Analysis of Microarrays (SAM) (Tusher et al., 2001), was performed for analysis of miRNA/genes significantly different between two classes (e.g. normal vs. cancer) in which case the t-test statistics was used (PTCL study). SAM calculated a score for each miRNA/gene on the basis of the change in expression relative to the standard deviation of all measurements. In PUVA +/- IFNα study stastistics based on the Cox model was used to identify genes correlated with overall response. SAM calculated the score for each gene by measuring the strength of its correlation with response. The aforementioned score is the maximum-likelihood score statistic from Cox-s proportional hazards model (Cox score).

A threshold of q-value ≤ 0.01 (PTCL study) and ≤ 0.25 (PUVA +/- IFNα study) was used and 1000 permutations were applied. The genes with >20% missing values were excluded. The biological functions of the significant genes, were assigned using the Gene Ontology (www.geneontology.org), EntrezGene, EntrezOMIM (http://www.ncbi.nlm.nih.gov/entrez/), Genecards (Rebhan et al., 1997; Rebhan et al., 1998) databases and using Ingenuity Pathways Analysis v.6.3 (Ingenuity Systems, Inc., Redwood City, CA, U.S.A.) (www.ingenuity.com).

2.4.6.2 Gene Set Enrichment Analysis (GSEA)

Gene Set Enrichment Analysis (GSEA) (Mootha et al., 2003; Subramanian et al., 2005) was performed to test for the sets of related genes that could be correlated with peripheral T-cell lymphoma pathogenesis (PTCL study) or PUVA +/- IFNα therapy resistance (PUVA +/- IFNα study). Briefly, this method identifies predefined database gene sets that are associated with phenotypic differences utilizing t-test statistics. Genes with >30% of missing values were excluded. We used the modified Biocarta database (www.biocarta.com) enriched in pathways derived from the literature and other databases, known to be involved in lymphoma pathogenesis. The rank positions of all members of the sets were identified, enrichment score was calculated and random class permutations (1000 permutations) were performed. Taking into consideration the low number of samples (29 patients) in PUVA +/- IFNα study and their uneven phenotypic distribution, the GSEA was used for stating and testing the hypothesis rather than for statistical analysis in this study.

2.4.6.3 Connectivity Map (cMap)

Identification of molecules (drugs) that could reverse the gene expression signatures associated with poor prognosis and drug resistance (PUVA +/- IFNα study) was performed using Connectivity Map (Lamb et al., 2006) (also known as cMap). cMap is a collection of genome-wide transcriptional expression data from cultured human cells treated with bioactive small molecules and simple pattern-matching algorithms that together enable the discovery of decisive functional connections between drugs, genes and diseases through the transitory feature of common gene expression changes. Enrichment of both the up- and downregulated genes from the submitted gene expression profiles for each treatment were estimated using a metric based on the Kolmogorov-Smirnov statistic and combined to produce the connectivity score (Lamb et al., 2006).

2.4.6.4 Short Time Series Expression Miner (STEM)

Assignment of genes to temporal expression profiles and detection of statistically enriched gene families within each profile was conducted using Short Time Series Expression Miner (STEM)(Ernst et al., 2005). Briefly, STEM implements a novel clustering method that depends on a set of distinct and representative short temporal expression profiles and each probe in the dataset is assigned to a profile with the closest match. The expected number of probes assigned to each profile is estimated by permutation and the statistically significantly over-expressed profiles are then identified. Genes were deemed to be upregulated or

downregulated if the expression change was at least 2-fold and the correlation between the duplicate arrays for each gene was at least 0.8. The p-values derived from STEM analysis were corrected for multiple hypotheses testing using a FDR of < 0.05. The significant genes were annotated and classified using FatiGO+ (Al-Shahrour et al., 2004) and Ingenuity Pathway Analysis software v.6.3 (Ingenuity Systems, Inc., Redwood City, CA, U.S.A.)

The significant genes were clustered by average linkage clustering using Cluster (Eisen et al., 1998) and visualized by TreeView v.1.6 (EisenSoftware, Berkley, CA). Interaction networks in PTCL study were depicted using Cytoscape bioinformatics software (Shannon et al., 2003) (www.cytoscape.org).

2.5 Fundamental molecular biology techniques

2.5.1 Bacterial Strains

Plasmids were produced in the TOP10 *E. coli* strain (Invitrogen) having the following genotype: F^- *mcr*A Δ(*mrr-hsd*RMS-*mcr*BC) ϕ80*lac*ZΔM15 ΔlacX74 *deo*R *rec*A1 *ara*D139 Δ(*ara-leu*)7697 *gal*U *gal*K *rps*L *end*A1 *nup*G and grown in low-salt Luria Bertani (LB) medium.

2.5.1.1 Production of chemicompetent cells

The TOP10 E. coli cells were pre-cultured in 10ml of LB medium (10g/l de triptone, 5g/l of yeast extract, 10g/l de NaCl, pH 7.0) at 37^{O}C, overnight with shaking. This culture was inoculated in 300ml of LB (1ml of miniculture for 100ml of LB medium) and incubated at 37^{O}C until the optical density at 600nm reached approximately 0.6. The culture was cooled on ice during 30min with ice-cold Cl_2Mg (100mM, 150ml). Following the mixture was centrifuged at 3,000 x g during 15min at 4^{O}C and cell pellet resuspended in 75ml of ice-cold $CaCl_2$ 100mM. Next, 30ml of 50% glycerol was added and the aliquots of 200-300μl were frozen immediately in liquid nitrogen and stored at -80^{O}C until use.

2.5.1.2 Transformation of chemicompetent cells

The necessary aliquots of chemicompetent cells were thawed on ice and the adequate quantity of plasmid DNA was added (1ng of plasmid for each kilobase in the gene of interest). Typically, 1μl of plasmid DNA is mixed with 100μl of bacteria. The mixture was incubated for 30min on ice and then placed in heat block previously set at 42^{O}C for 30sec. After that time, 250μl of SOC medium (20g/l de triptone, 5g/l of yeast extract, NaCl10mM, KCl 2.5mM, $MgCl_2$

10mM, $MgSO_4$ 10mM, glucose 20mM) was added and the mixture was incubated at 37^{O}C for 1h with shaking (350rpm) to allow expression of antibiotic resistance gene. Part of the culture (50-100μl) was spread over LB-agar plates containing appropriate antibiotics (ampicillin at a concentration of 100μg/ml). The plates were incubated at 37^{O}C for 14-16h. The obtained colonies were analyzed through restriction digestion of plasmid DNA and conserved at -80^{O}C in liquid culture LB medium with 20% glycerol.

2.5.2 Purification of DNA from agarose gel

The extraction of the DNA from agarose electrophoresis gel band was performed using QIAQuick Gel Extraction Kit (Qiagen). This system is based on the selective DNA adsorption to silico gel QIAQuick membrane. Briefly, the DNA fragment was excised from agarose gel and weighted. Following, three volumes of Buffer QG for 1 volume of gel were added and incubated at 50^{O}C for 10min to completely dissolve the gel. Next, the sample was applied on the QIAQuick column (to bind DNA) and centrifuged at 10,000 x g for 1min. After washing with Buffer PE, the DNA was eluted with H_2O.

2.5.3 DNA digestion with restriction enzymes

Typically, a mixture (of the total volume 20-50μl) containing 1-5μg of DNA, 2 units of enzyme per microgram of DNA, buffer appropriate for the enzyme mixture diluted to a concentration 1X in distilled water was prepared. The mixture was incubated during 1-3 hours at 37^{O}C and analyzed through running on electrophoresis gel.

2.5.4 Ligation

The ligation reactions were prepared by mixing purified restriction fragments (up to 7μl volume), 1μl of T4 DNA ligase (Invitrogen) and 2μl of enzyme reaction buffer (5X). The mixture was incubated at 16^{O}C for 12-16 hours and transformed in chemicompetent cells TOP10.

2.5.5 Miniprep plasmid purification

A small-scale isolation of plasmid DNA from bacterial culture was performed with the use of Wizard Plus SV Minipreps DNA Purification System (Promega Madison, WI) based on alkaline protease lysis procedure. This step is performed to inactivate endonucleases and nonspecifically degrade proteins, thus reducing the overall level of protein contaminants. The liquid culture (2-3ml) was grown in selective medium (LB supplemented with 100μg/ml ampicillin) during 14-16h at 37^{O}C with shaking. Cells were harvested by centrifugation for 5min

at 10,000 x g and thoroughly resuspended in 250μl of Cell Resuspension Solution (CRA). Next, 250μl of Cell Lysis Solution (CLA) was added, mixed by inverting the tube and incubated until the cell suspension cleared (1-5min). Following 10μl of Alkaline Protease Solution was added, mixed and incubated for 5min. The mixture was then neutralized by addition of 350μl of Neutralization Solution (NSB) and bacterial lysate was centrifuged at maximum speed in microcentrifuge for 10min at room temperature. The cleared lysate was transferred to the prepared Spin Column and centrifuged at the maximum speed for 1min. The Spin Column was then washed with 750μl of Column Wash Solution (CWA) (previously diluted with 95% ethanol). Finally, the plasmid DNA was eluted with 100μl of Nuclease-Free Water.

Composition of Buffers and Solutions

LB medium: casein peptone 10g, yeast extract 5g, NaCl 5g, agar (for plates only) 15g. Dissolved in 1L of distilled water, autoclaved and cooled to 55ºC before adding antibiotic.

Cell Resuspension Solution (CRA): 50mM Tris-HCL pH 7.5, 10mM EDTA pH 8.0, RNase A 100μg/ml.

Cell Lysis Solution (CLA): NaOH 0.2M, SDS 1%.

Neutralization Solution (NSB): 4.09M guanidine hydrochloride pH 4.8, potassium acetate 0.759M, glacial acetic acid 2.12M. Final pH of approximately 4.2.

Column Wash Solution (CWA): potassium acetate 162.8mM, 22.6mM Tris-HCl pH 7.5, 0.109mM EDTA pH 8.0. 35ml of 95% ethanol was added before use.

2.5.6 Maxiprep plasmid purification

A bigger-scale isolation of plasmid DNA from *E.coli* culture volume of 100-200ml of LB broth was performed using PureYield™ Plasmid Maxiprep System (Promega Madison, WI) following the manufacturer's instructions. Mainly, 100-200ml of transformed *E.coli* bacterial cell culture in selective medium (LB supplemented with 100μg/ml ampicillin) was grown overnight (16-21 hours) at 37^{O}C with shaking. The cells were pelleted by centrifugation at 5,000 x g for 10min and resuspended in 12ml of Cell Resuspension Solution (composition of all buffers and solutions can be found in the section 2.5.5). All steps of centrifugation were performed in Avanti J-25 centrifuge (Beckman) at 4^{O}C. Following, 12ml of Cell Lysis Solution was added, mixed gently and incubated for 3min at room temperature. The mixture was neutralized with 12ml of Neutralization Solution and mixed thoroughly to ensure complete precipitation of cellular debris. The lysate was centrifuged at 14,000 x g for 20min at room temperature in a fixed-angle rotor. Vacuum DNA purification has been performed by passing the supernatant

through PureYield™ Clearing Column assembled on the top of PureYield™ Maxi Binding Column to which membrane DNA binds. When all lysate has passed through both columns the PureYield™ Maxi Binding Column was washed with 5ml Endotoxin Removal Wash (prepared by adding 5.5ml (for 2 preps system) of isopropanol to the Endotoxin Removal Wash). Then the column was washed with 20ml of Column Wash and dried through applying vacuum for 5min. For DNA elution, the PureYield™ Maxi Binding Column was placed into a new 50ml disposable plastic centrifuge tube, 1.5ml of Nuclease-Free Water was added to the DNA binding membrane and the column was centrifuged in a swinging bucket rotor at 2,000 x g for 5min. The eluate was collected from the 50ml tube. Both the washing as well as elution steps were performed at room temperature.

2.6 Protein based techniques

2.6.1 Antibodies

The antibodies utilized in the present work together with its origin, type, clone, application, dilution and manufacturer are shown in Table 11.

Table 11. Characteristics of the antibodies used.

Antibody	Species	Type	Clone	Dilution	Manufacturer
BCL2	mouse	monoclonal	124	1:50 (IHC)	DakoCytomation
A20	mouse	monoclonal	59A426	1:50 (IHC)	Active Motif
CTSL2	mouse	monoclonal	----	1:50 (IHC)	Alexis Biochemicals
TRAF1	mouse	monoclonal	H-3	1:50 (IHC)	Santa Cruz Biotechn.
JUNB	mouse	monoclonal	C-11	1:50 (IHC)	Santa Cruz Biotechn.
STAT1	mouse	monoclonal	C-136	1:50 (IHC)	Santa Cruz Biotechn.
STAT3	mouse	monoclonal	F-2	1:50 (IHC)	Santa Cruz Biotechn.
STAT4	rabbit	polyclonal	C-20	1:50 (IHC)	Santa Cruz Biotechn.
ZAP70	goat	polyclonal	M-20	1:50 (IHC)	Santa Cruz Biotechn.
Ac-H2A	rabbit	polyclonal	----	1:2000 (WB)	Upstate
H2A	rabbit	polyclonal	----	1:2000 (WB)	Upstate
Ac-H2B	rabbit	polyclonal	----	1:400 (WB)	Abcam
H2B	rabbit	polyclonal	----	1:2000 (WB)	Upstate
Ac-H3	rabbit	polyclonal	----	1:20000 (WB)	Upstate
H3	rabbit	polyclonal	----	1:2000 (WB)	Abcam
Ac-H4	rabbit	polyclonal	----	1:2000 (WB)	Upstate
H4	rabbit	polyclonal	----	1:2000 (WB)	Upstate
p-ZAP70(Tyr493)	rabbit	polyclonal	----	1:1000 (WB)	Cell Signaling
p-ZAP70(Tyr319)/ SYK (Tyr352)	rabbit	polyclonal	----	1:1000 (WB)	Cell Signaling

ZAP70	goat	polyclonal	M-20	1:500 (WB)	Santa Cruz Biotechn.
p-AKT (Ser473)	rabbit	monoclonal	D9E	1:1000 (WB)	Cell Signaling
AKT	rabbit	polyclonal	----	1:1000 (WB)	Cell Signaling
p-ERK (p44/p42, Tyr204)	mouse	monoclonal	E-4	1:500 (WB)	Santa Cruz Biotechn.
ERK2	mouse	monoclonal	4C11C11C4	1:500 (WB)	Santa Cruz Biotechn.
BTLA	mouse	monoclonal	185B/E9	1:50 (IHC)	CNIO
PD-1	mouse	monoclonal	NAT105	1:50 (IHC)	CNIO
CD30	mouse	monoclonal	CON6D/B9	1:50 (IHC)	CNIO
CD10	mouse	monoclonal	56C6	1:50 (IHC)	DakoCytomation
ALK	mouse	monoclonal	ALK1	1:50 (IHC)	DakoCytomation
CXCL13	goat	polyclonal	BCA-1	1:50 (IHC)	R & D Systems
CD3	rabbit	polyclonal	----	1:50 (IHC)	DakoCytomation
CD56	mouse	monoclonal	123C3	1:50 (IHC)	DakoCytomation
FOXP3	mouse	monoclonal	206D/G7	1:50 (IHC)	CNIO
EBER	mouse	monoclonal	CS.1-4	1:50 (IHC)	DakoCytomation

2.6.2 Protein extraction

2.6.1.1 Histones extraction

Histones were obtained from cell lines treated with vorinostat and from respective DMSO controls. Histones were isolated by acidic extraction in 0.25M HCl and precipitation with acetone as previously described (Turner and Fellows, 1989). Briefly, 10^7 cells were harvested, washed with PBS and incubated overnight in 200µl of 0.25M HCl at 4^{O}C with shaking. For histone precipitation eight volumes of acetone were added to the supernatant, and histones were pelleted by centrifugation and washed with acetone. Histones were air-dried and resuspended in 0.25M HCl for subsequent immunoblot analysis.

2.6.2.2 Total protein extraction

Total protein extracts were prepared by lysing cells in RIPA lysis buffer (Sigma-Aldrich) containing protease inhibitor cocktail set III (Calbiochem, San Diego, CA) plus protease inhibitor cocktail set VIII (Calbiochem) for 20min on ice. Cell debris was removed by centrifugation (10,000 x g, 10min, 4^{O}C). The supernatant (protein extract) concentration was measured using Protein assays reagents A, B, and S (BioRad, Hercules, CA) following the manufacturer's instructions using bovine serum albumin (BSA) as a standard. Briefly, 1ml of Agent A was mixed with 20µl of Agent S. First, the adequate amount of either standard (BSA) or sample was applied to each well of 96-well plate, following 25µl of previously prepared

mixture was added. Finally, 200µl of Agent B was added and the whole preparation was incubated for 15min at RT and measured at a wavelength of 750nm.

Composition of RIPA buffer: : 150mM NaCl, 1.0% IGEPAL® CA-630, 0.5% sodium deoxycholate, 0.1% SDS, and 50mM Tris, pH 8.0. Just before use the protease inhibitor cocktail was added: 0.1mM sodium vanadate, 5µg/ml leupeptine, 5µg/ml aprotinine, 1mM phenylmethylsulphonyl fluoride (PMSF).

2.6.3 Western blotting

Histone acetylation was determined by Western Blot against acetyl forms of histones H2B (Abcam, Cambridge, UK), H2A, H3 and H4 (Upstate, Lake Placid, NY). Total histones H3 (Abcam), H2A, H2B and H4 (Upstate) were used as controls.
For phosphorylation studies the following primary antibodies has been used: p-ZAP70(Tyr493), p-ZAP70 (Tyr319)/SYK (Tyr352), p-AKT (Ser473), AKT (Cell Signaling Technology, Beverly, MA) and ZAP70 (Santa Cruz Biotechnology, Santa Cruz, CA). Antibody to α-tubulin was from Sigma Chemicals Co. (St. Louis, MO). Complete list of antibodies and dilutions used is presented in Table 11.
Western Blotting was performed according to standard protocols. First, the protein extracts were subjected to electrophoresis on sodium dodecyl sulfate polyacrylamide (SDS-PAGE) gels using the acrylamide concentration adequate for the size of the detected proteins (15% - histones and 10% - phosphoproteins) using Mini-Protean 3 system (BioRad).

Electrophoresis buffer 5X composition: TrisHCl 0.13M, glycine 0.95M, SDS 0.5%.
Sample buffer (Laemmli buffer) 4X composition: 62.5mM TrisHCl pH 6.8, glycerol 20%, SDS 2%, 2-mercaptoethanol 5%, bromophenol blue 0.025%.

Following electrophoresis, the proteins were wet-transferred onto nitrocellulose membranes (Whatman, Dassel, DE) using Mini Trans-Blot Cell equipment (BioRad). Transference was performed at 40mA during 12-20h at room temperature or 400mA during 1.5h at 4^{O}C.

Transference buffer 10X composition: TrisHCl 0.025M, glycine 0.2M, 20% of methanol

Membranes were blocked in PBS-T (phosphate-buffered saline with 0.1% Tween-20) during 1h with shaking and sequentially immunoprobed with primary antibodies at adequate dilution. Anti-histone antibodies were diluted in 5% milk PBS-T while anti-phospho antibodies were diluted in 5% BSA PBS-T. Antibody detection was performed using fluorescent-labeled

secondary antibodies (Alexa 680λm and Alexa 800λm, Rockland, Gilbertsville, PA, USA) and scanned with Odyssey Infrared System Scanner (LI-COR Biosciences, Lincoln, NE, USA). Band intensities were quantified using the ImageJ 1.34S software (National Institute of Health, Bethesda, MD, USA).

2.6.4 Immunohistochemistry

Immunohistochemical techniques were performed on paraffin-embedded tissue sections taken from 35 pre-treatment samples of patients included in the randomised clinical trial of PUVA vs. PUVA/IFNα treatment and 10 inflammatory dermatoses (ID) cases. All immunostaining was performed using the TechMate 500 (DAKO-Cytomation) automatic immunostaining device following LSAB Visualization System protocol (*labeled streptavidin-biotin*; DAKO). The slices were first dried at 56^{O}C for 16h through consecutive incubations in xylene (2X 10min), ethanol 100% (5min), ethanol 95% (5min), ethanol 70% (5min) and water (2min). A Heat-Induced Epitope Retrieval (HIER) step was performed in a 10mM solution of sodium citrate buffer pH 6.5 with 0.01M tri-sodium citrate solution, and heated for 2min in a conventional pressure cooker. After heating, slides were rinsed in cool running water for 5min. They were then quickly washed in Tris-buffered-saline pH 7.4, and incubated with monoclonal primary antibodies at appropriate dilutions for approx. 40min. The primary monoclonal antibodies used in this study and their dilutions are included in the Table 11.

Following incubation with the primary antibody, immunodetection was performed with biotinylated secondary antibody (25min), followed by peroxidase-labelled streptavidin-biotin (DAKO-Cytomation, Glostrup, Denmark) with diaminobenzidine chromogen as substrate and contrastained with hematoxilin (1min and washed with distilled water). The preparations were dehydrated through consecutive incubations with ethanol 95% (30sec), ethanol 100% (30sec) and xylene (1h), and mounted using automatic mounting Tissue-Tek SCA. Incubation omitting the specific antibody, including incubation including unrelated antibodies, was used as a control of the technique.

2.6.5 Tissue Microarrays

Tissue microarrays (TMAs) are used to analyze the expression of genes simultaneously in multiple individual tissue samples on one slide. TMAs are composed of small 0.6 - 3.0 mm cores of tissue from donor paraffin-embedded tissue blocks which are arrayed at a high density on a slide and are prepared as indicated in Figure 7. All tissues were obtained from the tissue archives of the CNIO Tumor Bank. Tissue Arrayer device (Beecher Instruments, Sun

Prairie, WI) was used to construct tissue microarray (TMA) blocks. All cases were histologically reviewed and representative areas were selected. In each case, 2 selected 1-mm-diameter cylinders from 2 different areas were included, along with 43 different controls to ensure the quality, reproducibility, and homogenous staining of the slides. The biopsies had been taken prior to treatment. The histological criteria used for diagnoses of cases were based on descriptions of the World Health Organization classification (Swerdlow, 2008). Thus, 7 different TMA blocks were constructed, containing a total of 547 cylinders. TMA blocks were sectioned and dried for 16 hours at 56^{O}C before being dewaxed in xylene and rehydrated through a graded ethanol series and washed with phosphate-buffered saline. Antigen retrieval was achieved by heat treatment in a pressure-cooker for 2min in 10mM citrate buffer (pH 6.5). Before staining the sections, endogenous peroxidase was blocked. Immunohistochemical staining was performed on these sections using antibodies described in Table 11. After incubation, immunodetection was performed with the LSAB Visualization System (DAKO, Glostrup, Denmark) employing diaminobenzidine chromogen as a substrate. Sections were counterstained with hematoxylin. The staining of the TMA sections was evaluated by a panel of pathologists using uniform criteria. In order to guarantee the reproducibility of this method, the straightforward and clear-cut criteria were employed. Briefly, the pattern of staining for each Ab was recorded as positive or negative, and high or low expression.

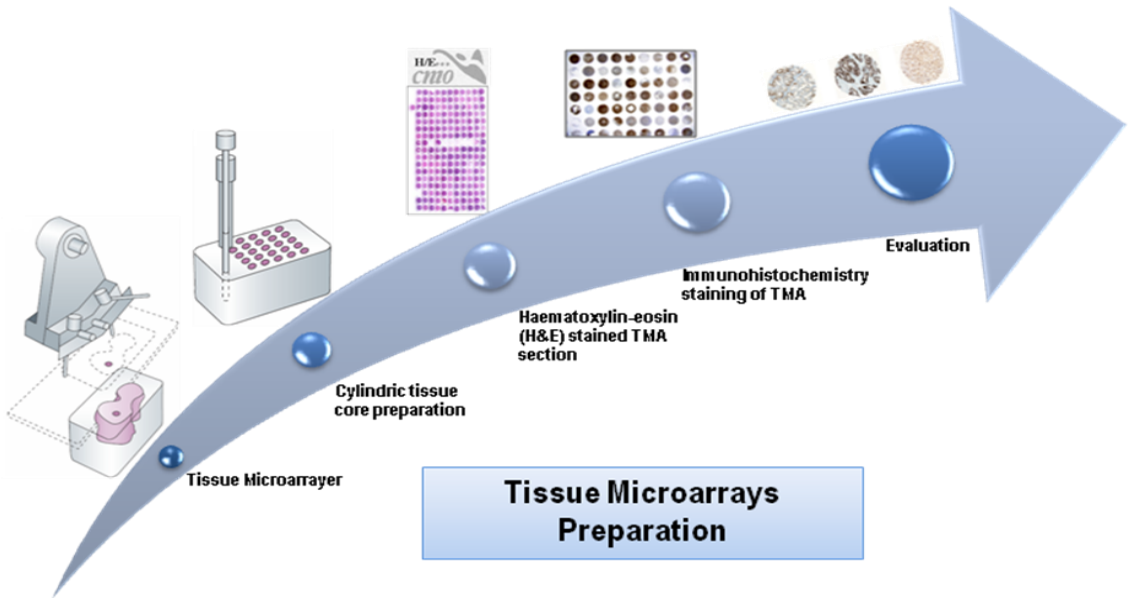

Figure 7. Tissue Microarrays preparation procedure.

2.7 Statistical Analysis

In PTCL study, the association between the different markers and disease specific survival (DSS) was estimated the log-rank test using the SPSS statistical program.

In order to identify statistically significant associations between differentially expressed microRNAs (FDR < 0.01) and gene expression signatures (FDR < 0.01), the analysis of consistency of predicted microRNA-mRNA targeting pairs with the pair components inverse regulation, and nonrandom association of the consistent pairs was performed. Briefly, for each differentially expressed microRNA a contingency table relating the microRNA and its predicted gene targets was produced, taking into consideration whether or not these targets were included in a consistent gene expression signature (downregulated targets for upregulated microRNAs etc.). Those microRNAs (FDR < 0.01) were subjected to Fisher's exact test and selected on the basis of their non-random association with the gene expression signature of interest (FDR < 0.01). Gene target predictions of human microRNAs were obtained from miRBase Targets Release v5.0 and TargetScan v5.1.

In the PUVA +/- IFNα study (MF99 trial), statistical differences between response and treatment arms were assessed using Pearson or Fisher exact statistics. For survival analysis Kaplan-Meier and Cox regression methods were used.

In the HDACi (vorinostat) study, group comparisons of parametric data were made by Student's t-test. Statistical analysis was performed with the SPSS software package, version 13.0 (SPSS, Chicago, IL). The differences were considered significant when the adjusted p-value was smaller than 0.05.

The mean inhibitory concentration 50% (IC50) was calculated using Graph Pad Prism software (sigmoidal dose response, variable slope) (GraphPad, San Diego, CA). Isobologram analyses using the Chou and Talalay method with Calcusyn (Biosoft, Ferguson, MO) were used to determine synergism (Chou and Talalay, 1984). A combination index (CI) value less than 1.0 indicates synergistic effects. A CI value equal to 1.0 indicates additive interactions. A CI value > 1 indicates antagonistic interactions.

RESULTS

RESULTS I

Peripheral T-cell lymphoma – molecular heterogeneity revealed by integrative genomic analysis

Peripheral T-cell lymphoma (PTCL) has been the subject of a relatively limited number of studies to elucidate the molecular pathogenesis. As a result, molecular classification of PTCL is still to be developed, targeted drugs are in very early development and clinical outcome is dismal. Recently, new technologies in genomic analysis have offered the opportunity to improve the knowledge regarding microRNA and gene expression signatures in T-cell lymphoma as well as the potential of microRNAs as prognostic markers in this disease.

Gene expression profiling (GEP) revealed twelve pathways significantly enriched in malignant tissue (FDR<0.1), including the ERK, EGF, CDK5, MET and cytokine induced signaling cascades. GEP data were analyzed trying to correlate the lymphoma cases with the signatures of different T-cell subpopulations including Th1, Th2, T-reg, Th17, T_{FH} and cytotoxic T-cells. The analysis of lymphoma samples revealed a group of 20% of cases with a null phenotype lacking any resemblance to normal T-cell subpopulations. A signature composed of 102 microRNAs was found to be differentially expressed in PTCL compared with reactive lymph node controls (LN), including the let-7 family, mir-10, mir-15, mir-16 and miR-101 ($p<0.0001$). MicroRNA and gene expression profiles of the cases with null-phenotype vs. differentiated-phenotype were compared and it was found that the former group expressed oncogenic microRNAs, such as the miR-17-92 cluster (Oncomir-1) and miR-181 family. In addition, a set of 67 microRNAs was lost in the null-phenotype group (FDR<0.0001). These microRNAs target genes of the insulin like growth factor 1 (IGF-1) pathway and oncogenic Ras family, signaling cascades that have been shown to function as potent proliferation stimuli.

In conclusion, molecular analysis of PTCL, facilitated by the comparison with normal T-cell subpopulations, revealed the existence of a null-phenotype PTCL, characterized by aggressive behavior and expressing a microRNA oncogenic signature. This research suggests possible and novel roles for microRNAs in the diagnosis and pathogenesis of T-cell lymphoma, and identifies promising therapeutic targets

3. Peripheral T-cell lymphoma – molecular heterogeneity revealed by integrative genomic analysis

3.1 Gene expression profile of peripheral T cell lymphomas

To explore the genetic alterations in the pathogenesis of PTCL, microarray analysis was performed comparing PTCL samples to normal lymph node (LN) tissue. The gene set enrichment analysis (GSEA) showed no significant pathways enriched in LN samples. However, the gene expression profile of PTCL series revealed several pathways significantly related to malignancy, 28 pathways with FDR lower than 0.25 among which 13 gene sets with FDR < 0.1 were enriched in PTCL. These included pathways known to be involved in cancer pathogenesis, such as extracellular signal-regulated kinases (MAPK/ERK), epidermal growth factor (EGF), erythropoietin (EPO), mesenchymal-epithelial transition factor (MET), BCL2 and inflammatory cytokine induced signaling cascades. Additionally, several cell cycle related pathways have been identified, such as cell cycle, cyclin-dependent kinase-5 (CDK5), GS, G1, G2 pathways. The complete list of the significant pathways enriched in PTCL is presented in Table 12.

Table 12. Pathways enriched in peripheral T-cell lymphoma identified by gene set enrichment analysis (GSEA).

NAME	SIZE	NOM p-val	FDR q-val
ERK PATHWAY	30	0	0.013
EGF PATHWAY	26	0	0.030
EPO PATHWAY	19	0	0.021
IL3 PATHWAY	15	0.004	0.019
RACCYCD PATHWAY	21	0	0.018
CDK5 PATHWAY	13	0.002	0.021
BCL2 FAMILY	21	0.002	0.050
IL2 PATHWAY	40	0.002	0.046
MET PATHWAY	35	0.004	0.045
IL6 PATHWAY	21	0.007	0.048
STAT3 PATHWAY	8	0.006	0.045
ERK5 PATHWAY	17	0.022	0.075
PROTEASOME PATHWAY	27	0.013	0.096
CXCR4 PATHWAY	23	0.024	0.103
IGF1 PATHWAY	20	0.033	0.112
MAPK PATHWAY	83	0.010	0.135
GS PATHWAY	5	0.043	0.127
MTOR PATHWAY	22	0.026	0.121
CREB PATHWAY	26	0.037	0.124
PLC PATHWAY	8	0.056	0.126
G2 PATHWAY	23	0.046	0.123
CELL CYCLE PATHWAY	22	0.048	0.134
G1 PATHWAY	26	0.060	0.178

VEGF PATHWAY	26	0.065	0.172
IL22BP PATHWAY	11	0.116	0.182
UBIQUITINS METAGENE	5	0.124	0.207
CDC25 PATHWAY	9	0.148	0.228
WNT PATHWAY	24	0.122	0.236

3.2 MicroRNA profile of peripheral T cell lymphomas

To date every type of tumor analyzed by microRNA profiling has shown significantly different microRNA profiles compared with normal cells from the same tissue. Emerging evidence suggests that altered microRNA expression contributes to tumorigenesis. In T-cell lymphoma little information is available regarding microRNA expression levels or the potential of microRNAs as prognostic markers in this disease. Therefore, a systematic miRNA expression profiling analysis of 711 mammalian microRNAs was performed on 20 peripheral T-cell lymphoma (PTCL) samples, including 11 PTCLU and 9 AITL, along with 7 reactive lymph nodes (LN) as a control samples. To identify microRNAs differentially expressed in PTCL compared with the LN, commercial human oligonucleotide microRNA platform from Agilent was used. microRNAs differentially expressed between PTCL and LN samples were identified using unpaired t-test implemented in significance analysis of microarrays (SAM) (Tusher et al., 2001) and permutation tests (10,000 permutations). A signature composed of 102 microRNAs was found to be differentially expressed in PTCL compared with LN, including the let-7 family, mir-10, mir-15, mir-16 and miR-101 (FDR<0.01). All of them were lost in PTCL samples (Figure 8). The complete list of significant microRNAs (FDR<0.01) with its corresponding fold change and FDR values are presented in the Supplementary Table 1. To investigate whether microRNA profiles were informative with regard to clinicopathological parameters, including patient's overall survival (OS), binary linear regression analysis was performed. This analysis identified 4 microRNAs significantly (p-value < 0.05) associated with survival, including miR-128a, miR-375, miR-425-3p and miR-608.

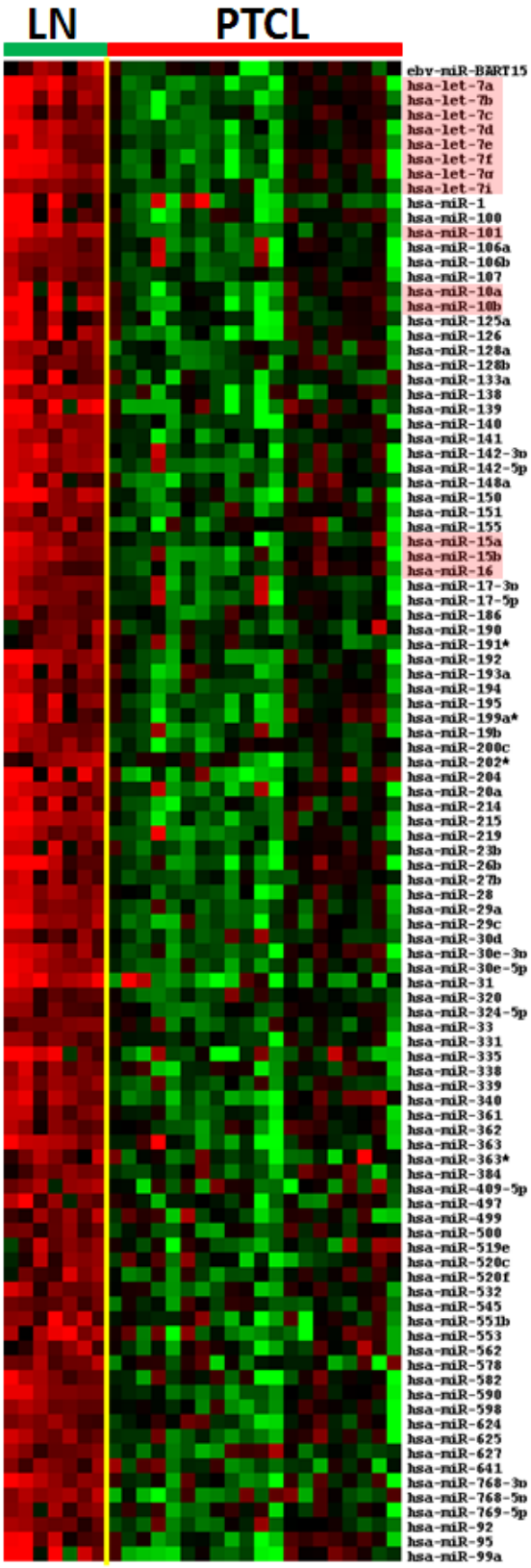

Figure 8. Heatmap representing differentially expressed microRNAs with FDR<0.0001 (SAM analysis) in LN and PTCL samples.

3.3 Association between miRNAs and mRNA signatures

Once the initial observation that microRNAs are differentially expressed within the cohort of patients analyzed so far was made, an integrated analysis of the microRNAs and mRNA expression profiles was carried out to identify putative microRNA targets. In order to identify statistically significant associations between differentially expressed microRNAs and gene expression signatures the consistency of predicted microRNA – mRNA (FDR<0.01) targeting pairs with the pair component inverse regulation was investigated, excluding the random associations. The genes targeted by significant microRNAs were first predicted with miRBase and TargetScan databases and Fisher's exact test was then applied to significant list of microRNAs and genes. These two databases jointly identified 18 microRNAs lost in PTCL with FDR<0.05 on the basis of a significant results of Fisher's exact tests (Figure 9A). Following, the microRNAs targets were filtered on nodes with at least 7 neighbors (within distance 1) to narrow the amount of targets to those genes targeted by higher number of microRNAs using Cytoscape software. Downregulated miRNAs with connections to upregulated genes are represented in the Figure 9B. Of note, microRNAs with the highest number of target genes included miR-607, miR-24 and miR-214 whereas among genes with high degree of connections comprised members of cell cycle pathway (E2F6, CDK6, CCND1), AKT (AKT2) , IGFR (IGF1R) and MAPK (MAP1A) signaling pathways (Figure 9B).

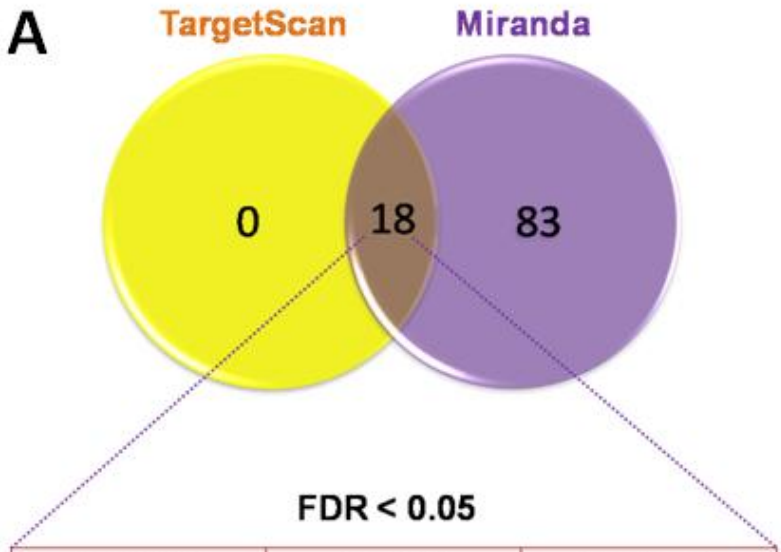

hsa-miR-637	hsa-miR-214	hsa-miR-155
hsa-miR-331-3p	hsa-miR-374a	hsa-miR-384
hsa-miR-142-5p	hsa-miR-28-5p	hsa-miR-339-5p
hsa-miR-340	hsa-miR-562	hsa-miR-15a
hsa-miR-380	hsa-miR-625	hsa-miR-24
hsa-miR-607	hsa-miR-101	hsa-miR-199a-3p

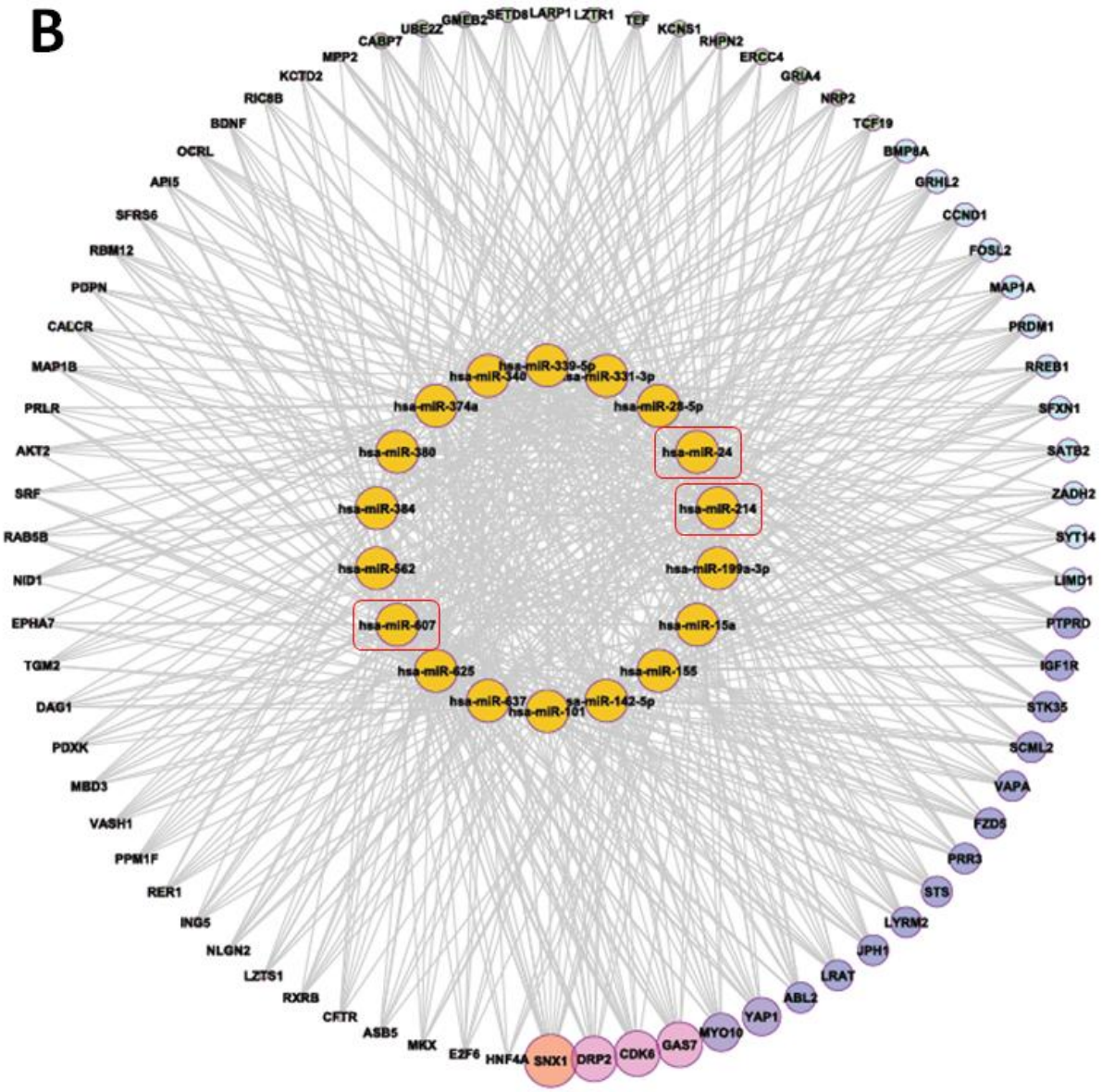

Figure 9. Correlation of significant microRNAs and genes differentially expressed between PTCL samples and LN controls. A) Downregulated miRNAs with connections to upregulated genes were subjected to Fisher analysis applying TargetScan and Miranda databases. Venn diagram represents significant microRNAs (FDR < 0.05) common to both databases. B) Network representing significant microRNAs and their correlation to target genes (filtered on 7 neighbours). miRNAs are indicated by yellow circles, while genes are represented by yellow to red circles (rainbow distribution) depending on the degree of connections. The size of circles representing genes is proportional to their degree of connectivity. Network visualization was performed with the use of Cytoscape software.

3.4 T-cell subsets signature differentiating two subtypes among peripheral T-cell lymphomas

The morphology and immunophenotype of the hematopietic tumors recapitulate the different normal subpopulations that are the counterpart for each type of tumor. The differentiation decision is governed predominantly by the cytokines in the microenvironment and, to some extent, by the strength of the interaction of the T cell antigen receptor with antigen. In normal T cells, upon interaction with cognate antigen, CD8+ T cells differentiate into T cytotoxic subtype, while CD4+ T cells can differentiate into a variety of effector subsets, including classical Th1 cells and Th2 cells, the more recently defined Th17 cells, follicular helper T (T_{FH}) cells, and induced regulatory T (iTreg) cells. Taking into consideration that PTCL is a malignancy of mature T lymphocytes, the hypothesis was stated whether there are any PTCL subtypes that could reflect the heterogeneity of the normal peripheral T-cell subsets and whether using this approach specific PTCL subtypes with distinctive molecular and clinical features could be identified. For this purpose gene expression profiling (GEP) data from a series of twenty PTCL patients was analyzed in attempt to correlate the lymphoma cases with the signatures of different T-cell subpopulations including CD4-positive Th1, Th2, iTreg, Th17, T_{FH} and CD8-positive cytotoxic T-cells. This analysis showed that most of PTCL re-express simultaneously genes that belong to different T-cell lineage subsets, but allowed to identify a subgroup of patients that essentially do not express markers for the specific T cell subpopulations (Figure 10). The PTCL subtypes identified were called differentiated or null-phenotype group, respectively. Furthermore, both groups were characterized on the clinicopathological, microRNA and gene expression level.

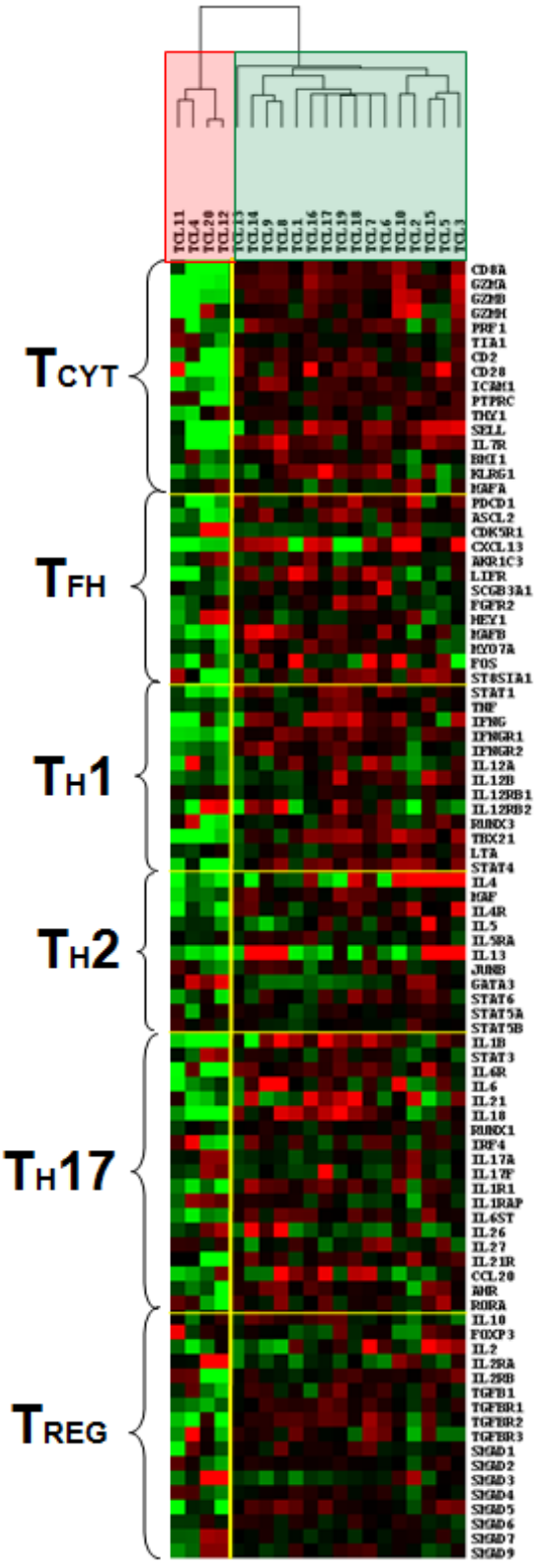

Figure 10. T-cell subsets (Tcytotoxic, T_{FH}, Th1, Th2, Th17 and Treg) signature in PTCL samples. Identification of two subtypes of patients with PTCL, null-phenotype and differentiated group. The tree node containing samples from null-phenotype group is highlighted in red and differentiated group in green.

Interestingly, both null-phenotype as well as differentiated groups were quite heterogeneous with respect to the diagnostics of the cases. While in the differentiated group equal distribution of PTCLU and AITL cases (8 PTCLU, 8 AITL) was observed, in the null-phenotype group PTCLU cases predominated (3 PTCLU, 1 AITL). The group of patients lacking resemblance to normal T cell subpopulations was found of particular interest, hence more attention to characterization of the mentioned group will be paid in this paragraph. Morphologically, in null-phenotype group large and medium-size pleomorphic cells were observed in 3 out of 4 cases (TCL4, TCL11 and TCL12) and typical for AITL small cells in TCL20 case (Figure 11A). The immunohistochemistry analysis revealed that in the group that lacks expression of T cell differentiation related genes, all cases expressed CD3, however, they lacked the genes regulating CD4 and CD8 cells differentiation suggesting other genes involved or their different differentiation level. Some of the cases weakly expressed CD4, despite not being classified as lymphoblastic lymphomas. All cases were negative for CD8, did not express CD56 (excluding the possibility of being NK lymphomas), TdT (excluding leukemias) and ALK (excluding ALCL). Two cases weakly expressed CD30 and all cases were of α/β T cell origin (TCR BF1 positive).

3.4.1 microRNA characterization of null-phenotype vs. differentiated subsets

Following, microRNA expression profiles of the cases with null-phenotype vs. differentiated-phenotype were compared. Of note, half of the patients in the null-phenotype group highly expressed oncogenic miR-17-92 cluster and mir-181 family (Figure 11B). The miR-17-92 cluster has been described to be functionally implicated in fundamental processes of development and cancer by targeting several mRNAs of proteins, regulating proliferation, apoptosis and differentiation (He et al., 2005). Similarly, miR-181-family has been previously found to actively participate in the process of differentiation (Naguibneva et al., 2006). In addition, all cases in this group showed enrichment in several EBV-related microRNAs including ebv-miR-BART4, ebv-miR-BART7, ebv-miR-BART13 and others (Figure 11C). However, approximately 50% of the samples showed upregulation of viral EBV related microRNAs suggesting that this phenomenon is not restricted to null-phenotype group. The tumoral cells in samples belonging to null-phenotype group did not express Epstein Barr-encoded RNA (EBER), hence the viral microRNA expression was ascribed to B cell blast (EBER+).

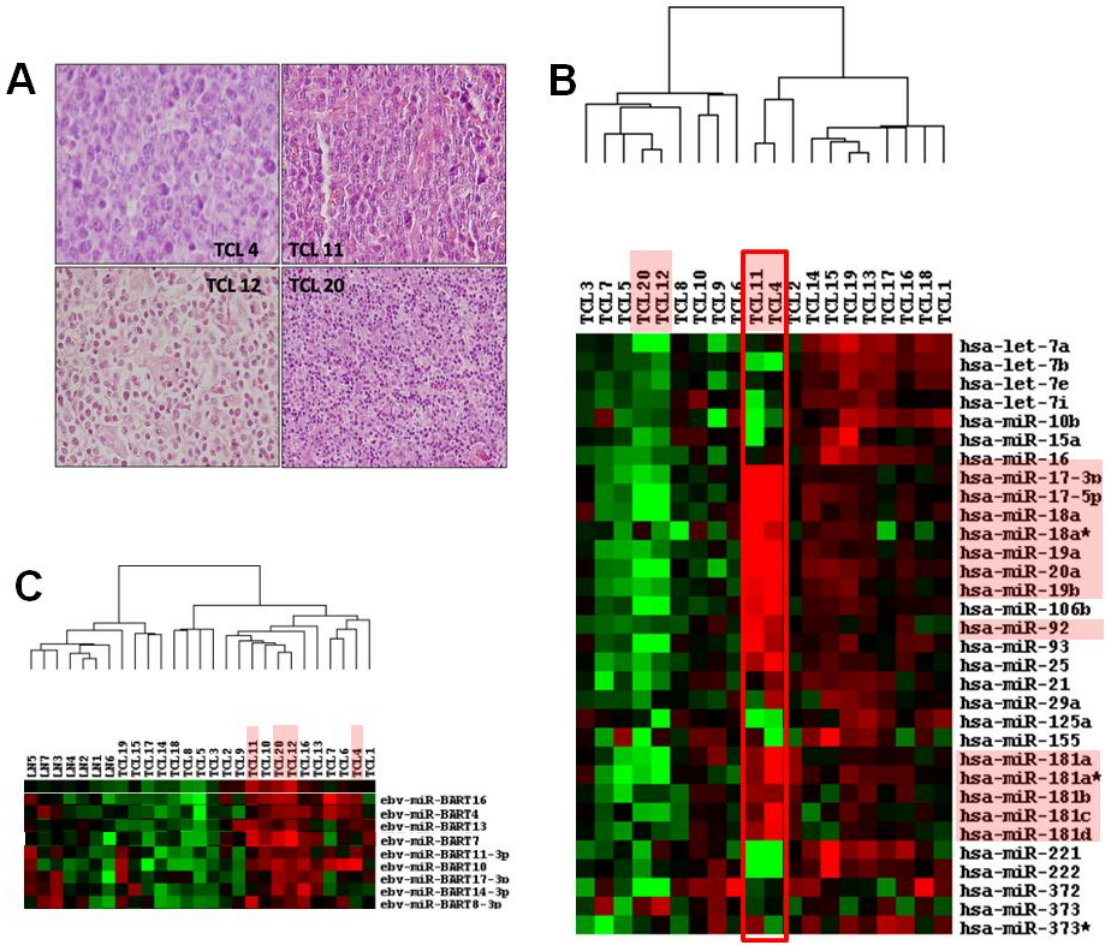

Figure 11. Characterization of null-phenotype vs. differentiated group of PTCL patients. A) Morphological assessment of patients constituting null-phenotype group (TCL4, TCL11, TCL12, TCL20) by hematoxylin-eosin stain. B) Heatmap representing high oncogenic microRNAs overexpression in two cases belonging to null-phenotype group: miR-17-92 cluster and miR-181 family (highlighted n red). C) Enrichment of Epstein Barr virus-related microRNAs in null-phenotype group.

In T cells, microRNAs have been shown to be key regulators of the lineage induction pathways, and to have strong role in the induction, function and maintenance of the T-cell lineage. In this context, the possibility whether the differences in microRNA expression could contribute to the distinct phenotypes of those two groups was investigated. Indeed, approximately 120 microRNAs were found to be differentially expressed (FDR<0.01), of those 67 had FDR-values lower than 0.0001. Among significant microRNAs 86 were upregulated and 34 microRNAs were downregulated in the differentiatied group. These included miR-223, miR-100, miR-498, miR-622, miR-610, miR-584, miR-518c and miR-510 which target genes of the insulin like growth factor 1 (IGF-1) pathway and oncogenic Ras family, signaling cascades that have been shown to function as potent proliferation stimuli (Figure 12).

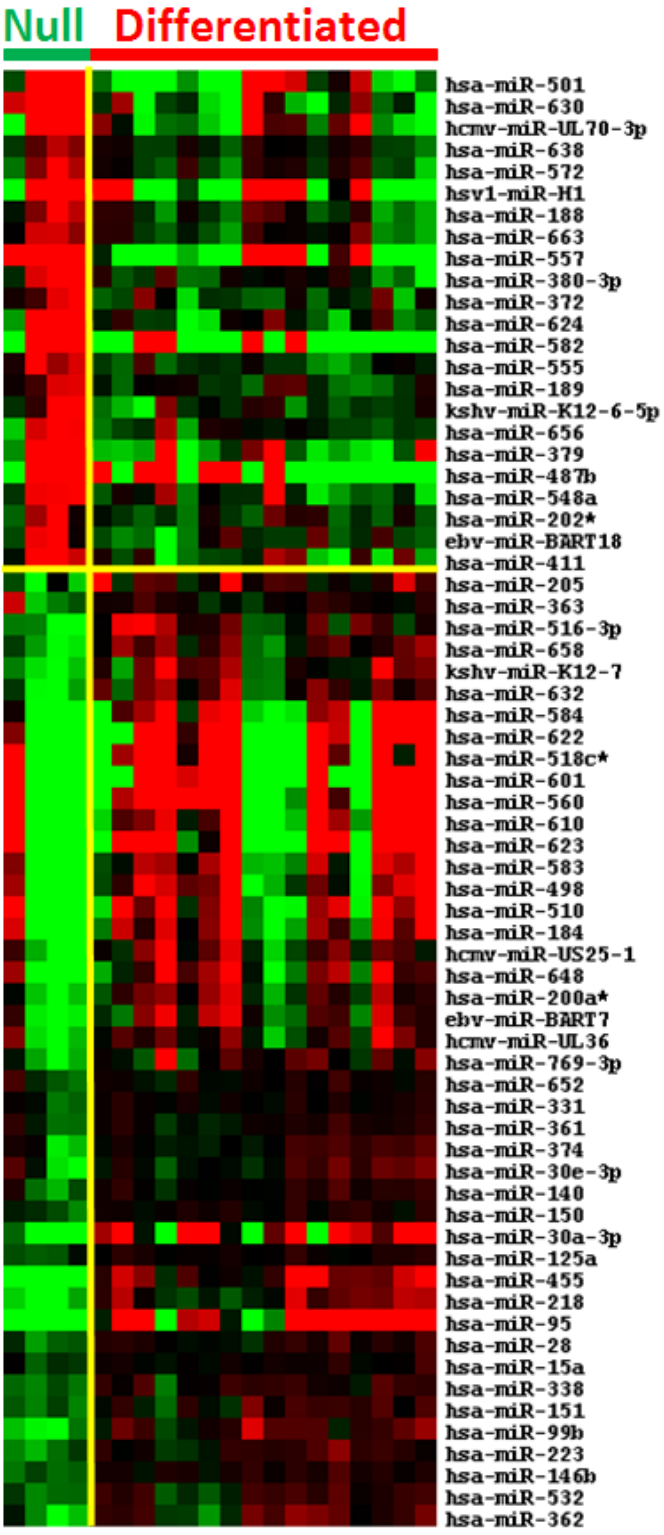

Gene ID	Fold Change	FDR - q value [%]
hsa-miR-501	0.131	0
hsa-miR-630	0.285	0
hcmv-miR-UL70-3p	0.286	0
hsa-miR-638	0.658	0
hsa-miR-572	0.550	0
hsv1-miR-H1	0.002	0
hsa-miR-188	0.512	0
hsa-miR-663	0.556	0
hsa-miR-557	0.042	0
hsa-miR-380-3p	0.336	0
hsa-miR-372	0.414	0
hsa-miR-624	0.337	0
hsa-miR-582	0.000	0
hsa-miR-555	0.386	0
hsa-miR-189	0.571	0
kshv-miR-K12-6-5p	0.352	0
hsa-miR-656	0.468	0
hsa-miR-379	0.258	0
hsa-miR-487b	0.000	0
hsa-miR-548a	0.471	0
hsa-miR-202*	0.448	0
ebv-miR-BART18	0.267	0
hsa-miR-411	0.294	0
hsa-miR-205	2.302	0
hsa-miR-363	1.494	0
hsa-miR-516-3p	2.347	0
hsa-miR-658	2.064	0
kshv-miR-K12-7	2.288	0
hsa-miR-632	2.150	0
hsa-miR-584	12.345	0
hsa-miR-622	1760.908	0
hsa-miR-518c*	49.389	0
hsa-miR-601	173147.513	0
hsa-miR-560	6157.129	0
hsa-miR-610	12.383	0
hsa-miR-623	495.797	0
hsa-miR-583	4.477	0
hsa-miR-498	6.011	0
hsa-miR-510	5.896	0
hsa-miR-184	3.319	0
hcmv-miR-US25-1	2.440	0
hsa-miR-648	3.067	0
hsa-miR-200a*	2.090	0
ebv-miR-BART7	2.406	0
hcmv-miR-UL36	2.239	0
hsa-miR-769-3p	2.058	0
hsa-miR-652	1.281	0
hsa-miR-331	1.267	0
hsa-miR-361	1.288	0
hsa-miR-374	1.505	0
hsa-miR-30e-3p	1.680	0
hsa-miR-140	1.470	0
hsa-miR-150	1.316	0
hsa-miR-30a-3p	33.372	0
hsa-miR-125a	1.240	0
hsa-miR-455	5.673	0
hsa-miR-218	2.321	0
hsa-miR-95	36.629	0
hsa-miR-28	1.453	0
hsa-miR-15a	1.232	0
hsa-miR-338	1.451	0
hsa-miR-151	1.453	0
hsa-miR-99b	2.140	0
hsa-miR-223	1.490	0
hsa-miR-146b	1.363	0
hsa-miR-532	1.478	0
hsa-miR-362	1.912	0

Figure 12. Expression patterns of microRNAs found to be significantly differentially expressed between null-phenotype and differentiated group. The heatmap represents only microRNAs with FDR-values < 0.0001 with indicated fold changes.

3.4.2 Identification of genes and pathways distinguishing two groups of patients

Consistently, Significance Analysis of Microarray (SAM) allowed identification of a total of 1439 differentially expressed genes, 1128 downregulated and 311 upregulated genes in null-phenotype vs. differentiated group. Many genes were targets of microRNAs that have been found to distinguish both groups. Significant differentially expressed genes (FDR < 0.01) were associated with T cell signaling and differentiation. Furthermore, gene set enrichment analysis (GSEA) was applied to identify gene sets correlated with the two groups of patients. Using a false discovery rate (FDR) of ≤ 0.25, 36 significant gene sets were found. Many of these gene sets were, as expected, related to inflammatory cytokine function and apoptosis. Due to the low number of samples in the null-phenotype group, only one pathway was found to be significantly enriched in this group of patients. Consistently with the microRNA results as outlined above, GSEA analysis demonstrated RACCYCD (Ras and Rho) pathway enrichment in the null-phenotype group (FDR = 0.175). This result could partly explain the increased proliferation of neoplastic cells in the null-phenotype group. Moreover, some genes of the RACCYCD pathway, such as E2F1 are targets of oncogenic microRNAs. In contrast, approximately 35 gene sets were significantly enriched in the differentiated group. These included cytokine (Inflammatory/Cytokine, IL4, IL5, IL7, IL12, IL10, IL18, IL22BP) and T cell subsets (Th1, T cytotoxic, Th2 and CD8-cells) related pathways. Besides, GSEA identified a number of pathways that mediated cell survival, proliferation and growth that were enriched in differentiated group, such as NFKB and RELA pathways that has previously been related to better prognosis in PTCLU, cell death and apoptosis related BCL2 family, caspase and death pathways. Moreover, B cell, dendritic cell (DC) and natural killer cell (NK) signaling, possibly contributed by the tumor microenvironment, were also found to be enriched in a group of patients with differentiated phenotype. By GSEA, the gene set designated “NOTCH signaling pathway” showed the regulation pattern of differentiated group. The TNFR and IFN response (IFNG and IFNA) pathways are involved in the expression of many inflammatory cytokines/chemokines. Among highly ranked genes, Toll like receptor 1 and TALL1, another upstream activators of NFKB were noticed. The complete list of enriched gene sets is presented in Table 13.

Table 13. Pathways significantly enriched in null-phenotype and differentiated group identified by gene set enrichment analysis (GSEA).

Gene sets enriched in the null-phenotype group			
NAME	**SIZE**	**NOM p-val**	**FDR q-val**
RACCYC PATHWAY	21	0.008	0.175

Gene sets enriched in the differentiated group			
NAME	**SIZE**	**NOM p-val**	**FDR q-val**
NKT PATHWAY	25	0	0
TH1 PATHWAY	14	0	0
INFLAMMATORY/CYTOKINE PATHWAY	22	0	3.75E-04
DC PATHWAY	17	0	0.001
IL12 PATHWAY	20	0	0.002
T CYTOTOXIC PATHWAY	15	0.002	0.005
IL10 PATHWAY	12	0.005	0.005
IL18 PATHWAY	6	0	0.005
NFKB PATHWAY	36	0	0.005
IL22BP PATHWAY	11	0	0.005
CTL PATHWAY	10	0.002	0.009
IFNG PATHWAY	6	0	0.011
B LYMPHOCYTE PATHWAY	8	0.003	0.012
TH2 PATHWAY	7	0.007	0.031
BCR PATHWAY	33	0.009	0.045
NOTCH PATHWAY	6	0.014	0.046
CD8 CELLS	6	0.007	0.050
IL5 PATHWAY	7	0.015	0.050
IL7 PATHWAY	16	0.027	0.067
CASPASE PATHWAY	21	0.043	0.077
CCR5 PATHWAY	17	0.048	0.081
TOLL PATHWAY	33	0.026	0.083
NK CELLS PATHWAY	19	0.024	0.088
MAPK PATHWAY	82	0.011	0.088
IL4 PATHWAY	11	0.046	0.089
TALL1 PATHWAY	15	0.041	0.091
DEATH PATHWAY	32	0.047	0.092
TNFR PATHWAY	39	0.048	0.099
RELA PATHWAY	15	0.101	0.149
TCR PATHWAY	10	0.089	0.151
IFNA PATHWAY	8	0.107	0.154
IL3 PATHWAY	14	0.105	0.155
BCL2 FAMILY	20	0.136	0.190
IL17 PATHWAY	11	0.112	0.201

3.5 Validation of selected genes by tissue microarrays

Some of the most significant gene expression data have been validated in Tissue Microarrays (TMA) on a extended number of 275 PTCL samples. So far, five markers have been evaluated in TMA, which includes three genes upregulated in the differentiated group (BTLA, STAT1, NFATC1) and two genes upregulated in the null-phenotype group (TOP2A, GATA3). The genes were selected based on its significance (FDR values) in SAM analysis, fold change and the biological function. As shown in Figure 13A, all genes were able to clearly distinguish between null-phenotype and differentiated group. The initial analysis comparing the percentage of cases that expressed or not a specific marker was compared and related to the percentage of null-phenotype patients in the hybridized cases. Most of the markers selected (GATA3, BTLA, STAT1 and NFATC1), except TOP2A, roughly corresponded with the expected values regarding positive or negative expression (Figure 13B). B and T lymphocyte associated gene (BTLA) was used as a surrogate marker differentiating two subgroups of patients and from all the markers selected gave the closest match of TMA results and gene expression data (Figure 13B-D). BTLA, a gene induced during T cell activation with a gradual inhibitory effect on TCR signaling, was found to be 44 times upregulated in a differentiated group. Based on TMA analysis lack of BTLA expression in 29% of samples was observed. This number approximately corresponds to the percentage of null-phenotype patients, which is 20%. Signal transducer and activator of transcription 1 (STAT1), a member of JAK/STAT pathway, was found to be lost in 32% of patients. Furthermore, loss of nuclear factor of activated T-cells, cytoplasmic, calcineurin-dependent 1 (NFATC1) was detected in 14% of patients. In addition, loss of expression of GATA binding protein 3 (GATA3), an important regulator of T-cell development, was observed in majority of cases (92%). Topoisomerase (DNA) II alpha (TOP2A) has been previously found to be a member of proliferation signature and related to shorter survival of PTCL patients (Cuadros et al., 2007) and is the only gene which did not correspond with the microarray data. However, higher percentage of patients with no or less than 25% expression (36.4%) trend has been observed for this gene.

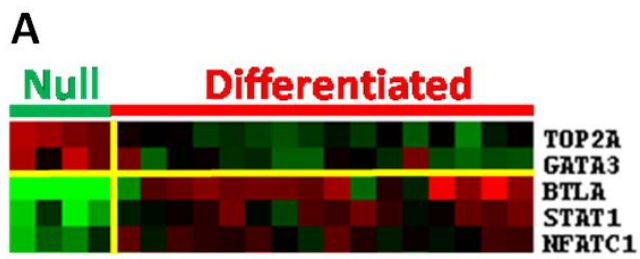

Gene name	Fold change	FDR
TOP2A	0.227	0
GATA3	0.289	0.0059
BTLA	44.601	0
STAT1	4.408	0
NFATC1	3.746	0

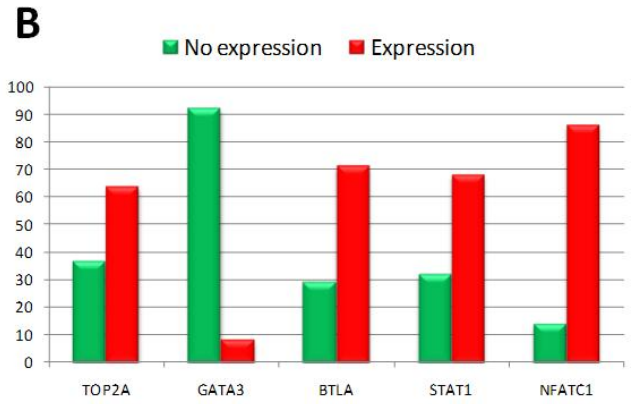

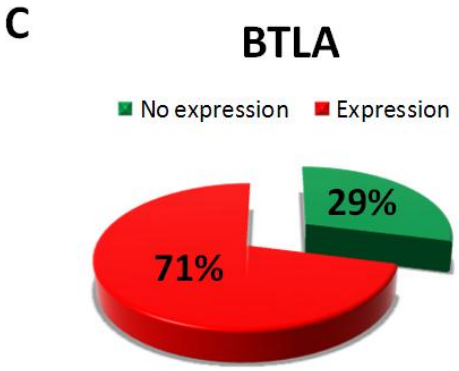

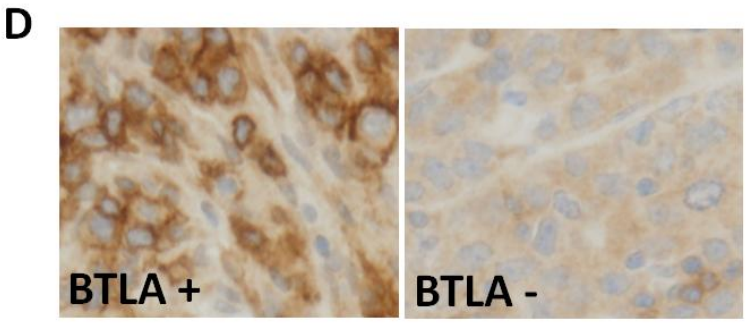

Figure 13. Validation of gene expression profiling by Tissue Micoarrays. A) Heatmap and table representing fold change and significance of the genes selected for validation. B) Chart showing the percentage of cases expressing or not the selected markers overexpressed in null-phenotype group (TOP2A, GATA3) and differentiated group (BTLA, STAT1, NFATC1). The analysis was performed on the total of 275 PTCL cases included in the Tissue Microarray. C) Pie chart representing BTLA expression in PTCL patients. D) Immunohistochemistry images presenting examples of BTLA staining considered positive (left panel) or negative (right panel).

RESULTS II

PUVA ± IFNα treatment resistance in MF: the role of tumor microenvironment, NF-κB and TCR pathways

Interferon alpha (IFNα) is widely used in the treatment of Mycosis Fungoides (MF) and when used in combination with photo-chemotherapy (PUVA), both improved response and duration of complete remission have been reported. However, in spite of encouraging results of the initial studies, currently there are no specific prognostic factors enabling prediction of patients' resistance to treatment. In order to identify factors responsible for resistance to PUVA +/- IFNα treatment in MF patients, the gene expression profiling of pre-treatment samples from 29 MF patients enrolled in a randomized clinical trial was analyzed using cDNA microarrays. A Cox model (SAM) and Gene Set Enrichment Analysis (GSEA) were used for identification of genes and biologically significant pathways related to resistance to treatment. Genes involved in NF-κB signaling, T-cell receptor (TCR) signaling, cytokine signaling and proliferation were differentially expressed between responders and non-responders. Interestingly, expression of markers representative of those pathways was found not only in the tumoral cells, but also in specific subpopulations of macrophages, dendritic cells and other non-neoplastic cell types constituting the tumor microenvironment, likely involved in the promotion of survival and proliferation of cutaneous T-cell lymphoma. Some pro-inflammatory factors such as NF-κB, inflammatory cytokines and their receptors in addition to TCR associated molecules could be promising, targets for MF treatment. Furthermore, the resistance-associated signature was connected to the drug-associated profiles using Connectivity Maps (cMaps) in order to identify molecules that could potentially reverse a drug resistance signature. This screen indicated that Hsp90 inhibitors (17-AAG, geldanamycin) and HDAC inhibitors match the PUVA +/- IFNα sensitivity profile.

4. PUVA ± IFNα treatment resistance in MF: the role of tumor microenvironment, NF-κB and TCR pathways

4.1 Patient characteristics

The MF99 randomized study of early-stage MF patients testing the efficacy of PUVA vs. PUVA + IFNα showed similar response rates of both regimens. Twenty nine pre-treatment samples (PUVA: 18 patients; PUVA + IFNα: 11 patients) from patients enrolled in MF99 randomized clinical trial were profiled in order to assess the genes related and pathways involved in good or poor response to the treatment. The clinical trial protocol allowed 24 weeks of treatment, which was a rational cut-off used to distinguish between good and poor responders. Complete remission (CR) was defined as disappearance of all clinically detectable disease manifestations. After 24 weeks, 22/29 patients achieved CR, 4/29 did not respond to therapy and 3/29 progressed. The patients treated with PUVA alone showed similar response rates to the patients treated with the combination of PUVA and IFNα. Of 12 patients subjected to PUVA + IFNα therapy, 9 obtained CR, 2 did not and 1 progressed (Table 14). Of 22 patients that obtained CR, 20 patients experienced a relapse (median duration of CR: 66 weeks). Previous treatments had no statistical relationship with therapy response. Since both treatment arms showed similar response rates, the 29 pre-treatment samples (PUVA: 18 patients; PUVA + IFNα: 11 patients) from both arms were combined in one analysis, in order to assess the genes related to and pathways involved in sensitivity or resistance to treatment. Clinical and pathologic characteristics of patients enrolled are summarized in Table 14.

Table 14. Clinical and Pathologic Characteristics of Patients

Patient characteristics		All Patients (N=29) No. of patients (%)	Responders (N=22) No. of patients (%)	Non-Responders (N=7) No. of patients (%)	P-value
Gender	Male	12 (41)	7 (32)	5 (71)	
	Female	17 (59)	15 (68)	2 (29)	0.080
Age	Median (years)	52	52	45	
	Range (years)	18-78	21-78	18-62	
	<40	8 (28)	5 (23)	3 (43)	
	40-59	12 (41)	9 (41)	3 (43)	
	>59	9 (31)	8 (36)	1 (14)	0.445
Stage	IA	14 (48)	10 (45)	4 (57)	
	IB	6 (21)	3 (14)	3 (43)	
	IIA	9 (31)	9 (41)	0 (0)	0.074
Skin Phototype	II	3 (10)	3 (14)	0 (0)	
	III	26 (90)	19 (86)	7 (100)	0.421
β2-microglobulin*	Median	0.05	0.05	0.05	
	Range	0.03-0.42	0.03-0.26	0.05-0.42	
	≤0.05	13 (45)	11 (50)	2 (29)	
	>0.05	4 (14)	3 (14)	1 (14)	0.579
Soluble IL-2R*	Median	1118	871	1252	
	Range	0-3260	0-3260	1148-2001	
	≤1118	9 (31)	9 (41)	0 (0)	
	>1118	9 (31)	5 (23)	4 (57)	0.041
Extension	Median (%BS)	10	10	8.5	
	Range (%BS)	1.5-44	2-33	1.5-44	
	≤10%	14 (48)	11 (50)	3 (43)	
	>10%	15 (52)	11 (50)	4 (57)	0.542
Accum. PUVA*#	Median	60.81	48.69	122.65	
	Range	19.32-570	22.38-570	19.32-250.65	
	≤60	14 (48)	13 (59)	1 (14)	
	>60	15 (52)	9 (41)	6 (86)	0.049
Previous Treatments	None	13 (45)	10 (45)	3 (43)	
	Yes	16 (55)	12 (55)	4 (57)	0.626
Previous Treatments	No PUVA and/or IFNα	19 (66)	14 (64)	5 (71)	
	PUVA and/or IFNα	10 (34)	8 (36)	2 (29)	0.541
Treatment distribution	PUVA	17 (59)	13 (59)	4 (57)	
	PUVA+IFNα	12 (41)	9 (41)	3 (43)	0.631
Results					
CR at 24 weeks	Yes	22 (76)	22 (100)	0 (0)	
	No	7 (24)	0 (0)	7 (100)	
Time to CR	Median (weeks)	16	13	---	
Duration of CR	Median (weeks)	93	66	---	

Abbreviations:* There is no data available for some patients; # J/CM^2 of received PUVA dose; CR: Complete Remission; BS: Body Surface.

4.2 Identification of genes correlated with response to PUVA +/- IFNα treatment

To identify a gene expression profile correlated with the prediction of response to PUVA +/- IFNα treatment, the SAM bioinformatics tool based on the Cox model was used. This method identified a total of 52 probes corresponding to 42 unique genes significantly associated with therapy response, 4 of which were associated with good response to treatment and 38 of which were related to poor response or resistance (Table 15) (q-value $\leq$ 0.25). The genes significantly overexpressed in the responders group included: *CTSL2* (cathepsin L2), *ENTPD6* (ectonucleoside triphosphate diphosphohydrolase 6), *PSMD2* (proteasome 26S subunit) and *LHFPL2* (lipoma HMGIC fusion partner-like 2).

The genes that were associated with the non-responder group are related to a wide range of processes favoring growth, differentiation, migration, proliferation and survival of malignant cells and tumor accompanying cells, such as *ENG, TNC, WNT4, CD69, NFKB2, FYN* and *ELF4*. Most of these genes have previously been described as being upregulated in several tumors and many of them are involved in regulation of transcription (*ASH1L, LRRFIP1, UBTF, IRF2BP*, and *CRI1*) and signal transduction. Several genes, such as *CH25H, HSXIAPAF1, NFKB2, SOCS1, FYN, MAF, PFN1,* and *STOM* show mutual interactions. These genes either regulate each other or are regulated by the factors involved in pathways known to be involved in the pathogenesis of MF, such as the NF-κB pathway and associated cytokine genes (*IL2, IL4, IL6, IL7, IL8, IL10* and *IL13*). In addition, T-cell receptor signaling, TNF and the JAK/STAT pathway were also implicated (www.ingenuity.com).

4.3 Identification of signaling pathways associated with resistance to PUVA +/- IFNα treatment in MF clinical samples

To examine the possibility that the response or resistance to treatment might be associated with the alterations in biological pathway signaling or co-regulated gene sets rather than with individual genes, gene set enrichment analysis (GSEA) was performed. Genes were rank-ordered from highest to lowest by degree of differential expression (using t-test) between the R and NR groups. A heat map of the 50 best scoring genes in each group is shown in Figure 14. GSEA identified 79 gene sets meeting the gene set size criteria (min=1, max=500 genes) that were used in the analysis.

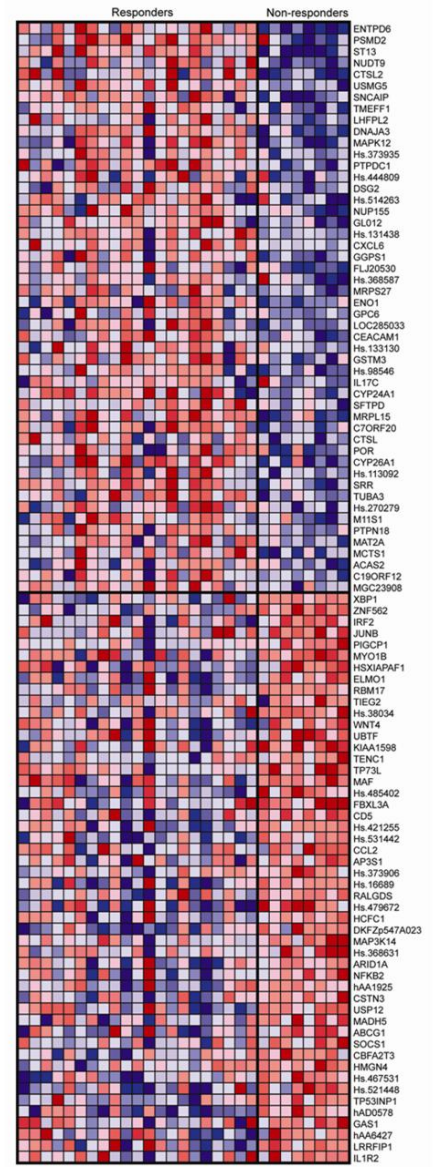

Figure 14. The gene expression heat map of the 29 MF patient samples including 22 responders and 7 non-responders to treatment. The heat map shows an expression data set sorted by correlation with response (t-test) of the 50 genes with the best enrichment score in each group.

Twenty-two pathways potentially associated with good response to treatment were identified in this analysis, including apoptosis and cell-cycle regulation. The apoptosis pathway genes included *TRAF6*, *CASP9*, *survivin* (*BIRC5*) and *NME2* involved in the caspase cascade and intrinsic apoptosis pathways. The main cell-cycle genes included cyclins, cyclin-dependent kinase inhibitors (CDKNs) and transcription factors controlling cell-cycle. The top-score genes included *CDC25A, CDKN2B, E2F1, CDC25C, CHEK1* and the CDK5 pathway enriched in *NGFR, CDK5 and MAPK3* (Table 15).

Table 15. Genes and pathways associated with good response

GENES (SAM)	FUNCTION	GSEA PATHWAYS	GENES GSEA
CTSL2	Cathepsin, lysosomal cysteine proteinase	Apoptosis (8)	BIRC5, CASP9, NME2, TRAF6
		ACE2 Signalling (4)	AGT, COL4A6
		B-Lymphocyte Signalling (2)	CR2, ICAM1
		Caspase Signalling (10)	BIRC4, CASP9
		CDC25 Signalling (6)	CDC25A, CDC25C, CHEK1, WEE1
		CDK5 Signalling (8)	CDK5, MAPK3, NGFR
		CK1 Signalling (8)	CDK5, PPP1R1B, PRKAR1A, PRKAR2B
		EGF Signalling (17)	EGF, MAPK3, RASA1, PIK3R1
		EGFR/SMRTE Signalling (6)	EGF, RARA
		G1 Cell Cycle Pathway (21)	CDC25A, CDKN2B, DHFR, E2F1, HDAC1, TGFB2
		G2 Cell Cycle Pathway (14)	BRCA1,CHEK1, CDC34, CDC25A, CDC25C, MDM2, WEE1
		IGF1 Signalling (12)	IGF1, MAPK3, PIK3R1, RASA1
		IL10 Signalling (9)	BLVRB
		Lymphocyte Signalling (6)	ICAM1, ITGA4, SELP
ENTPD6	Purine and pyrimidine metabolism		
PSMD2	Proteasome regulatory subunit, Ubiquitination, TNF signalling		
LHFPL2	Lipoma HMGIC fusion partner		

[a]Correlation between all analyses used in the study showing genes significantly associated with treatment response (SAM), gene functions and where applicable, GSEA pathways enriched in good or bad response signatures, including gene set size (in parentheses) and genes enriching particular GSEA pathways.

Among the pathways associated with poor response to treatment, gene sets related to cytokine inflammatory responses and T helper 2 (Th2) cell response promotions were identified, including T-cell activating pathways through IL2R, inflammatory IL6 signaling involved in STAT3 activation and IL3 and IL7 signaling pathways implicated in the cell survival and proliferation signals necessary for T-cell development. IL2 signaling (enriched by *IL2RB, IL2RG, SOCS1, CFLAR, JAK3, JUN, PIK3CA, HRAS, PTPN6, SOS1, SYK, SOCS3, BCL2, NMI*) can not only activate T-cells and stimulate their proliferation but could also block T-cell apoptosis through several pathways including activation of anti-apoptotic BCL-xL. This activation of T-cell signaling could lead to upregulation of the NF-κB pathway associated gene set (NOM p=0.053), including genes such as *NIK* (*MAP3K14*), *A20* (*TNFAIP3*), *IKBA* (*NFKBIA*), *NEMO* (*IKBKG*) and *TGF1*α (*MAP3K7*) and NF-κB target genes (*NFKB2*, *TNFAIP3*, *TRAF1*, *ID2*, *CXCL9* and *BIRC3*).

Table 16. Genes and pathways associated with poor response

GENES (SAM)	FUNCTION	GSEA PATHWAYS	GENES GSEA
NFKB2	NFKB subunit	NFKB Signalling (23)	BIRC3, TRAF1, MAP3K7, NFKBIA, CXCL9, TNFAIP3, ID2, NFKB2, IKBKG, MAP3K14
CH25H#	Cholesterol/ lipid metabolism		
SOCS1*	Negative regulation of JAK/STAT signalling	IL4 Signalling (4)	IL2RG, JAK3
MAF*	Transcription regulation, Oncogene		
STOM#	Stomatin, cation conductance	IL6 Signalling (14)	HRAS, IL6R, JAK3, JUN, SOS1, STAT3
RGL1#	Rho GTPase	TNFR Signalling (24)	CASP8, IKBKG, JUN, MAP3K7, MAP3K14, NFKB1A, PRKDC, TANK, TNFAIP3, TRAF1, TRAF3
		CCR5 Signalling (6)	CCL2, CCR5, CXCL12, JUN, MAPK14, PRKCA
		Cytokines (2)	CCL2, CXCL9
		FAS Signalling (12)	CASP8, CFLAR, DAXX, FAF, JUN, MAP3K7, PRKDC
		IL2 Signalling (27)	BCL2, CFLAR, HRAS, IL2RB, IL2RG, JAK3, JUN, LCK, NMI, PIK3CA, PTPN6, SOCS1, SOCS3, SOS1, SYK
		IL3 Signalling (9)	CSF2RB, HRAS, SOS1, PTPN6
		IL7 Signalling (13)	BCL2, CREBBP, FYN, IL2RG, JAK3, LCK, NMI, PIK3CA
		MTOR Signalling (12)	EIF3S10, EIF4A1, EIF4A2, MKNK1, PIK3CA, RPS6
		NOTCH Signalling (2)	ADAM17, FURIN
		Plasma Cell Differentiation (1)	XBP1
		Regulatory T-cell Signalling (7)	CD4, IL2RB, PDCD1
AI429215	Unknown		
ANTXR1	Anthrax toxin receptor, Tumor endothelial marker		
ARHE	Rho family GTPase, Cell adhesion, Actin cytoskeleton organization and biogenesis		
ARL2BP	ADP-ribosylation factor binding protein		
ASH1L	Histone methyltransferase, Transcription regulation		
CCNL1	Transcriptional regulation, splicing, candidate proto-oncogene, cell cycle control		
CD69	Lymphocyte proliferation, Signal transduction		
CRI1	Negative regulation of transcription		
DSP	Cytoskelton organization		
ELF4	ETS family transcription factor, development and function of NK and NK T-cells		
ELMO1	Engulfment and cell motility 1		
ENG	Angiogenesis, Cell adhesion		
EVI2A	Ecotropic viral integration site, Transmembrane receptor activity		
FBXO9	Ubiquitin-protein ligase activity		
FYN	oncogene related to SRC, FGR, YES, T-cell signaling regulation, control of cell growth		
HSXIAPAF1#	BIRC4/XIAF binding protein		
IPO8	Nuclear protein import, Ran GTPase binding, Signal transduction		
IRF2BP2	Ubiquitin cycle, Interferon regulatory factor 2-binding protein		
LRRFIP1	Transcriptional repressor, Regulation of TNF, EGFR and PDGFA expression		
MBNL1	Development, mRNA splice site selection		
MYO1B	Cell migration, vesicular transport		
PAPD5	DNA polymerase, DNA repair, Cell cycle control		
PCDHB10	Protocadherin beta 10 precursor, Cell adhesion		
PFN1	Profilin, Actin binding, transcription regulation, cytoskeleton organization and biogenesis		
RBM17	Splicing		
SAT	Enzyme which catalyzes the acetylation of polyamines, regulation of polyamine transport, transferase activity		
TNC	Cell adhesion, signal transduction, cell communication		
TNKS2	Vesicle trafficking and sub-cellular distribution, Regulation of telomere length, Transferase activity, Regulation of body size		
UBTF	Transcription activation		

USP12	Ubiquitin specific protease
WNT4	Development, Signal transduction, Cell-Cell signalling, Extracellular matrix structural constituent
ZNF521	Zinc finger protein

[a]Correlation between all analyses used in the study showing genes significantly associated with treatment response (SAM), gene functions and where applicable, GSEA pathways enriched in good or bad response signatures, including gene set size (in parentheses) and genes enriching particular GSEA pathways. [b]Genes regulated by each other. [c]Core genes with the highest enrichment score (ES) in the GSEA pathway.

GSEA also highlighted gene sets in poor responders correlated with chemokine receptors that are differentially expressed by different T-cell subsets and play a role in T-cell migration and homing, including *CCL2, CXCL12* and *CCR5.* CCR5 is associated with homing to inflamed tissues and together with CCR3 is abundantly expressed on T-helper cells (Table 16). Finally, the immunosuppressive T-regulatory cell pathway, Notch, mTOR and FAS pathways have been found to be enriched in the group of patients with poor treatment outcome.

4.4 Involvement of NF-κB activation, TNF signaling and Th2 inflammatory cytokine signaling in poor response of MF patients to treatment

Two different systems for analysis of the expression profiles of patients undergoing treatment in the PUVA +/- IFNα randomized clinical trial were used. These systems apply different approaches such as: expression of particular genes in relation to time to CR (Cox model: SAM) and enrichment of pathways with genes overexpressed in good or bad responders (t-test: GSEA). Both bioinformatic methods used to identify genes and gene sets significantly associated with response to treatment have pinpointed several common pathways. Upregulation of NF-κB pathway genes and inflammatory cytokines related to T-cell signaling (mainly Th2) seemed to play a central role in the poor response to treatment. There appear to be important mutual interactions between pathways indicated by both bioinformatics tools. The upregulation of IL2, IL3, IL4, IL6 and IL7 signaling pathways could lead to activation and proliferation of T lymphocytes and the activation and enrichment of the TNF receptor pathway could jointly cause the activation of NF-κB leading to growth, proliferation and survival of malignant cells. The remaining pathways identified by only one of the approaches such as mTOR or CCR5 pathways could enhance the effect triggered by NF-κB, TNF signaling or cytokine signaling and contribute to proliferation and migration of the neoplastic cells.

4.5 Immunohistochemical evaluation of the expression of representative genes related to response to therapy

The results obtained from the gene expression analysis were further validated at the protein level by immunohistochemistry (IHC) on MF samples and ID controls, for markers representative of the pathways identified by GSEA as follows: (1) NF-κB pathway: A20 (TNFAIP3) and TRAF1 and apoptosis-related targets of NF-κB pathway (BCL2); (2) JAK/STAT and TCR signalling: STAT1, STAT3, STAT4, ZAP70; (3) immune response: CTSL2 and (4) oncogenes: JUNB.

Interestingly, the genes selected were expressed not only by the tumoral cells, but also by specific subpopulations of macrophages, dendritic cells and other non-neoplastic accompanying cell types present in MF. Three of the markers — antiapoptotic BCL2, TCR-signal transducer ZAP70 and NF-κB target A20 — were expressed mainly by tumoral cells, and their expression could drive tumor proliferation and apoptosis escape. The remaining markers were expressed not only by neoplastic cells but also in the cytoplasm of macrophages (TRAF1, STAT4) and nucleus of epithelial cells (JUNB). The expression of markers implicated in the JAK⁄STAT pathway (STAT3, STAT1) and immune response (CTSL2) was absent in the malignant cells of MF cases but present in macrophages and dendritic cells (Figure 15A). Cytoplasmic and nuclear expression of STAT3 were observed, the latter suggesting the presence of the constitutive active form of the protein in accompanying cells.

In inflammatory dermatitis (ID) control cases (psoriasis, psoriasiform dermatitis and spongiotic dermatitis), STAT1, STAT3, TRAF1, STAT4 and CTSL2 were observed only in nonlymphoid cells such as dendritic cells, histiocytes, macrophages and epithelial cells, while JUNB was found in both stroma and lymphocytes. Furthermore, expression of those markers found only in the surrounding cells in ID cases was usually less intense (Figure 15B) compared with MF, with the exception of chronic inflammatory diseases such as lichen planus, which showed comparable expression.

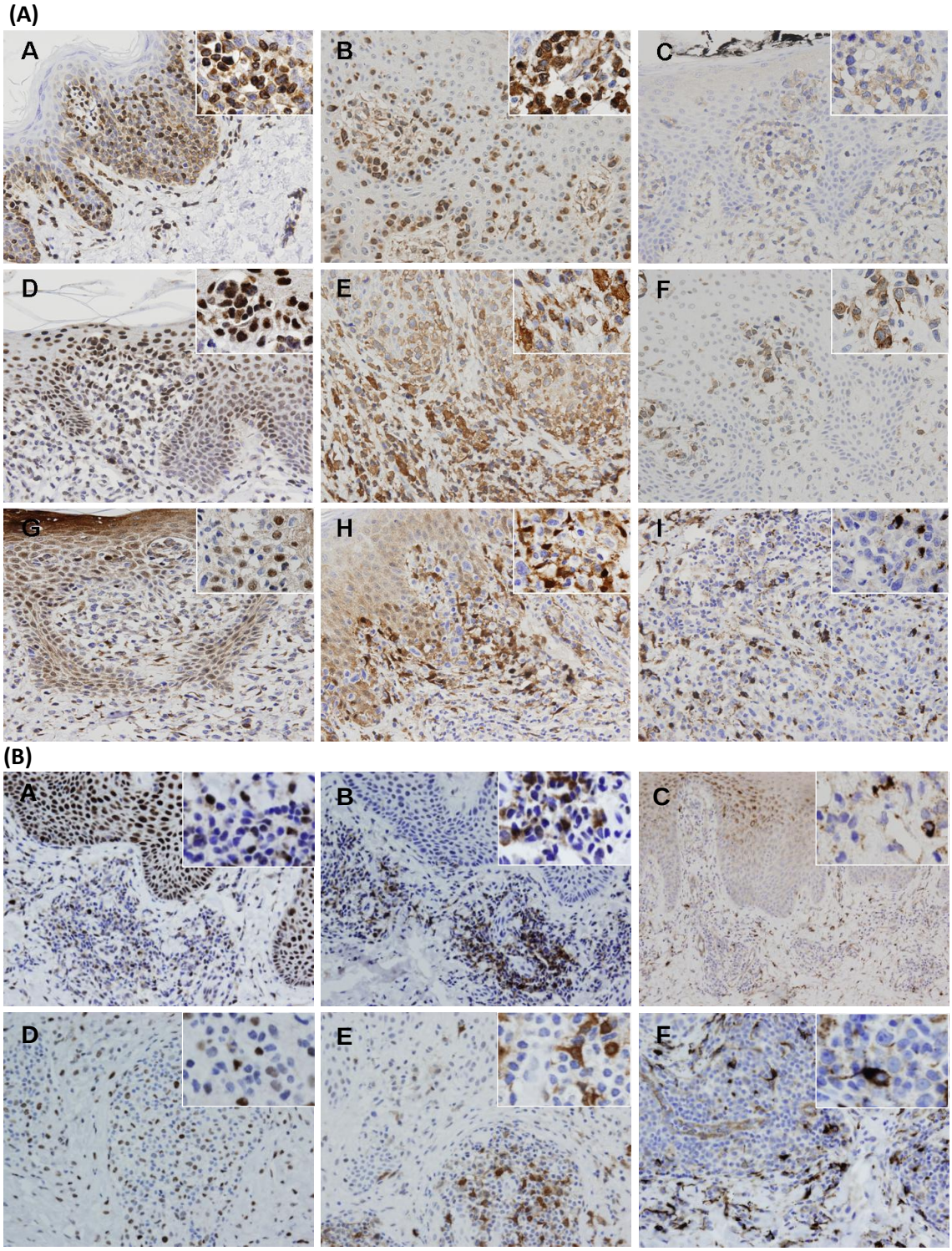

Figure 15. Immunohistochemistry on selected markers in mycosis fungoides cases and control inflammatory dermatitis samples. (A) Immunohistochemical staining for markers expressed in tumor cells: BCL2 (A), ZAP70 (B) and A20 (C); tumour and stroma cells: JUNB (D), STAT4 (E) and TRAF-1 (F); and only by stroma cells: STAT3 (G), STAT-1 (H), (A, B, C) CTSL2 (I). (B) Immunohistochemical staining for JUNB (A, D), TRAF1 (B, E) and CTSL2 (C, F) in benign control samples. Upper panel of (B), psoriasis (A, B, C); bottom panel of (B), psoriasiform dermatitis (D, E, F). Immersion oil; original magnification x 40 (main images) and x 100 insert images.

4.6 Identification of compounds that could reverse the PUVA +/- IFNα therapy resistance signature

Having identified a signature of to PUVA +/- IFNα treatment by SAM and GSEA analyses, a clinical application of this information was sought. The knowledge of resistance signature was applied to identify molecules that could reverse the drug resistance signature. For this purpose Connectivity Maps (cMaps) was used. This bioinformatics tool allowed rapid in silico assessment of molecules contained in the database with regards to their ability to reverse signatures related to specific drug resistance or disease state profiles. This screen indicated several hits (Table 17), such as protein kinase C inhibitor H-7 (p-value < 0.0001), HSP90 inhibitors: geldanamycin (p-value < 0.0001), tanespimycin (17-allylamino-geldanamycin 17-AAG; p-value < 0.0001), HDAC inhibitors: vorinostat (SAHA; p-value = 0.0002), scriptaid (p-value = 0.00673), CDK2 inhibitor – GW-8510 (p-value = 0.00084), cyclosporins and anti-bacterial and anti-protozoal agents.

Table 17. Connectivity Map (cMap, version 2) hits - potential molecules able to reverse PUVA +/- IFNα resistance signature.

cMap Molecules	Dose [μM]	Cell lines	# instances	Enrichment score	p-value
H-7	100	PC3, MCF7	4	-0.96	0
Geldanamycin	1	HL60, PC3, MCF7	15	-0.586	0
Tanespimycin (17-AAG)	0.1-1	HL60, PC3, MCF7	62	-0.373	0
Vorinostat (SAHA, Zolinza™)	10	HL60, PC3, MCF7	12	-0.591	0.0002
GW-8510	10	MCF7, PC3	4	-0.854	0.00084
Ciclosporin	1-3	PC3, MCF7	6	-0.708	0.00153
Alsterpaullone	10	MCF7,PC3	3	-0.863	0.00527
Dantrolene	12	HL60, PC3, MCF7	6	-0.647	0.00534
Scriptaid	10	MCF7, PC3	3	-0.849	0.00673

Cefotetan	7	HL60, PC3, MCF7	3	-0.84	0.00815
Diloxanide	12	HL60, PC3, MCF7	4	-0.744	0.00849

The highest scoring molecules included histone deacetylase inhibitors (HDACi): vorinostat (SAHA, Zolinza^{TM}) and Scriptaid (Takai et al., 2006) as well as known anticancer antibiotics that bind heat shock protein 90 (Hsp90) which antitumor activity has been shown in both leukemias (Meyer et al., 2008) and solid cancers (Zsebik et al., 2006), such as Tanespimycin (17-AAG) and geldanamycin. Furthermore, H-7 – protein kinase C (PKC) inhibitor – has been found to inhibit tumor cell invasion and metastasis in melanoma cells via suppression of phosphorylated extracellular signal-regulated kinase 1/2 (ERK1/2) (Tsubaki et al., 2007). Additionally, two selective cyclin-dependent kinase (CDK) inhibitors: GW-8510 (CDK2 inhibitor) (Sielecki et al., 2000) and Alsterpaullone (GSK-3β, CDK5/p25 and CDK1/cyclin B inhibitor) (Schultz et al., 1999) have been selected by cMap. Other molecules identified include Cyclosporin which possess a potent inhibitory action on T lymphocytes and interleukin release leading to reduced function of effector T-cells (Berth-Jones, 2005) and Dantrolene (acting trough decreasing intracellular calcium concentration) (Krause et al., 2004). It seems that many of the molecules identified by cMap either directly or indirectly negatively regulate T lymphocytes proliferation and signaling which could explain their antitumor activity in CTCL.

4.7 Validation of the best cMap hit with clinical application (17-AAG) in a model of advanced disease (CTCL cell lines)

The cMap analysis revealed 17-AAG and vorinostat (SAHA) as one of the most significant hits negatively connected with the resistance versus sensitive signature and suggested the hypothesis that this small molecules could induce the PUVA +/- IFNα sensitivity (reverse resistance to PUVA +/- IFNα) in resistant patients. As representation of resistance SS and MF cell lines were selected that could serve as a model of advanced CTCL. In order to further assess the activity and ability of the candidate molecules to downregulate the resistance signature, the viability, apoptosis, cell cycle and gene expression studies were performed on 17-AAG and vorinostat (Results III).

To determine the antilymphoma activity of Hsp90 inhibitor – 17-AAG – a panel of CTCL cell lines was exposed to increasing concentrations of 17-AAG (0.01, 0.05, 0.15, 0.5, 1.25, 4, 10, 35,

100μM) for 72 hours. The inhibitory effect of 17-AAG on the CTCL cells viability was assessed using CellTiter-Glo proliferation assay. All CTCL cell lines were sensitive to investigated Hsp90 inhibitor. 17-AAG suppressed the growth of CTCL cells at nanomolar concentrations with the IC50 values in a range 146nM (Myla cells) – 803nM (HH cells) (Figure 16A). Similarly, 17-AAG killed CTCL cells in a dose- and time-dependent manner, preferentially through induction of apoptosis, as shown by Annexin V and PI staining. Higher apoptosis levels were observed in Myla, SeAx and MJ cells (approximately 60-70%) following 72h treatment with the drug (Figure 16B). The effect of 17-AAG on cell cycle arrest was further explored. Surprisingly, the effect of 17-AAG on cell cycle in CTCL cells seemed to be rather cytotoxic as in all cell lines a significant increase in sub-G0 was observed following treatment with 1μM concentration of Hsp90 inhibitor both for 24 and 48 hours. Only modest G0/G1 cell cycle arrest was recorded for Myla and HuT78 cells as shown in Figure 16C.

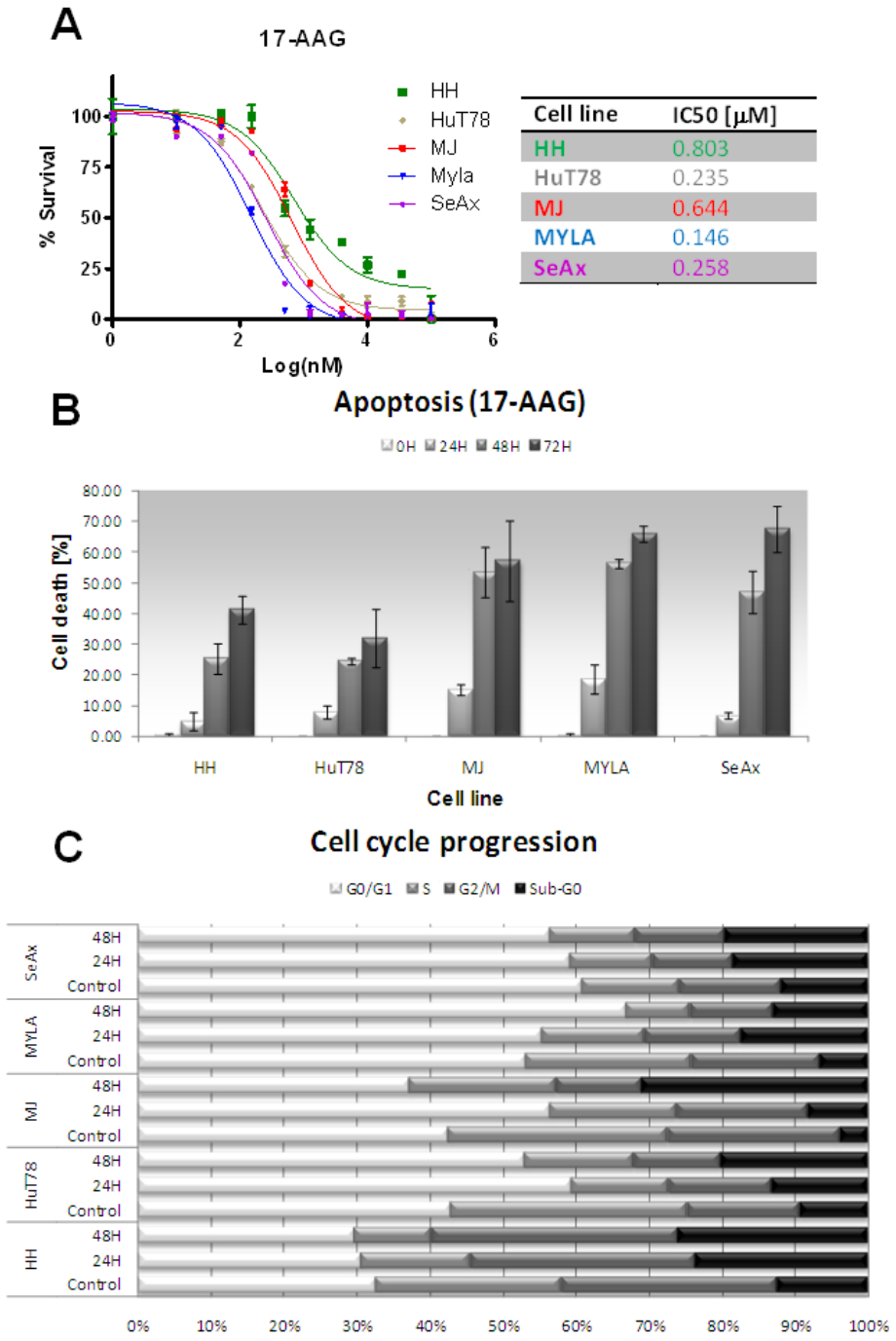

Figure 16. Effect of 17-AAG on viability, apoptosis and cell cycle in cutaneous T cell lymphoma (CTCL) cell lines. HH, HuT78, MJ, Myla, and SeAx cell lines were treated with or without 17-AAG (1µM).

A) Sensitivity to 17-AAG for a panel of CTCL cell lines was established by the proliferation/viability assay (CellTiter-Glo Viability Assay) following 72 hours of treatment. The IC50 values were calculated using GraphPad Prism software.

B) Apoptosis: Each point represented the percentage of annexin V^+PI^-, annexin V^+PI^+ and annexin V^-PI^+ cells. The cell death of control DMSO was subtracted from each value (error bar represents mean±SD of n=3 determinations).

C) Cell-cycle distributions were determined by DNA content analysis with propidium iodide (PI) staining and flow cytometry.

To further characterize the actions of 17-AAG in CTCL, cells were treated with 1μM 17-AAG over 4, 8, 12, 24 hour time course and gene expression profiling was performed. In total, approximately 3400 genes were downregulated and 2450 were upregulated by exposure to 17-AAG in all the cell lines following Short Time Series Expression Miner (STEM) analysis. The least number of genes was altered in the HH cell line (283) which in proliferation assays has shown the highest IC50 value. Consistently, in HuT78, Myla and SeAx cells the higher number of genes was changed following 17-AAG treatment leading to the conclusion that the amount of genes modulated by the Hsp90 inhibitor used was clearly related to their sensitivity levels. The numbers of genes enriched in downregulated and upregulated profiles in CTCL cells upon exposure to 17-AAG is presented in Figure 17.

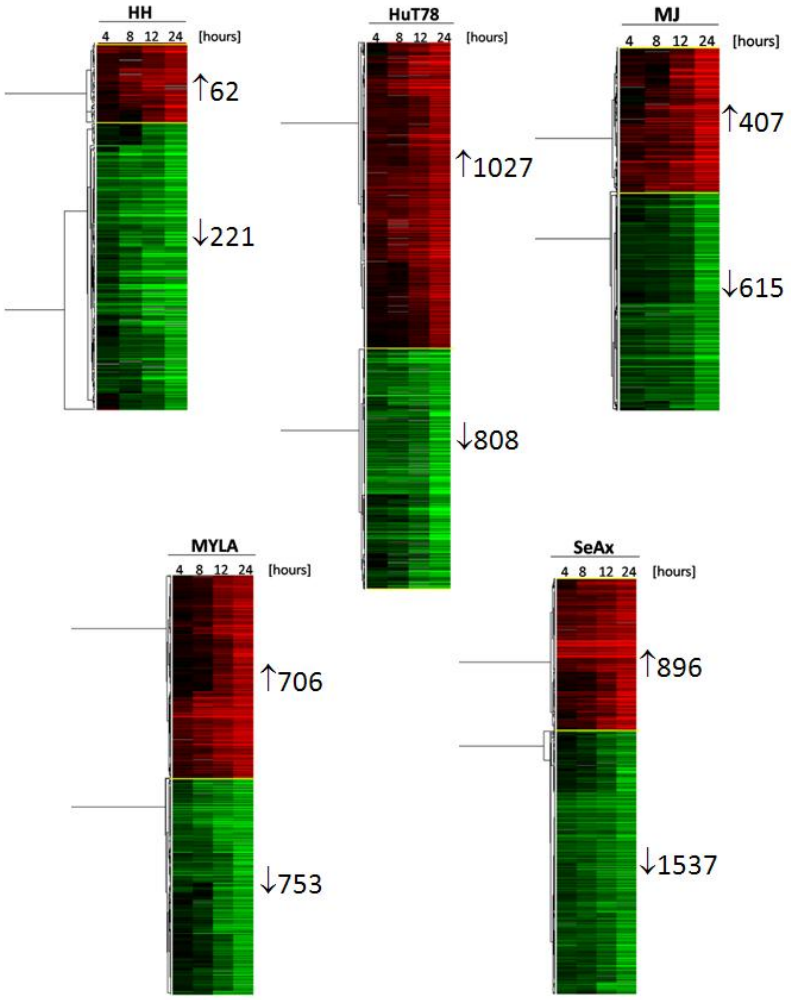

Figure 17. Gene expression profiles of 17-AAG-regulated genes in CTCL cells. The figure represents selected up- and down- regulated profiles obtained from the Short Time Series Expression Miner (STEM) analysis. The significant genes within selected profiles are visualized for each cell line. Genes selected as differentially expressed were clustered using CLUSTER and visualized by TreeView.

The list of downregulated genes was enriched for those involved in cytokine-cytokine receptor interactions, MAPK signaling pathway, antigen processing, NK-mediated cytotoxicity, apoptosis, WNT signaling and TCR signaling pathways. The downregulation of the latter pathway could partially confirm the ability of 17-AAG to reverse PUVA +/- IFNα resistance signature as TCR – associated genes were found to be upregulated in poor responders. Furthermore, the upregulated genes were enriched for metabolism, focal adhesion, cytokine-cytokine receptor interactions, MAPK signaling, JAK/STAT signaling. The complete list of pathways modulated by 17-AAG and enriched genes is presented in Table 18.

Table 18. Pathways and genes altered following 17-AAG (1μM) treatment. Functional analysis of the significant genes was performed using FatiGO Search.

Genes downregulated by 17-AAG	
Pathway	**Genes Enriched**
Cytokine-cytokine receptor interaction (hsa04060)	IL28RA, CCL3, FAS, TNFRSF10A, IL1A, LTB, TNFSF11, LTA, IL13RA1, CCL21, TNFRSF1B, IL3RA, TNFRSF8, TNFSF10, IL6
MAPK signaling pathway (hsa04010)	PPP3R2, RAP1A, PPP3CB, JUND, A_24_P204414, ATF4, CRK, DDIT3, CACNA1S, RASGRP3, FAS, IL1A, RAP1B
Antigen processing and presentation (hsa04612)	PSME2, HLA-DQB2, HLA-DPB1, IFI30, TAP1, HLA-DQA2, LTA, CD74, HLA-DOA, CREB1, HLA-B, CALR
Natural killer cell mediated cytotoxicity (hsa04650)	PLCG1, PPP3R2, PPP3CB, TNFSF10, HLA-B, PIK3R3, FAS, TNFRSF10A, ICAM2, ULBP2
Apoptosis (hsa04210)	TNFRSF10A, IL1A, PPP3R2, IL3RA, PPP3CB, TNFSF10, PIK3R3, FAS
Calcium signaling pathway (hsa04020)	PPP3R2, PPP3CB, SLC25A6, PHKG1, CACNA1S, PLCD3, PLCG1, GNAQ
Purine metabolism (hsa00230)	A_24_P400815, POLR2F, ADSS, ATIC, FHIT, NME1, ENTPD8, PDE7A
Wnt signaling pathway (hsa04310)	TCF7, NKD2, WNT7A, PPP3R2, PPP3CB, APC2, LRP5
Cell adhesion molecules (CAMs) (hsa04514)	ICAM2, HLA-DQB2, HLA-DPB1, HLA-DQA2, HLA-DOA, HLA-B
Regulation of actin cytoskeleton (hsa04810)	APC2, PIK3R3, NCKAP1L, CRK, A_24_P689479, PFN1
T cell receptor signaling pathway (hsa04660)	CDK4, PLCG1, PPP3R2, PPP3CB, PIK3R3

Genes upregulated by 17-AAG	
Pathway	**Genes Enriched**
Purine metabolism (hsa00230)	PDE9A, AMPD3, ENPP3, ENST00000371207, ADK, PDE3B, ENST00000327299, POLD4, ENTPD1
Focal adhesion (hsa04510)	SHC1, BAD, ITGB1, PDGFB, LAMC3, MYLC2PL, MRCL3
Regulation of actin cytoskeleton (hsa04810)	CD14, MYLC2PL, MRCL3, A_24_P689479, ITGB1, MRAS, PDGFB
Cytokine-cytokine receptor interaction (hsa04060)	PRL, IL2RA, PDGFB, IL13, IL12A, CCR5
MAPK signaling pathway (hsa04010)	MRAS, CACNA2D1, PDGFB, CD14, ATF2, CACNA1E, RASGRP2
Toll-like receptor signaling	CD14, TICAM2, TLR1, TLR3, IL12A

pathway (hsa04620)	
Calcium signaling pathway (hsa04020)	GRIN1, CACNA1E, SLC25A6, TNNC2, CYSLTR2
Insulin signaling pathway (hsa04910)	SHC1, BAD, PDE3B, TSC1
Jak-STAT signaling pathway (hsa04630)	PRL, IL2RA, IL13, IL12A

RESULTS III

Vorinostat interferes with the signaling transduction pathway of TCR and synergizes with PI3K inhibitors in CTCL

Vorinostat (SAHA), an orally administered inhibitor of class I and II histone deacetylases, has been approved by FDA for the treatment of cutaneous T-cell lymphoma (CTCL). In spite of emerging information on vorinostat effect on many cancer types, there is still little knowledge on mechanism and the kinetics of gene expression, essential for its effective use in combination therapy. In this chapter the alterations in gene expression profile (GEP) in CTCL cells treated with vorinostat over time were investigated. Subsequently, the evaluation of PI3K, PIM and HSP90 inhibitors as potential combination agents with HDAC inhibitors – HDACi (vorinostat and panobinostat) was performed. The functional analysis of gene expression data suggested that vorinostat modifies signaling of T cell receptor (TCR). The phosphorylation studies of ZAP70 (Tyr319, Tyr493) and its downstream target AKT (Ser473) revealed that this HDACi inhibits phosphorylation of these kinases. Based on the expression analysis, vorinostat was combined with PI3K, PIM and HSP90 inhibitors. The combination with PI3K inhibitors resulted in synergy while cytotoxic antagonism was observed when combining vorinostat with HSP90 inhibitor in CTCL. These results demonstrate the potential targets of vorinostat which shares many biological pathways with other HDACi studied – panobinostat and underline the importance of TCR signaling inhibition following vorinostat treatment. Furthermore, these findings show that concomitant administration of vorinostat/panobinostat and PI3K inhibitors (LY249002 and new ETP-45658) results in synergism and can potentially be efficacious for the treatment of CTCL. In addition, vorinostat and PIM inhibitors showed an additive effect while the use of vorinostat and HSP90 inhibitor (17-AAG) produces antagonistic reaction.

5. Vorinostat interferes with the signaling transduction pathway of TCR and synergizes with PI3K inhibitors in CTCL

5.1 Vorinostat induces cell death and cell cycle arrest in cutaneous T-cell lymphoma (CTCL) cells

In a previous chapter cMap analysis identified vorinostat as one of the molecules able to revert a signature of resistance to PUVA +/- IFNα treatment. Taking into consideration the high significance in cMap screen (Figure 18) and the demonstrated clinical benefit for CTCL patients (Duvic et al., 2007), the mechanisms of vorinostat action in CTCL cells were explored in depth.

vorinostat

rank	batch	cmap name		dose	cell	score	up	down	instance_id
1026	603	vorinostat		10 µM	PC3	.470	.072	-.086	1220
3545	767	vorinostat		10 µM	MCF7	0	-.063	-.072	6939
3793	626	vorinostat		10 µM	MCF7	0	-.072	-.080	1645
5123	765	vorinostat		10 µM	MCF7	-.504	-.066	.077	6980
5143	513	vorinostat		10 µM	MCF7	-.509	-.063	.080	1058
5368	506	vorinostat		10 µM	MCF7	-.569	-.071	.089	1000
5437	757	vorinostat		10 µM	MCF7	-.583	-.095	.069	5580
5442	725	vorinostat		10 µM	MCF7	-.584	-.107	.058	5217
5650	727	vorinostat		10 µM	PC3	-.641	-.093	.088	4444
5854	602	vorinostat		10 µM	HL60	-.713	-.140	.061	1161
5927	750	vorinostat		10 µM	HL60	-.740	-.147	.061	6179
6035	650	vorinostat		10 µM	HL60	-.816	-.121	.110	2680

Figure 18. Result of cMap screen for vorinostat. Screen shot from web browser represents the dose, cell line used and enrichment score.

The inhibitory effect of vorinostat on the viability of CTCL cell lines was examined through a CellTiter-Glo Assay using various concentrations of vorinostat (0.01, 0.05, 0.15, 0.5, 1.25, 4, 10, 35, 100µM) for 72 hours. All CTCL cell lines were sensitive to investigated HDAC inhibitor. The inhibitory effect of vorinostat was reflected as a dose-dependent reduction in cell proliferation/viability. Vorinostat suppressed the growth of CTCL cells in a dose-dependent manner. The IC50 of proliferation was determined at 0.146 µM in HH cells, at 2.062 µM in HuT78 cells, at 2.697 µM in MJ cells, at 1.375 µM in MYLA and at 1.510 µM in SeAx cells, respectively (Table 19).

Table 19. Sensitivity to Vorinostat for a panel of CTCL cell lines from the proliferation/viability assays (CellTiter-Glo Viability Assay). Proliferation/viability was analyzed following 72 hours of treatment.

Cell lines		
Name	**Source**	**IC50 [μM]**
HH	Peripheral blood of patient with aggressive CTCL	0.146
HuT78	Peripheral blood of patient with Sézary syndrome	2.062
MJ	Peripheral blood of patient with Mycosis fungoides	2.697
MYLA	Peripheral blood of patient with Mycosis fungoides	1.375
SeAx	Peripheral blood of patient with Sézary syndrome	1.510

In addition, the relation between the observed sensitization effect to the increase in apoptosis was investigated. To study this aspect of vorinostat treatment, HH, Hut78, MJ, Myla and SeAx cells were treated with various doses of vorinostat. Apoptosis was detected after 24-48h through Annexin V and propidum iodide (PI) staining. In all cells a time- and dose-dependent increase in the population of apoptotic cells was observed (Figure 19A). HH cells were most responsive to vorinostat and showed 18 $\pm$ 3.9 percent of apoptosis after only 24 hours and 44 $\pm$ 1.6 after 48 hours. HuT78 cells were less sensitive to vorinostat with 3.4 $\pm$ 1.3 and 17 $\pm$ 3.9 percent of death at 24 and 48 hours, respectively. MJ, Myla and SeAx cell lines showed approximately 26% cell death after 48 hours.

Furthermore, the effect of vorinostat on the cell cycle progression in CTCL cell lines was investigated. Cell cycle analysis of CTCL cell lines treated with vorinostat or vehicle alone (DMSO) was performed for 24 and 48 hours and analyzed for cell cycle distribution by flow cytometry. The S phase decreased in MJ and SeAx cells compared with control. G2/M cell cycle arrest was induced in HuT78, while a G0/G1 phase arrest was detected in Myla, MJ and SeAx cells (Figure 19B).

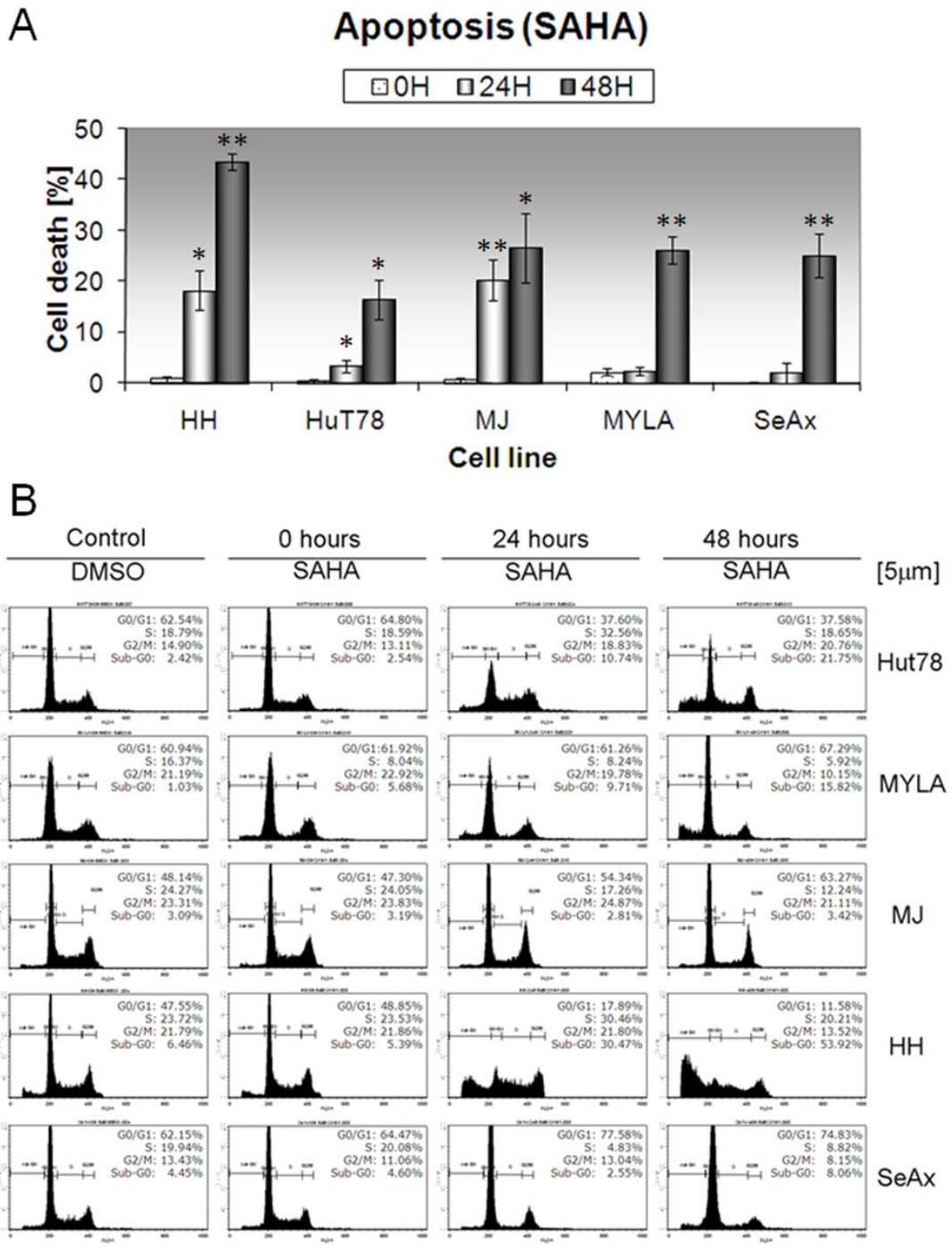

Figure 19. Effect of vorinostat (SAHA) on apoptosis and cell cycle in cutaneous T cell lymphoma (CTCL) cell lines. HH, HuT78, MJ, Myla, and SeAx cell lines were treated with or without vorinostat (5µM) for 24 and 48 h.

A) Apoptosis: Each point represented the percentage of annexin V^+PI^-, annexin V^+PI^+ and annexin V^-PI^+cells. The cell death of control DMSO was subtracted from each value (error bar represents mean±SD of n=3-8 determinations). * $p<0.05$, ** $p<0.001$.

B) Cell-cycle distributions were determined by DNA content analysis with propidium iodide (PI) staining and flow cytometry.

5.2 Vorinostat treatment leads to accumulation of acetylated histones in CTCL cell lines

The effect of vorinostat on histone acetylation status in human CTCL cell lines was determined by Western blot analysis. CTCL cells were exposed to 5μM SAHA for 0, 0.5, 1, 2, 4, 8, 12 and 24h. As shown in Figure 3, all four core nucleosomal histones (H2A, H2B, H3, and H4) become hyperacetylated following culture in the presence of vorinostat when compared to DMSO control. These effects were visible after 0.5h exposure (Myla) and showed a time dependent increase (Figure 20).

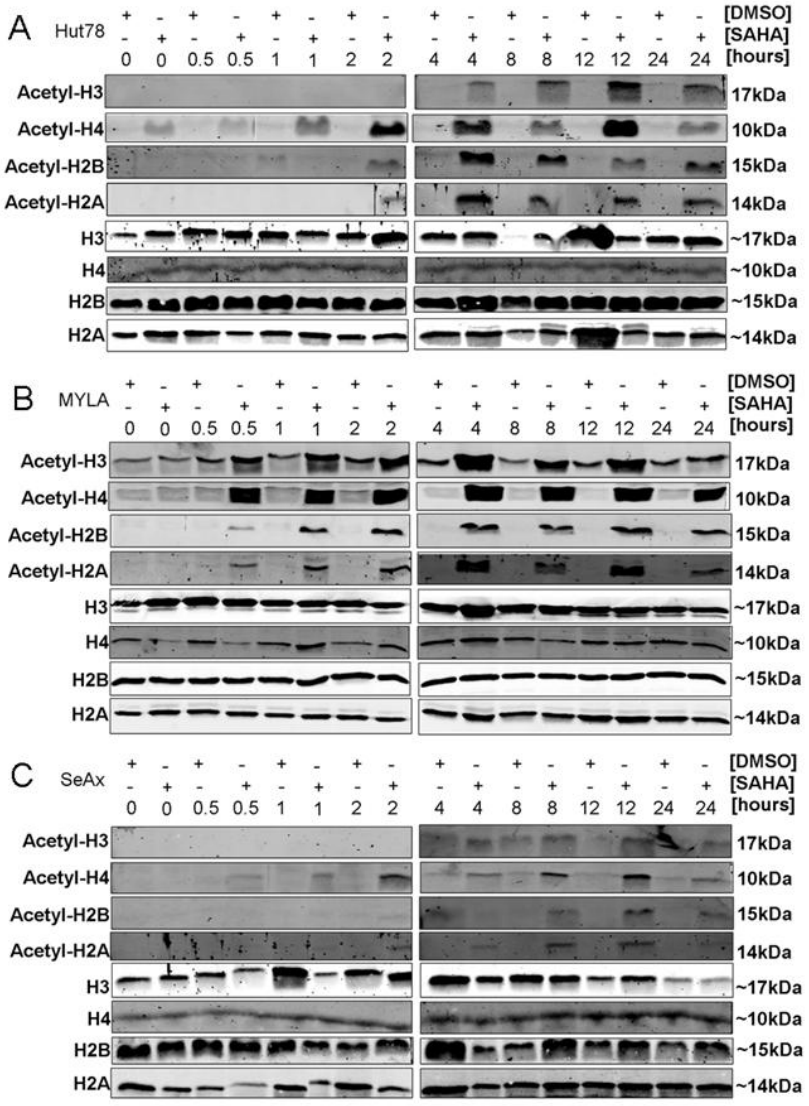

Figure 20. Effect of vorinostat on acetylation of histones. CTCL cell lines: HuT78 (A), Myla (B) and SeAx (C) were exposed to vorinostat (SAHA) (5μM) for 0.5, 1, 2, 4, 8, 12, 24 hours. Histones were extracted and analysed by Western Blot. The acetylation of histones H3, H4, H2B and H2A was determined. Nonacetylated histone H3, H4, H2A and H2B were used as a loading control.

5.3 Transcriptional profile of vorinostat treatment

Based on flow cytometry data, the CTCL cells were cultured in the presence of vorinostat over a 24-hours time course. Gene expression data were obtained from two independent microarray hybridizations for each time point. Data were then analyzed using STEM and genes with a significant up- or down-regulated profile (FDR<0.05) were used for further analysis. The number of genes altered progressively increased following 24-hours treatment (Figure 21A-B). Around 20% of genes on the array were significantly activated or repressed in response to vorinostat. The number of genes that were modulated in response to treatment, increased from 318 (HH), 424 (HuT78), 528 (MJ), 301 (Myla) and 155 (SeAx) at 4 hours to 3512 (HH), 2379 (HuT78), 3081 (MJ), 2022 (Myla) and 3275 (SeAx) at 24 hours.

The functional analysis of up- and down- regulated genes in response to vorinostat treatment revealed pathways that have previously been identified as being altered by the drug. They include cell proliferation, apoptosis and cell cycle related genes, as well as new pathways that have not been reported previously but could crucially contribute to the understanding of the mechanism of action of above mentioned drug (Supplementary Table 2).

Consistent with the previous findings of Ruefli *et al* (Ruefli et al., 2001) vorinostat modulated expression of key apoptosis genes, such as *IRAK1, FAS, CASP6, BID, BIRC4, cFLAR, CAPN2, BCL2L1, TNFRSF1A* and *TNFRSF10A*. Multiple MAPK signaling pathway members were also altered by vorinostat. Interestingly, the expression of genes involved in signal transduction and response to stress (*MAPK12, MAP3K6, MAPK13, MAP4K1*) was inhibited, while the genes playing a role in induction of apoptosis (*MAPK1, MAPK8, MAPK9, MAPK10, MAPK14 MAP2K6, MAP3K7, MAP3K10, MAP4K2, MAP2K2*) were upregulated.

HDAC inhibition of CTCL cells modulates the expression of genes involved in cell cycle (Mitsiades et al., 2004; Zhang et al., 2005). Thus, vorinostat downregulated genes required for G1/S transition (often aberrantly expressed in tumor cells), including *E2F1, E2F4, E2F5, SKP2* (Latres et al., 2001)*, CDC25A, CDK4, CDK6, CDC6, CDC25B* and several cyclins (cyclins *A2, D2, D3, E2*), as well as G2/M phase regulators (*CDC23, CDC25B, CHEK1*). Furthermore, vorinostat treatment induced expression of genes with an antiproliferative or arrest functions (*CDKN2A, CDKN2B, CDKN2C, CDKN2D, CDKN1A, CDKN1C*) (Supplementary Figure S1).

Additionally, significant changes after vorinostat treatment were observed in members of JAK/STAT pathway, cytokine-cytokine receptor interactions and expression of the members of tumor necrosis factor (TNF) receptor superfamily. Vorinostat also showed significant alterations in the network of interleukins (ILs) and their receptors; inhibits expression of *IL4, IL5, IL10, IL11, IL13, IL15A, IL19, IL21, IL29, IL2RB, IL4R, IL6R, IL10RA, IL15RA*; and enhances expression of *IL1A, IL6, IL9, IL12A, IL15, IL22, IL23A, IL24, IL1RAP, IL3RA*. Interestingly, many of the repressed interleukins are known to enhance cell growth, proliferation and promote Th2 responses, which is a hallmark of CTCL pathogenesis. Furthermore, we found that upon vorinostat treatment a set of chemokines and their receptors also experienced a shift in expression profile. Among the downregulated set we encountered genes related to T-cell migration and chemotaxis, such as: *CCL1, CCL22, CCL26, CCL28, CXCL10, CXCL13, CXCL16, CCRA, CCR4, CCR6, CXCR3* and *CXCR4*; the genes induced by vorinostat include: *CCL19, CCL20, CCL27, CXCL9, CXCL11, CX3CL1, CCR2* and *CCR6*. Besides, we observed alterations in expression of the remaining members of JAK/STAT pathway, among them suppression of *STAT6, STAT5A, SOCS2, SOCS6* and *SOS* accompanied by enhanced expression of *STAT1, STAT2, STAT3, STAT5B, SOCS3, IFNAR2, INFG, IFNGR1* and *JAK1*.

Finally, the repressive influence of vorinostat on the TCR pathway signaling was shared by all the CTCL cell lines. Thus, vorinostat repressed a remarkably large set of genes directly associated with the TCR, together with molecules acting downstream, including *ZAP70, LAT, VAV2, CD247, CD3D, CD3E, CD3G, CD4, IL4, IL5, IL10, IL13, IL4R, IL6R, PTPN6, PAK2, PAK6, ICAM1, NMI, FOXP3,* while upregulated genes included: *FYN, IFNG, IFNGR1, IL12A* and others (Figure 21C). TCR signaling has also being found as associated with resistance to PUVA +/- IFNα (Wozniak et al., 2009), which could partly explain why vorinostat sensitizes PUVA +/- IFNα resistant patients.

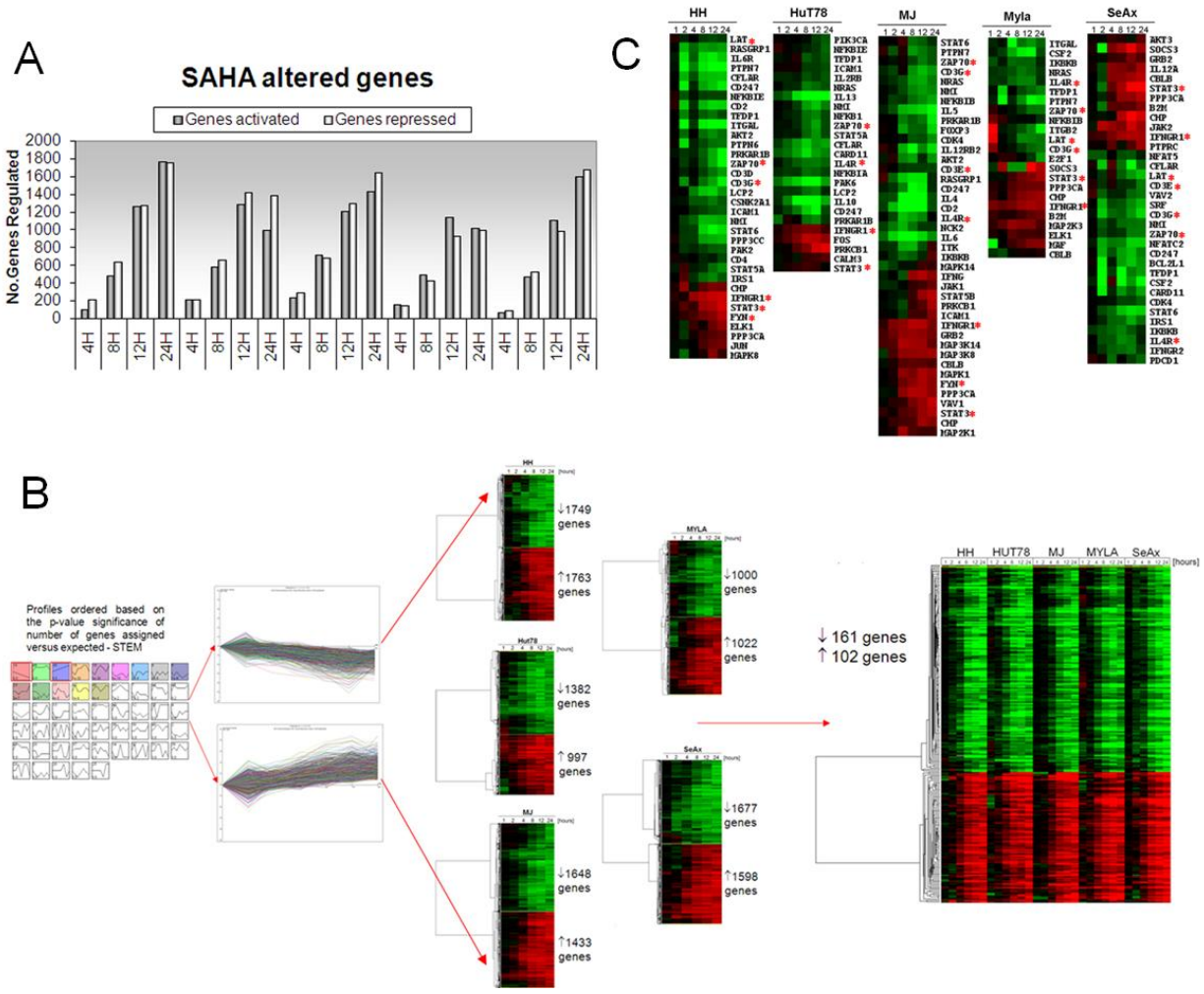

Figure 21. Gene expression profiles of vorinostat-regulated genes.

A) Numbers of genes up- and down-regulated at each time point after treatment with vorinostat. Number of genes with significant profile that were differentialy expressed by at least 2-fold from time 0 h to at least one later time point in response to vorinostat are shown.

B) Short time series expression miner (STEM) analysis flowchart. The figure represents selected up- and down- regulated profiles and significant genes within selected profiles are visualized for each cell line. Genes selected as differentially expressed were clustered using CLUSTER and visualized by TreeView. Genes were hierarchically clustered based on standard correlation coefficients.

C) Functional clustering of vorinostat-regulated T-cell receptor associated genes. The red asterisks indicate genes chosen for qRT-PCR validation.

5.4 Analysis of early and late response genes after vorinostat treatment

During the first two hours of treatment with vorinostat no significant change in gene expression profile was observed. At four hours of exposure to vorinostat between 155 (SeAx) and 528 (MJ) genes were altered. Genes that were demonstrated to be downregulated included TNF receptor associated factor 2 (*TRAF2*), telomerase reverse transcriptase (*TERT*), histone methyltransferase (*SUV39H1*), BCL6 co-repressor *BCOR*, interferon regulatory factor 2

binding protein (IRF2BP2) and metabolism related lipoyltransferase 1 (*LIPT1*). In the group of genes that were upregulated by vorinostat after 4 hours of treatment we identified genes associated with JAK-STAT signaling (*IFNGR1, TSLP*), calcium signaling (*ADRB2*), metabolic processes (*PFKFB4, IDH1, CYB5R1*) and MAPK pathway (*MAP3K*).

After 8 hours a dramatic change in gene expression was observed in all cell lines. During this time vorinostat altered from 912 (Myla) to 1389 (MJ) genes. At 8h, SAHA induced downregulation of cell adhesion molecules (ICAMs) including: *ICAM2, CD58, CD2*, cytokine receptors (*IL4R, IL15RA*), Notch signaling (*CTBP1, GCN5L2*), TCR (*LCP2*) and Wnt pathway (*CTBP1*). Moreover, HDACi further upregulated JAK-STAT pathway (*STAT1, STAT3, SOCS3*), apoptosis (*CASP7, BCL2L12*), cell cycle (*CDKN2D, CCND3, PTTG1, CDC6*) and oxidative phosphorylation (*ATP6V1G2*).

Furthermore, after 12 hours vorinostat changed the expression of over 2000 genes in each of the cell lines: 2069 (Myla) – 2704 (HuT78). At this time point vorinostat continued its repressive effect on TCR signaling (*ZAP70, LAT, CARD11, CD3G, PTPN7*), cytokine interactions (*CCL28, FAS, CCR4, CXCR3, IL6R*), apoptosis (*IRAK1, FAS, BIRC4, CFLAR, LMNB2,CAD*), purine and pyrimidine metabolism (*ATIC,ADSS,AMPD3/ DTYMK,TYMS*). Vorinostat also further increased the expression of MAPK pathway members (*MAP3K9, MAP3K7*), cell cycle (*CDKN1A, CDK7, CDKN2D, CDKN1C*) and JAK-STAT signaling (*JAK2, IL15, SPRY1*).

5.5 Validation of Expression Profiles of Selected Genes by Quantitative Real-Time PCR

To verify changes in gene expression detected by our microarray analysis, quantitative real-time PCR analysis on 8 genes belonging to the T-cell receptor pathway, where expression profiles were altered by vorinostat in at least two cell lines was performed. These genes included: *Zap70, STAT3, FYN, IFNGR1, CD3G, LAT, IL4R* and *CD3E*. As shown in Figure 22A-5H there was a high correlation between the microarray and real-time PCR data for all 8 genes.

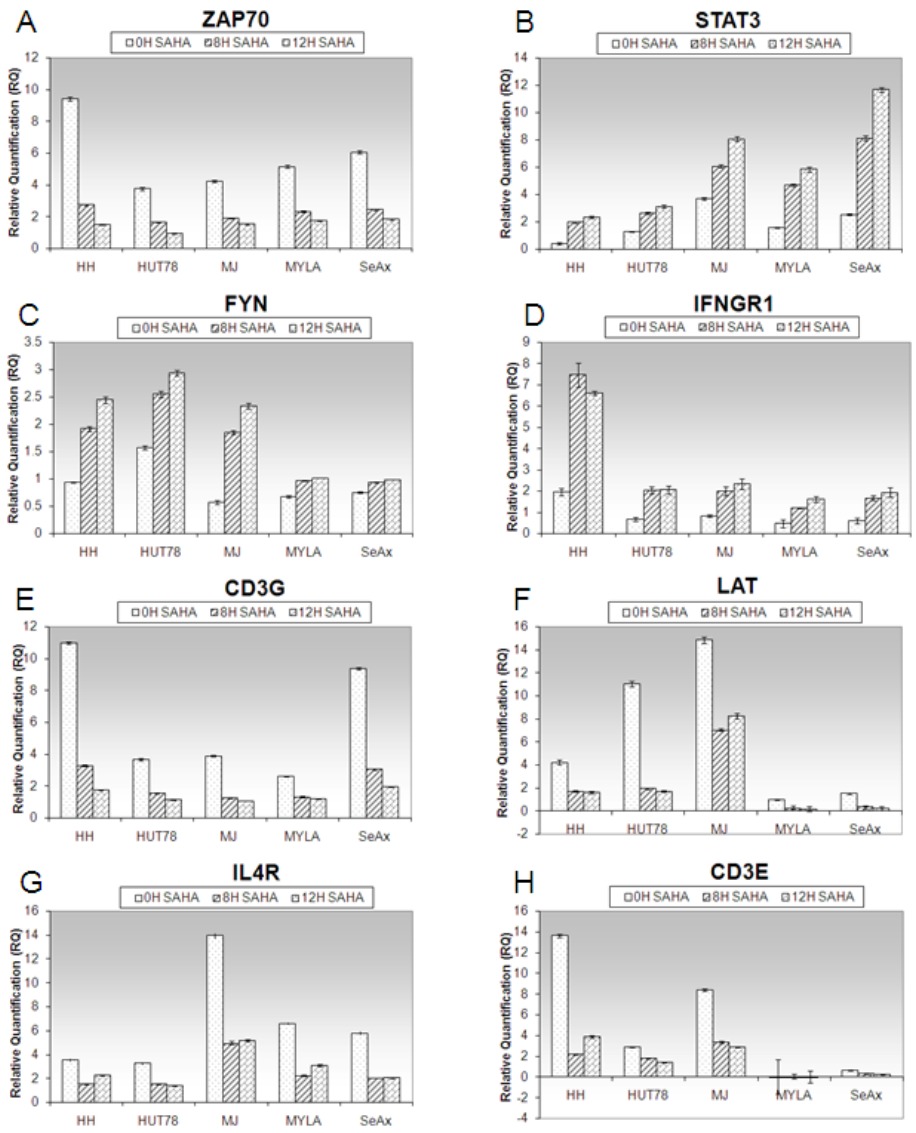

Figure 22. Validation of microarray data by TaqMan quantitative real time PCR.
The influence of vorinostat on mRNA expression of ZAP70 (A), STAT3 (B), FYN (C), IFNGR1(D), CD3G (E), LAT (F), IL4R (G) and CD3E (H) for all cell lines before and after 8 and 12 hours of treatment. Values for each gene were normalized to expression levels of HGUSB endogenous control. Data were performed in triplicates.

Furthermore, the changes in expression of *ZAP70* and *FYN* in peripheral blood tumoral lymphocytes samples from a leukemic MF patient treated with vorinostat were analyzed. The samples were taken before and after 1, 3, 6, 24, 48, 120 and 360 hours of treatment. The expression profiles of *ZAP70* and *FYN* in the leukemic cells after vorinostat treatment closely matched those obtained in the cell lines, with a slight delay in the beginning of the action attributed to the pharmacokinetics of vorinostat in vivo; thus after the first 6 hours a contradictory effect (upregulation of *ZAP70* and downregulation of *FYN*) occurred, followed by

downregulation of *ZAP70* and upregulation of *FYN,* both more profound after 15 days of treatment (Supplementary Figure S2).

5.6 Vorinostat decreases the TCR activation through inhibition of kinase phosphorylation

Considering the critical role of ZAP70 in transmitting signals from the TCR signaling complex, the ability of vorinostat to inhibit the tyrosine phosphorylation in two of the CTCL cell lines was examined. Two representative cell lines: HuT78 (SS) and Myla (MF) cells were treated with vorinostat for 0.5, 1, 6 and 24 hours at the concentration of 5 and 25μM. Phosphorylation of Tyr319 and Tyr493 within the activation loop results in enzymatic activation of ZAP70 (Watts et al., 1994; Williams et al., 1999). Decrease in phosphorylation of ZAP70 on Tyr493 after vorinostat treatment was observed after 0.5h (25μM) and 1h (5μM) in HuT78 and after 1h in Myla for both concentrations. Phosphorylation of Tyr319 was diminished after 1 h (25μM) and 6 h (5μM) in HuT78 and 1h in Myla (25μM) (Figure 23A). In both cases the inhibition of tyrosine phosphorylation was time and concentration dependent. Meanwhile, vorinostat modestly decreased total ZAP70 cellular level.

Tyrosine phosphorylation of ZAP70 correlates well with its increased kinase activity and downstream signaling events. To extend the understanding of the potential impact of vorinostat on the T-cell signaling the downstream effector molecules were evaluated. PI3K/AKT pathway has been shown to be implicated in signal transmission leading to activation, differentiation as well as cellular survival of T-lymphocytes (Bauer and Baier, 2002). The activating phosphorylation of AKT within the carboxy terminus at Ser473 was decreased already after 0.5h at 25μM concentration and was further reduced at 1, 6 and 24h in HuT78. In the Myla cell line slight reduction in AKT (Ser473) phosphorylation was observed after 1h followed by significant reduction after 24h. Vorinostat also decreased the total AKT levels in a dose-dependent manner (Figure 23B).

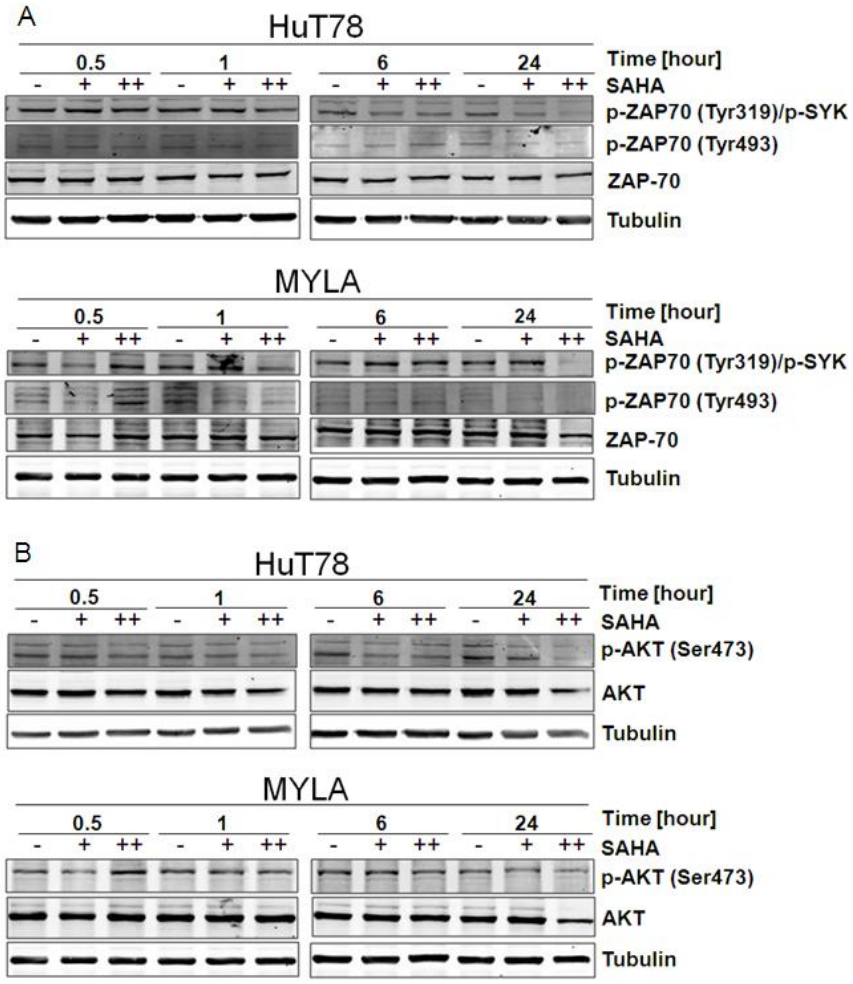

Figure 23. Effect of vorinostat on TCR related genes.

A, B, C) HuT78 and Myla cells were incubated with 5μM (+) or 25μM (++) of vorinostat for 0.5, 1, 6 and 24 hours. Whole cell lysates were examined by Western Blotting for phospho-ZAP70 (Tyr319 and Tyr493) (A) and phosphor-AKT (Ser473) (B). Total ZAP-70 and AKT were used as controls, respectively. Tubulin was used as a loading control of total proteins.

5.7 Overexression of ZAP70 does not increase vorinostat resistance

To test the hypothesis that the increased expression of ZAP70 could correlate with vorinostat resistance or decreased sensitivity in CTCL cells, ZAP70 was successfully overexpressed in MYLA cells. Due to relatively high initial expression of ZAP70 in CTCL cells, approximately 16-30% increase in ZAP70 levels was achieved. The effect of ZAP70 overexpression was assessed by cell viability/proliferation assays; however, increase of 16-30% in ZAP70 kinase expression (and overexpression of ZAP70 alone) was not sufficient and did not correlate with vorinostat sensitivity (Figure 24).

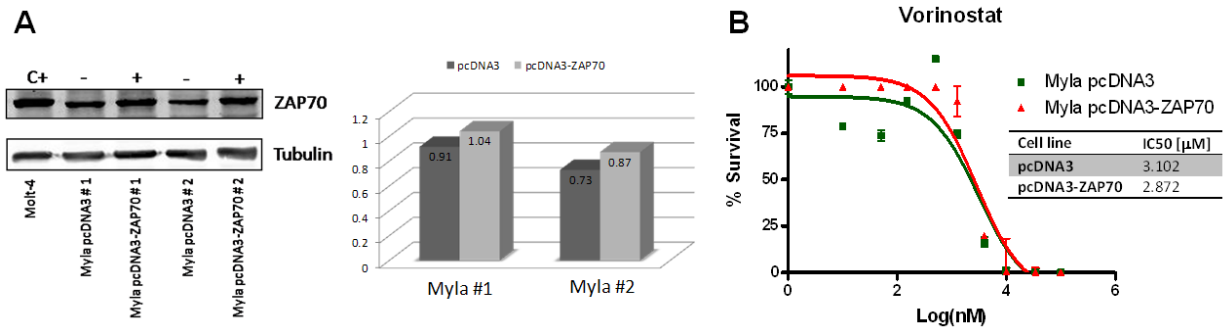

Figure 24. Overexpression of ZAP70 after microporation with pcDNA3 vector in Myla cells. (A) Myla cells were microporated with 2 pulses of 1300V with pcDNA3 (empty vector) or with pcDNA3-ZAP70 (containing ZAP70 insert). After 24 hours, cells were incubated with 800μg/ml of G418 (Geneticin) antibiotic for selection of transfected cells. Following, cell lysates were prepared for western blot (WB) analysis. ZAP70 was detected with anti-ZAP70 antibody and α-tubulin was used as a loading control. Right panel represents quantification of WB analysis using the ImageJ 1.34S software; the ratio of ZAP70 vs. Tubulin is represented. (B) Viability/Proliferation assays of Myla cells with empty vector or ZAP70-containing vector following vorinostat treatment. The results are represented as the percentage of DMSO vehicle control. IC50 values were calculated using Graph Pad Prism software.

5.8 Combination of Vorinostat with PI3K, PIM and HSP90 inhibitors

Vorinostat, being a multi-HDAC inhibitor, could be suitable for use in a combination therapy with other anti-neoplastic agents. As candidates for combination therapy PI3K inhibitors (LY294002, ETP-45658), PIM kinase family inhibitor (ETP-39010) and HSP90 inhibitor (17-AAG) were selected. This selection was done following the analysis of the genes targeted by vorinostat (PI3Ki, PIMi) or cMAP data. Thus, GSK-3β (PI3K substrate) and PIM1/PIM2 were upregulated after vorinostat treatment (Figure 25A). HSP90 (target of 17-AAG) was downregulated, but was included in this analysis since it has the best score in the cMap analysis (Table 17).

The sensitivity of CTCL cells to each of the compounds after 72 hours of exposure individually or in combination was determined by Luminescent Cell Viability Assay. The IC50 values for LY294002 ranged between 1.797μM (HH) and 34.669μM (SeAx). Additionally, a more potent and selective PI3K inhibitor – ETP-45658 was used, with the IC50s of a magnitude from 0.442μM (HH) to 1.5μM (SeAx), being 4-28 times lower than those of LY294002. The inhibitor of PIM kinases family – ETP-39010 was also tested which resulted to have the IC50 values varying from 1.286μM (MJ) to 5.042μM (HH) after 72-hour exposure and from 3.083μM (MJ) to 17.051μM (HH) after 48-hour treatment. The IC50 values for the HSP90 inhibitor – 17-AAG

(17-allylamino-geldanamycin) were in the nanomolar range for all the cell lines, with MYLA being the most sensitive (146nM) and HH having the highest value of 803nM (Table 20).

Table 20. Sensitivity of CTCL cells to ETP-45628, LY294002, ETP-39010, 17-AAG. Proliferation/viability was analyzed using CellTiter-Glo Viability Assay after 3 days of treatment unless stated otherwise.

Cell lines	IC50 [μM]				
Name	**ETP-45628**	**LY294002**	**ETP-39010***	**ETP-39010**	**17-AAG**
HH	0.442	1.797	17.051	5.042	0.803
HuT78	1.444	10.853	5.977	2.695	0.235
MJ	0.603	10.158	3.083	1.286	0.644
MYLA	1.033	28.776	4.639	2.708	0.146
SeAx	1.500	34.669	4.194	3.190	0.258

* Proliferation/viability was analyzed after 48 hours.

To study the possible synergy between vorinostat and the combination drugs, approximately equipotent concentration of each drug were used. Combination Index (CI) values were calculated using CalcuSyn software with a formula initially proposed by Chou and Talay (Chou and Talalay, 1984). The drugs were used in constant ratios to determine the effectiveness of combinations. When at least 80% of CI values for combination in all cell lines were less than 1, the drug combination was considered to be synergistic. Similarly, if more than 80% of CI was higher than 1 the drug was considered antagonistic. Otherwise, the drug was asserted to be additive with a synergistic/antagonistic tendency.

Combined treatment of vorinostat with LY294002 demonstrated moderate to strong synergy, usually with the best CI values for IC50 concentrations and above for all CTCL cell lines, with the SeAx cell line showing the strongest synergy. Coadministration of vorinostat with more potent and selective PI3K inhibitor ETP-45658 also showed clearly synergistic relation at the concentration of 0.5 times IC50 and above (Figure 25B). Concomitant as well as sequential addition (addition of the drug after 24 hour pretreatment with vorinostat) of PIM inhibitor (ETP-39010) resulted in additive to synergistic effect in HuT78 and SeAx - SS cell lines, additive to antagonistic effect was observed in MYLA and varying results were obtained for HH and MJ cell lines (Figure 25C). Clear antagonism was observed when concomitantly administering vorinostat with the inhibitor of HSP90 – 17-AAG (Figure 25D). The combination results seemed to be conversely related to the expression changes of the targets of inhibitors used following treatment with vorinostat. In summary, synergistic/additive combination effect was demonstrated for the compounds targeting genes whose expression was upregulated by vorinostat.

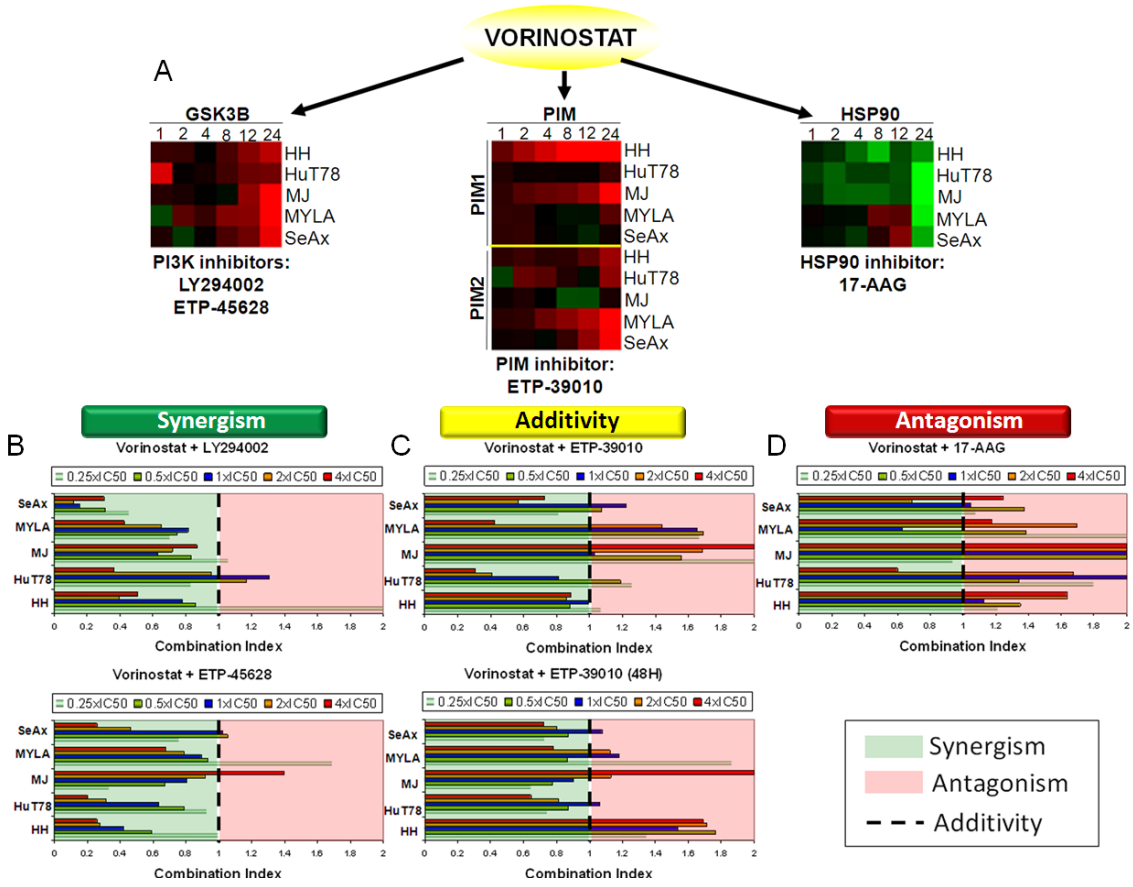

Figure 25. Combination studies of vorinostat with PI3K, PIM and HSP90 inhibitors in cutaneous T-cell lymphoma (CTCL) cells. (A) Effect of vorinostat on the targets of the inhibitors used for combination studies: PI3K inhibitors (GSK-3β - left panel), PIM inhibitor (PIM1 and PIM2 – middle panel) and HSP90 inhibitor HSP90 – right panel) in five CTCL cell lines. The HH, HuT78, MJ, MYLA, SeAx cells were treated with 5μM of vorinostat over 24h time course. The gene expression values were normalized with respect to time 0 hours. The selected genes were visualized using CLUSTER and TreeView. (B) Synergistic interactions between vorinostat and PI3K inhibitors (LY294002 and ETP-45658). (C) Additive interactions for concomitant and sequential coadministration of vorinostat with PIM inhibitor (ETP-39010). (D) Antagonistic interactions between vorinostat and HSP90 inhibitor (17-AAG).
B, C, D) Synergistic, additive, or antagonistic effects of the drug combinations were determined by calculating the combination index value (CI) by isobologram analysis with CalcuSyn software. A CI < 1 indicates synergism, CI ± 1 indicates additivity and CI > 1 indicates antagonism.

5.9. Validation of vorinostat (SAHA) mechanism of action using a different histone deacetylase inhibitor - panobinostat (LBH589)

Multiple HDACi have been developed to date and several are in clinical investigation. The hydroxamic acid based HDACi, vorinostat and panobinostat are pan-inhibitors of class I and II HDACs that have demonstrated potent cytotoxicity in vitro against a variety of solid tumor cell lines. While vorinostat is FDA-approved treatment for CTCL, panobinostat is under extensive clinical investigation in CTCL and several solid tumors. Is the mechanism of action and synergy with PI3K inhibitors identified in the previous paragraphs common for pan-HDACi or specific for vorinostat? In this section the similarities in the effects of these two clinically relevant HDACi were analyzed.

5.9.1 Panobinostat similarly to vorinostat inhibits the growth and induces cell cycle arrest and apoptosis of CTCL cells

The CTCL cell lines were analyzed to determine the effects on cellular proliferation using CellTiter-Glo Assay. Cells were exposed to increasing concentrations of each drug for 72 hours and subsequently analyzed for the luminescent signal. The IC50 values for all cell lines following panobinostat treatment were 2-30 times smaller than that for vorinostat and were in the nanomolar range (Figure 26A).

Subsequently, flow cytometry was utilized to examine the effects of panobinostat on apoptosis and cell cycle distribution in CTCL cells and its comparison to vorinostat. HH, Hut78, MJ, Myla and SeAx cells were treated with 50nM concentration of panobinostat and followed by apoptosis examination at 24, 48 and 72 hours. Similarly to vorinostat, all cell lines showed sensitivity to panobinostat with 10% (SeAx) to 45% (MJ) cell death following 48-hour treatment (Figure 26B). This result together with IC50 values demonstrates higher potency of panobinostat over vorinostat in CTCL.

Analysis of the cell cycle distribution of CTCL cells after treatment with panobinostat showed that this drug similarly to vorinostat caused an increase in G0-G1 in Myla and SeAx cells, decrease in S phase in HuT78, MJ, Myla and SeAx and decrease in G2/M in HH, Myla and SeAx (Figure 26C).

A

Cell line	IC50 [nM]
HH	77.45
HuT78	77.29
MJ	80.33
MYLA	76.55
SeAx	76.40

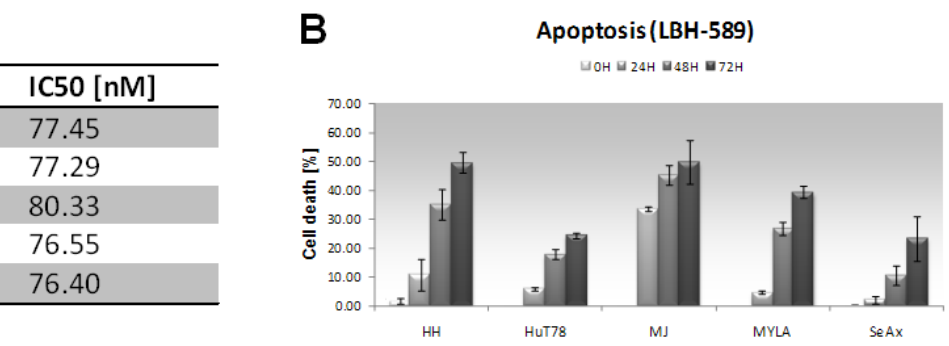

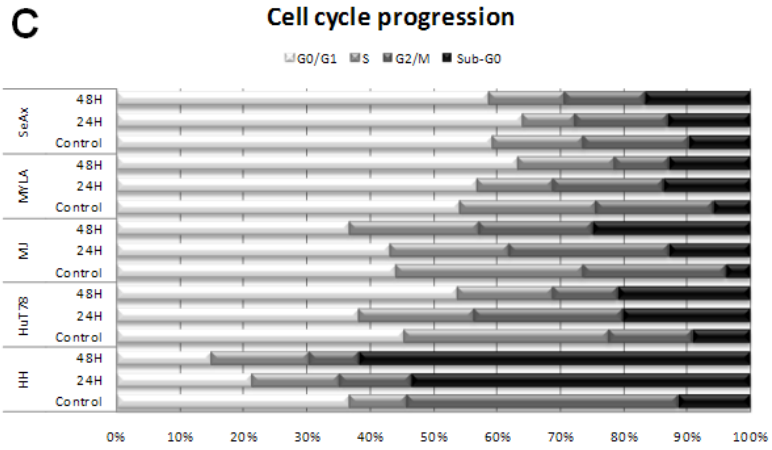

Figure 26. In vitro characterization of panobinostat (LBH589) in CTCL cells. Proliferation (A), apoptosis (B) and cell cycle (C) analysis was measured in HH, HuT78, MJ, MYLA and SeAx cells following treatment with panobinostat. (B, C) Cells were treated with a concentration of 50nM panobinostat. DMSO was used as a vehicle control. Error bar represents mean±SD of all determinations).

5.9.2 Microarray profiling in HDACi treated CTCL cells

To compare the molecular events which occur in response to HDAC inhibition, CTCL cells were treated with the clinically relevant concentration of 50nM panobinostat and analyzed using microarray platform as outlined in the methods section. Genes with a FDR-adjusted p-value of < 0.05 following STEM analysis were considered differentially expressed genes relative to vehicle treated controls over time.

5.9.3 Differentially expressed genes in response to HDACi treatment

To check for the similarities of the effects exerted by both HDACi, Venn analysis was performed. Based on flow cytometry data, the CTCL cells were cultured in the presence of panobinostat over a 24-hours time course. Similarly to vorinostat, the number of genes altered by panobinostat increased continuously following 24-hours treatment. Panobinostat modulated approximately 2000 genes in each of the cell lines. The number of genes modified

in response to treatment included the decrease in expression of 1283 (HH), 861 (HuT78), 1079 (MJ), 1029 (Myla) and 973 (SeAx) genes and increase in the level of 941 (HH), 1293 (HuT78), 1182 (MJ), 965 (Myla) and 938 (SeAx) genes. Up to 50% of the genes altered by panobinostat were common with those modulated by vorinostat (Figure 27) suggesting a substantial overlap in the mechanism exerted by both HDACi. The classification of the common genes according to functional categories indicated that the downregulated genes were involved in purine and pyrimidine metabolism, apoptosis, cytokine-cytokine receptor interaction, TCR and MAPK signaling. In addition, the genes upregulated following treatment with both HDACi were related to metabolism, apoptosis, regulation of actin cytoskeleton and tight junction, axon guidance and MAPK signaling. The down- and up- regulated genes common for both inhibitors are presented in the Supplementary Table 3.

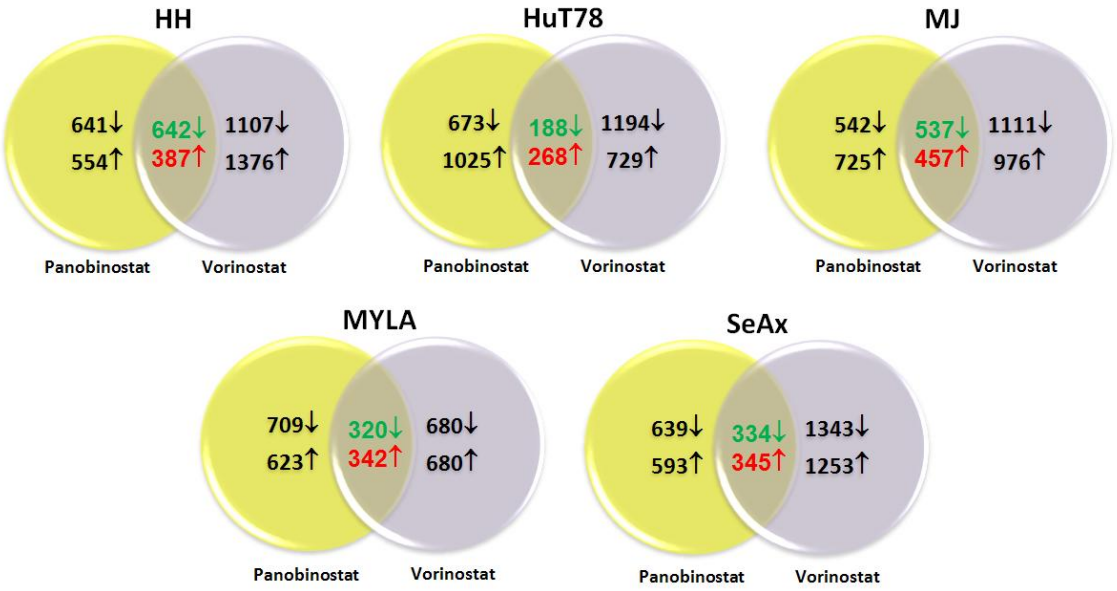

Figure 27. Venn analysis of differentially expressed genes in panobinostat (LBH589) and vorionstat (SAHA) – treated CTCL cells. HH, HuT78, MJ, MYLA and SeAx cells were treated with either 50nM panobinostat or 5μM vorinostat over 24-hour time course. Significant genes were subjected to Venn analysis.

5.9.4 Panobinostat similarly to vorinostat synergize with PI3K inhibitors.

To investigate whether panobinostat likewise vorinostat potentiate the activity of other agents, such as PI3K inhibitors, CTCL were treated with serial dilutions of panobinostat and PI3K inhibitor (LY294002) individually or with both drugs simultaneously at a fixed ratio of doses 0.25, 0.5, 1, 2, 4 times the individual IC_{50} (ED_{50}) values (Figure 26A, Table 20, respectively). Similarly to vorinostat, coadministration of panobinostat with PI3K inhibitor

demonstrated a strong synergy (the lowest CI values) for the concentrations of 1- and 2- times IC50 in all CTCL cell lines (Figure 28). These results confirm our hypothesis that HDACi in combination with PI3K inhibitors could be of significant benefit to PTCL patients.

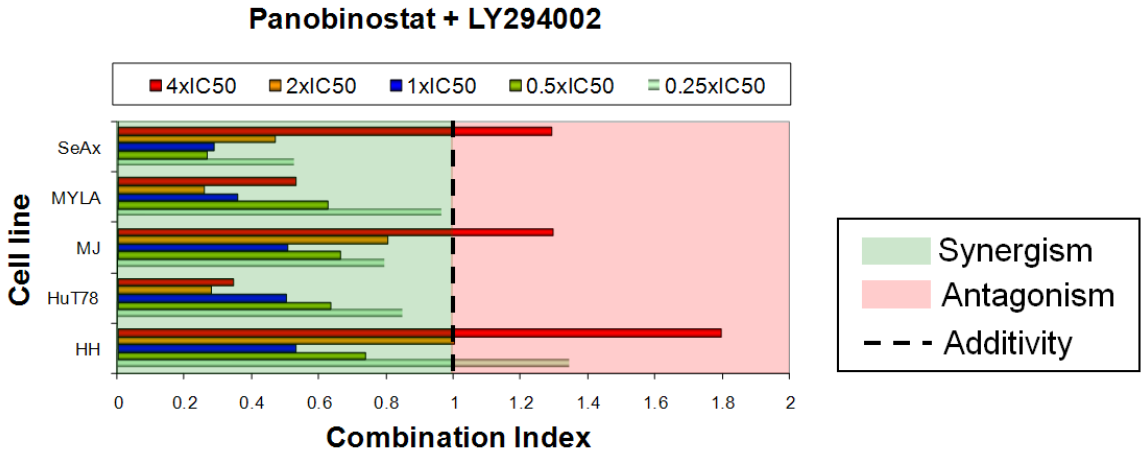

Figure 28. Synergistic effect of panobinostat and PI3K inhibitor in cutaneous T-cell lymphoma (CTCL) cells. Cells were treated with each drug both individually and in combination. After 72h of exposure, the luminescence was measured using CellTiter-Glo Assay. Combination effects of the drug combinations were determined by calculating the combination index value (CI) using CalcuSyn software (CI < 1 indicates synergistic effect).

DISCUSSION

7. Discussion

Cancer is the end result of the accumulation of genetic mutations that function cooperatively to promote neoplastic transformation. These lesions provide many advantages to transformed cells, including an increased ability to grow and proliferate and insensitivity to programmed cell death or apoptosis. Two major categories of mutated genes are oncogenes and tumor suppressor genes. Mutational and regulatory changes in specific oncogenes may have important implications for diagnosis, therapy, and prognosis, which have fueled multiple research studies on the molecular biology of lymphomas during the past two decades. The development of new cytogenetic and molecular techniques have led to a wealth of information on lymphomagenesis and its impact on the diagnosis, prognosis, and management of lymphoma, which will continue into the next decade. However, in contrast to B-cell lymphomas, peripheral T-cell lymphomas (PTCL) have been the subject of only a limited number of studies to elucidate their pathobiology and identify novel pharmacological approaches. Understanding of the biology and optimal treatment of PTCL has been limited due to only recent recognition of PTCL in addition to disease rarity and histologic subtype heterogeneity. With the development of new technologies in genomic analysis new opportunities arose to improve the current knowledge as far as microRNA and gene expression signatures are concerned.

In the present manuscript, different approaches were undertaken to investigate alterations in gene and microRNA expression of a series of PTCL samples. Furthermore, the mechanisms of action and resistance of CTCL treatments were studied and possible new therapies were suggested.

7.1 Identification of microRNAs, genes and biological pathways implicated in pathogenesis of peripheral T cell lymphoma

Peripheral T-cell lymphoma represents an orphan pathology. This can be explained by their relatively low prevalence, diagnostic difficulties and dismal prognosis. One of the drawbacks of the functional studies is because of the lack of suitable cell lines in most of the aggressive PTCL, such as PTCLU or AITL, indicating the difficulty to establish cell lines from these tumors, and probably, a relevant role played by the infiltrating reactive cells in these PTCLs. Thus, most studies have been performed on cutaneous T-cell lymphoma (CTCL), ALCL and lymphoblastic T-cell lymphoma. However, an improved understanding of the biology of the PTCL should allow development of better treatments for these disorders.

Aberrant microRNA expression patterns have been described in various hematological and solid cancers, and alterations in microRNA expression correlate highly with progression and prognosis of human malignant diseases. However, profiles of microRNAs differ and need to be investigated in every type of tumor. In the first study, substantial associations between differential expression of specific microRNAs and course of disease and prognosis of peripheral T-cell lymphoma were recorded. The global microRNA expression comparing a series of PTCL samples with LN tissue revealed loss of 102 microRNAs. The most remarkably down-regulated microRNAs belonged to the families of let-7, miR-10, miR-101, miR-29, miR-215, miR-150, miR-139, miR-126 and miR-195 which regulate stemness, stress response, apoptosis, proliferation, angiogenesis, and expression of genes. The significant decrease in most members of let-7 was observed (FDR < 0.0001) which correlates with the enrichment of RACCYCD (Ras and Rho) pathway (FDR = 0.018) in PTCL patients. The Ras family of oncogenes has been previously described to be regulated by the let-7 family in solid tumors (lung cancer) (Esquela-Kerscher et al., 2008; Kumar et al., 2008). Additionally, in tumor-initiating cells of breast cancer (which have stem cell like properties), let-7 regulates self-renewal (by silencing HRAS) and differentiation (by silencing HMGA2). Furthermore, miR-101, significantly repressed microRNA with the highest score in SAM analysis was shown to be downregulated in hepatocellular carcinoma and colon cancer (Strillacci et al., 2009). Interestingly, decrease in miR-101 expression was found during cancer progression. In addition, it was suggested that miR-101 could exert its proapoptotic function via targeting MCL1, an important prognostic factor in NHL (Kuramoto et al., 2002; Su et al., 2009; Varambally et al., 2008). Moreover, miR-101 turned out to be significant (FDR < 0.05) in the Fisher analysis correlating microRNA and mRNA expression in the presented series of PTCL. Taken together, this data suggest an important role of miR-101 in the molecular etiology of cancer (including PTCL) and implicate the potential application of miR-101 in cancer therapy. Importantly, the loss of miR-15 and miR-16, known to act as tumor suppressors was observed which is consistent with previous reports of downregulation of the mentioned microRNAs in chronic lymphocytic leukemia (CLL), pituitary adenomas, and prostate carcinoma. Expression of these miRNAs inhibits cell proliferation, promotes apoptosis of cancer cells, and suppresses tumorigenicity both in vitro and in vivo, possibly through targeting multiple oncogenes, including BCL2, MCL1, CCND1, and WNT3A (Aqeilan et al.; Cimmino et al., 2005). Of note is the fact that miR-15a has also been found to be significant in Fisher analysis which makes it an attractive candidate for further studies in PTCL. Other significant microRNAs, including miR-215, miR-10 and miR-126, were previously described to be downregulated in lung and colon cancers (Georges et al., 2008; Guo et al., 2008; Izzotti et

al., 2009; Sun et al.). Moreover, tumor suppressor function of miR-215 could be related to their suppression of cancerogenesis through CDKN1A/p21 accumulation and cell cycle arrest (Braun et al., 2008). As the protein encoded by CDKN1A binds to and inhibits the activity of cyclin-CDK2 or -CDK4 complexes, and thus regulates cell cycle progression at G1, these data reflect the alterations of G1 and cell cycle pathways identified by gene expression data (FDR equal to 0.178 and 0.134, respectively). Furthermore, miR-126, in addition to controlling cell proliferation, negatively regulates the angiogenesis through targeting vascular endothelial growth factor (VEGF) (Guo et al., 2008). Besides, miR-10a, miR-150 and miR-29, likewise in the presented PTCL series, were found to be downregulated in other hematological malignancies, such as chronic myeloid leukemia (miR-10a, miR-150) as well as mantle cell lymphoma (miR-29, miR-150) (Agirre et al., 2008; Zhao et al.). Down-regulation of miR-10a was related to the increase in levels of USF2 and hence contribution to the increase in cell proliferation of chronic myeloid leukemia cells (Agirre et al., 2008). On the other hand, ectopic expression of miR-150 in breast cancer and leukemic cells was associated with repressed endogenous c-Myb at both messenger RNA (mRNA) and protein levels (Lin et al., 2008). Notably, changes in the expression levels of miR-29 family were previously reported to be associated with disease prognosis (mantle cell lymphoma). The patients with significant downregulated miR-29 had shorter survival as compared to those who express relative high level of miR-29. In addition, a mechanism through which miR-29 exerts its function was suggested to be through overexpression of cyclin D1 and activation of CDK4/6 (Zhao et al.). Similar mechanism was implied for miR-195 which downregulation was described in various types of cancers, including hepatocellular carcinoma and bladder cancer (Ichimi et al., 2009; Xu et al., 2009). Xu *et al* showed that miR-195 may block the G1/S transition by repressing Rb-E2F signaling through targeting multiple molecules, including cyclin D1, CDK6, and E2F3 (Xu et al., 2009).

In summary, this review of the microRNAs most significantly repressed in PTCL samples (Fold change < 0.2) suggests, as expected, alterations in such important pathways as apoptosis (through BCL2 signaling), cell cycle (CDK, G2, G1 pathways), proliferation (WNT, RACCYCD pathway) and angiogenesis (VEGF pathway). This confirms the gene sets identified by gene set enrichment analysis, in addition to ERK and EGF pathways with high level of significance (FDR: 0.013 and 0.030, respectively).

Taking into consideration the heterogeneity of PTCL tumors and limited data on microRNA and gene expression patterns, we sought to identify also genes and microRNA related to various

subsets of PTCL. In the attempt to verify the immune profile of a series of PTCL cases, two groups were identified with distinct T-cell subsets signature. Interestingly, the null-phenotype group lacked expression of genes characterizing normal T-cell subtypes (both CD4+ and CD8+). In contrast, higher plasticity of T cell lineages than previously appreciated was observed in the differentiated group. Even though the division into null-phenotype and differentiated group did not show a reflection in the cases diagnostics, the microRNA as well as gene expression characterization of both groups brought along interesting findings.

Interestingly, half of the patients in the null-phenotype group highly expressed oncogenic miR-17-92 cluster (oncomir-1) and miR-181 family. miR-17-92 cluster expression is described to concomitantly reduce E2F1 protein expression, regulating proliferation and/or apoptosis E2F1 protein levels, thereby enhancing survival of leukemic T-cells (Mu et al., 2009; Nagel et al., 2009). Moreover, He *et al* showed that enforced expression of the miR-17-92 cluster accelerated MYC-induced lymphomagenesis, suggesting the oncogenic potential of the overexpressed microRNAs (He et al., 2005). miR-17-92 cluster and miR-181 were also delineated to have a 'permissive' function in the maturation, proliferation and differentiation of myeloid and lymphoid cells. Importantly, these actions of miRNAs often involve interactions with transcription factors (Tsitsiou and Lindsay, 2009). Among the most significant microRNAs, able to distinguish between the null-phenotype and differentiated group, many have not been previously described in any cancer types. However, overexpression of oncogenic miR-372 in the null-phenotype group was observed, which could be related to the increased proliferation of neoplastic cells in this group as this microRNA plays a role in controlling cell growth, cell cycle, and apoptosis through down-regulation of a tumor suppressor gene, LATS2 (Cho et al., 2009). In contrast, the increase of tumor suppressor microRNAs was observed in the differentiated group, including miR-205 and miR200a. The fact that downregulation of these microRNAs might be an important step in tumor progression could give a rationale for the worst outcome of patients with the null-phenotype. miR-205 inhibits tumor cell migration through down-regulating the expression of the LDL receptor-related protein 1 (Song and Bu, 2009) and possibly through its direct targets ErbB3 and vascular endothelial growth factor A (VEGF-A) (Wu et al., 2009). Similarly, miR-200a was reported to affect the metastatic potential of cervical cancer cells by coordinate suppression of multiple genes controlling cell motility (Hu et al.) and inhibit ovarian cancer cell migration. Moreover, low-level expression of miR-200 is thought to predict poor survival (Hu et al., 2009). Furthermore, upregulation of miR-601, miR-331 and miR-146b in differentiated group could have an impact on regulation of actin

cytoskeleton and Fas-induced apoptosis (mir-601) (Ohdaira et al., 2009), cell proliferation and survival (through miR-331 putative target - SOCS1) (Zanette et al., 2007), and inhibition of invasion and migration (miR-146b) (Hurst et al., 2009). Increased expression of miR-15a and miR-223 could also be indicative of better course and disease outcome in the differentiated group of patients as miR-15a is known to induce apoptosis in other hematological malignancies (Cimmino et al., 2005) and enhanced levels of miR-223 are described to restore cell differentiation (Fazi et al., 2007). Several pathways identified as significantly differentially expressed between null-phenotype and differentiated group have the representation in targets of significant microRNAs, including BCL2 family, caspase and death pathways enriched in differentiated group or RACCYCD pathway in null-phenotype group.

Prognostic biomarkers are urgently needed to identify patients at high risk for peripheral T-cell lymphoma. microRNA expression profiles have been linked to the clinical features of several cancers; this suggests that some microRNAs have potential as diagnostic and prognostic markers. In the present study, microRNA expression profiles were assessed in PTCL and several attractive targets for more in depth investigation were found. However, further studies are needed to establish whether the microRNAs identified in the presented study have full potential as either biomarkers or therapeutic targets in PTCL as the number of samples used was quite limited and lacking clinical information did not allow final validation. The association between aberrant expression of microRNAs and malignancy is now so compelling that research is rapidly focusing on the therapeutic use of these molecules. Perhaps one of the biggest problems/limitations facing the use of microRNAs and/or associated agents as therapeutics is their pleiotropic mode of action. As a single microRNA can target several hundred genes their perturbation may be expected to give rise to a complex phenotype that may not be readily predictable. It is therefore imperative that such therapeutics is precisely delivered in order to mitigate effects on non-targeted cells.

7.2 Identification of new pathways associated with resistance to PUVA +/- IFNα therapy

There are several treatment options, such as skin directed therapies (topical corticosteroids, carmustine, bexarotene gel, total skin electron bean therapy or PUVA), systemic therapies (retinoids, rexinoids, HDAC inhibitors, denileukin diftitox, IFNα, monoclonal antibodies) and other treatment modalities available for treatment of CTCL (Kim et al., 2005; Wollina and Dummer, 2006). IFNα therapy is frequently used and found to be effective in the treatment of

early stages of MF, especially in combination with PUVA (Chiarion-Sileni et al., 2002; Roenigk et al., 1990). Some authors report very promising results of 80% CR rate when using the combination of IFNα and PUVA showing higher response rate and longer duration that PUVA or IFNα monotherapies (Kuzel et al., 1990; Kuzel et al., 1995; Mostow et al., 1993; Roenigk et al., 1990). However, it is not clear why some patients respond better to the therapy than the others and what could be the underlying molecular mechanisms contributing to treatment resistance.

In this study, gene expression profiling and response data from early stage MF patients enrolled in a randomised clinical trial of PUVA alone or in combination with IFNα was used in order to identify markers associated with lack of remission and resistance to treatment. The randomized clinical trial of PUVA +/- IFNα performed here showed no significant difference between the treatment arms. The patients treated with PUVA alone showed similar response rates to the patients treated with PUVA and IFNα, nevertheless, lower UVA doses can be used during the combined treatment. However, the information and clinical samples obtained allowed identification patients resistant to treatment and to describe that the molecular signature of resistance in these early stage MF patients is composed by a combination of signals derived from NF-κB activation, known to be important in the MF lymphomagenesis (Tracey et al., 2003), T-cell receptor signaling, inflammatory cytokine signaling and JAK/STAT signaling.

The poor response-associated group of genes, interesting for the identification of markers associated with therapy resistance, highlighted characteristics of CTCL cells as well as non-malignant cells present in the tumor tissue. Many of the genes and pathways identified in this study confer a survival advantage on tumoral T-cells, including genes important for T-lymphocyte activation and proliferation (*CD69*, *FYN*, *TNC, MAF*), migration (*ENG*, *TNC*, *MYO1B*, *FYN*) and survival (*WNT4*, *NFKB2*). Additionally, IFN signaling pathway genes such as *SOCS1* and *IRF2BP2* were associated with treatment outcome. SOCS1 negatively regulates IFN activity and therefore it is not surprising that its expression was associated with poor response. Moreover, its expression has previously been associated with poor response to IFNα in chronic myeloid leukaemia (Roman-Gomez et al., 2004). IRF2BP2 is a co-repressor of IRF2, which is induced by IFNα treatment. This induction is correlated with the clinical response of IFNα treatment in carcinoid tumours (Zhou et al., 2000), shedding some light on the association of IRF2BP2 with poor response to treatment in MF patients. Although the molecular mechanisms by which PUVA

acts are not well understood, it has been described that the exposure may lead to expression of inflammatory cytokines (IL10, IL8, IL6) that could influence IFNγ and TNFα (Kim-Han et al., 2001; Wolf et al., 2006). The *in vivo* elevation of SOCS and IRFBP2 gene expression found may be part of the host/tumour response, as has been suggested in other tumors (Raccurt et al., 2003). Treatment resistance is a complex and dynamic process involving interactions between many pathways. Using GSEA we identified several pathways related to unfavorable response to treatment, which could interact with each other and cause a series of subsequent events leading to activation and/or up regulation of the other pathways contributing to treatment outcome. The pathways highlighted by GSEA analysis showed similar results to Ingenuity Pathway Analysis. In addition, signaling by the CCR5 chemokine, FAS, MAPK, T-regulatory cells, Notch and mTOR were found to be of importance. Finally, separate analysis of only PUVA-treated patients and PUVA/IFNα-treated patients also revealed the importance of the same pathways. In summary, gene expression profiling showed that the cytokine inflammatory response, TCR and NF-κB pathway activation, as well as expression of certain chemokine receptors promoting migration and homing of T-cells to skin and inflamed tissues are an important determinant of treatment outcome. Full understanding of the interaction between the mentioned pathways could be predictive of survival and the patient response to the therapy at the time of diagnosis.

Tumor microenvironment is an important factor in conferring drug resistance, and one of the major causes underlying treatment failure and relapse in cancer (Herreros et al., 2007). The epithelial cells, squamous cells, fibroblasts, macrophages and dendritic cells are the important cells constituting the tumor microenvironment. Emerging information highlights the importance of tumour-accompanying non-neoplastic cells in cancer progression. Those cells could promote production of immunosuppressive factors and inhibit anti-tumor immune responses promoting growth, survival and proliferation of tumor cells. The interaction between the cytokines, chemokines, growth factors and matrix degrading enzymes produced in the tumor microenvironment have complex functions and account for various cell interactions and regulation of differentiation, activation, proliferation and survival of different cell types (Galmarini and Galmarini, 2003; Li and Dalton, 2006). For example, stromal dendritic cells can protect from apoptosis, stimulate proliferation, and induce tumoral T-cell homing to the skin through expression and secretion of specific chemokines and cytokines (Shurin et al., 2006).

Other cells such as macrophages, dendritic cells, epithelial cells and non-malignant lymphocytes also interact directly with neoplastic cells. A high density of tumor-associated macrophages is associated with chronic inflammation, resulting in suppression of the anti-tumor immune response (Balkwill et al., 2005) and NF-κB activation, a key player in the tumorigenesis of MF (Tracey et al., 2003). This interplay between the neoplastic cells and the tumor microenvironment could promote cell-cycle progression and survival, thereby conferring increased drug resistance to malignant cells. Many of the markers identified in this study, are expressed not only by tumoral cells but also by the tumor microenvironment, underlining the important role of the stroma in conferring therapy resistance in MF.

In MF, it appears that activation of the NF-κB pathway and T-cell signaling in both tumor cells as well as in the microenvironment plays a central role in treatment resistance. The activation of the JAK/STAT pathway in MF reported here suggests that this pathway may play a role in the pathogenesis of cutaneous T-cell lymphomas, as has been previously described in other T-cell lymphomas (Zhang et al., 1996). Notch signaling, recently described to play a role in T-cell leukemogenesis (Gothert et al., 2007), was also associated with poor response and may play a role in treatment outcome as has been shown in other hematological malignancies (Nefedova et al., 2004). Furthermore, Notch signaling is known to induce secretion of IL6 (Li and Dalton, 2006), which leads to constitutive activation of STAT3, an oncogene expressed in tumor stage MF cases and thought to be a characteristic feature of MF neoplastic transformation. In earlier stage cases, as studied here, STAT3 expression is more clearly observed in the tumor microenvironment, with constitutively active STAT3 expression observed in NK cells, neutrophils and macrophages of the tumor stroma (Sommer et al., 2004). STAT3 can alter the cell-cycle, prevent apoptosis, and mediate the proliferation and survival of tumor cells and it is known to have a negative influence on Th1-type inflammation (Brender et al., 2001; Takeda et al., 1999) attenuating the inflammatory properties of type 1 cytokines. Meanwhile the expansion of Th2 phenotype is recognized as one of the hallmarks of MF progression(Whittaker, 2006). Constitutive activation of NF-κB and STAT3 play an important role in resistance to chemotherapy in other tumor types (Bhardwaj et al., 2007), and have previously been linked with resistance to IFNα and other treatments in MF (Sors et al., 2006; Tracey et al., 2004; Yang et al., 1998). Taken together, these data point towards the importance of mutual interactions and overlap of signaling pathways in the resistance to PUVA +/- IFNα therapy. Many of these markers, as shown by immunohistochemistry, are expressed not only by the tumor but also in the tumor microenvironment, suggesting the important role

that the stroma may play in conferring therapy resistance. In many other haematological malignancies, the tumor microenvironment is thought to provide nutrition and survival factors to the tumor contributing to disease progression. Among the factors related to survival and growth in haematological malignancies are vascular endothelial growth factor (VEGF), IL6, IL3, TNF super family members and many others (Li and Dalton, 2006). Many of those factors are also angiogenic factors that indirectly promote tumor progression through angiogenesis and metastasis (Yu et al., 2007). Those factors utilize several signaling pathways such as JAK/STAT, MAPK, NF-κB and the others. Seemingly, activation of the NF-κB pathway in both tumor cells as well as in the microenvironment plays a central role in treatment resistance. The up-regulation of T-cell signalling (Th2 cytokine profile, T-regulatory cells) and TNF signaling leading to NF-κB pathway activation seem to play an essential role in the phenomenon of resistance.

Furthermore, the use of Connectivity Maps has identified the potential molecules that could be used in combination for treatment of PUVA +/- IFNα resistant patients. As described in Results section the potential molecules for use in a combination therapy included histone deacetylase inhibitors (HDACi): Vorinostat (SAHA, Zolinza™) and Scriptaid, known anticancer antibiotics binding to heat shock protein 90 (Hsp90): Tanespimycin (17-AAG) and geldanamycin. Moreover, 17-AAG, tested *in vitro* in CTCL cells, has shown potent cytotoxic activity. Toyooka *et al* showed that the HDACi, remarkably enhanced the cell killing effect of psoralen plus UVA (PUVA) in several cancer cell lines including skin melanoma. Moreover, HDACi (sodium butyrate)-induced augmentation of the cell killing effect was more dramatic in combination with PUVA than with anticancer drugs. The immediate potential application of HDACi-PUVA treatment could be in therapy of CTCL as both PUVA and HDACi (suberoylanilide hydroxamic acid – vorinostat), are presently used as monotherapy for CTCL. Additionally, HDACi-PUVA treatment killed the CTCL cells more effectively than PUVA treatment alone (Toyooka and Ibuki, 2009).

The results gleaned from these studies illustrate that not only are gene expression changes in the tumor important for drug resistance, but also changes in the tumor microenvironment are an important determinant of treatment outcome. Treatment resistance can be conferred by both direct and indirect interaction between the tumor cells and the tumor microenvironment. These bi-directional interactions provide survival and proliferation signals by pathways involved in up-regulation of anti-apoptotic molecules and promotion of cell growth and proliferation, and identify potential therapeutic targets expressed by inflammatory cells.

Therefore, the tumor microenvironment plays a crucial role in response to treatment and survival of the malignant cells. Some pro-inflammatory factors such as NF-κB, TFNα and interleukins such as IL6 and their respective receptors in addition to STAT3 could be promising targets for MF treatment, and their inhibitors could help to overcome treatment resistance in combination with other drugs, such as Hsp90 or HDAC inhibitors.

7.3 Identification of mechanism of action and synergistic agents for HDACi

Recent reports have highlighted the pre-clinical activity of HDAC inhibitors in human leukemia and lymphoma cells (Marks and Breslow, 2007; Ungerstedt et al., 2005), as well as the promising results in a substantial proportion of patients with advanced CTCL (response rate of around 30%) (Duvic et al., 2007), leading to its approval by FDA. Presently, the therapeutic use of vorinostat focuses on application in combination therapies which is reflected in undergoing numerous clinical trials. However, the mechanism of action, essential for efficient use and combination, has not been fully identified. A likely model for the anti-tumor action of vorinostat is that the inhibition of HDAC activity, and subsequent accumulation of acetylated nucleosomal histones, leads to the alteration of genes involved in regulation of differentiation, apoptosis and tumor growth (Marks et al., 2001). The study presented in chapter 5 shows that vorinostat at the concentration of 5μM induces CTCL cell apoptosis via several different but nonexclusive mechanisms. Cellular kinetics of particular tumors is an important consideration in the design of antineoplastic drug regimens and may influence the dosing schedules and timing intervals of treatment.

In CTCL the balance between cell proliferation and cell death is altered, which contribute to a clonal expansion of cancer cells. Zhang *et al* (Zhang et al., 2003) .investigated the expression of apoptosis regulators in CTCL cells reporting shift of the equilibrium between inducers and inhibitors to the side of inhibitors. The expression of *BCL2L1 (BCL-xL), MCL1, BAD* and *BAX*, but not *BCL-x* was found to be expressed in CTCL and could be sufficient for survival of malignant CTCL cells. Similarly to Rosato *et al.*(Rosato et al., 2003) we observe decrease in expression of *BCL2L1, MCL1, BCL2, BID* which indicate enhanced apoptosis upon treatment with vorinostat Moreover, our data reveal alterations in both intrinsic (*CASP9, CASP7, APAF1*) as well as extrinsic (*FAS, BID, cFLAR*) apoptosis pathways following vorinostat treatment. Similarly to previous observations in leukemic cells (Mitsiades et al., 2004; Peart et al., 2005; Ruefli et al., 2001) we noted activation of intrinsic apoptotic pathway through upregulation of *CASP9* and a key downstream effector of the pathway - *APAF1*. Furthermore, we identified decrease in

expression of important members of extrinsic apoptosis pathway upon treatment with vorinostat, such as *FAS BID, cFLAR (CASP8).* The extrinsic apoptotic pathway, either alone or together with intrinsic pathway, has been previously described to be altered upon treatment with HDACi in other cancer types, including leukemias (Rosato et al., 2003), breast (Mitchell et al., 2007), lung (Kim et al., 2006a) and head and neck (Gillenwater et al., 2007) malignancies. As vorinostat promotes upregulation and activation of multiple proapoptotic factors we reckon that downregulation of *FAS, BID* and *cFLAR* could be a compensating mechanism of CTCL cells in response to treatment. Additionally, vorinostat inhibited members of TNF receptor superfamily and their downstream signaling cascades, expressed in activated T cells, which are responsible for transduction of survival and proliferation signals while upregulated genes mediating signals for apoptosis (Tracey et al., 2003). Consistent with the previous findings of Duvic *et al* (Duvic et al., 2007) and Fantin *et al* (Fantin et al., 2008) modulation of JAK/STAT pathway was observed, including suppression of *STAT6, STAT5A, SOCS2, SOCS6* and *SOS* accompanied by enhanced expression of *STAT1, STAT2, STAT3, STAT5B, SOCS3, IFNAR2, INFG, IFNGR1* and *JAK1*.

Finally, vorinostat repressed several members of TCR as well as factors acting downstream. vorinostat treatment caused downregulation of *ZAP70, LAT, VAV2, CD247, CD3D, CD3E, CD3G, CD4, IL4, IL5, IL10, IL13, IL4R, IL6R, PTPN6, PAK2, PAK6, ICAM1, NMI, FOXP3* but upregulated genes included: *FYN, IFNG, IFNGR1, IL12A* suggesting a shift in the balance of T helper cells from Th2 (phenotype of malignant T cells) to Th1. In chapter 4 relation between TCR pathway and PUVA +/- IFNα treatment resistance was established. To my knowledge, this is the first report that identifies TCR signaling pathway as a target for vorinostat.

T-lymphocytes play a crucial role in the immune response, both as direct effector cells and as regulatory cells that modulate functions of other cell types. Among the earliest recognizable events after T-cell receptor (TCR) stimulation are the activation of LCK (p56lck) and FYN (p59fyn), which result in phosphorylation of tyrosine residues(Zamoyska et al., 2003). Subsequently, ZAP70 (ζ-associated protein 70) tyrosine kinase is recruited to the TCR where it is activated by LCK through tyrosine phosphorylation (Iwashima et al., 1994). ZAP70 is a key signaling molecule in T cells, where it couples the antigen-activated T-cell receptor (TCR) to downstream signaling pathways (Chu et al., 1998). Once ZAP70 is activated, LCK and ZAP70 presumably act synergistically to phosphorylate specific downstream substrates, which in turn orchestrate the cytoplasmic signaling cascades leading to T-cell activation. These central roles

of LCK and ZAP70 in TCR signaling have been amply documented. ZAP70 causes phosphorylation of LAT (linker for activation of T-cells), which in turn activates important downstream signaling pathways, including protein kinase C (PKC), protein kinase B (PKB), and mitogen-activated protein kinases (MAPKs), such as extracellular signal-regulated kinase (ERK), p38 MAPK, c-JUN N-terminal kinase (JNK) (Janeway and Bottomly, 1994). The PI3K/AKT pathway is also necessary for the survival of T-lymphocytes through both increased expression of BCL-XL and as a consequence of the role AKT plays in supporting metabolism in proliferating lymphocytes (Juntilla and Koretzky, 2008). Activation of ERKs in response to TCR stimulation is largely, but not entirely, dependent on ZAP70 (Griffith et al., 1998). We examined the activation of TCR through evaluation of phosphorylation of ZAP70 and its downstream factors such as ERK and AKT. Consequently, we observed a reduction in activating phosphorylation of all members including ZAP70, ERK and AKT which confirms that vorinostat inhibits TCR signaling by both downregulation of the expression of several members of the pathway as well as phosphorylation of key tyrosine kinases.

Due to the broad activity of vorinostat, the inhibition of other kinases affecting T-cell function cannot be excluded. The increase of the SRC family tyrosine kinase FYN, which is also participating in activation of TCR, also observed by Peart *et al* (Peart et al., 2005), seems to be a compensating mechanism in response to stress caused by vorinostat to tumoral cells, and likely indicating that fine tuning of TCR signaling is essential for vorinostat action in CTCL cells.

Clinical trials of vorinostat, both alone or in combination therapy, are on-going and show promising anti-cancer activities in both hematologic as well as solid tumors. The molecular events underlying the synergistic effect using vorinostat in combination remain to be fully elucidated; the mechanisms will plausibly be dependent on the tumor cell type, specific molecular events and the precise added agent. So far a limited amount of reports have focused on describing the interactions of HDACi (including vorinostat) and inhibitors targeting phosphoinositide 3-kinase (PI3K) and all of these efforts have centred on LY294002 (Rahmani et al., 2003b). Our current work indicates that a more potent and selective, hence less toxic, inhibitor of PI3K - ETP-45658, demonstrates comparable to LY294002 synergy with vorinostat. Several properties that are critical for therapeutic agents differentiate ETP-45658 from previously tested PI3K inhibitors, including wortmannin and LY294002 (Bain et al., 2007; Hennessy et al., 2005; Nagata et al., 2004), mainly ETP-45658 is highly selective for class IA PI3K (Link et al., 2009). These make ETP-45658 an attractive candidate for further clinical studies in combination with vorinostat and other HDACi. For combination of vorinostat and 17-

AAG, we observed the opposite effect to the one described in human leukemia cells (Rahmani et al., 2005; Rahmani et al., 2003a) and mantle cell lymphoma (Rao et al., 2009). Our data show that coadministration of vorinostat and 17-AAG results in antagonistic interaction, which could be related to the fact that vorinostat by itself already inhibits expression of HSP90 (Fiskus et al., 2007). This result suggests that coadministration of vorinostat and 17-AAG should be avoided in CTCL. Moreover, we observed a correlation between the expression levels of targets of the inhibitors used following vorinostat treatment and the effect of the combination. Whenever the molecule targeted by the inhibitor was upregulated (GSK-3β, PIM), the combination therapy resulted in synergistic or additive interaction. Furthermore, downregulation of HSP90 (target of 17-AAG) upon vorinostat treatment showed an antagonistic effect of coadministration of 17-AAG with vorinostat. This suggests that inhibitors of the genes whose levels significantly increase following vorinostat treatment could be the potential candidates for successful combination therapy.

The presented data provide substantial new information improving our knowledge and understanding of vorinostat action, and suggest that clinical trials of vorinostat, either alone or in combination, performed in CTCL should evaluate its in vivo effect on the signal transduction of TCR and correlate the results with the treatment response. In addition, several clinical implications can be drawn from our studies. First, PI3K inhibitors, such as ETP-45658 could be used in combination with vorinostat-based therapies, and, based on our current study, it is anticipated that the combination could be highly effective. Therefore, combining vorinostat with PI3K inhibitors is a rational approach to increase the cytotoxic effects in CTCL. These results provide proof-of- principle that a comprehensive understanding of the mechanisms of vorinostat action is central to designing rational combination approaches using HDACi.

CONCLUSIONS

1. Peripheral T-cell lymphomas (PTCL) showed a characteristic microRNA signature including downregulation of microRNAs let-7 family, miR-10, miR-15, miR-16, miR-101, miR-29, miR-215, miR-150, miR-139, miR-126 and miR-195 regulating stemness, stress response, apoptosis, proliferation, angiogenesis, and cell cycle pathways.

2. Neoplastic T cells in most cases of peripheral T-cell lymphoma (PTCL) were endowed with functional plasticity, expressing simultaneously genes that identify different normal peripheral T-cell subpopulations.

3. A group of peripheral T-cell lymphoma (PTCL) with a null-phenotype (lacking normal T-cell subpopulations' markers) has been identified, expressing oncogenic microRNA signature. This group showed an increased proliferation with enrichment of Ras and Rho associated pathways.

4. The gene signature associated with activation of NF-κB survival pathway, inflammatory cytokine and T cell signaling pathway were found to be of importance in prognosis of response to PUVA and IFNα treatment in mycosis fungoides (MF) patients.

5. Many of the markers identified as related to PUVA and IFNα resistance, were expressed not only by tumoral cells but also by the tumor microenvironment, underlining the important role of the stroma in conferring therapy resistance in mycosis fungoides (MF)

6. The Connectivity Map analysis revealed molecules that could potentially reverse the PUVA and IFNα resistance signature, including 17-AAG and vorinostat.

7. HDACi inhibited proliferation, increased acetylation of histones, induced cell death and cell cycle arrest in cutaneous T-cell lymphoma (CTCL) cells

8. HDACi decreased T-cell receptor (TCR) signaling through inhibition of kinase phosphorylation (ZAP70, AKT) in cutaneous T-cell lymphoma (CTCL) cells.

9. The combination of HDACi with phosphatidylinositol 3-kinase (PI3K) inhibitors resulted in synergy while cytotoxic antagonism was observed when combining vorinostat with heat shock protein 90 (HSP90) inhibitor in cutaneous T-cell lymphoma (CTCL) suggesting that combination therapies involving histone deacetylase (HDAC) and PI3K inhibitors can potentially be efficacious for the treatment of CTCL.

CONCLUSIONES

1. Los linfomas periféricos de célula T (LPCT) presentan un perfil de microARNs característico, incluyendo una disminución en la expresión de los microARNs de la familia de let-7, miR-10, miR-15, miR-16, miR-101, miR-29, miR-215, miR-150, miR-139, miR-126 y miR-195 que regulan las rutas responsables de las propiedades de células troncales, respuesta al estrés, apoptosis, proliferación, angiogénesis y ciclo celular.

2. En la mayoría de los casos estudiados, las células T tumorales estaban dotadas de plasticidad funcional y expresaban genes que identificaban a las diferentes subpoblaciones de células T periféricas normales.

3. Se identificó un grupo de linfomas periféricos de célula T (LPCT) con un fenotipo nulo (carecen de los marcadores de subpoblaciones normales de células T) que expresaba un conjunto de microARNs oncogénicos. Este grupo mostraba una mayor proliferación y una mayor activación de las rutas asociadas a Ras y Rho.

4. Se descubrió que el perfil genético asociado a la activación de las rutas de supervivencia de NF-κB, citoquinas inflamatorias y señalización de células T son importantes en el pronóstico y la respuesta al tratamiento con PUVA e IFNα en pacientes con micosis fungoides (MF).

5. Muchos de los marcadores identificados como relacionados con la resistenacia a PUVA e IFNα se expresaban no sólo en la población de células tumorales sino también en el microambiente del tumor, subrayando la importancia del estroma en otorgar resistencia a la terapia en micosis fungoides.

6. El análisis in silico realizado con el "Connectivity Map" reveló algunas moléculas como 17-AAG y vorinostat que podrían, potencialmente, revertir el perfil de expresión asociado a la resistencia a PUVA e IFNα.

7. Los HDACi inhiben la proliferación, incrementan los niveles de acetilación de histonas e inducen muerte celular y parada del ciclo celular en células de linfoma cutáneo de célula T (LCCT).

8. Los HDACi disminuyen la señalización del receptor de célula T mediante la inhibición de la fosforilación de quinasas (ZAP70, AKT) en células de linfoma cutáneo de célula T (LCCT).

9. La combinación de HDACi con inhibidores de la fosfatidilinositol 3-quinasa (PI3K) resultó en un efecto sinérgico. Sin embargo, se observó antagonismo citotóxico cuando se combinó el vorinostat con el inhibidor de HSP90 (*Heat shock protein 90*) en linfoma cutáneo de célula T (LCCT) lo cual sugiere que las terapias combinadas de inhibidores de histona desacetilasas y fosfatidilinositol 3-quinasas pueden, potencialmente, ser eficaces en el tratamiento de LCCT.

BIBLIOGRAPHY

References List:

Abramovich, C., Shulman, L. M., Ratovitski, E., Harroch, S., Tovey, M., Eid, P., and Revel, M. (1994). Differential tyrosine phosphorylation of the IFNAR chain of the type I interferon receptor and of an associated surface protein in response to IFN-alpha and IFN-beta. Embo J *13*, 5871-5877.

Agirre, X., Jimenez-Velasco, A., San Jose-Eneriz, E., Garate, L., Bandres, E., Cordeu, L., Aparicio, O., Saez, B., Navarro, G., Vilas-Zornoza, A.*, et al.* (2008). Down-regulation of hsa-miR-10a in chronic myeloid leukemia CD34+ cells increases USF2-mediated cell growth. Mol Cancer Res *6*, 1830-1840.

Al-Shahrour, F., Diaz-Uriarte, R., and Dopazo, J. (2004). FatiGO: a web tool for finding significant associations of Gene Ontology terms with groups of genes. Bioinformatics *20*, 578-580.

Al-Shamkhani, A. (2004). The role of CD30 in the pathogenesis of haematopoietic malignancies. Curr Opin Pharmacol *4*, 355-359.

Altiok, S., Batt, D., Altiok, N., Papautsky, A., Downward, J., Roberts, T. M., and Avraham, H. (1999). Heregulin induces phosphorylation of BRCA1 through phosphatidylinositol 3-Kinase/AKT in breast cancer cells. J Biol Chem *274*, 32274-32278.

Amaravadi, R., and Thompson, C. B. (2005). The survival kinases Akt and Pim as potential pharmacological targets. J Clin Invest *115*, 2618-2624.

Amson, R., Sigaux, F., Przedborski, S., Flandrin, G., Givol, D., and Telerman, A. (1989). The human protooncogene product p33pim is expressed during fetal hematopoiesis and in diverse leukemias. Proc Natl Acad Sci U S A *86*, 8857-8861.

An, W. G., Schulte, T. W., and Neckers, L. M. (2000). The heat shock protein 90 antagonist geldanamycin alters chaperone association with p210bcr-abl and v-src proteins before their degradation by the proteasome. Cell Growth Differ *11*, 355-360.

Aqeilan, R. I., Calin, G. A., and Croce, C. M. miR-15a and miR-16-1 in cancer: discovery, function and future perspectives. Cell Death Differ *17*, 215-220.

Armitage, J. O., and Coiffier, B. (2000). Activity of interferon-alpha in relapsed patients with diffuse large B-cell and peripheral T-cell non-Hodgkin's lymphoma. Ann Oncol *11*, 359-361.
Armitage, J. O., Vose, J. M., and Weisenburger, D. D. (2004). Towards understanding the peripheral T-cell lymphomas. Ann Oncol *15*, 1447-1449.

Atadja, P., Hsu, M., Kwon, P., Trogani, N., Bhalla, K., and Remiszewski, S. (2004). Molecular and cellular basis for the anti-proliferative effects of the HDAC inhibitor LAQ824. Novartis Found Symp *259*, 249-266; discussion 266-248, 285-248.

Bachmann, M., Hennemann, H., Xing, P. X., Hoffmann, I., and Moroy, T. (2004). The oncogenic serine/threonine kinase Pim-1 phosphorylates and inhibits the activity of Cdc25C-associated kinase 1 (C-TAK1): a novel role for Pim-1 at the G2/M cell cycle checkpoint. J Biol Chem *279*, 48319-48328.
Bachmann, M., Kosan, C., Xing, P. X., Montenarh, M., Hoffmann, I., and Moroy, T. (2006). The oncogenic serine/threonine kinase Pim-1 directly phosphorylates and activates the G2/M specific phosphatase Cdc25C. Int J Biochem Cell Biol *38*, 430-443.

Bachmann, M., and Moroy, T. (2005). The serine/threonine kinase Pim-1. Int J Biochem Cell Biol *37*, 726-730.

Bagatell, R., Khan, O., Paine-Murrieta, G., Taylor, C. W., Akinaga, S., and Whitesell, L. (2001). Destabilization of steroid receptors by heat shock protein 90-binding drugs: a ligand-independent approach to hormonal therapy of breast cancer. Clin Cancer Res *7*, 2076-2084.

Bagot, M. (2008). Introduction: cutaneous T-cell lymphoma (CTCL)--classification, staging, and treatment options. Dermatol Clin *26 Suppl 1*, 3-12.

Bain, J., Plater, L., Elliott, M., Shpiro, N., Hastie, C. J., McLauchlan, H., Klevernic, I., Arthur, J. S., Alessi, D. R., and Cohen, P. (2007). The selectivity of protein kinase inhibitors: a further update. Biochem J *408*, 297-315.

Bakels, V., Van Oostveen, J. W., Geerts, M. L., Gordijn, R. L., Walboomers, J. M., Scheffer, E., Meijer, C. J., and Willemze, R. (1993). Diagnostic and prognostic significance of clonal T-cell receptor beta gene rearrangements in lymph nodes of patients with mycosis fungoides. J Pathol *170*, 249-255.

Balkwill, F., Charles, K. A., and Mantovani, A. (2005). Smoldering and polarized inflammation in the initiation and promotion of malignant disease. Cancer Cell *7*, 211-217.

Ballester, B., Ramuz, O., Gisselbrecht, C., Doucet, G., Loi, L., Loriod, B., Bertucci, F., Bouabdallah, R., Devilard, E., Carbuccia, N.*, et al.* (2006). Gene expression profiling identifies molecular subgroups among nodal peripheral T-cell lymphomas. Oncogene *25*, 1560-1570.

Basso, A. D., Solit, D. B., Chiosis, G., Giri, B., Tsichlis, P., and Rosen, N. (2002). Akt forms an intracellular complex with heat shock protein 90 (Hsp90) and Cdc37 and is destabilized by inhibitors of Hsp90 function. J Biol Chem *277*, 39858-39866.

Bauer, B., and Baier, G. (2002). Protein kinase C and AKT/protein kinase B in CD4+ T-lymphocytes: new partners in TCR/CD28 signal integration. Mol Immunol *38*, 1087-1099.

Baylin, S. B., and Ohm, J. E. (2006). Epigenetic gene silencing in cancer - a mechanism for early oncogenic pathway addiction? Nat Rev Cancer *6*, 107-116.

Bekkenk, M. W., Vermeer, M. H., Jansen, P. M., van Marion, A. M., Canninga-van Dijk, M. R., Kluin, P. M., Geerts, M. L., Meijer, C. J., and Willemze, R. (2003). Peripheral T-cell lymphomas unspecified presenting in the skin: analysis of prognostic factors in a group of 82 patients. Blood *102*, 2213-2219.

Benharroch, D., Meguerian-Bedoyan, Z., Lamant, L., Amin, C., Brugieres, L., Terrier-Lacombe, M. J., Haralambieva, E., Pulford, K., Pileri, S., Morris, S. W.*, et al.* (1998). ALK-positive lymphoma: a single disease with a broad spectrum of morphology. Blood *91*, 2076-2084.

Bentwich, I., Avniel, A., Karov, Y., Aharonov, R., Gilad, S., Barad, O., Barzilai, A., Einat, P., Einav, U., Meiri, E.*, et al.* (2005). Identification of hundreds of conserved and nonconserved human microRNAs. Nat Genet *37*, 766-770.
Berezikov, E., Guryev, V., van de Belt, J., Wienholds, E., Plasterk, R. H., and Cuppen, E. (2005). Phylogenetic shadowing and computational identification of human microRNA genes. Cell *120*, 21-24.

Berth-Jones, J. (2005). The use of ciclosporin in psoriasis. J Dermatolog Treat *16*, 258-277.
Bhalla, K. N. (2005). Epigenetic and chromatin modifiers as targeted therapy of hematologic malignancies. J Clin Oncol *23*, 3971-3993.

Bhardwaj, A., Sethi, G., Vadhan-Raj, S., Bueso-Ramos, C., Takada, Y., Gaur, U., Nair, A. S., Shishodia, S., and Aggarwal, B. B. (2007). Resveratrol inhibits proliferation, induces apoptosis, and overcomes chemoresistance through down-regulation of STAT3 and nuclear factor-kappaB-regulated antiapoptotic and cell survival gene products in human multiple myeloma cells. Blood *109*, 2293-2302.

Bhattacharya, N., Wang, Z., Davitt, C., McKenzie, I. F., Xing, P. X., and Magnuson, N. S. (2002). Pim-1 associates with protein complexes necessary for mitosis. Chromosoma *111*, 80-95.
Blagosklonny, M. V., Toretsky, J., Bohen, S., and Neckers, L. (1996). Mutant conformation of p53 translated in vitro or in vivo requires functional HSP90. Proc Natl Acad Sci U S A *93*, 8379-8383.

Bolden, J. E., Peart, M. J., and Johnstone, R. W. (2006). Anticancer activities of histone deacetylase inhibitors. Nat Rev Drug Discov *5*, 769-784.

Bonzheim, I., Geissinger, E., Roth, S., Zettl, A., Marx, A., Rosenwald, A., Muller-Hermelink, H. K., and Rudiger, T. (2004). Anaplastic large cell lymphomas lack the expression of T-cell receptor molecules or molecules of proximal T-cell receptor signaling. Blood *104*, 3358-3360.

Bradford, P. T., Devesa, S. S., Anderson, W. F., and Toro, J. R. (2009). Cutaneous lymphoma incidence patterns in the United States: a population-based study of 3884 cases. Blood *113*, 5064-5073.

Braun, C. J., Zhang, X., Savelyeva, I., Wolff, S., Moll, U. M., Schepeler, T., Orntoft, T. F., Andersen, C. L., and Dobbelstein, M. (2008). p53-Responsive micrornas 192 and 215 are capable of inducing cell cycle arrest. Cancer Res *68*, 10094-10104.

Brender, C., Nielsen, M., Kaltoft, K., Mikkelsen, G., Zhang, Q., Wasik, M., Billestrup, N., and Odum, N. (2001). STAT3-mediated constitutive expression of SOCS-3 in cutaneous T-cell lymphoma. Blood *97*, 1056-1062.

Broderick, D. K., Di, C., Parrett, T. J., Samuels, Y. R., Cummins, J. M., McLendon, R. E., Fults, D. W., Velculescu, V. E., Bigner, D. D., and Yan, H. (2004). Mutations of PIK3CA in anaplastic oligodendrogliomas, high-grade astrocytomas, and medulloblastomas. Cancer Res *64*, 5048-5050.

Bullock, A. N., Debreczeni, J. E., Fedorov, O. Y., Nelson, A., Marsden, B. D., and Knapp, S. (2005). Structural basis of inhibitor specificity of the human protooncogene proviral insertion site in moloney murine leukemia virus (PIM-1) kinase. J Med Chem *48*, 7604-7614.

Bunn, P. A., Jr., and Lamberg, S. I. (1979). Report of the Committee on Staging and Classification of Cutaneous T-Cell Lymphomas. Cancer Treat Rep *63*, 725-728.

Butler, L. M., Zhou, X., Xu, W. S., Scher, H. I., Rifkind, R. A., Marks, P. A., and Richon, V. M. (2002). The histone deacetylase inhibitor SAHA arrests cancer cell growth, up-regulates thioredoxin-binding protein-2, and down-regulates thioredoxin. Proc Natl Acad Sci U S A *99*, 11700-11705.

Caffieri, S., Di Lisa, F., Bolesani, F., Facco, M., Semenzato, G., Dall'Acqua, F., and Canton, M. (2007). The mitochondrial effects of novel apoptogenic molecules generated by psoralen photolysis as a crucial mechanism in PUVA therapy. Blood *109*, 4988-4994.

Calin, G. A., and Croce, C. M. (2006). MicroRNA-cancer connection: the beginning of a new tale. Cancer Res *66*, 7390-7394.

Calin, G. A., and Croce, C. M. (2007). Investigation of microRNA alterations in leukemias and lymphomas. Methods Enzymol *427*, 193-213.

Campbell, I. G., Russell, S. E., Choong, D. Y., Montgomery, K. G., Ciavarella, M. L., Hooi, C. S., Cristiano, B. E., Pearson, R. B., and Phillips, W. A. (2004). Mutation of the PIK3CA gene in ovarian and breast cancer. Cancer Res *64*, 7678-7681.

Carbone, A., Cozzi, M., Gloghini, A., and Pinto, A. (1994). CD26/dipeptidyl peptidase IV expression in human lymphomas is restricted to CD30-positive anaplastic large cell and a subset of T-cell non-Hodgkin's lymphomas. Hum Pathol *25*, 1360-1365.

Carbone, A., Gloghini, A., Zagonel, V., Aldinucci, D., Gattei, V., Degan, M., Improta, S., Sorio, R., Monfardini, S., and Pinto, A. (1995). The expression of CD26 and CD40 ligand is mutually exclusive in human T-cell non-Hodgkin's lymphomas/leukemias. Blood *86*, 4617-4626.

Chen, G., Cao, P., and Goeddel, D. V. (2002a). TNF-induced recruitment and activation of the IKK complex require Cdc37 and Hsp90. Mol Cell *9*, 401-410.

Chen, X. P., Losman, J. A., Cowan, S., Donahue, E., Fay, S., Vuong, B. Q., Nawijn, M. C., Capece, D., Cohan, V. L., and Rothman, P. (2002b). Pim serine/threonine kinases regulate the stability of Socs-1 protein. Proc Natl Acad Sci U S A *99*, 2175-2180.

Cheney, I. W., Yan, S., Appleby, T., Walker, H., Vo, T., Yao, N., Hamatake, R., Hong, Z., and Wu, J. Z. (2007). Identification and structure-activity relationships of substituted pyridones as inhibitors of Pim-1 kinase. Bioorg Med Chem Lett *17*, 1679-1683.

Cheng, A. L., Su, I. J., Chen, Y. C., Uen, W. C., and Wang, C. H. (1993). Characteristic clinicopathologic features of Epstein-Barr virus-associated peripheral T-cell lymphoma. Cancer *72*, 909-916.

Cheson, B. D. (2007). Clinical management of T-cell malignancies: current perspectives, key issues, and emerging therapies. Semin Oncol *34*, S3-7.

Chiarion-Sileni, V., Bononi, A., Fornasa, C. V., Soraru, M., Alaibac, M., Ferrazzi, E., Redelotti, R., Peserico, A., Monfardini, S., and Salvagno, L. (2002). Phase II trial of interferon-alpha-2a plus psolaren with ultraviolet light A in patients with cutaneous T-cell lymphoma. Cancer *95*, 569-575.

Cho, W. J., Shin, J. M., Kim, J. S., Lee, M. R., Hong, K. S., Lee, J. H., Koo, K. H., Park, J. W., and Kim, K. S. (2009). miR-372 regulates cell cycle and apoptosis of ags human gastric cancer cell line through direct regulation of LATS2. Mol Cells *28*, 521-527.

Chou, T. C., and Talalay, P. (1984). Quantitative analysis of dose-effect relationships: the combined effects of multiple drugs or enzyme inhibitors. Adv Enzyme Regul *22*, 27-55.

Chu, D. H., Morita, C. T., and Weiss, A. (1998). The Syk family of protein tyrosine kinases in T-cell activation and development. Immunol Rev *165*, 167-180.

Chuang, T. Y., Su, W. P., and Muller, S. A. (1990). Incidence of cutaneous T cell lymphoma and other rare skin cancers in a defined population. J Am Acad Dermatol *23*, 254-256.

Cibull, T. L., Jones, T. D., Li, L., Eble, J. N., Ann Baldridge, L., Malott, S. R., Luo, Y., and Cheng, L. (2006). Overexpression of Pim-1 during progression of prostatic adenocarcinoma. J Clin Pathol *59*, 285-288.

Cimmino, A., Calin, G. A., Fabbri, M., Iorio, M. V., Ferracin, M., Shimizu, M., Wojcik, S. E., Aqeilan, R. I., Zupo, S., Dono, M.*, et al.* (2005). miR-15 and miR-16 induce apoptosis by targeting BCL2. Proc Natl Acad Sci U S A *102*, 13944-13949.

Claudio, J. O., Masih-Khan, E., Tang, H., Goncalves, J., Voralia, M., Li, Z. H., Nadeem, V., Cukerman, E., Francisco-Pabalan, O., Liew, C. C.*, et al.* (2002). A molecular compendium of genes expressed in multiple myeloma. Blood *100*, 2175-2186.

Colamonici, O. R., Domanski, P., Platanias, L. C., and Diaz, M. O. (1992). Correlation between interferon (IFN) alpha resistance and deletion of the IFN alpha/beta genes in acute leukemia cell lines suggests selection against the IFN system. Blood *80*, 744-749.

Cooper, D. L., Braverman, I. M., Sarris, A. H., Durivage, H. J., Saidman, B. H., Davis, C. A., and Hait, W. N. (1993). Cyclosporine treatment of refractory T-cell lymphomas. Cancer *71*, 2335-2341.

Cress, W. D., and Seto, E. (2000). Histone deacetylases, transcriptional control, and cancer. J Cell Physiol *184*, 1-16.

Cuadros, M., Dave, S. S., Jaffe, E. S., Honrado, E., Milne, R., Alves, J., Rodriguez, J., Zajac, M., Benitez, J., Staudt, L. M., and Martinez-Delgado, B. (2007). Identification of a proliferation signature related to survival in nodal peripheral T-cell lymphomas. J Clin Oncol *25*, 3321-3329.

Cuypers, H. T., Selten, G., Quint, W., Zijlstra, M., Maandag, E. R., Boelens, W., van Wezenbeek, P., Melief, C., and Berns, A. (1984). Murine leukemia virus-induced T-cell lymphomagenesis: integration of proviruses in a distinct chromosomal region. Cell *37*, 141-150.

Dai, H., Li, R., Wheeler, T., Diaz de Vivar, A., Frolov, A., Tahir, S., Agoulnik, I., Thompson, T., Rowley, D., and Ayala, G. (2005). Pim-2 upregulation: biological implications associated with disease progression and perinueral invasion in prostate cancer. Prostate *65*, 276-286.

Dalton, W. S., Grogan, T. M., Rybski, J. A., Scheper, R. J., Richter, L., Kailey, J., Broxterman, H. J., Pinedo, H. M., and Salmon, S. E. (1989). Immunohistochemical detection and quantitation of P-glycoprotein in multiple drug-resistant human myeloma cells: association with level of drug resistance and drug accumulation. Blood *73*, 747-752.
Datta, S. R., Brunet, A., and Greenberg, M. E. (1999). Cellular survival: a play in three Akts. Genes Dev *13*, 2905-2927.

Datta, S. R., Ranger, A. M., Lin, M. Z., Sturgill, J. F., Ma, Y. C., Cowan, C. W., Dikkes, P., Korsmeyer, S. J., and Greenberg, M. E. (2002). Survival factor-mediated BAD phosphorylation raises the mitochondrial threshold for apoptosis. Dev Cell *3*, 631-643.

de Leval, L., Rickman, D. S., Thielen, C., Reynies, A., Huang, Y. L., Delsol, G., Lamant, L., Leroy, K., Briere, J., Molina, T.*, et al.* (2007). The gene expression profile of nodal peripheral T-cell lymphoma demonstrates a molecular link between angioimmunoblastic T-cell lymphoma (AITL) and follicular helper T (TFH) cells. Blood *109*, 4952-4963.

Dhanasekaran, S. M., Barrette, T. R., Ghosh, D., Shah, R., Varambally, S., Kurachi, K., Pienta, K. J., Rubin, M. A., and Chinnaiyan, A. M. (2001). Delineation of prognostic biomarkers in prostate cancer. Nature *412*, 822-826.

Di Venuti, G., Nawgiri, R., and Foss, F. (2003). Denileukin diftitox and hyper-CVAD in the treatment of human T-cell lymphotropic virus 1-associated acute T-cell leukemia/lymphoma. Clin Lymphoma *4*, 176-178.

Diamandidou, E., Colome, M., Fayad, L., Duvic, M., and Kurzrock, R. (1999). Prognostic factor analysis in mycosis fungoides/Sezary syndrome. J Am Acad Dermatol *40*, 914-924.

Dogan A, G. P., Jaffe ES, Swerdlow SH, Campo E, Harris NL (2008). Pathology and Genetics of Tumours of Haematopoietic and Lymphoid Tissues. World Health Organization Classification of Tumours. Chapter: Angioimmunoblastc T-cell lymphoma., 4th edn: IARC press).

Dokmanovic, M., Clarke, C., and Marks, P. A. (2007). Histone deacetylase inhibitors: overview and perspectives. Mol Cancer Res *5*, 981-989.

Dorfman, D. M., Brown, J. A., Shahsafaei, A., and Freeman, G. J. (2006). Programmed death-1 (PD-1) is a marker of germinal center-associated T cells and angioimmunoblastic T-cell lymphoma. Am J Surg Pathol *30*, 802-810.

Drummond, D. C., Noble, C. O., Kirpotin, D. B., Guo, Z., Scott, G. K., and Benz, C. C. (2005). Clinical development of histone deacetylase inhibitors as anticancer agents. Annu Rev Pharmacol Toxicol *45*, 495-528.

Dummer, R., Michie, S. A., Kell, D., Gould, J. W., Haeffner, A. C., Smoller, B. R., Warnke, R. A., and Wood, G. S. (1995). Expression of bcl-2 protein and Ki-67 nuclear proliferation antigen in benign and malignant cutaneous T-cell infiltrates. J Cutan Pathol *22*, 11-17.

Dunleavy, K., and Wilson, W. H. (2007). Angioimmunoblastic T-cell lymphoma: immune modulation as a therapeutic strategy. Leuk Lymphoma *48*, 449-451.

Dupuis, J., Boye, K., Martin, N., Copie-Bergman, C., Plonquet, A., Fabiani, B., Baglin, A. C., Haioun, C., Delfau-Larue, M. H., and Gaulard, P. (2006a). Expression of CXCL13 by neoplastic cells in angioimmunoblastic T-cell lymphoma (AITL): a new diagnostic marker providing evidence that AITL derives from follicular helper T cells. Am J Surg Pathol *30*, 490-494.

Dupuis, J., Emile, J. F., Mounier, N., Gisselbrecht, C., Martin-Garcia, N., Petrella, T., Bouabdallah, R., Berger, F., Delmer, A., Coiffier, B.*, et al.* (2006b). Prognostic significance of Epstein-Barr virus in nodal peripheral T-cell lymphoma, unspecified: A Groupe d'Etude des Lymphomes de l'Adulte (GELA) study. Blood *108*, 4163-4169.

Duvic, M., Hymes, K., Heald, P., Breneman, D., Martin, A. G., Myskowski, P., Crowley, C., and Yocum, R. C. (2001). Bexarotene is effective and safe for treatment of refractory advanced-stage cutaneous T-cell lymphoma: multinational phase II-III trial results. J Clin Oncol *19*, 2456-2471.

Duvic, M., Talpur, R., Ni, X., Zhang, C., Hazarika, P., Kelly, C., Chiao, J. H., Reilly, J. F., Ricker, J. L., Richon, V. M., and Frankel, S. R. (2007). Phase 2 trial of oral vorinostat (suberoylanilide hydroxamic acid, SAHA) for refractory cutaneous T-cell lymphoma (CTCL). Blood *109*, 31-39.

Eberwine, J. (1996). Amplification of mRNA populations using aRNA generated from immobilized oligo(dT)-T7 primed cDNA. Biotechniques *20*, 584-591.

Edelson, R. L. (1980). Cutaneous T cell lymphoma: mycosis fungoides, Sezary syndrome, and other variants. J Am Acad Dermatol *2*, 89-106.
Eichmann, A., Yuan, L., Breant, C., Alitalo, K., and Koskinen, P. J. (2000). Developmental expression of pim kinases suggests functions also outside of the hematopoietic system. Oncogene *19*, 1215-1224.

Eisen, M. B., Spellman, P. T., Brown, P. O., and Botstein, D. (1998). Cluster analysis and display of genome-wide expression patterns. Proc Natl Acad Sci U S A *95*, 14863-14868.

Enblad, G., Hagberg, H., Erlanson, M., Lundin, J., MacDonald, A. P., Repp, R., Schetelig, J., Seipelt, G., and Osterborg, A. (2004). A pilot study of alemtuzumab (anti-CD52 monoclonal antibody) therapy for patients with relapsed or chemotherapy-refractory peripheral T-cell lymphomas. Blood *103*, 2920-2924.

Engelman, J. A. (2009). Targeting PI3K signalling in cancer: opportunities, challenges and limitations. Nat Rev Cancer *9*, 550-562.

Engelman, J. A., Luo, J., and Cantley, L. C. (2006). The evolution of phosphatidylinositol 3-kinases as regulators of growth and metabolism. Nat Rev Genet *7*, 606-619.

Ernst, J., Nau, G. J., and Bar-Joseph, Z. (2005). Clustering short time series gene expression data. Bioinformatics *21 Suppl 1*, i159-168.

Esquela-Kerscher, A., Trang, P., Wiggins, J. F., Patrawala, L., Cheng, A., Ford, L., Weidhaas, J. B., Brown, D., Bader, A. G., and Slack, F. J. (2008). The let-7 microRNA reduces tumor growth in mouse models of lung cancer. Cell Cycle *7*, 759-764.

Evens, A. M., and Gartenhaus, R. B. (2004). Treatment of T-cell non-Hodgkin's lymphoma. Curr Treat Options Oncol *5*, 289-303.

Falini, B., Pileri, S., Zinzani, P. L., Carbone, A., Zagonel, V., Wolf-Peeters, C., Verhoef, G., Menestrina, F., Todeschini, G., Paulli, M.*, et al.* (1999). ALK+ lymphoma: clinico-pathological findings and outcome. Blood *93*, 2697-2706.

Fantin, V. R., Loboda, A., Paweletz, C. P., Hendrickson, R. C., Pierce, J. W., Roth, J. A., Li, L., Gooden, F., Korenchuk, S., Hou, X. S.*, et al.* (2008). Constitutive activation of signal transducers and activators of transcription predicts vorinostat resistance in cutaneous T-cell lymphoma. Cancer Res *68*, 3785-3794.

Fazi, F., Racanicchi, S., Zardo, G., Starnes, L. M., Mancini, M., Travaglini, L., Diverio, D., Ammatuna, E., Cimino, G., Lo-Coco, F.*, et al.* (2007). Epigenetic silencing of the myelopoiesis regulator microRNA-223 by the AML1/ETO oncoprotein. Cancer Cell *12*, 457-466.

Feinberg, A. P. (2008). Epigenetics at the epicenter of modern medicine. Jama *299*, 1345-1350.

Ferrarini, M., Heltai, S., Zocchi, M. R., and Rugarli, C. (1992). Unusual expression and localization of heat-shock proteins in human tumor cells. Int J Cancer *51*, 613-619.

Fisher, R. I., Gaynor, E. R., Dahlberg, S., Oken, M. M., Grogan, T. M., Mize, E. M., Glick, J. H., Coltman, C. A., Jr., and Miller, T. P. (1993). Comparison of a standard regimen (CHOP) with three intensive chemotherapy regimens for advanced non-Hodgkin's lymphoma. N Engl J Med *328*, 1002-1006.

Fiskus, W., Ren, Y., Mohapatra, A., Bali, P., Mandawat, A., Rao, R., Herger, B., Yang, Y., Atadja, P., Wu, J., and Bhalla, K. (2007). Hydroxamic acid analogue histone deacetylase inhibitors attenuate estrogen receptor-alpha levels and transcriptional activity: a result of hyperacetylation and inhibition of chaperone function of heat shock protein 90. Clin Cancer Res *13*, 4882-4890.

Fox, C. J., Hammerman, P. S., Cinalli, R. M., Master, S. R., Chodosh, L. A., and Thompson, C. B. (2003). The serine/threonine kinase Pim-2 is a transcriptionally regulated apoptotic inhibitor. Genes Dev *17*, 1841-1854.

Fox, C. J., Hammerman, P. S., and Thompson, C. B. (2005). The Pim kinases control rapamycin-resistant T cell survival and activation. J Exp Med *201*, 259-266.

Fraga, M. F., Ballestar, E., Paz, M. F., Ropero, S., Setien, F., Ballestar, M. L., Heine-Suner, D., Cigudosa, J. C., Urioste, M., Benitez, J.*, et al.* (2005a). Epigenetic differences arise during the lifetime of monozygotic twins. Proc Natl Acad Sci U S A *102*, 10604-10609.

Fraga, M. F., Ballestar, E., Villar-Garea, A., Boix-Chornet, M., Espada, J., Schotta, G., Bonaldi, T., Haydon, C., Ropero, S., Petrie, K.*, et al.* (2005b). Loss of acetylation at Lys16 and trimethylation at Lys20 of histone H4 is a common hallmark of human cancer. Nat Genet *37*, 391-400.

Fruman, D. A. (2004). Towards an understanding of isoform specificity in phosphoinositide 3-kinase signalling in lymphocytes. Biochem Soc Trans *32*, 315-319.

Galmarini, C. M., and Galmarini, F. C. (2003). Multidrug resistance in cancer therapy: role of the microenvironment. Curr Opin Investig Drugs *4*, 1416-1421.

Gamero, A. M., Sakamoto, S., Montenegro, J., and Larner, A. C. (2004). Identification of a novel conserved motif in the STAT family that is required for tyrosine phosphorylation. J Biol Chem *279*, 12379-12385.

Garrido, C., Gurbuxani, S., Ravagnan, L., and Kroemer, G. (2001). Heat shock proteins: endogenous modulators of apoptotic cell death. Biochem Biophys Res Commun *286*, 433-442.

Gascoyne, R. D., Aoun, P., Wu, D., Chhanabhai, M., Skinnider, B. F., Greiner, T. C., Morris, S. W., Connors, J. M., Vose, J. M., Viswanatha, D. S*., et al.* (1999). Prognostic significance of anaplastic lymphoma kinase (ALK) protein expression in adults with anaplastic large cell lymphoma. Blood *93*, 3913-3921.

Georges, S. A., Biery, M. C., Kim, S. Y., Schelter, J. M., Guo, J., Chang, A. N., Jackson, A. L., Carleton, M. O., Linsley, P. S., Cleary, M. A., and Chau, B. N. (2008). Coordinated regulation of cell cycle transcripts by p53-Inducible microRNAs, miR-192 and miR-215. Cancer Res *68*, 10105-10112.

Gillenwater, A. M., Zhong, M., and Lotan, R. (2007). Histone deacetylase inhibitor suberoylanilide hydroxamic acid induces apoptosis through both mitochondrial and Fas (Cd95) signaling in head and neck squamous carcinoma cells. Mol Cancer Ther *6*, 2967-2975.

Gisselbrecht, C., Gaulard, P., Lepage, E., Coiffier, B., Briere, J., Haioun, C., Cazals-Hatem, D., Bosly, A., Xerri, L., Tilly, H*., et al.* (1998). Prognostic significance of T-cell phenotype in aggressive non-Hodgkin's lymphomas. Groupe d'Etudes des Lymphomes de l'Adulte (GELA). Blood *92*, 76-82.

Gootenberg, J. E., Ruscetti, F. W., Mier, J. W., Gazdar, A., and Gallo, R. C. (1981). Human cutaneous T cell lymphoma and leukemia cell lines produce and respond to T cell growth factor. J Exp Med *154*, 1403-1418.

Gothert, J. R., Brake, R. L., Smeets, M., Duhrsen, U., Begley, C. G., and Izon, D. J. (2007). NOTCH1 pathway activation is an early hallmark of SCL T-leukemogenesis. Blood.

Gray, S. G., Qian, C. N., Furge, K., Guo, X., and Teh, B. T. (2004). Microarray profiling of the effects of histone deacetylase inhibitors on gene expression in cancer cell lines. Int J Oncol *24*, 773-795.

Gregoretti, I. V., Lee, Y. M., and Goodson, H. V. (2004). Molecular evolution of the histone deacetylase family: functional implications of phylogenetic analysis. J Mol Biol *338*, 17-31.

Griffith, C. E., Zhang, W., and Wange, R. L. (1998). ZAP-70-dependent and -independent activation of Erk in Jurkat T cells. Differences in signaling induced by H2o2 and Cd3 cross-linking. J Biol Chem *273*, 10771-10776.

Gui, C. Y., Ngo, L., Xu, W. S., Richon, V. M., and Marks, P. A. (2004). Histone deacetylase (HDAC) inhibitor activation of p21WAF1 involves changes in promoter-associated proteins, including HDAC1. Proc Natl Acad Sci U S A *101*, 1241-1246.

Guitart, J., Camisa, C., Ehrlich, M., and Bergfeld, W. F. (2003). Long-term implications of T-cell receptor gene rearrangement analysis by Southern blot in patients with cutaneous T-cell lymphoma. J Am Acad Dermatol *48*, 775-779.

Guo, C., Sah, J. F., Beard, L., Willson, J. K., Markowitz, S. D., and Guda, K. (2008). The noncoding RNA, miR-126, suppresses the growth of neoplastic cells by targeting phosphatidylinositol 3-kinase signaling and is frequently lost in colon cancers. Genes Chromosomes Cancer *47*, 939-946.

Hartl, F. U., and Hayer-Hartl, M. (2002). Molecular chaperones in the cytosol: from nascent chain to folded protein. Science *295*, 1852-1858.
He, L., Thomson, J. M., Hemann, M. T., Hernando-Monge, E., Mu, D., Goodson, S., Powers, S., Cordon-Cardo, C., Lowe, S. W., Hannon, G. J., and Hammond, S. M. (2005). A microRNA polycistron as a potential human oncogene. Nature *435*, 828-833.

Heald, P., Yan, S. L., and Edelson, R. (1994). Profound deficiency in normal circulating T cells in erythrodermic cutaneous T-cell lymphoma. Arch Dermatol *130*, 198-203.

Hellman, S., Mauch P.M. (1999). Hodgkin's Disease. Chapter 1., 1999 edn: Lippincott Williams & Wilkins).

Hennessy, B. T., Smith, D. L., Ram, P. T., Lu, Y., and Mills, G. B. (2005). Exploiting the PI3K/AKT pathway for cancer drug discovery. Nat Rev Drug Discov *4*, 988-1004.

Herling, M., Rassidakis, G. Z., Jones, D., Schmitt-Graeff, A., Sarris, A. H., and Medeiros, L. J. (2004). Absence of Epstein-Barr virus in anaplastic large cell lymphoma: a study of 64 cases classified according to World Health Organization criteria. Hum Pathol *35*, 455-459.

Herrero, J., Diaz-Uriarte, R., and Dopazo, J. (2003). Gene expression data preprocessing. Bioinformatics *19*, 655-656.

Herreros, B., Sanchez-Aguilera, A., and Piris, M. A. (2007). Lymphoma microenvironment: culprit or innocent? Leukemia.

Holder, S., Lilly, M., and Brown, M. L. (2007a). Comparative molecular field analysis of flavonoid inhibitors of the PIM-1 kinase. Bioorg Med Chem *15*, 6463-6473.

Holder, S., Zemskova, M., Zhang, C., Tabrizizad, M., Bremer, R., Neidigh, J. W., and Lilly, M. B. (2007b). Characterization of a potent and selective small-molecule inhibitor of the PIM1 kinase. Mol Cancer Ther *6*, 163-172.

Hoover, D., Friedmann, M., Reeves, R., and Magnuson, N. S. (1991). Recombinant human pim-1 protein exhibits serine/threonine kinase activity. J Biol Chem *266*, 14018-14023.

Hoppe, R. T., Medeiros, L. J., Warnke, R. A., and Wood, G. S. (1995). CD8-positive tumor-infiltrating lymphocytes influence the long-term survival of patients with mycosis fungoides. J Am Acad Dermatol *32*, 448-453.

Hostein, I., Robertson, D., DiStefano, F., Workman, P., and Clarke, P. A. (2001). Inhibition of signal transduction by the Hsp90 inhibitor 17-allylamino-17-demethoxygeldanamycin results in cytostasis and apoptosis. Cancer Res *61*, 4003-4009.

Hu, X., Macdonald, D. M., Huettner, P. C., Feng, Z., El Naqa, I. M., Schwarz, J. K., Mutch, D. G., Grigsby, P. W., Powell, S. N., and Wang, X. (2009). A miR-200 microRNA cluster as prognostic marker in advanced ovarian cancer. Gynecol Oncol *114*, 457-464.

Hu, X., Schwarz, J. K., Lewis, J. S., Jr., Huettner, P. C., Rader, J. S., Deasy, J. O., Grigsby, P. W., and Wang, X. A MicroRNA Expression Signature for Cervical Cancer Prognosis. Cancer Res.
Hurst, D. R., Edmonds, M. D., Scott, G. K., Benz, C. C., Vaidya, K. S., and Welch, D. R. (2009). Breast cancer metastasis suppressor 1 up-regulates miR-146, which suppresses breast cancer metastasis. Cancer Res *69*, 1279-1283.

Iannitto, E., Ferreri, A. J., Minardi, V., Tripodo, C., and Kreipe, H. H. (2008). Angioimmunoblastic T-cell lymphoma. Crit Rev Oncol Hematol *68*, 264-271.

Ichimi, T., Enokida, H., Okuno, Y., Kunimoto, R., Chiyomaru, T., Kawamoto, K., Kawahara, K., Toki, K., Kawakami, K., Nishiyama, K.*, et al.* (2009). Identification of novel microRNA targets based on microRNA signatures in bladder cancer. Int J Cancer *125*, 345-352.

Iqbal, J., Weisenburger, D. D., Greiner, T. C., Vose, J. M., McKeithan, T., Kucuk, C., Geng, H., Deffenbacher, K., Smith, L., Dybkaer, K.*, et al.* (2009). Molecular signatures to improve diagnosis in peripheral T-cell lymphoma and prognostication in angioimmunoblastic T-cell lymphoma. Blood.

Ishida, T., Inagaki, H., Utsunomiya, A., Takatsuka, Y., Komatsu, H., Iida, S., Takeuchi, G., Eimoto, T., Nakamura, S., and Ueda, R. (2004). CXC chemokine receptor 3 and CC chemokine receptor 4 expression in T-cell and NK-cell lymphomas with special reference to clinicopathological significance for peripheral T-cell lymphoma, unspecified. Clin Cancer Res *10*, 5494-5500.

Iwashima, M., Irving, B. A., van Oers, N. S., Chan, A. C., and Weiss, A. (1994). Sequential interactions of the TCR with two distinct cytoplasmic tyrosine kinases. Science *263*, 1136-1139.

Izban, K. F., Ergin, M., Martinez, R. L., and Alkan, S. (2000). Expression of the tumor necrosis factor receptor-associated factors (TRAFs) 1 and 2 is a characteristic feature of Hodgkin and Reed-Sternberg cells. Mod Pathol *13*, 1324-1331.

Izzotti, A., Calin, G. A., Arrigo, P., Steele, V. E., Croce, C. M., and De Flora, S. (2009). Downregulation of microRNA expression in the lungs of rats exposed to cigarette smoke. FASEB J *23*, 806-812.

Jacobs, M. D., Black, J., Futer, O., Swenson, L., Hare, B., Fleming, M., and Saxena, K. (2005). Pim-1 ligand-bound structures reveal the mechanism of serine/threonine kinase inhibition by LY294002. J Biol Chem *280*, 13728-13734.

Jaffe, E. S., Harris, N.L., Stein, H. and Vardiman, J.W. (2001). Pathology and genetics of tumours of haematopoietic and lymphoid tissues. World health organization classification of tumours., (Lyon: IARC Press.).

Jaffe ES, H. N., Stein H and Vardiman JW., Janeway, C. A., Jr., and Bottomly, K. (1994). Signals and signs for lymphocyte responses. Cell *76*, 275-285.

John, B., Enright, A. J., Aravin, A., Tuschl, T., Sander, C., and Marks, D. S. (2004). Human MicroRNA targets. PLoS Biol *2*, e363.

Johnstone, R. W., and Licht, J. D. (2003). Histone deacetylase inhibitors in cancer therapy: is transcription the primary target? Cancer Cell *4*, 13-18.

Jonasch, E., and Haluska, F. G. (2001). Interferon in oncological practice: review of interferon biology, clinical applications, and toxicities. Oncologist *6*, 34-55.

Jones, L. K., and Saha, V. (2002). Chromatin modification, leukaemia and implications for therapy. Br J Haematol *118*, 714-727.

Jun, S. M., Hong, Y. S., Seo, J. S., Ko, Y. H., Yang, C. W., and Lee, S. K. (2008). Viral microRNA profile in Epstein-Barr virus-associated peripheral T cell lymphoma. Br J Haematol.
Juntilla, M. M., and Koretzky, G. A. (2008). Critical roles of the PI3K/Akt signaling pathway in T cell development. Immunol Lett *116*, 104-110.

Kadin, M. E., Sako, D., Berliner, N., Franklin, W., Woda, B., Borowitz, M., Ireland, K., Schweid, A., Herzog, P., Lange, B., and et al. (1986). Childhood Ki-1 lymphoma presenting with skin lesions and peripheral lymphadenopathy. Blood *68*, 1042-1049.

Kallinich, T., Muche, J. M., Qin, S., Sterry, W., Audring, H., and Kroczek, R. A. (2003). Chemokine receptor expression on neoplastic and reactive T cells in the skin at different stages of mycosis fungoides. J Invest Dermatol *121*, 1045-1052.

Kaltoft, K., Bisballe, S., Dyrberg, T., Boel, E., Rasmussen, P. B., and Thestrup-Pedersen, K. (1992). Establishment of two continuous T-cell strains from a single plaque of a patient with mycosis fungoides. In Vitro Cell Dev Biol *28A*, 161-167.

Kaltoft, K., Bisballe, S., Rasmussen, H. F., Thestrup-Pedersen, K., Boehncke, W. H., Volker, H., and Sterry, W. (1988). C-type particles are inducible in Se-Ax, a continuous T-cell line from a patient with Sezary's syndrome. Arch Dermatol Res *280*, 264-267.

Katakami, N., Kaneto, H., Hao, H., Umayahara, Y., Fujitani, Y., Sakamoto, K., Gorogawa, S., Yasuda, T., Kawamori, D., Kajimoto, Y.*, et al.* (2004). Role of pim-1 in smooth muscle cell proliferation. J Biol Chem *279*, 54742-54749.

Katso, R., Okkenhaug, K., Ahmadi, K., White, S., Timms, J., and Waterfield, M. D. (2001). Cellular function of phosphoinositide 3-kinases: implications for development, homeostasis, and cancer. Annu Rev Cell Dev Biol *17*, 615-675.

Kim-Han, J. S., Reichert, S. A., Quick, K. L., and Dugan, L. L. (2001). BMCP1: a mitochondrial uncoupling protein in neurons which regulates mitochondrial function and oxidant production. J Neurochem *79*, 658-668.

Kim, C. H., Lim, H. W., Kim, J. R., Rott, L., Hillsamer, P., and Butcher, E. C. (2004). Unique gene expression program of human germinal center T helper cells. Blood *104*, 1952-1960.

Kim, E. J., Hess, S., Richardson, S. K., Newton, S., Showe, L. C., Benoit, B. M., Ubriani, R., Vittorio, C. C., Junkins-Hopkins, J. M., Wysocka, M., and Rook, A. H. (2005). Immunopathogenesis and therapy of cutaneous T cell lymphoma. J Clin Invest *115*, 798-812.

Kim, H. R., Kim, E. J., Yang, S. H., Jeong, E. T., Park, C., Lee, J. H., Youn, M. J., So, H. S., and Park, R. (2006a). Trichostatin A induces apoptosis in lung cancer cells via simultaneous activation of the death receptor-mediated and mitochondrial pathway? Exp Mol Med *38*, 616-624.

Kim, T. Y., Bang, Y. J., and Robertson, K. D. (2006b). Histone deacetylase inhibitors for cancer therapy. Epigenetics *1*, 14-23.

Kim, W. Y., and Kaelin, W. G. (2004). Role of VHL gene mutation in human cancer. J Clin Oncol *22*, 4991-5004.

Kim, Y. H., Liu, H. L., Mraz-Gernhard, S., Varghese, A., and Hoppe, R. T. (2003). Long-term outcome of 525 patients with mycosis fungoides and Sezary syndrome: clinical prognostic factors and risk for disease progression. Arch Dermatol *139*, 857-866.

King, C., Tangye, S. G., and Mackay, C. R. (2008). T follicular helper (TFH) cells in normal and dysregulated immune responses. Annu Rev Immunol *26*, 741-766.

Kitano, H. (2003). Cancer robustness: tumour tactics. Nature *426*, 125.

Kluin, P. M., Feller, A., Gaulard, P., Jaffe, E. S., Meijer, C. J., Muller-Hermelink, H. K., and Pileri, S. (2001). Peripheral T/NK-cell lymphoma: a report of the IXth Workshop of the European Association for Haematopathology. Histopathology *38*, 250-270.

Kojima, H., Hasegawa, Y., Suzukawa, K., Mukai, H. Y., Kaneko, S., Kobayashi, T., Kamoshita, M., Shinagawa, A., Komeno, T., Komatsu, T.*, et al.* (2004). Clinicopathological features and prognostic factors of Japanese patients with "peripheral T-cell lymphoma, unspecified" diagnosed according to the WHO classification. Leuk Res *28*, 1287-1292.

Krause, T., Gerbershagen, M. U., Fiege, M., Weisshorn, R., and Wappler, F. (2004). Dantrolene--a review of its pharmacology, therapeutic use and new developments. Anaesthesia *59*, 364-373.

Krenacs, L., Schaerli, P., Kis, G., and Bagdi, E. (2006). Phenotype of neoplastic cells in angioimmunoblastic T-cell lymphoma is consistent with activated follicular B helper T cells. Blood *108*, 1110-1111.

Kumar, M. S., Erkeland, S. J., Pester, R. E., Chen, C. Y., Ebert, M. S., Sharp, P. A., and Jacks, T. (2008). Suppression of non-small cell lung tumor development by the let-7 microRNA family. Proc Natl Acad Sci U S A *105*, 3903-3908.

Kumar, R., and Atlas, I. (1992). Interferon alpha induces the expression of retinoblastoma gene product in human Burkitt lymphoma Daudi cells: role in growth regulation. Proc Natl Acad Sci U S A *89*, 6599-6603.

Kuramoto, K., Sakai, A., Shigemasa, K., Takimoto, Y., Asaoku, H., Tsujimoto, T., Oda, K., Kimura, A., Uesaka, T., Watanabe, H., and Katoh, O. (2002). High expression of MCL1 gene related to vascular endothelial growth factor is associated with poor outcome in non-Hodgkin's lymphoma. Br J Haematol *116*, 158-161.

Kuzel, T. M., Gilyon, K., Springer, E., Variakojis, D., Kaul, K., Bunn, P. A., Jr., Evans, L., Roenigk, H. H., Jr., and Rosen, S. T. (1990). Interferon alfa-2a combined with phototherapy in the treatment of cutaneous T-cell lymphoma. J Natl Cancer Inst *82*, 203-207.

Kuzel, T. M., Roenigk, H. H., Jr., Samuelson, E., Herrmann, J. J., Hurria, A., Rademaker, A. W., and Rosen, S. T. (1995). Effectiveness of interferon alfa-2a combined with phototherapy for mycosis fungoides and the Sezary syndrome. J Clin Oncol *13*, 257-263.

Lachenal, F., Berger, F., Ghesquieres, H., Biron, P., Hot, A., Callet-Bauchu, E., Chassagne, C., Coiffier, B., Durieu, I., Rousset, H., and Salles, G. (2007). Angioimmunoblastic T-cell lymphoma: clinical and laboratory features at diagnosis in 77 patients. Medicine (Baltimore) *86*, 282-292.

Lamant, L., de Reynies, A., Duplantier, M. M., Rickman, D. S., Sabourdy, F., Giuriato, S., Brugieres, L., Gaulard, P., Espinos, E., and Delsol, G. (2007). Gene-expression profiling of systemic anaplastic large-cell lymphoma reveals differences based on ALK status and two distinct morphologic ALK+ subtypes. Blood *109*, 2156-2164.

Lamb, J., Crawford, E. D., Peck, D., Modell, J. W., Blat, I. C., Wrobel, M. J., Lerner, J., Brunet, J. P., Subramanian, A., Ross, K. N.*, et al.* (2006). The Connectivity Map: using gene-expression signatures to connect small molecules, genes, and disease. Science *313*, 1929-1935.

Landgraf, P., Rusu, M., Sheridan, R., Sewer, A., Iovino, N., Aravin, A., Pfeffer, S., Rice, A., Kamphorst, A. O., Landthaler, M.*, et al.* (2007). A mammalian microRNA expression atlas based on small RNA library sequencing. Cell *129*, 1401-1414.

Landolfo, S., Guarini, A., Riera, L., Gariglio, M., Gribaudo, G., Cignetti, A., Cordone, I., Montefusco, E., Mandelli, F., and Foa, R. (2000). Chronic myeloid leukemia cells resistant to interferon-alpha lack STAT1 expression. Hematol J *1*, 7-14.

Latres, E., Chiarle, R., Schulman, B. A., Pavletich, N. P., Pellicer, A., Inghirami, G., and Pagano, M. (2001). Role of the F-box protein Skp2 in lymphomagenesis. Proc Natl Acad Sci U S A *98*, 2515-2520.

Lawrie, C. H. (2008). MicroRNA expression in lymphoid malignancies: new hope for diagnosis and therapy? J Cell Mol Med *12*, 1432-1444.

Lebeau, J., Le Chalony, C., Prosperi, M. T., and Goubin, G. (1991). Constitutive overexpression of a 89 kDa heat shock protein gene in the HBL100 human mammary cell line converted to a tumorigenic phenotype by the EJ/T24 Harvey-ras oncogene. Oncogene *6*, 1125-1132.

Lewis, B. P., Burge, C. B., and Bartel, D. P. (2005). Conserved seed pairing, often flanked by adenosines, indicates that thousands of human genes are microRNA targets. Cell *120*, 15-20.
Lewis, B. P., Shih, I. H., Jones-Rhoades, M. W., Bartel, D. P., and Burge, C. B. (2003). Prediction of mammalian microRNA targets. Cell *115*, 787-798.

Li, Z. W., and Dalton, W. S. (2006). Tumor microenvironment and drug resistance in hematologic malignancies. Blood Rev *20*, 333-342.

Lin, Y. C., Kuo, M. W., Yu, J., Kuo, H. H., Lin, R. J., Lo, W. L., and Yu, A. L. (2008). c-Myb is an evolutionary conserved miR-150 target and miR-150/c-Myb interaction is important for embryonic development. Mol Biol Evol *25*, 2189-2198.

Link, W., Oyarzabal, J., Serelde, B. G., Albarran, M. I., Rabal, O., Cebria, A., Alfonso, P., Fominaya, J., Renner, O., Peregrino, S*., et al.* (2009). Chemical interrogation of FOXO3a nuclear translocation identifies potent and selective inhibitors of phosphoinositide 3-kinases. J Biol Chem.

Lu, D., Duvic, M., Medeiros, L. J., Luthra, R., Dorfman, D. M., and Jones, D. (2001). The T-cell chemokine receptor CXCR3 is expressed highly in low-grade mycosis fungoides. Am J Clin Pathol *115*, 413-421.

Lu, D., Patel, K. A., Duvic, M., and Jones, D. (2002). Clinical and pathological spectrum of CD8-positive cutaneous T-cell lymphomas. J Cutan Pathol *29*, 465-472.

Lu, J., Getz, G., Miska, E. A., Alvarez-Saavedra, E., Lamb, J., Peck, D., Sweet-Cordero, A., Ebert, B. L., Mak, R. H., Ferrando, A. A*., et al.* (2005). MicroRNA expression profiles classify human cancers. Nature *435*, 834-838.

Lum, A. M., Wang, B. B., Li, L., Channa, N., Bartha, G., and Wabl, M. (2007). Retroviral activation of the mir-106a microRNA cistron in T lymphoma. Retrovirology *4*, 5.

Lund, A. H., and van Lohuizen, M. (2004). Epigenetics and cancer. Genes Dev *18*, 2315-2335.

Lytle, J. R., Yario, T. A., and Steitz, J. A. (2007). Target mRNAs are repressed as efficiently by microRNA-binding sites in the 5' UTR as in the 3' UTR. Proc Natl Acad Sci U S A *104*, 9667-9672.

Ma, Y. Y., Wei, S. J., Lin, Y. C., Lung, J. C., Chang, T. C., Whang-Peng, J., Liu, J. M., Yang, D. M., Yang, W. K., and Shen, C. Y. (2000). PIK3CA as an oncogene in cervical cancer. Oncogene *19*, 2739-2744.

Mack, G. S. (2006). Epigenetic cancer therapy makes headway. J Natl Cancer Inst *98*, 1443-1444.

Mann, B. S., Johnson, J. R., Cohen, M. H., Justice, R., and Pazdur, R. (2007). FDA approval summary: vorinostat for treatment of advanced primary cutaneous T-cell lymphoma. Oncologist *12*, 1247-1252.

Marks, P., Rifkind, R. A., Richon, V. M., Breslow, R., Miller, T., and Kelly, W. K. (2001). Histone deacetylases and cancer: causes and therapies. Nat Rev Cancer *1*, 194-202.

Marks, P. A., and Breslow, R. (2007). Dimethyl sulfoxide to vorinostat: development of this histone deacetylase inhibitor as an anticancer drug. Nat Biotechnol *25*, 84-90.

Marks, P. A., and Dokmanovic, M. (2005). Histone deacetylase inhibitors: discovery and development as anticancer agents. Expert Opin Investig Drugs *14*, 1497-1511.

Marks, P. A., and Jiang, X. (2005). Histone deacetylase inhibitors in programmed cell death and cancer therapy. Cell Cycle *4*, 549-551.

Marks, P. A., Richon, V. M., Miller, T., and Kelly, W. K. (2004). Histone deacetylase inhibitors. Adv Cancer Res *91*, 137-168.

Martinez-Delgado, B., Cuadros, M., Honrado, E., Ruiz de la Parte, A., Roncador, G., Alves, J., Castrillo, J. M., Rivas, C., and Benitez, J. (2005). Differential expression of NF-kappaB pathway genes among peripheral T-cell lymphomas. Leukemia *19*, 2254-2263.

McKendry, R., John, J., Flavell, D., Muller, M., Kerr, I. M., and Stark, G. R. (1991). High-frequency mutagenesis of human cells and characterization of a mutant unresponsive to both alpha and gamma interferons. Proc Natl Acad Sci U S A *88*, 11455-11459.

Melamed, D., Tiefenbrun, N., Yarden, A., and Kimchi, A. (1993). Interferons and interleukin-6 suppress the DNA-binding activity of E2F in growth-sensitive hematopoietic cells. Mol Cell Biol *13*, 5255-5265.

Mercieca, J., Matutes, E., Dearden, C., MacLennan, K., and Catovsky, D. (1994). The role of pentostatin in the treatment of T-cell malignancies: analysis of response rate in 145 patients according to disease subtype. J Clin Oncol *12*, 2588-2593.

Meyer, P. N., Roychowdhury, S., Kini, A. R., and Alkan, S. (2008). HSP90 inhibitor 17AAG causes apoptosis in ATRA-resistant acute promyelocytic leukemia cells. Leuk Res *32*, 143-149.

Mikkers, H., Nawijn, M., Allen, J., Brouwers, C., Verhoeven, E., Jonkers, J., and Berns, A. (2004). Mice deficient for all PIM kinases display reduced body size and impaired responses to hematopoietic growth factors. Mol Cell Biol *24*, 6104-6115.

Miller, P., Schnur, R. C., Barbacci, E., Moyer, M. P., and Moyer, J. D. (1994). Binding of benzoquinoid ansamycins to p100 correlates with their ability to deplete the erbB2 gene product p185. Biochem Biophys Res Commun *201*, 1313-1319.

Minet, E., Mottet, D., Michel, G., Roland, I., Raes, M., Remacle, J., and Michiels, C. (1999). Hypoxia-induced activation of HIF-1: role of HIF-1alpha-Hsp90 interaction. FEBS Lett *460*, 251-256.

Mitchell, C., Park, M. A., Zhang, G., Yacoub, A., Curiel, D. T., Fisher, P. B., Roberts, J. D., Grant, S., and Dent, P. (2007). Extrinsic pathway- and cathepsin-dependent induction of mitochondrial dysfunction are essential for synergistic flavopiridol and vorinostat lethality in breast cancer cells. Mol Cancer Ther *6*, 3101-3112.

Mitsiades, C. S., Mitsiades, N. S., McMullan, C. J., Poulaki, V., Shringarpure, R., Hideshima, T., Akiyama, M., Chauhan, D., Munshi, N., Gu, X.*, et al.* (2004). Transcriptional signature of histone deacetylase inhibition in multiple myeloma: biological and clinical implications. Proc Natl Acad Sci U S A *101*, 540-545.

Mizoguchi, M., Nutt, C. L., Mohapatra, G., and Louis, D. N. (2004). Genetic alterations of phosphoinositide 3-kinase subunit genes in human glioblastomas. Brain Pathol *14*, 372-377.

Mochizuki, T., Kitanaka, C., Noguchi, K., Muramatsu, T., Asai, A., and Kuchino, Y. (1999). Physical and functional interactions between Pim-1 kinase and Cdc25A phosphatase. Implications for the Pim-1-mediated activation of the c-Myc signaling pathway. J Biol Chem *274*, 18659-18666.

Montagnani, M., Chen, H., Barr, V. A., and Quon, M. J. (2001). Insulin-stimulated activation of eNOS is independent of Ca2+ but requires phosphorylation by Akt at Ser(1179). J Biol Chem *276*, 30392-30398.

Mootha, V. K., Lindgren, C. M., Eriksson, K. F., Subramanian, A., Sihag, S., Lehar, J., Puigserver, P., Carlsson, E., Ridderstrale, M., Laurila, E.*, et al.* (2003). PGC-1alpha-responsive genes involved in oxidative phosphorylation are coordinately downregulated in human diabetes. Nat Genet *34*, 267-273.

Mostow, E. N., Neckel, S. L., Oberhelman, L., Anderson, T. F., and Cooper, K. D. (1993). Complete remissions in psoralen and UV-A (PUVA)-refractory mycosis fungoides-type cutaneous T-cell lymphoma with combined interferon alfa and PUVA. Arch Dermatol *129*, 747-752.

Mu, P., Han, Y. C., Betel, D., Yao, E., Squatrito, M., Ogrodowski, P., de Stanchina, E., D'Andrea, A., Sander, C., and Ventura, A. (2009). Genetic dissection of the miR-17~92 cluster of microRNAs in Myc-induced B-cell lymphomas. Genes Dev *23*, 2806-2811.

Nagata, Y., Lan, K. H., Zhou, X., Tan, M., Esteva, F. J., Sahin, A. A., Klos, K. S., Li, P., Monia, B. P., Nguyen, N. T.*, et al.* (2004). PTEN activation contributes to tumor inhibition by trastuzumab, and loss of PTEN predicts trastuzumab resistance in patients. Cancer Cell *6*, 117-127.

Nagel, S., Venturini, L., Przybylski, G. K., Grabarczyk, P., Schmidt, C. A., Meyer, C., Drexler, H. G., Macleod, R. A., and Scherr, M. (2009). Activation of miR-17-92 by NK-like homeodomain proteins suppresses apoptosis via reduction of E2F1 in T-cell acute lymphoblastic leukemia. Leuk Lymphoma *50*, 101-108.

Naguibneva, I., Ameyar-Zazoua, M., Polesskaya, A., Ait-Si-Ali, S., Groisman, R., Souidi, M., Cuvellier, S., and Harel-Bellan, A. (2006). The microRNA miR-181 targets the homeobox protein Hox-A11 during mammalian myoblast differentiation. Nat Cell Biol *8*, 278-284.

Nanbo, A., Inoue, K., Adachi-Takasawa, K., and Takada, K. (2002). Epstein-Barr virus RNA confers resistance to interferon-alpha-induced apoptosis in Burkitt's lymphoma. Embo J *21*, 954-965.

Nefedova, Y., Cheng, P., Alsina, M., Dalton, W. S., and Gabrilovich, D. I. (2004). Involvement of Notch-1 signaling in bone marrow stroma-mediated de novo drug resistance of myeloma and other malignant lymphoid cell lines. Blood *103*, 3503-3510.

Neill, G. W., and Kelsell, D. P. (2001). Spotting prostate cancer. Trends Mol Med *7*, 432.
NHL-Group (1997). A clinical evaluation of the International Lymphoma Study Group classification of non-Hodgkin's lymphoma. The Non-Hodgkin's Lymphoma Classification Project. Blood *89*, 3909-3918.

Nielsen, M., Kaestel, C. G., Eriksen, K. W., Woetmann, A., Stokkedal, T., Kaltoft, K., Geisler, C., Ropke, C., and Odum, N. (1999). Inhibition of constitutively activated Stat3 correlates with altered Bcl-2/Bax expression and induction of apoptosis in mycosis fungoides tumor cells. Leukemia *13*, 735-738.

Ohdaira, H., Nakagawa, H., and Yoshida, K. (2009). Profiling of molecular pathways regulated by microRNA 601. Comput Biol Chem *33*, 429-433.

Ohshima, K., Karube, K., Kawano, R., Tsuchiya, T., Suefuji, H., Yamaguchi, T., Suzumiya, J., and Kikuchii, M. (2004). Classification of distinct subtypes of peripheral T-cell lymphoma unspecified, identified by chemokine and chemokine receptor expression: Analysis of prognosis. Int J Oncol *25*, 605-613.

Olsen, E., Duvic, M., Frankel, A., Kim, Y., Martin, A., Vonderheid, E., Jegasothy, B., Wood, G., Gordon, M., Heald, P.*, et al.* (2001). Pivotal phase III trial of two dose levels of denileukin diftitox for the treatment of cutaneous T-cell lymphoma. J Clin Oncol *19*, 376-388.

Olsen, E., Vonderheid, E., Pimpinelli, N., Willemze, R., Kim, Y., Knobler, R., Zackheim, H., Duvic, M., Estrach, T., Lamberg, S. I.*, et al.* (2007). Revisions to the staging and classification of mycosis fungoides and Sezary syndrome: a proposal of the International Society for Cutaneous Lymphomas (ISCL) and the Cutaneous Lymphoma Task Force of the European Organization of Research and Treatment of Cancer (EORTC). Blood.

Olsen, E. A. (2003). Interferon in the treatment of cutaneous T-cell lymphoma. Dermatol Ther *16*, 311-321.

Parrish, J. A., Fitzpatrick, T. B., Tanenbaum, L., and Pathak, M. A. (1974). Photochemotherapy of psoriasis with oral methoxsalen and longwave ultraviolet light. N Engl J Med *291*, 1207-1211.

Pautier, P., Devidas, A., Delmer, A., Dombret, H., Sutton, L., Zini, J. M., Nedelec, G., Molina, T., Marolleau, J. P., and Brice, P. (1999). Angioimmunoblastic-like T-cell non Hodgkin's lymphoma: outcome after chemotherapy in 33 patients and review of the literature. Leuk Lymphoma *32*, 545-552.

Peart, M. J., Smyth, G. K., van Laar, R. K., Bowtell, D. D., Richon, V. M., Marks, P. A., Holloway, A. J., and Johnstone, R. W. (2005). Identification and functional significance of genes regulated by structurally different histone deacetylase inhibitors. Proc Natl Acad Sci U S A *102*, 3697-3702.

Peltola, K. J., Paukku, K., Aho, T. L., Ruuska, M., Silvennoinen, O., and Koskinen, P. J. (2004). Pim-1 kinase inhibits STAT5-dependent transcription via its interactions with SOCS1 and SOCS3. Blood *103*, 3744-3750.

Pescarmona, E., Pignoloni, P., Puopolo, M., Martelli, M., Addesso, M., Guglielmi, C., and Baroni, C. D. (2001). p53 over-expression identifies a subset of nodal peripheral T-cell lymphomas with a distinctive biological profile and poor clinical outcome. J Pathol *195*, 361-366.

Piccaluga, P. P., Agostinelli, C., Califano, A., Carbone, A., Fantoni, L., Ferrari, S., Gazzola, A., Gloghini, A., Righi, S., Rossi, M.*, et al.* (2007). Gene expression analysis of angioimmunoblastic lymphoma indicates derivation from T follicular helper cells and vascular endothelial growth factor deregulation. Cancer Res *67*, 10703-10710.

Pircher, T. J., Zhao, S., Geiger, J. N., Joneja, B., and Wojchowski, D. M. (2000). Pim-1 kinase protects hematopoietic FDC cells from genotoxin-induced death. Oncogene *19*, 3684-3692.

Pogacic, V., Bullock, A. N., Fedorov, O., Filippakopoulos, P., Gasser, C., Biondi, A., Meyer-Monard, S., Knapp, S., and Schwaller, J. (2007). Structural analysis identifies imidazo[1,2-b]pyridazines as PIM kinase inhibitors with in vitro antileukemic activity. Cancer Res *67*, 6916-6924.

Popovic, M., Sarin, P. S., Robert-Gurroff, M., Kalyanaraman, V. S., Mann, D., Minowada, J., and Gallo, R. C. (1983). Isolation and transmission of human retrovirus (human t-cell leukemia virus). Science *219*, 856-859.

Potapenko, A. (1991). Mechanisms of photodynamic effects of furocoumarins. J Photochem Photobiol B *9*, 1-33.

Prince, H. M., McCormack, C., Ryan, G., O'Keefe, R., Seymour, J. F., and Baker, C. (2003). Management of the primary cutaneous lymphomas. Australas J Dermatol *44*, 227-240; quiz 241-222.

Pulford, K., Morris, S. W., and Turturro, F. (2004). Anaplastic lymphoma kinase proteins in growth control and cancer. J Cell Physiol *199*, 330-358.

Querfeld, C., Rosen, S. T., Guitart, J., and Kuzel, T. M. (2005). The spectrum of cutaneous T-cell lymphomas: new insights into biology and therapy. Curr Opin Hematol *12*, 273-278.

Quiros, P. A., Kacinski, B. M., and Wilson, L. D. (1996). Extent of skin involvement as a prognostic indicator of disease free and overall survival of patients with T3 cutaneous T-cell lymphoma treated with total skin electron beam radiation therapy. Cancer *77*, 1912-1917.

Raccurt, M., Tam, S. P., Lau, P., Mertani, H. C., Lambert, A., Garcia-Caballero, T., Li, H., Brown, R. J., McGuckin, M. A., Morel, G., and Waters, M. J. (2003). Suppressor of cytokine signalling gene expression is elevated in breast carcinoma. Br J Cancer *89*, 524-532.

Raetz, E. A., and Moos, P. J. (2004). Impact of microarray technology in clinical oncology. Cancer Invest *22*, 312-320.

Rahmani, M., Reese, E., Dai, Y., Bauer, C., Kramer, L. B., Huang, M., Jove, R., Dent, P., and Grant, S. (2005). Cotreatment with suberanoylanilide hydroxamic acid and 17-allylamino 17-demethoxygeldanamycin synergistically induces apoptosis in Bcr-Abl+ Cells sensitive and resistant to STI571 (imatinib mesylate) in association with down-regulation of Bcr-Abl, abrogation of signal transducer and activator of transcription 5 activity, and Bax conformational change. Mol Pharmacol *67*, 1166-1176.

Rahmani, M., Yu, C., Dai, Y., Reese, E., Ahmed, W., Dent, P., and Grant, S. (2003a). Coadministration of the heat shock protein 90 antagonist 17-allylamino- 17-demethoxygeldanamycin with suberoylanilide hydroxamic acid or sodium butyrate synergistically induces apoptosis in human leukemia cells. Cancer Res *63*, 8420-8427.

Rahmani, M., Yu, C., Reese, E., Ahmed, W., Hirsch, K., Dent, P., and Grant, S. (2003b). Inhibition of PI-3 kinase sensitizes human leukemic cells to histone deacetylase inhibitor-mediated apoptosis through p44/42 MAP kinase inactivation and abrogation of p21(CIP1/WAF1) induction rather than AKT inhibition. Oncogene *22*, 6231-6242.

Ramanathan, R. K., Trump, D. L., Eiseman, J. L., Belani, C. P., Agarwala, S. S., Zuhowski, E. G., Lan, J., Potter, D. M., Ivy, S. P., Ramalingam, S*., et al.* (2005). Phase I pharmacokinetic-pharmacodynamic study of 17-(allylamino)-17-demethoxygeldanamycin (17AAG, NSC 330507), a novel inhibitor of heat shock protein 90, in patients with refractory advanced cancers. Clin Cancer Res *11*, 3385-3391.

Rao, R., Lee, P., Fiskus, W., Yang, Y., Joshi, R., Wang, Y., Buckley, K., Balusu, R., Chen, J., Koul, S*., et al.* (2009). Co-treatment with heat shock protein 90 inhibitor 17-dimethylaminoethylamino-17-demethoxygeldanamycin (DMAG) and vorinostat: A highly active combination against human mantle cell lymphoma (MCL) cells. Cancer Biol Ther *8*.

Rasheed, W. K., Johnstone, R. W., and Prince, H. M. (2007). Histone deacetylase inhibitors in cancer therapy. Expert Opin Investig Drugs *16*, 659-678.

Rassidakis, G. Z., Jones, D., Lai, R., Ramalingam, P., Sarris, A. H., McDonnell, T. J., and Medeiros, L. J. (2003). BCL-2 family proteins in peripheral T-cell lymphomas: correlation with tumour apoptosis and proliferation. J Pathol *200*, 240-248.

Rassidakis, G. Z., Sarris, A. H., Herling, M., Ford, R. J., Cabanillas, F., McDonnell, T. J., and Medeiros, L. J. (2001). Differential expression of BCL-2 family proteins in ALK-positive and ALK-negative anaplastic large cell lymphoma of T/null-cell lineage. Am J Pathol *159*, 527-535.

Rebhan, M., Chalifa-Caspi, V., Prilusky, J., and Lancet, D. (1997). GeneCards: integrating information about genes, proteins and diseases. Trends Genet *13*, 163.

Rebhan, M., Chalifa-Caspi, V., Prilusky, J., and Lancet, D. (1998). GeneCards: a novel functional genomics compendium with automated data mining and query reformulation support. Bioinformatics *14*, 656-664.
Redner, R. L., Wang, J., and Liu, J. M. (1999). Chromatin remodeling and leukemia: new therapeutic paradigms. Blood *94*, 417-428.

Resnitzky, D., Tiefenbrun, N., Berissi, H., and Kimchi, A. (1992). Interferons and interleukin 6 suppress phosphorylation of the retinoblastoma protein in growth-sensitive hematopoietic cells. Proc Natl Acad Sci U S A *89*, 402-406.

Rice, J. C., and Allis, C. D. (2001). Histone methylation versus histone acetylation: new insights into epigenetic regulation. Curr Opin Cell Biol *13*, 263-273.

Richon, V. M., Sandhoff, T. W., Rifkind, R. A., and Marks, P. A. (2000). Histone deacetylase inhibitor selectively induces p21WAF1 expression and gene-associated histone acetylation. Proc Natl Acad Sci U S A *97*, 10014-10019.

Richter, K., and Buchner, J. (2001). Hsp90: chaperoning signal transduction. J Cell Physiol *188*, 281-290.

Rodriguez-Abreu, D., Filho, V. B., and Zucca, E. (2008). Peripheral T-cell lymphomas, unspecified (or not otherwise specified): a review. Hematol Oncol *26*, 8-20.

Rodriguez-Antona, C., Leskela, S., Zajac, M., Cuadros, M., Alves, J., Moneo, M. V., Martin, C., Cigudosa, J. C., Carnero, A., Robledo, M.*, et al.* (2007). Expression of CYP3A4 as a predictor of response to chemotherapy in peripheral T-cell lymphomas. Blood *110*, 3345-3351.

Rodriguez, J., Gutierrez, A., Martinez-Delgado, B., and Perez-Manga, G. (2008). Current and future aggressive peripheral T-cell lymphoma treatment paradigms, biological features and therapeutic molecular targets. Crit Rev Oncol Hematol.

Roenigk, H. H., Jr., Kuzel, T. M., Skoutelis, A. P., Springer, E., Yu, G., Caro, W., Gilyon, K., Variakojis, D., Kaul, K., Bunn, P. A., Jr., and et al. (1990). Photochemotherapy alone or combined with interferon alpha-2a in the treatment of cutaneous T-cell lymphoma. J Invest Dermatol *95*, 198S-205S.

Roman-Gomez, J., Jimenez-Velasco, A., Castillejo, J. A., Cervantes, F., Barrios, M., Colomer, D., Heiniger, A., and Torres, A. (2004). The suppressor of cytokine signaling-1 is constitutively expressed in chronic myeloid leukemia and correlates with poor cytogenetic response to interferon-alpha. Haematologica *89*, 42-48.

Roncador, G., Garcia Verdes-Montenegro, J. F., Tedoldi, S., Paterson, J. C., Klapper, W., Ballabio, E., Maestre, L., Pileri, S., Hansmann, M. L., Piris, M. A.*, et al.* (2007). Expression of two markers of germinal center T cells (SAP and PD-1) in angioimmunoblastic T-cell lymphoma. Haematologica *92*, 1059-1066.

Rosato, R. R., Almenara, J. A., Dai, Y., and Grant, S. (2003). Simultaneous activation of the intrinsic and extrinsic pathways by histone deacetylase (HDAC) inhibitors and tumor necrosis factor-related apoptosis-inducing ligand (TRAIL) synergistically induces mitochondrial damage and apoptosis in human leukemia cells. Mol Cancer Ther *2*, 1273-1284.

Rudiger, T., Weisenburger, D. D., Anderson, J. R., Armitage, J. O., Diebold, J., MacLennan, K. A., Nathwani, B. N., Ullrich, F., and Muller-Hermelink, H. K. (2002). Peripheral T-cell lymphoma (excluding anaplastic large-cell lymphoma): results from the Non-Hodgkin's Lymphoma Classification Project. Ann Oncol *13*, 140-149.

Ruefli, A. A., Ausserlechner, M. J., Bernhard, D., Sutton, V. R., Tainton, K. M., Kofler, R., Smyth, M. J., and Johnstone, R. W. (2001). The histone deacetylase inhibitor and chemotherapeutic agent suberoylanilide hydroxamic acid (SAHA) induces a cell-death pathway characterized by cleavage of Bid and production of reactive oxygen species. Proc Natl Acad Sci U S A *98*, 10833-10838.

Rupoli, S., Goteri, G., Pulini, S., Filosa, A., Tassetti, A., Offidani, M., Filosa, G., Mozzicafreddo, G., Giacchetti, A., Brandozzi, G.*, et al.* (2005). Long-term experience with low-dose interferon-alpha and PUVA in the management of early mycosis fungoides. Eur J Haematol *75*, 136-145.

Saed, G., Fivenson, D. P., Naidu, Y., and Nickoloff, B. J. (1994). Mycosis fungoides exhibits a Th1-type cell-mediated cytokine profile whereas Sezary syndrome expresses a Th2-type profile. J Invest Dermatol *103*, 29-33.

Saffer, H., Wahed, A., Rassidakis, G. Z., and Medeiros, L. J. (2002). Clusterin expression in malignant lymphomas: a survey of 266 cases. Mod Pathol *15*, 1221-1226.

Sakamoto, H., Yasukawa, H., Masuhara, M., Tanimura, S., Sasaki, A., Yuge, K., Ohtsubo, M., Ohtsuka, A., Fujita, T., Ohta, T.*, et al.* (1998). A Janus kinase inhibitor, JAB, is an interferon-gamma-inducible gene and confers resistance to interferons. Blood *92*, 1668-1676.

Sangfelt, O., Erickson, S., Castro, J., Heiden, T., Gustafsson, A., Einhorn, S., and Grander, D. (1999). Molecular mechanisms underlying interferon-alpha-induced G0/G1 arrest: CKI-mediated regulation of G1 Cdk-complexes and activation of pocket proteins. Oncogene *18*, 2798-2810.

Sato, S., Fujita, N., and Tsuruo, T. (2000). Modulation of Akt kinase activity by binding to Hsp90. Proc Natl Acad Sci U S A *97*, 10832-10837.

Sausville, E. A., Eddy, J. L., Makuch, R. W., Fischmann, A. B., Schechter, G. P., Matthews, M., Glatstein, E., Ihde, D. C., Kaye, F., Veach, S. R., and et al. (1988). Histopathologic staging at initial diagnosis of mycosis fungoides and the Sezary syndrome. Definition of three distinctive prognostic groups. Ann Intern Med *109*, 372-382.

Savage, K. J. (2007). Peripheral T-cell lymphomas. Blood Rev *21*, 201-216.

Savage, K. J., Chhanabhai, M., Gascoyne, R. D., and Connors, J. M. (2004). Characterization of peripheral T-cell lymphomas in a single North American institution by the WHO classification. Ann Oncol *15*, 1467-1475.

Saven, A., Carrera, C. J., Carson, D. A., Beutler, E., and Piro, L. D. (1992). 2-Chlorodeoxyadenosine: an active agent in the treatment of cutaneous T-cell lymphoma. Blood *80*, 587-592.

Schrock, E., du Manoir, S., Veldman, T., Schoell, B., Wienberg, J., Ferguson-Smith, M. A., Ning, Y., Ledbetter, D. H., Bar-Am, I., Soenksen, D.*, et al.* (1996). Multicolor spectral karyotyping of human chromosomes. Science *273*, 494-497.

Schulte, T. W., Blagosklonny, M. V., Romanova, L., Mushinski, J. F., Monia, B. P., Johnston, J. F., Nguyen, P., Trepel, J., and Neckers, L. M. (1996). Destabilization of Raf-1 by geldanamycin leads to disruption of the Raf-1-MEK-mitogen-activated protein kinase signalling pathway. Mol Cell Biol *16*, 5839-5845.

Schultz, C., Link, A., Leost, M., Zaharevitz, D. W., Gussio, R., Sausville, E. A., Meijer, L., and Kunick, C. (1999). Paullones, a series of cyclin-dependent kinase inhibitors: synthesis, evaluation of CDK1/cyclin B inhibition, and in vitro antitumor activity. J Med Chem *42*, 2909-2919.

Shannon, P., Markiel, A., Ozier, O., Baliga, N. S., Wang, J. T., Ramage, D., Amin, N., Schwikowski, B., and Ideker, T. (2003). Cytoscape: a software environment for integrated models of biomolecular interaction networks. Genome Res *13*, 2498-2504.

Shao, Y., Gao, Z., Marks, P. A., and Jiang, X. (2004). Apoptotic and autophagic cell death induced by histone deacetylase inhibitors. Proc Natl Acad Sci U S A *101*, 18030-18035.

Shayesteh, L., Lu, Y., Kuo, W. L., Baldocchi, R., Godfrey, T., Collins, C., Pinkel, D., Powell, B., Mills, G. B., and Gray, J. W. (1999). PIK3CA is implicated as an oncogene in ovarian cancer. Nat Genet *21*, 99-102.

Shiotsu, Y., Neckers, L. M., Wortman, I., An, W. G., Schulte, T. W., Soga, S., Murakata, C., Tamaoki, T., and Akinaga, S. (2000). Novel oxime derivatives of radicicol induce erythroid differentiation associated with preferential G(1) phase accumulation against chronic myelogenous leukemia cells through destabilization of Bcr-Abl with Hsp90 complex. Blood *96*, 2284-2291.

Shirogane, T., Fukada, T., Muller, J. M., Shima, D. T., Hibi, M., and Hirano, T. (1999). Synergistic roles for Pim-1 and c-Myc in STAT3-mediated cell cycle progression and antiapoptosis. Immunity *11*, 709-719.

Shurin, M. R., Shurin, G. V., Lokshin, A., Yurkovetsky, Z. R., Gutkin, D. W., Chatta, G., Zhong, H., Han, B., and Ferris, R. L. (2006). Intratumoral cytokines/chemokines/growth factors and tumor infiltrating dendritic cells: friends or enemies? Cancer Metastasis Rev *25*, 333-356.

Sielecki, T. M., Boylan, J. F., Benfield, P. A., and Trainor, G. L. (2000). Cyclin-dependent kinase inhibitors: useful targets in cell cycle regulation. J Med Chem *43*, 1-18.

Skinner, H. D., Zheng, J. Z., Fang, J., Agani, F., and Jiang, B. H. (2004). Vascular endothelial growth factor transcriptional activation is mediated by hypoxia-inducible factor 1alpha, HDM2, and p70S6K1 in response to phosphatidylinositol 3-kinase/AKT signaling. J Biol Chem *279*, 45643-45651.

Smith, B. D., and Wilson, L. D. (2003). Management of mycosis fungoides: Part 2. Treatment. Oncology (Williston Park) *17*, 1419-1428; discussion 1430, 1433.

Sommer, V. H., Clemmensen, O. J., Nielsen, O., Wasik, M., Lovato, P., Brender, C., Eriksen, K. W., Woetmann, A., Kaestel, C. G., Nissen, M. H*., et al.* (2004). In vivo activation of STAT3 in cutaneous T-cell lymphoma. Evidence for an antiapoptotic function of STAT3. Leukemia *18*, 1288-1295.

Song, H., and Bu, G. (2009). MicroRNA-205 inhibits tumor cell migration through down-regulating the expression of the LDL receptor-related protein 1. Biochem Biophys Res Commun *388*, 400-405.

Sors, A., Jean-Louis, F., Pellet, C., Laroche, L., Dubertret, L., Courtois, G., Bachelez, H., and Michel, L. (2006). Down-regulating constitutive activation of the NF-kappaB canonical pathway overcomes the resistance of cutaneous T-cell lymphoma to apoptosis. Blood *107*, 2354-2363.
Stadler, R. (2003). Clinical trial comparing PUVA vs PUVA + IFN in mycosis fungoides. . Paper presented at: EORTC cutaneous lymphoma task force clinical meeting. (Helsinki).

Stark, G. R., Kerr, I. M., Williams, B. R., Silverman, R. H., and Schreiber, R. D. (1998). How cells respond to interferons. Annu Rev Biochem *67*, 227-264.

Starkebaum, G., Loughran, T. P., Jr., Waters, C. A., and Ruscetti, F. W. (1991). Establishment of an IL-2 independent, human T-cell line possessing only the p70 IL-2 receptor. Int J Cancer *49*, 246-253.

Stein, H., Mason, D. Y., Gerdes, J., O'Connor, N., Wainscoat, J., Pallesen, G., Gatter, K., Falini, B., Delsol, G., Lemke, H., and et al. (1985). The expression of the Hodgkin's disease associated antigen Ki-1 in reactive and neoplastic lymphoid tissue: evidence that Reed-Sternberg cells and histiocytic malignancies are derived from activated lymphoid cells. Blood *66*, 848-858.

Stepanova, L., Leng, X., Parker, S. B., and Harper, J. W. (1996). Mammalian p50Cdc37 is a protein kinase-targeting subunit of Hsp90 that binds and stabilizes Cdk4. Genes Dev *10*, 1491-1502.

Stern, R. S. (2007). Psoralen and ultraviolet a light therapy for psoriasis. N Engl J Med *357*, 682-690.

Strillacci, A., Griffoni, C., Sansone, P., Paterini, P., Piazzi, G., Lazzarini, G., Spisni, E., Pantaleo, M. A., Biasco, G., and Tomasi, V. (2009). MiR-101 downregulation is involved in cyclooxygenase-2 overexpression in human colon cancer cells. Exp Cell Res *315*, 1439-1447.

Su, H., Yang, J. R., Xu, T., Huang, J., Xu, L., Yuan, Y., and Zhuang, S. M. (2009). MicroRNA-101, down-regulated in hepatocellular carcinoma, promotes apoptosis and suppresses tumorigenicity. Cancer Res *69*, 1135-1142.

Subramanian, A., Tamayo, P., Mootha, V. K., Mukherjee, S., Ebert, B. L., Gillette, M. A., Paulovich, A., Pomeroy, S. L., Golub, T. R., Lander, E. S., and Mesirov, J. P. (2005). Gene set enrichment analysis: a knowledge-based approach for interpreting genome-wide expression profiles. Proc Natl Acad Sci U S A *102*, 15545-15550.

Sun, W. H., Pabon, C., Alsayed, Y., Huang, P. P., Jandeska, S., Uddin, S., Platanias, L. C., and Rosen, S. T. (1998). Interferon-alpha resistance in a cutaneous T-cell lymphoma cell line is associated with lack of STAT1 expression. Blood *91*, 570-576.

Sun, Y., Bai, Y., Zhang, F., Wang, Y., Guo, Y., and Guo, L. miR-126 inhibits non-small cell lung cancer cells proliferation by targeting EGFL7. Biochem Biophys Res Commun *391*, 1483-1489.

Swerdlow, S. H., Campo, E., Harris, N.L., Jaffe, E.S., Pileri, S.A., Stein, H., Thiele, J., Vardiman, J.W (2008). WHO Classification of Tumours of Haematopoietic and Lymphoid Tissues, Fourth Edition., Vol 2, 4 edn: IARC Press).

Takai, N., Ueda, T., Nishida, M., Nasu, K., and Narahara, H. (2006). A novel histone deacetylase inhibitor, Scriptaid, induces growth inhibition, cell cycle arrest and apoptosis in human endometrial cancer and ovarian cancer cells. Int J Mol Med *17*, 323-329.
Takeda, K., Clausen, B. E., Kaisho, T., Tsujimura, T., Terada, N., Forster, I., and Akira, S. (1999). Enhanced Th1 activity and development of chronic enterocolitis in mice devoid of Stat3 in macrophages and neutrophils. Immunity *10*, 39-49.

Thompson, M. A., Stumph, J., Henrickson, S. E., Rosenwald, A., Wang, Q., Olson, S., Brandt, S. J., Roberts, J., Zhang, X., Shyr, Y., and Kinney, M. C. (2005). Differential gene expression in anaplastic lymphoma kinase-positive and anaplastic lymphoma kinase-negative anaplastic large cell lymphomas. Hum Pathol *36*, 494-504.

Tiefenbrun, N., Melamed, D., Levy, N., Resnitzky, D., Hoffman, I., Reed, S. I., and Kimchi, A. (1996). Alpha interferon suppresses the cyclin D3 and cdc25A genes, leading to a reversible G0-like arrest. Mol Cell Biol *16*, 3934-3944.

Timmermann, S., Lehrmann, H., Polesskaya, A., and Harel-Bellan, A. (2001). Histone acetylation and disease. Cell Mol Life Sci *58*, 728-736.

Tosca, A., Linardopoulos, S., Malliri, A., Hatziolou, E., Nicolaidou, A., and Spandidos, D. A. (1991). Implication of the ras and myc oncoproteins in the pathogenesis of mycosis fungoides. Anticancer Res *11*, 1433-1438.

Toyooka, T., and Ibuki, Y. (2009). Histone deacetylase inhibitor sodium butyrate enhances the cell killing effect of psoralen plus UVA by attenuating nucleotide excision repair. Cancer Res *69*, 3492-3500.

Tracey, L., Spiteri, I., Ortiz, P., Lawler, M., Piris, M. A., and Villuendas, R. (2004). Transcriptional response of T cells to IFN-alpha: changes induced in IFN-alpha-sensitive and resistant cutaneous T cell lymphoma. J Interferon Cytokine Res *24*, 185-195.

Tracey, L., Villuendas, R., Dotor, A. M., Spiteri, I., Ortiz, P., Garcia, J. F., Peralto, J. L., Lawler, M., and Piris, M. A. (2003). Mycosis fungoides shows concurrent deregulation of multiple genes involved in the TNF signaling pathway: an expression profile study. Blood *102*, 1042-1050.

Tracey, L., Villuendas, R., Ortiz, P., Dopazo, A., Spiteri, I., Lombardia, L., Rodriguez-Peralto, J. L., Fernandez-Herrera, J., Hernandez, A., Fraga, J., *et al.* (2002). Identification of genes involved in resistance to interferon-alpha in cutaneous T-cell lymphoma. Am J Pathol *161*, 1825-1837.

Trautinger, F., Knobler, R., Willemze, R., Peris, K., Stadler, R., Laroche, L., D'Incan, M., Ranki, A., Pimpinelli, N., Ortiz-Romero, P., *et al.* (2006). EORTC consensus recommendations for the treatment of mycosis fungoides/Sezary syndrome. Eur J Cancer *42*, 1014-1030.

Tsitsiou, E., and Lindsay, M. A. (2009). microRNAs and the immune response. Curr Opin Pharmacol *9*, 514-520.

Tsubaki, M., Matsuoka, H., Yamamoto, C., Kato, C., Ogaki, M., Satou, T., Itoh, T., Kusunoki, T., Tanimori, Y., and Nishida, S. (2007). The protein kinase C inhibitor, H7, inhibits tumor cell invasion and metastasis in mouse melanoma via suppression of ERK1/2. Clin Exp Metastasis *24*, 431-438.

Tsuchiya, T., Ohshima, K., Karube, K., Yamaguchi, T., Suefuji, H., Hamasaki, M., Kawasaki, C., Suzumiya, J., Tomonaga, M., and Kikuchi, M. (2004). Th1, Th2, and activated T-cell marker and clinical prognosis in peripheral T-cell lymphoma, unspecified: comparison with AILD, ALCL, lymphoblastic lymphoma, and ATLL. Blood *103*, 236-241.

Turgeon, M. L. (2005). Clinical hematology: theory and procedures. Frequency of lymphoid neoplasms.: Lippincott Williams & Wilkins.).

Turner, B. M., and Fellows, G. (1989). Specific antibodies reveal ordered and cell-cycle-related use of histone-H4 acetylation sites in mammalian cells. Eur J Biochem *179*, 131-139.

Tusher, V. G., Tibshirani, R., and Chu, G. (2001). Significance analysis of microarrays applied to the ionizing radiation response. Proc Natl Acad Sci U S A *98*, 5116-5121.

Ungerstedt, J. S., Sowa, Y., Xu, W. S., Shao, Y., Dokmanovic, M., Perez, G., Ngo, L., Holmgren, A., Jiang, X., and Marks, P. A. (2005). Role of thioredoxin in the response of normal and transformed cells to histone deacetylase inhibitors. Proc Natl Acad Sci U S A *102*, 673-678.

van Doorn, R., Dijkman, R., Vermeer, M. H., Starink, T. M., Willemze, R., and Tensen, C. P. (2002). A novel splice variant of the Fas gene in patients with cutaneous T-cell lymphoma. Cancer Res *62*, 5389-5392.

Van Gelder, R. N., von Zastrow, M. E., Yool, A., Dement, W. C., Barchas, J. D., and Eberwine, J. H. (1990). Amplified RNA synthesized from limited quantities of heterogeneous cDNA. Proc Natl Acad Sci U S A *87*, 1663-1667.

Vanden Berghe, T., Kalai, M., van Loo, G., Declercq, W., and Vandenabeele, P. (2003). Disruption of HSP90 function reverts tumor necrosis factor-induced necrosis to apoptosis. J Biol Chem *278*, 5622-5629.

Varambally, S., Cao, Q., Mani, R. S., Shankar, S., Wang, X., Ateeq, B., Laxman, B., Cao, X., Jing, X., Ramnarayanan, K., *et al.* (2008). Genomic loss of microRNA-101 leads to overexpression of histone methyltransferase EZH2 in cancer. Science *322*, 1695-1699.

Vonderheid, E. C., Bernengo, M. G., Burg, G., Duvic, M., Heald, P., Laroche, L., Olsen, E., Pittelkow, M., Russell-Jones, R., Takigawa, M., and Willemze, R. (2002). Update on erythrodermic cutaneous T-cell lymphoma: report of the International Society for Cutaneous Lymphomas. J Am Acad Dermatol *46*, 95-106.

Vose, J. M. (2008). Peripheral T-cell non-Hodgkin's lymphoma. Hematol Oncol Clin North Am *22*, 997-1005, x.

Vowels, B. R., Lessin, S. R., Cassin, M., Jaworsky, C., Benoit, B., Wolfe, J. T., and Rook, A. H. (1994). Th2 cytokine mRNA expression in skin in cutaneous T-cell lymphoma. J Invest Dermatol *103*, 669-673.

Wang, C. L., Wang, B. B., Bartha, G., Li, L., Channa, N., Klinger, M., Killeen, N., and Wabl, M. (2006). Activation of an oncogenic microRNA cistron by provirus integration. Proc Natl Acad Sci U S A *103*, 18680-18684.

Wang, Z., Bhattacharya, N., Meyer, M. K., Seimiya, H., Tsuruo, T., Tonani, J. A., and Magnuson, N. S. (2001). Pim-1 negatively regulates the activity of PTP-U2S phosphatase and influences terminal differentiation and apoptosis of monoblastoid leukemia cells. Arch Biochem Biophys *390*, 9-18.

Wang, Z., Bhattacharya, N., Mixter, P. F., Wei, W., Sedivy, J., and Magnuson, N. S. (2002). Phosphorylation of the cell cycle inhibitor p21Cip1/WAF1 by Pim-1 kinase. Biochim Biophys Acta *1593*, 45-55.

Wasik, M. A., Vonderheid, E. C., Bigler, R. D., Marti, R., Lessin, S. R., Polansky, M., and Kadin, M. E. (1996). Increased serum concentration of the soluble interleukin-2 receptor in cutaneous T-cell lymphoma. Clinical and prognostic implications. Arch Dermatol *132*, 42-47.

Watts, J. D., Affolter, M., Krebs, D. L., Wange, R. L., Samelson, L. E., and Aebersold, R. (1994). Identification by electrospray ionization mass spectrometry of the sites of tyrosine phosphorylation induced in activated Jurkat T cells on the protein tyrosine kinase ZAP-70. J Biol Chem *269*, 29520-29529.

Wegele, H., Muller, L., and Buchner, J. (2004). Hsp70 and Hsp90--a relay team for protein folding. Rev Physiol Biochem Pharmacol *151*, 1-44.

Weinstock, M. A., and Gardstein, B. (1999). Twenty-year trends in the reported incidence of mycosis fungoides and associated mortality. Am J Public Health *89*, 1240-1244.

Went, P., Agostinelli, C., Gallamini, A., Piccaluga, P. P., Ascani, S., Sabattini, E., Bacci, F., Falini, B., Motta, T., Paulli, M., *et al.* (2006). Marker expression in peripheral T-cell lymphoma: a proposed clinical-pathologic prognostic score. J Clin Oncol *24*, 2472-2479.

Whitesell, L., and Lindquist, S. L. (2005). HSP90 and the chaperoning of cancer. Nat Rev Cancer *5*, 761-772.

Whittaker, S. (2006). Biological insights into the pathogenesis of cutaneous T-cell lymphomas (CTCL). Semin Oncol *33*, S3-6.

Wiemer, E. A. (2007). The role of microRNAs in cancer: no small matter. Eur J Cancer *43*, 1529-1544.

Willemze, R., Kerl, H., Sterry, W., Berti, E., Cerroni, L., Chimenti, S., Diaz-Perez, J. L., Geerts, M. L., Goos, M., Knobler, R., *et al.* (1997). EORTC classification for primary cutaneous lymphomas: a proposal from the Cutaneous Lymphoma Study Group of the European Organization for Research and Treatment of Cancer. Blood *90*, 354-371.

Williams, B. L., Irvin, B. J., Sutor, S. L., Chini, C. C., Yacyshyn, E., Bubeck Wardenburg, J., Dalton, M., Chan, A. C., and Abraham, R. T. (1999). Phosphorylation of Tyr319 in ZAP-70 is required for T-cell antigen receptor-dependent phospholipase C-gamma1 and Ras activation. Embo J *18*, 1832-1844.

Winn, L. M., Lei, W., and Ness, S. A. (2003). Pim-1 phosphorylates the DNA binding domain of c-Myb. Cell Cycle *2*, 258-262.

Woenckhaus, J., Steger, K., Werner, E., Fenic, I., Gamerdinger, U., Dreyer, T., and Stahl, U. (2002). Genomic gain of PIK3CA and increased expression of p110alpha are associated with progression of dysplasia into invasive squamous cell carcinoma. J Pathol *198*, 335-342.

Wolf, P., Nghiem, D. X., Walterscheid, J. P., Byrne, S., Matsumura, Y., Matsumura, Y., Bucana, C., Ananthaswamy, H. N., and Ullrich, S. E. (2006). Platelet-activating factor is crucial in psoralen and ultraviolet A-induced immune suppression, inflammation, and apoptosis. Am J Pathol *169*, 795-805.

Wollina, U., and Dummer, R. (2006). [Peripheral T-cell lymphoma: diagnosis and treatment]. Dtsch Med Wochenschr *131*, 1884; author reply 1884.

Wood, G. S., Tung, R. M., Haeffner, A. C., Crooks, C. F., Liao, S., Orozco, R., Veelken, H., Kadin, M. E., Koh, H., Heald, P., and et al. (1994). Detection of clonal T-cell receptor gamma gene rearrangements in early mycosis fungoides/Sezary syndrome by polymerase chain reaction and denaturing gradient gel electrophoresis (PCR/DGGE). J Invest Dermatol *103*, 34-41.

Wozniak, M. B., Tracey, L., Ortiz-Romero, P. L., Montes, S., Alvarez, M., Fraga, J., Fernandez Herrera, J., Vidal, S., Rodriguez-Peralto, J. L., Piris, M. A., and Villuendas Deceased, R. (2009). Psoralen plus ultraviolet A +/- interferon-alpha treatment resistance in mycosis fungoides: the role of tumour microenvironment, nuclear transcription factor-kappaB and T-cell receptor pathways. Br J Dermatol *160*, 92-102.

Wu, H., Zhu, S., and Mo, Y. Y. (2009). Suppression of cell growth and invasion by miR-205 in breast cancer. Cell Res *19*, 439-448.

Xie, R. L., Gupta, S., Miele, A., Shiffman, D., Stein, J. L., Stein, G. S., and van Wijnen, A. J. (2003). The tumor suppressor interferon regulatory factor 1 interferes with SP1 activation to repress the human CDK2 promoter. J Biol Chem *278*, 26589-26596.

Xu, T., Zhu, Y., Xiong, Y., Ge, Y. Y., Yun, J. P., and Zhuang, S. M. (2009). MicroRNA-195 suppresses tumorigenicity and regulates G1/S transition of human hepatocellular carcinoma cells. Hepatology *50*, 113-121.

Yan, B., Zemskova, M., Holder, S., Chin, V., Kraft, A., Koskinen, P. J., and Lilly, M. (2003). The PIM-2 kinase phosphorylates BAD on serine 112 and reverses BAD-induced cell death. J Biol Chem *278*, 45358-45367.

Yang, C. H., Murti, A., and Pfeffer, L. M. (1998). STAT3 complements defects in an interferon-resistant cell line: evidence for an essential role for STAT3 in interferon signaling and biological activities. Proc Natl Acad Sci U S A *95*, 5568-5572.

Yoo, E. K., Rook, A. H., Elenitsas, R., Gasparro, F. P., and Vowels, B. R. (1996). Apoptosis induction of ultraviolet light A and photochemotherapy in cutaneous T-cell Lymphoma: relevance to mechanism of therapeutic action. J Invest Dermatol *107*, 235-242.

Yoshida, S., Kaneita, Y., Aoki, Y., Seto, M., Mori, S., and Moriyama, M. (1999). Identification of heterologous translocation partner genes fused to the BCL6 gene in diffuse large B-cell lymphomas: 5'-RACE and LA - PCR analyses of biopsy samples. Oncogene *18*, 7994-7999.

Young, J. C., Agashe, V. R., Siegers, K., and Hartl, F. U. (2004). Pathways of chaperone-mediated protein folding in the cytosol. Nat Rev Mol Cell Biol *5*, 781-791.

Yu, H., Kortylewski, M., and Pardoll, D. (2007). Crosstalk between cancer and immune cells: role of STAT3 in the tumour microenvironment. Nat Rev Immunol *7*, 41-51.

Yu, X., Guo, Z. S., Marcu, M. G., Neckers, L., Nguyen, D. M., Chen, G. A., and Schrump, D. S. (2002). Modulation of p53, ErbB1, ErbB2, and Raf-1 expression in lung cancer cells by depsipeptide FR901228. J Natl Cancer Inst *94*, 504-513.

Zamoyska, R., Basson, A., Filby, A., Legname, G., Lovatt, M., and Seddon, B. (2003). The influence of the src-family kinases, Lck and Fyn, on T cell differentiation, survival and activation. Immunol Rev *191*, 107-118.

Zanette, D. L., Rivadavia, F., Molfetta, G. A., Barbuzano, F. G., Proto-Siqueira, R., Silva-Jr, W. A., Falcao, R. P., and Zago, M. A. (2007). miRNA expression profiles in chronic lymphocytic and acute lymphocytic leukemia. Braz J Med Biol Res *40*, 1435-1440.

Zhang, C., Richon, V., Ni, X., Talpur, R., and Duvic, M. (2005). Selective induction of apoptosis by histone deacetylase inhibitor SAHA in cutaneous T-cell lymphoma cells: relevance to mechanism of therapeutic action. J Invest Dermatol *125*, 1045-1052.

Zhang, C. L., Kamarashev, J., Qin, J. Z., Burg, G., Dummer, R., and Dobbeling, U. (2003). Expression of apoptosis regulators in cutaneous T-cell lymphoma (CTCL) cells. J Pathol *200*, 249-254.

Zhang, Q., Nowak, I., Vonderheid, E. C., Rook, A. H., Kadin, M. E., Nowell, P. C., Shaw, L. M., and Wasik, M. A. (1996). Activation of Jak/STAT proteins involved in signal transduction pathway mediated by receptor for interleukin 2 in malignant T lymphocytes derived from cutaneous anaplastic large T-cell lymphoma and Sezary syndrome. Proc Natl Acad Sci U S A *93*, 9148-9153.

Zhang, Y., Wang, Z., and Magnuson, N. S. (2007). Pim-1 kinase-dependent phosphorylation of p21Cip1/WAF1 regulates its stability and cellular localization in H1299 cells. Mol Cancer Res *5*, 909-922.

Zhao, J. J., Lin, J., Lwin, T., Yang, H., Guo, J., Kong, W., Dessureault, S., Moscinski, L. C., Rezania, D., Dalton, W. S.*, et al.* microRNA expression profile and identification of miR-29 as a prognostic marker and pathogenetic factor by targeting CDK6 in mantle cell lymphoma. Blood.

Zhou, B. P., Liao, Y., Xia, W., Spohn, B., Lee, M. H., and Hung, M. C. (2001). Cytoplasmic localization of p21Cip1/WAF1 by Akt-induced phosphorylation in HER-2/neu-overexpressing cells. Nat Cell Biol *3*, 245-252.

Zhou, Y., Wang, S., Gobl, A., and Oberg, K. (2000). The interferon-alpha regulation of interferon regulatory factor 1 (IRF-1) and IRF-2 has therapeutic implications in carcinoid tumors. Ann Oncol *11*, 707-714.

Zimmermann, S., and Moelling, K. (1999). Phosphorylation and regulation of Raf by Akt (protein kinase B). Science *286*, 1741-1744.

Zsebik, B., Citri, A., Isola, J., Yarden, Y., Szollosi, J., and Vereb, G. (2006). Hsp90 inhibitor 17-AAG reduces ErbB2 levels and inhibits proliferation of the trastuzumab resistant breast tumor cell line JIMT-1. Immunol Lett *104*, 146-155.

APPENDIX

APPENDIX I

SUPPLEMENTARY MATERIAL

SUPPLEMENTARY FIGURES

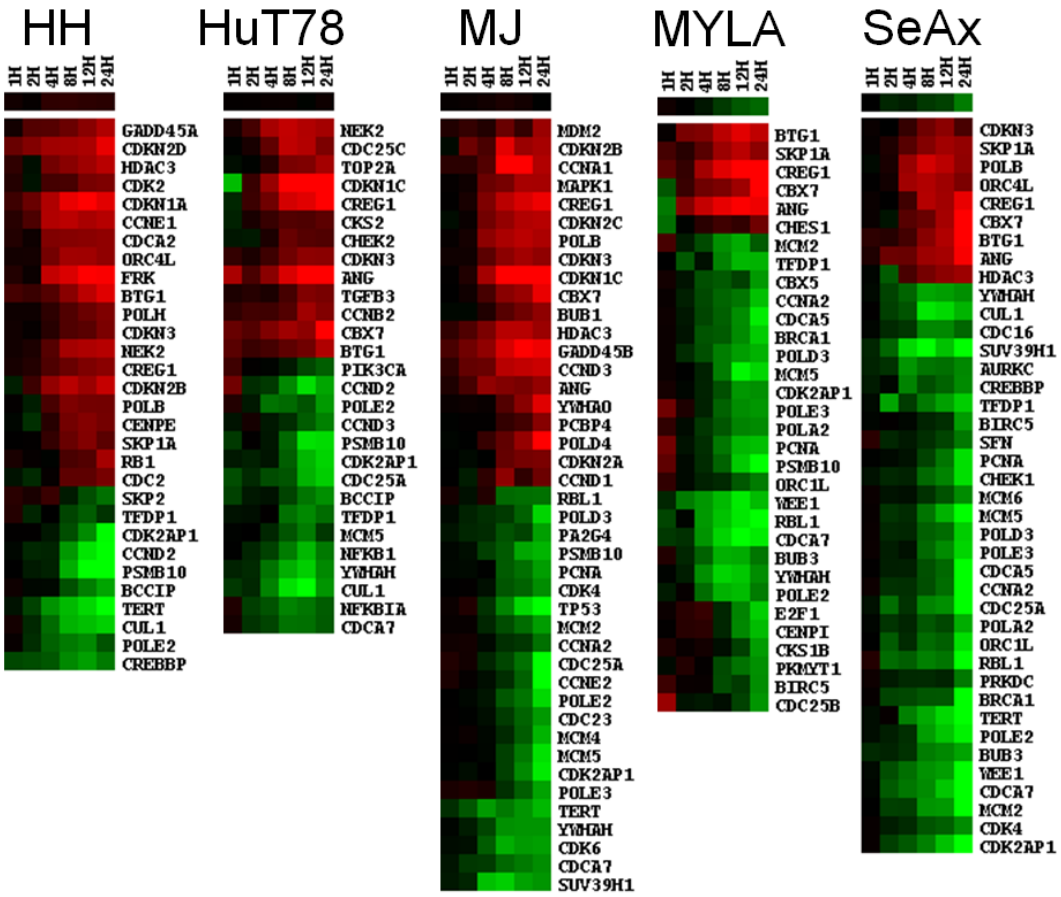

Figure S1. Functional clustering of vorinostat-regulated cell cycle associated genes.

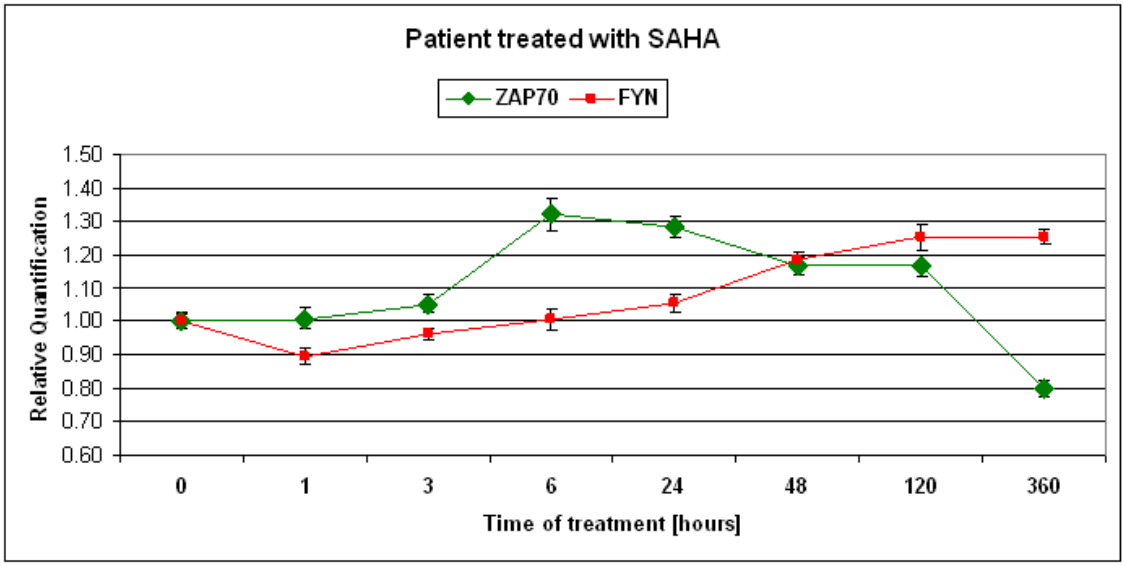

Figure S2. Validation of microarray data by TaqMan quantitative real time PCR in CTCL patient. Effect on vorinostat on mRNA expression of ZAP-70 and FYN in a treated patient. A patient with high load of tumoral cells was treated with vorinostat (24h dose schedule) and the samples were taken before and after 1, 3, 6, 24, 48, 120 and 360 hours from the commencement of the treatment. The figure represents RT-qPCR results for ZAP70 and FYN. The expression values before treatment were set to 1 and the percent of alteration was calculated.

APPENDIX II

PUBLICATIONS